

DESCRIPTION OF HETEROGENEOUS  
RESERVOIRS  
USING PRESSURE AND TRACER DATA

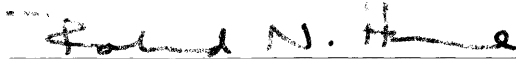
A DISSERTATION  
SUBMITTED TO THE DEPARTMENT OF PETROLEUM ENGINEERING  
AND THE COMMITTEE ON GRADUATE STUDIES  
OF STANFORD UNIVERSITY  
IN PARTIAL FULFILLMENT OF THE REQUIREMENTS  
FOR THE DEGREE OF  
DOCTOR OF PHILOSOPHY

By  
Xianfa Deng  
March 1996

AQTL 1397

© Copyright 1996 by Xianfa Deng  
All Rights Reserved

I certify that I have read this dissertation and that in my opinion it is fully adequate, in scope and in quality, as a dissertation for the degree of Doctor of Philosophy.



---

Roland N. Horne  
(Principal Advisor)

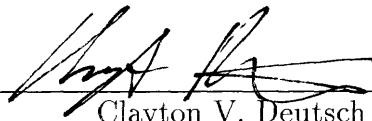
I certify that I have read this dissertation and that in my opinion it is fully adequate, in scope and in quality, as a dissertation for the degree of Doctor of Philosophy.



---

Thomas A. Hewett

I certify that I have read this dissertation and that in my opinion it is fully adequate, in scope and in quality, as a dissertation for the degree of Doctor of Philosophy.



---

Clayton V. Deutsch

Approved for the University Committee on Graduate Studies:



# Abstract

This study investigated methods of characterizing areally heterogeneous reservoirs through the interpretation of pressure data and tracer data. The analysis of pressure data and the analysis of tracer data were studied both individually and simultaneously.

A nonlinear least square method was applied to interpret multiwell transient pressure data from interference tests. Several models, including anisotropic reservoir, circular discontinuity, no-flow linear boundary and interaction among multiple wells were investigated. Their solutions were reformulated to fit into the nonlinear regression algorithm. Results showed that using multiwell data avoids inconsistent results for the selected reservoir model, increases the tolerance to noise in the data, increases the confidence of the interpretation and improves the convergence of the regression search.

Analytical solutions to tracer flow were obtained for three cases: radial flow, linearly varying dispersivity and linear flow in composite reservoir. Another semi-analytical solution to tracer flow in two dimensional reservoirs based on the characteristic method is presented.

The method of Green's functions has been a powerful tool to solve unsteady flow problems in homogeneous reservoirs. The application of the Green's function method was extended to diffusivity problems in heterogeneous reservoirs. A fundamental formula was obtained to express the general pressure solution to the diffusivity equation with nonhomogeneous initial and boundary conditions in terms of Green's functions. Through practical examples, appropriate methods were suggested for obtaining Green's functions that are more difficult to find in heterogeneous problems than in

homogeneous ones. Reciprocity is a basic and useful property which facilitates the understanding to porous media flow problems. With the Green's function method developed, the conditions under which the Principle of Reciprocity holds in heterogeneous formation were studied. The application of the Green's function method to convection-dispersion equation and its limitations are also discussed.

After the analysis of pressure data and tracer data are described individually, direct method is presented to simultaneously interpret pressure data and tracer data from multiple wells to characterize the areal permeability distribution in heterogeneous reservoirs. Since tracer data are more sensitive to heterogeneity than pressure data, integration of the two kinds of data should give a better description of the reservoir. A correlation between permeability and dispersivity was investigated, and used to reformulate the convection-dispersion equation and diffusion equation to a system of first-order equations in permeability. The system of equations can then be solved to yield the permeability distribution for appropriate boundary conditions. Advantages and disadvantages of this new scheme are discussed. As an example, the time function method was applied to the interpretation of pressure and tracer data of a multiwell reservoir with a circular discontinuity.

# Acknowledgements

In completing this dissertation, I am indebted to many people and organizations. First, I thank my advisor, Dr. Roland N. Horne, for his guidance, suggestions, and continuous encouragement during the course of this study and for his encouragement extended beyond this study. I wish to express my gratitude to Dr. Thomas A. Hewett and Dr. Clayton V. Deutsch for serving on the reading committee, and to Dr. Martin Blunt for participating on the examination committee. Appreciation is extended to the faculty, staff, and students of the Department of Petroleum Engineering, who have made my life as a graduate student so enjoyable.

I thank my family for all the love that they have given me and will give me in the future. Without their supports and understandings, this work would never have been completed.

This material is based upon the work supported financially by the U.S. Department of Energy under grant DE-FG07-90 ID12934 to the Stanford Geothermal Program. This financial support is gratefully acknowledged.

# Contents

<b>Abstract</b>	<b>iv</b>
<b>Acknowledgements</b>	<b>vi</b>
<b>1 Introduction</b>	<b>1</b>
<b>2 Use of Pressure Data from Multiple Wells</b>	<b>7</b>
2.1 Multiwell Data of Anisotropic Reservoir . . . . .	7
2.1.1 Mathematical Considerations . . . . .	8
2.1.2 Field Example . . . . .	9
2.2 Heterogeneity of the Circular Discontinuity Type . . . . .	16
2.2.1 Discontinuity Without Wellbore Storage . . . . .	17
2.2.2 Discontinuity with Wellbore Storage . . . . .	24
2.2.3 Transformation of Coordinate System . . . . .	26
2.2.4 Objective Function . . . . .	28
2.2.5 Examples . . . . .	35
2.2.6 A Special Case - Concentric Active Well . . . . .	38
2.3 Analysis of Drawdown-Buildup Pressure Data in Multiwell Systems .	47
2.4 No-Flow Linear Boundary . . . . .	59
2.5 Interpreting Multiwell Pressure Data of Ohaaki Geothermal Field . .	63
<b>3 Green's Functions and the Reciprocity Principle in Heterogeneous Media</b>	<b>72</b>
3.1 Definition of Green's Functions . . . . .	72

3.2	Properties of Green's Functions . . . . .	75
3.3	Pressure in Terms of Green's Functions . . . . .	76
3.4	Examples of Green's Functions . . . . .	76
3.4.1	<u>Case 1: Separation of Variables</u> . . . . .	76
3.4.2	<u>Case 2: Fourier Transformation</u> . . . . .	78
3.4.3	<u>Case 3: Working in Laplace Space</u> . . . . .	80
3.4.4	<u>Case 4: Decomposition</u> . . . . .	82
3.5	Anisotropic and Heterogeneous Reservoirs . . . . .	84
3.6	Principle of Reciprocity . . . . .	85
3.7	Effects of Wellbore Storage and Skin . . . . .	86
3.8	Green's Functions for Tracer Flow Problems . . . . .	88
<b>4</b>	<b>Analytical Solutions to Tracer Flow</b>	<b>90</b>
4.1	Convection-Dispersion Equation with Linearly Changing Dispersivity	92
4.2	Linear Tracer Flow in a Composite Reservoir . . . . .	95
4.3	Radial Convection-Dispersion Tracer Flow in Homogeneous Reservoir	103
4.4	Streamlines in an Infinite Reservoir with a Circular Discontinuity . .	104
<b>5</b>	<b>Using Tracer and Pressure Data Simultaneously</b>	<b>113</b>
5.1	Dispersivity and Permeability Correlation . . . . .	113
5.2	Integrating Tracer and Pressure Data in Heterogeneous Reservoirs . .	115
5.3	Ill-posedness . . . . .	116
5.4	Permeability Constraints . . . . .	118
5.5	Direct Method for Tracer Data . . . . .	121
5.6	Example . . . . .	125
<b>6</b>	<b>Conclusions</b>	<b>136</b>
<b>A</b>	<b>Equivalence of two Anisotropic Solutions</b>	<b>142</b>
<b>B</b>	<b>Pressure Expression in Green's Function</b>	<b>146</b>
<b>C</b>	<b>Reciprocity of Green's Function</b>	<b>150</b>



<b>D Two-Dimensional Green's Functions in Problems with Variable Permeability</b>	<b>154</b>
<b>E Pressure and Tracer Solutions for a Multiwell Heterogeneous System</b>	<b>158</b>
<b>Nomenclature</b>	<b>164</b>
<b>Bibliography</b>	<b>168</b>

# List of Tables

- 2.1 Water-injection interference pressure rise above the initial pressure . . . 11
- 2.2 Configuration of the formation . . . . . 28
- 2.3 Generated pressure data for the reservoir of Example 1 . . . . . 36
- 2.4 Properties of the reservoir in Example 1 . . . . . **37**
- 2.5 Initial guess, matching result and true value . . . . . 38
- 2.6 Generated pressure data of Example 2 . . . . . **39**
- 2.7 Properties of the reservoir for Example 2 . . . . . 40
- 2.8 Initial guess, matching result and true value . . . . . 40

# List of Figures

2.1	Field well pattern in an anisotropic reservoir . . . . .	10
2.2	Using three sets of pressure data in an anisotropic reservoir example .	12
2.3	Using nine sets of pressure data in an anisotropic reservoir example .	14
2.4	Using another three sets of pressure data in an anisotropic reservoir example . . . . .	15
2.5	Infinite reservoir with a circular discontinuity . . . . .	18
2.6	Pressure response versus compressibility of first region . . . . .	20
2.7	Pressure response versus permeability of first region . . . . .	20
2.8	Pressure response versus compressibility of second region . . . . .	21
2.9	Pressure response versus permeability of second region . . . . .	21
2.10	Pressure response versus position of active well (distance) . . . . .	22
2.11	Pressure response versus position of active well (angle) . . . . .	22
2.12	Pressure response versus radius of discontinuity . . . . .	23
2.13	Comparison of pressure response in active well with or without wellbore storage . . . . .	25
2.14	Comparison of pressure response in observation well with or without wellbore storage . . . . .	25
2.15	Transformation of two coordinate systems . . . . .	27
2.16	Well pattern for an infinite reservoir with a circular discontinuity . .	29
2.17	Objective function versus various position of active well . . . . .	30
2.18	Objective function versus various position of active well . . . . .	31
2.19	Objective function versus various position of active well . . . . .	32
2.20	Objective function versus various position of active well . . . . .	<b>33</b>

2.21 Comparison of pressure responses between skin factor approach and discontinuity approach . . . . .	42
2.22 Comparison of pressure responses between skin factor approach and discontinuity model approach . . . . .	43
2.23 Matching result for concentric model . . . . .	44
2.24 Matching result for concentric model . . . . .	45
2.25 Interference pressure response versus production time . . . . .	48
2.26 Pressure response versus production time and wellbore storage effect .	48
2.27 Pressure response versus production time and wellbore storage effect .	49
2.28 Pressure response versus production time and wellbore storage effect .	49
2.29 Pressure response versus production time . . . . .	51
2.30 Pressure response versus production time and wellbore storage effect .	51
2.31 Pressure buildup response versus time after shut-in . . . . .	52
2.32 Pressure buildup versus time after shut-in and wellbore storage effect	52
2.33 Configuration of six-well and infinite-well systems . . . . .	53
2.34 Pressure response versus production time . . . . .	55
2.35 Pressure response versus production time and wellbore storage effect .	55
2.36 Pressure buildup response versus time after shut-in . . . . .	56
2.37 Pressure buildup versus time after shut-in and wellbore storage effect	56
2.38 Drawdown pressure response versus production time . . . . .	58
2.39 Drawdown pressure response versus production time . . . . .	58
2.40 Well pattern for an infinite reservoir with a linear no-flow boundary .	60
2.41 Contour of objective function using two sets of pressure data . . . . .	61
2.42 Contour of objective function using three sets of pressure data . . . . .	62
2.43 Approximate matching results from <i>Leaver et al</i> (1988) . . . . .	66
2.44 Matching results without weights and initial pressures as parameters .	67
<b>2.45</b> Matching results with initial pressures as parameters . . . . .	68
2.46 Matching results with weights emphasizing early data . . . . .	69
2.47 Matching results with initial pressures as parameters . . . . .	70
2.48 Matching results with weights and initial pressures as parameters . .	71

3.1	Distribution of mobility and storativity . . . . .	82
4.1	Tracer responses(incorrect) calculated by Stehfest algorithm . . . . .	93
4.2	Tracer response(correct) calculated by Crump algorithm . . . . .	93
<b>4.3</b>	<b>Comparison of constant dispersivity and linearly changing dispersivity</b>	<b>94</b>
4.4	Linear tracer flow in composite region . . . . .	96
4.5	Tracer profile in one dimensional uniform region . . . . .	98
4.6	Tracer profile in one dimension with two different dispersivities . . . . .	98
4.7	Tracer profile in one dimension with two different dispersivities . . . . .	99
4.8	Tracer profile in one dimension with two different porosities . . . . .	99
4.9	Pressure distribution of two wells in discontinuous reservoir . . . . .	106
4.10	Streamlines of two wells in a homogeneous reservoir . . . . .	107
4.11	Streamlines of two wells with a discontinuity of lower permeability . . . . .	108
4.12	Streamlines of two wells with a discontinuity of higher permeability . . . . .	109
4.13	Tracer profile in a doublet system of infinite reservoir . . . . .	111
4.14	Tracer profile in a doublet system of infinite reservoir . . . . .	111
5.1	Propagation of concentration of discontinuity at $x = 0$ . . . . .	124
5.2	x-y-t diagram showing characteristic surface for the concentration of radial flow . . . . .	124
5.3	Pressure distribution of multiwell system with a circular discontinuity	126
5.4	Pressure contour of multiwell system with a circular discontinuity . . . . .	126
5.5	Streamline of multiwell system with a circular discontinuity . . . . .	128
5.6	Streamline of multiwell system but without the circular discontinuity	128
5.7	Concentration front in the multiwell system with a circular discontinuity	129
5.8	Concentration front in the multiwell system without the circular discontinuity . . . . .	130
5.9	x-y-t diagram showing the time at which the concentration front arrives as a function of $(\mathbf{x}, y)$ . . . . .	131
5.10	The time at which the concentration front arrives as a function of $(x, y)$	131
5.11	Permeability distribution calculated using pressure and tracer data from <b>300</b> by <b>300</b> observation points . . . . .	<b>133</b>

5.12 Permeability distribution calculated using pressure and tracer data from <b>100</b> by 100 observation points . . . . .	134
5.13 Permeability distribution calculated using pressure and tracer data from <b>30</b> by <b>30</b> observation points . . . . .	135

# Chapter 1

## Introduction

Pressure tests and tracer tests are used frequently to estimate parameters and identify flow paths in geothermal reservoirs that are often controlled by the large heterogeneity in permeability due to fractures.

The use of tracer tests to determine the nature of the flow paths in geothermal and groundwater reservoirs was studied broadly in the 1980s. *Jensen and Home* (1983) developed a matrix model to obtain the tracer returns from fractured reservoirs. A similar model was used to forecast the thermal breakthrough from tracer test data by *Walkup and Horne* (1982). A single well tracer test in fractured geothermal reservoirs was studied by *Kocabas and Home* (1987). Due to the geometric complexity in representing the fractures, all these models were applied only to systems with one or two fractures. There has been little work done in solving the tracer problem for a multiply fractured reservoir that also includes the geometric effects of the fractures.

Tracer tests are believed to be more sensitive to heterogeneity than pressure tests. Pressure interference tests are good for determining directional permeability trends and the average properties between two wells, while well-to-well tracer tests indicate the extent of heterogeneity that is merely averaged in the pressure interference tests. These two types of tests describe different characteristics of the reservoir. Thus, running both tests may be helpful. In addition, obtaining both pressure and tracer data should help in reducing the uncertainty or nonuniqueness in the solutions. Nonuniqueness always arises with either tracer test analysis or pressure test analysis

alone because the property identification problem is under-determined when the heterogeneity is represented as a spatial function. It is important to coordinate different studies, such as geology, geophysics, coring, well logging, pressure testing and tracer testing etc. so that the interpreted properties of the reservoir are compatible with all the sources of information. The central emphasis of this work is on combining pressure data and tracer data from multiple wells.

Among the efforts to integrate tracer data with other type of data, *Hyndman* (1993) presented the Split Inversion Method to combine crosswell seismic and natural gradient tracer tests data in a process-oriented parameter estimation algorithm. This iterative method can estimate the location and shape of large-scale lithologic zones, and the mean seismic velocity, hydraulic conductivity, and dispersivity within each zone. *Peters and Afzal* (1992) made effort in other direction by using CT imaging data of the media to estimate permeability and porosity distributions. The model developed was for one-dimensional linear incompressible flow of stable displacement in laboratory-scale porous media.

The convection-dispersion equation has been the model used most commonly to describe transport phenomena in porous media. *Bear* (1961) considered the concentration distribution, in two dimensions, resulting from a point tracer injection into a uniform macro-flow and showed that an approximated variance of this concentration distribution yields a tensorial coefficient of dispersions  $D_{ij}$ , and that this tensor could be related to a fourth rank dispersivity tensor  $a_{ijkl}$ , the components of which were determined by geometrical characteristics of the porous medium only. *De Josselin de Jong and Bossen* (1961) subsequently established a dispersion equation on this basis, valid for three-dimensional convective tracer transport through an isotropic porous medium. *De Josselin de Jong and Bossen* (1961) showed that the dispersion tensor resulting from *Bear's* analysis could be written

$$D_{ij} + a_L |v| \delta_{ij} + (a_L - a_T) \frac{v_i v_j}{|v|}. \quad (1.1)$$

*Abbaszadeh-Dehghani* (1982) developed the analytical solutions to immiscible displacements for a variety of repeated flooding pattern. The dispersion effects were



considered by computing the concentration of the displacing fluid along the streamlines. For heterogeneity, *Abbaszadeh-Dehghani* (1982) studied a stratified model without layer communication. These noncommunicating layered systems were further investigated by *Mishra* (1987) together with both pressure and tracer data. The result *Mishra* (1987) reached indicated that tracer data convey more information than pressure data for describing layered systems. *Mishra* (1987) also introduced the heterogeneity index  $\sigma_{ln(k)}^2 \lambda_D$  defined as the product of permeability variance and a dimensionless correlation length scale to describe the permeability difference. The effects of large or small heterogeneity index on tracer flow were compared.

*Yu* (1984) studied a one-dimensional, uniform, vertical flow of radioactive nuclide in a homogeneous, saturated porous medium with instantaneous adsorption and the linear Freundlich isotherm. Linear and nonlinear least square methods were used to estimate the parameters iteratively.

Compared to the tracer problem, pressure problems are usually easier to solve analytically. There are a wide variety of analytical well test analysis models in the literature. In particular, the Green's function method has been found to be an effective analytical tool to construct pressure responses in homogeneous reservoirs.

Using the Green's function method to solve linear ordinary and partial differential equations is not a new idea. However, many of the textbooks of mathematics only cover the application of this method to simple equations. *Starkgold* (1979) and *Roach* (1982) showed some examples how to use this method for equations of parabolic and hyperbolic equations with constant coefficients. The method of Green's functions has been a powerful tool to solve unsteady flow problems for homogeneous reservoirs in petroleum engineering. *De Wiest* (1969) used this method in a problem of water flowing through porous media. *Gringarten* and *Ramey* (1973) made this approach practically useful in petroleum engineering by giving tables of Green's functions for pressure diffusion in homogeneous or anisotropic reservoirs. *Ozkan and Raghavan* (1991) extended these tables and provided solutions in Laplace space, as well as for naturally fractured reservoirs. *Carslaw and Jaeger* (1959) discussed the Green's function approach for problems of heat conduction; however, their definition of Green's function is less useful if applied to composite or heterogeneous regions.

A subtle, yet important aspect of using Green's functions in heterogeneous problems is their dependence on the Principle of Reciprocity. By investigating the conditions under which reciprocity holds, we were able to illustrate those problems whose solutions are accessible by use of Green's functions.

The principle of reciprocity is also useful in understanding reservoir physics. *McKinley et al.* (1968) investigated the effect of this property in the analysis of interference well testing. *Ogbe* (1984) studied this principle in the presence of wellbore storage and skin effect for infinite reservoirs. *McKinley et al.* (1968) proved that this principle holds if the mobility and storativity are continuously distributed. We were able to show that the principle can also be extended to discontinuous distributions of reservoir properties, and also investigated the influence of wellbore storage on reciprocity.

Most studies of well test analysis start by solving the diffusivity equation in which permeability or dispersivity and porosity are treated as coefficients. For instance, the pressure equation is solved to yield pressure for specific boundary conditions. Once this mathematical model is formed, the pressure response can be calculated for any given permeability and porosity. The remaining work in the analysis is to compute the correct pressure curve to match the real data and infer the needed permeability. In computer-aided interpretation, an initial permeability value is estimated, then the pressure response is obtained and compared with the observed pressure data. Based on the difference, the estimate is adjusted iteratively. This iterative process is referred to as the *Output Error Criterion* by *Yeh* (1986). When a large set of data is involved, this approach will require a large amount of calculation and sometimes becomes inefficient and impractical. One of the solutions to this problem is to put a filter in front of the interpreter. The filter serves to choose a subset from the whole set of data. The question then becomes which subset is a good representation and how to avoid inconsistent results interpreted from different subsets. This problem is not easy to solve either. Moreover, the minimization of an error criterion defined on the difference between the computed and observed data may be associated with multiple local convergences.

There also exist cases that defeat the output error procedure as shown by *Falk* (1983).

Even though conditions can be specified to guarantee the unique determination of the permeability  $k(x, y)$ , the optimization approximations  $k_{ij}$  do not necessarily converge to the unique function  $k(x, y)$  as the grid spacing decreases. Nonetheless, for the output error procedure, the possibility of using regularization method or constrained optimization can make the methods attractive in some cases.

Besides this conventional approach, there have been some attempts to identify the parameters by solving the diffusivity equation from the opposite direction. One type of the parameter identification approach was called the Direct Method in aquifer studies, e.g. *Sagar et al. (1975)*, also referred to as the *Equation Error Criterion* by *Yeh (1986)*. In this approach, taking the equation

$$\frac{\partial}{\partial x} \left( k \frac{\partial p}{\partial x} + k \frac{\partial p}{\partial y} \right) + \frac{\partial}{\partial y} \left( k \frac{\partial p}{\partial x} + k \frac{\partial p}{\partial y} \right) = \frac{q\mu}{h} \quad (1.2)$$

as an example, the permeability values are considered as dependent variables of pressure in the form of a formal boundary value problem. If the pressure  $p$  is known everywhere, then  $\frac{\partial p}{\partial x}$ ,  $\frac{\partial p}{\partial y}$ ,  $\frac{\partial^2 p}{\partial x^2}$  and  $\frac{\partial^2 p}{\partial y^2}$  are also known, and the equation becomes a linear first-order hyperbolic equation in terms of permeabilities. *Yeh et al. (1983)* applied this method to an unsteady flow in a heterogeneous, isotropic, and confined aquifer. There, kriging was used as a presampling filter for reconstruction and the parameter was estimated by using a multiobjective optimization criterion to find the optimum dimension.

*Nelson (1968)* presented a direct method for a steady flow system called the *energy dissipation method* which was based on the characteristic equation. This method requires a boundary condition on permeability since the equation was reduced to a first-order partial differential equation in the unknown permeability. For pressure interpretation, the finite element method has also been employed in approximating pressure and permeability, e.g. *Frind et al. (1973)* and *Yeh et al. (1983)*. An algebraic method was developed by *Sagar (1975)* and its error bound was obtained by *Yakowitz (1976)*. This technique utilized the idea that the effect of the permeability value at a location is uniquely determined by values of pressure in a neighborhood of the location.

The direct approach has not yet been widely applied to the tracer equation. With

the assumption that there is a correlation between dispersivity coefficients and permeabilities, both the tracer equation and the pressure equation will have permeabilities as parameters, then permeabilities could be solved directly as unknowns in both the pressure and tracer equations. The interpretation of pressure data and tracer data together should provide a better estimation of the permeability distribution in heterogeneous reservoirs.

The goal of this study was the interpretation of pressure data and tracer data for multiwell systems. First, the multiwell pressure data were investigated for several heterogeneous models with analytical pressure solutions. The methods for finding solutions to tracer problems were studied with an emphasis on analytical methods. Then, the Green's function method was established for both diffusivity equation and convection-dispersion equation with an investigation of the principle of reciprocity. Finally, an approach to integrate pressure and tracer data to estimate areal permeability distribution was investigated.

## **Chapter 2**

# **Use of Pressure Data from Multiple Wells**

Considering the amount of data collected in well test analysis, there are two opposite scenarios that require special attention: more data than necessary and insufficient data. In the first case, interpretation results by conventional methods may be nonunique depending on the sufficient subset of data chosen and usually, it is difficult to tell which answer is correct or better. One way to avoid the nonuniqueness in this approach is to interpret all the applicable data sets simultaneously.

In this chapter, a nonlinear least square method is presented to analyze multiwell transient pressure data for various reservoir models that have simple heterogeneities such as anisotropy, circular discontinuity or no-flow boundary. In a multiwell system, neighbor wells in production have influence on the buildup pressure data from observation wells. The interaction among multiple active and testing wells is discussed in Section 2.3. Section 2.5 applies the nonlinear least square method to interpret multiwell data from the Ohaaki geothermal field.

### **2.1 Multiwell Data of Anisotropic Reservoir**

For an anisotropic formation, the directional permeabilities are the parameters of interest as they play an important role on planning reservoir development such as fluid

injection. In the 1960s, there appeared a series of papers on the well test analysis for anisotropic aquifers in groundwater hydrology. The type-curve matching method for multiple observation wells recommended by *Papadopoulos (1965)* and *Walton (1970)* averages the pressure-scale match points to avoid different pressure-scale matches that may be found for various observation wells. Based on the observation that the pressure scale in pounds per square inch is the same for all the sets of field data, as indicated in the solution of anisotropic formation, *Ramey (1975)* outlined another approach to simply align the pressure scale and adjust the time scale until all sets of field data match. However, due to noise in real data, the pressure scale matched from the pressure data of one well may not be the same as that matched from other wells. Nonunique results may arise when the matching starts with the pressure data of a different well. Furthermore, the method can only make use of pressure data from three wells. Choosing a typical set of three wells from multiple wells is not easy.

### 2.1.1 Mathematical Considerations

The theory of fluid flow through an anisotropic medium has been well established. Consider a well producing at a constant rate in an infinite anisotropic medium with three permeability components as  $k_{xx}$ ,  $k_{xy}$ ,  $k_{yy}$ . The thickness  $h$  and porosity  $\phi$  of the medium are constant.

*Collins (1961)* chose the permeability axes as the coordinates system axes. A solution to the governing equation

$$k_{XX} \frac{\partial^2 p}{\partial x^2} + k_{YY} \frac{\partial^2 p}{\partial y^2} = \phi \mu c_t \frac{\partial p}{\partial t} \quad (2.1)$$

for infinite-acting radial flow was obtained as

$$\sqrt{k_{XX} k_{YY}} \frac{h(p_i - p_{x,y,t})}{141.2qB\mu} = -\frac{1}{2} Ei \left[ -\frac{\phi \mu c_t (k_{XX} y^2 + k_{YY} x^2)}{0.001056 k_{XX} k_{YY} t} \right] \quad (2.2)$$

where  $k_{XX}$  and  $k_{YY}$  are principal permeabilities. From the general governing equation

$$k_{xx} \frac{\partial^2 p}{\partial x^2} + 2k_{xy} \frac{\partial^2 p}{\partial x \partial y} + k_{yy} \frac{\partial^2 p}{\partial y^2} = \phi \mu c_t \frac{\partial p}{\partial t} \quad (2.3)$$

*Papadopoulos (1965)* derived another solution using Fourier transformation and Laplace transformation

$$\sqrt{k_{xx}k_{yy} - k_{xy}^2} \frac{h (p_i - p_{x,y,t})}{141.2qB\mu} = -\frac{Ei}{2} \left[ \frac{-\phi\mu c}{0.001056t} \left( \frac{k_{xx}y^2 + k_{yy}x^2 - 2k_{xy}xy}{k_{xx}k_{yy} - k_{xy}^2} \right) \right] \quad (2.4)$$

$$k_{XX} = \frac{1}{2} \left[ (k_{xx} + k_{yy}) + \sqrt{(k_{xx} - k_{yy})^2 + 4k_{xy}^2} \right] \quad (2.5)$$

$$k_{YY} = \frac{1}{2} \left[ (k_{xx} + k_{yy}) - \sqrt{(k_{xx} - k_{yy})^2 + 4k_{xy}^2} \right] \quad (2.6)$$

$$\theta = \arctan \left( \frac{k_{XX} - k_{xx}}{k_{xy}} \right) \quad (2.7)$$

Though these two solutions are mathematically equivalent as shown in Appendix A, the solution presented by *Papadopoulos* (1965) is more convenient for the analysis of observed pressure data since the permeabilities or permeability axes are unknowns in well test analysis.

When more pressure data than needed are present, using all the sets of data can be achieved by nonlinear least square regression. Estimating the directional permeabilities is transformed as to minimize the following objective function

$$j(\alpha, \beta, \gamma) = \sum_{i=1}^n (\Delta p_i - p'_i)^2 \quad (2.8)$$

$$p'_i = \frac{1}{2} \left\{ -\frac{141.2qB\mu}{h\alpha} Ei \left[ -\frac{\phi\mu c_t}{0.001056\Delta t_i \alpha^2} \left( \beta y_i^2 + \gamma x_i^2 - 2x_i y_i \sqrt{\beta\gamma - \alpha^2} \right) \right] \right\} \quad (2.9)$$

where  $a = \sqrt{k_{xx}k_{yy} - k_{xy}^2}$ ,  $\beta = k_{xx}$ ,  $\gamma = k_{yy}$  and  $\Delta p_i, \Delta t_i$  are the measured pressure and time;  $x_i, y_i$  are the positions of wells from which  $\Delta p_i, \Delta t_i$  are measured. There exist many methods to solve nonlinear least square problems. Among them, the *Marquardt* (1963) method works well for anisotropic formations if a restriction is posed that  $\beta\gamma - a = 0.001$  when  $\beta\gamma - \alpha < 0$ .

## 2.1.2 Field Example

The field example presented by *Ramey* (1975) was interpreted in this section using the nonlinear square approach.

In order to determine whether directional permeability would influence the production in a watered out formation, an injection well test was run. Fig. 2.1 represents

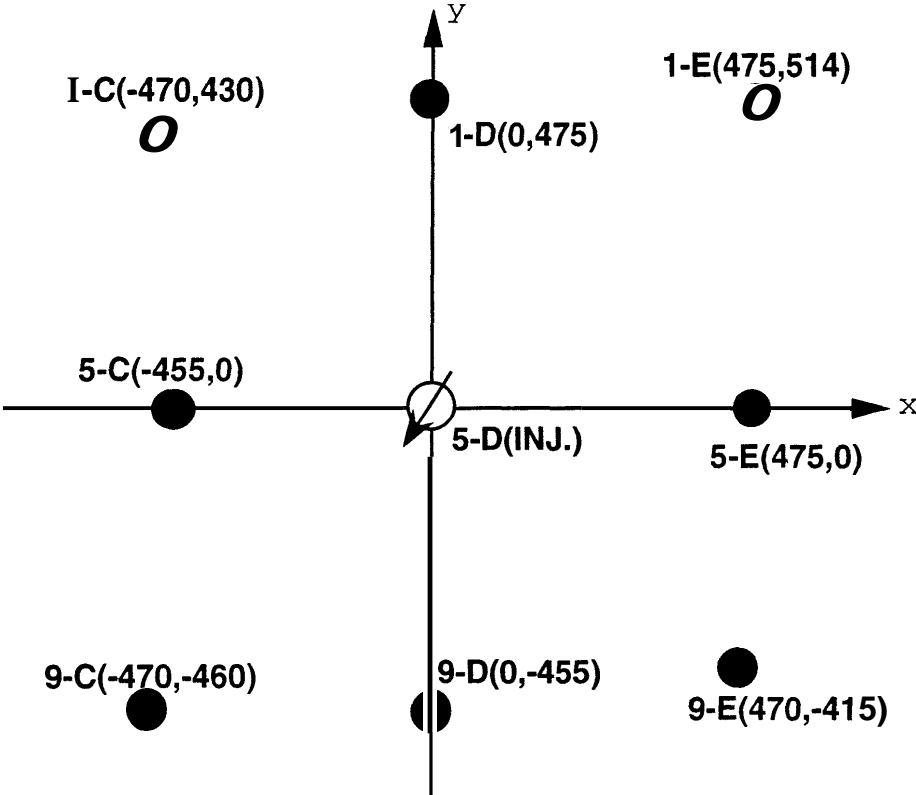


Figure 2.1: Field well pattern in an anisotropic reservoir



Table 2.1: Water-injection interference pressure rise above the initial pressure

Well 1-D	Well 1-E		Well 5-C				Well 9-C		Well 9-D		Well 9-E		
	$\Delta p$	$At$	$\Delta p$	$At$	$Ap$	$At$	$Ap$	$At$	$\Delta p$	$At$	$\Delta p$		
95	6.7	27.5	3	47	10	21	4	24	4	23.5	8.2	21	3
	7.2	47	5	71	17.2	47	11	47	8	28.5	9.3	47	3
	15	72	11	94	24	72	16.3	72	13	51	17	71	3
	20	95	13	113	25.1	94	21.2	94	17.7	75	23.2	94	10
	25	115	16	124	26	115	22	115	18	95	27.2	115	12.5
		125	16			122	25	126	18	120	27	125	13

the well pattern where well 5-D served as a single injection well and the surrounding wells (5-E, 1-E, 1-D, 1-C, 5-C, 9-C, 9-D and 9-E) were observation wells. The rising parts of the pressure(*psi*) and time(*hours*) are presented in Table 2.1. Table 2.1 represents a set of interference data from seven wells, which is more than required to obtain a unique result since only three sets of the data are needed to determine  $k_{,,}$ ,  $k_{xy}$ ,  $k_{yy}$  and  $\phi c$ . Using Wells 5-E,1-E and 1-D, Ramey (1975) obtained by manual type curve matching:

$$\begin{aligned}
 k_{xx} &= 15.2 \text{ md} \\
 k_{yy} &= 19.4 \text{ md} \\
 k_{xy} &= 3.12 \text{ md},
 \end{aligned}$$

while for the same set of data, a nonlinear least square method gives the solution

$$\begin{aligned}
 k_{xx} &= 15.59 \text{ md} \\
 k_{,,} &= 19.59 \text{ md} \\
 k_{xy} &= 2.07 \text{ md}
 \end{aligned}$$

as shown in Fig. 2.2. The noticeable difference is the  $k_{xy}$  value. The initial guesses used in the nonlinear least square algorithm are:

$$\begin{aligned}
 k_{,,} &= 5 \\
 k_{yy} &= 4 \\
 k_{xy} &= 1
 \end{aligned}$$

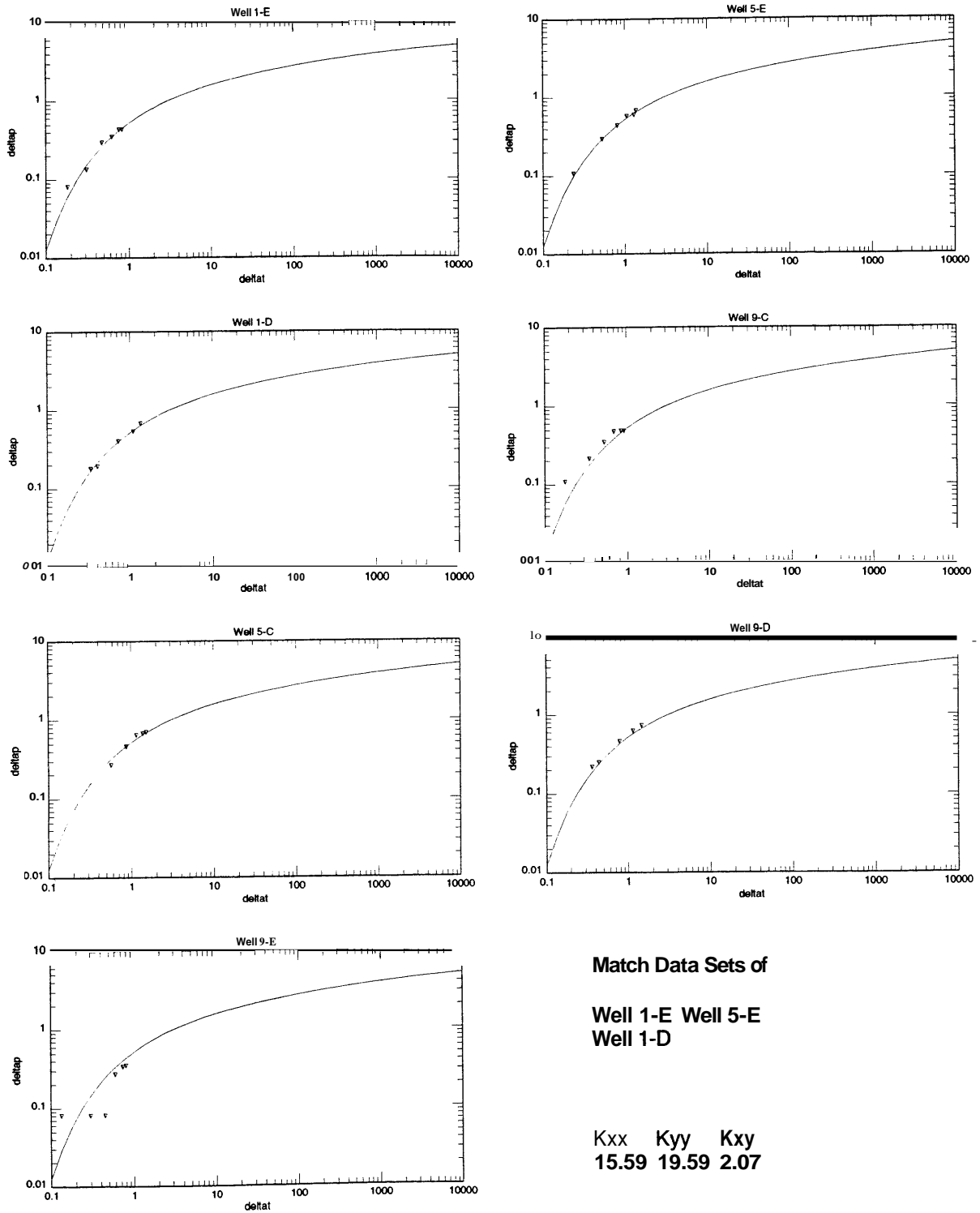


Figure 2.2: Using three sets of pressure data in an anisotropic reservoir example

This set of initial guesses was used also in all the other matches described below. When pressure data from all the seven wells are used, the matched curves are shown in Fig. 2.3 and the permeability solution is

$$\begin{aligned}k_x &= 13.96 \text{ md} \\k_{yy} &= 18.60 \text{ md} \\k_{xy} &= 3.56 \text{ md}\end{aligned}$$

If another set of three wells, for example, Well 9-D, 5-C, 9-E are chosen, then the  $k_{xx}, k_{xy}, k_x$  solution to the nonlinear square problem is shown in Fig. 2.4

$$\begin{aligned}k_x &= 11.88 \text{ md} \\k_{yy} &= 16.30 \text{ md} \\k_{xy} &= 4.50 \text{ md}\end{aligned}$$

The two results generated from the two sets of wells are modestly different. There is no definite way to tell which one is the correct answer. If the residual is used as an indicator of preference, Fig. 2.3 shows a better match to the data set of each well. The small difference among the matching results from different well combinations most likely means there is no strong heterogeneity present in this example. The homogeneous anisotropic model is a good approximation to the reservoir. During the matching process, if the data from some wells are believed to be affected by noise, the data set that has the worst behavior can be identified by matching all the well data except for one well each time.

Through the investigation of this field example, it can be seen that the nonlinear least square method is useful for estimating the anisotropic permeabilities from multiple well interference data. Though the application is shown only for homogeneous anisotropic formations here, it is not difficult to extend the nonlinear least square method to other reservoir configurations, for instance, a reservoir with a circular discontinuous region.

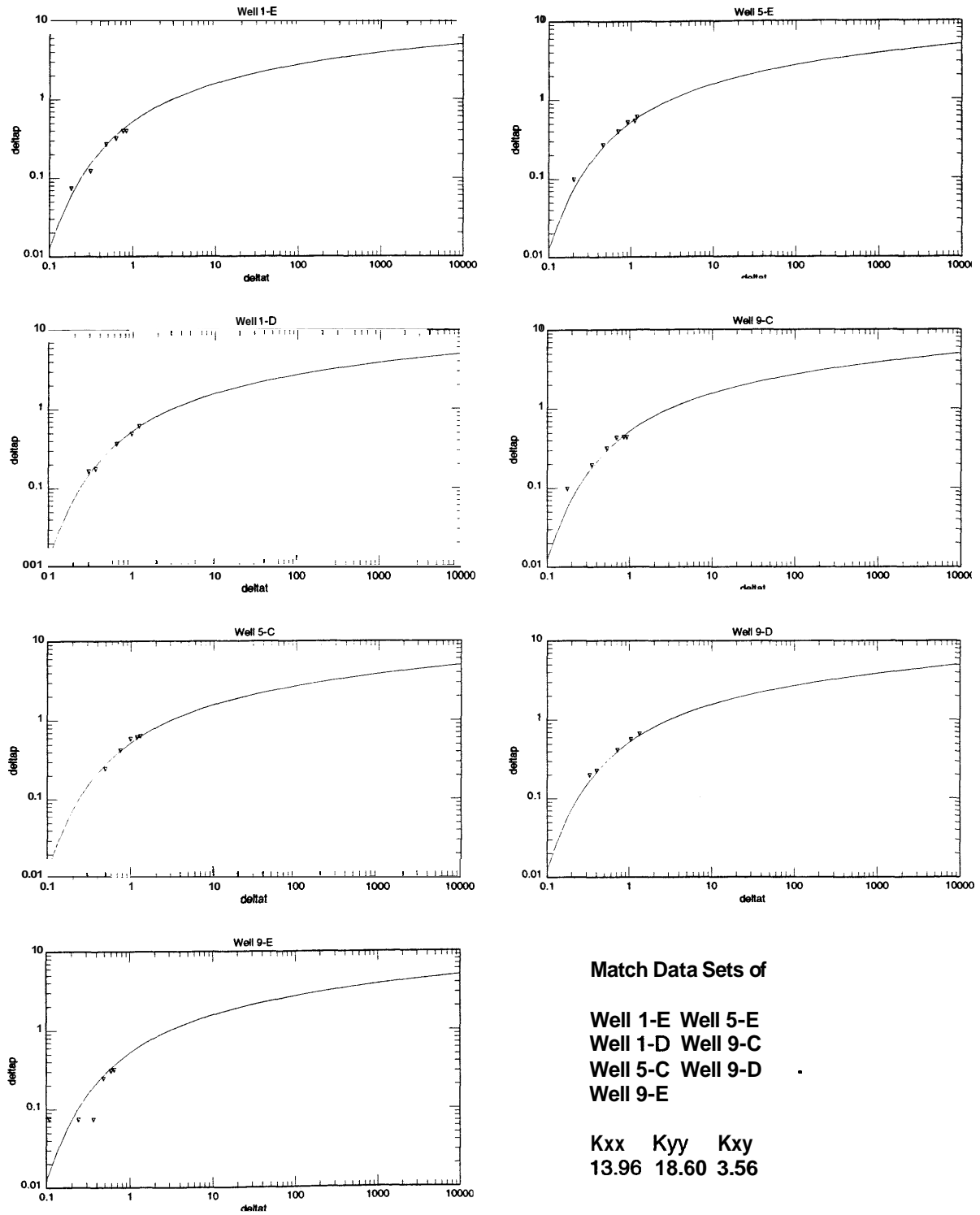


Figure 2.3: Using nine sets of pressure data in an anisotropic reservoir example

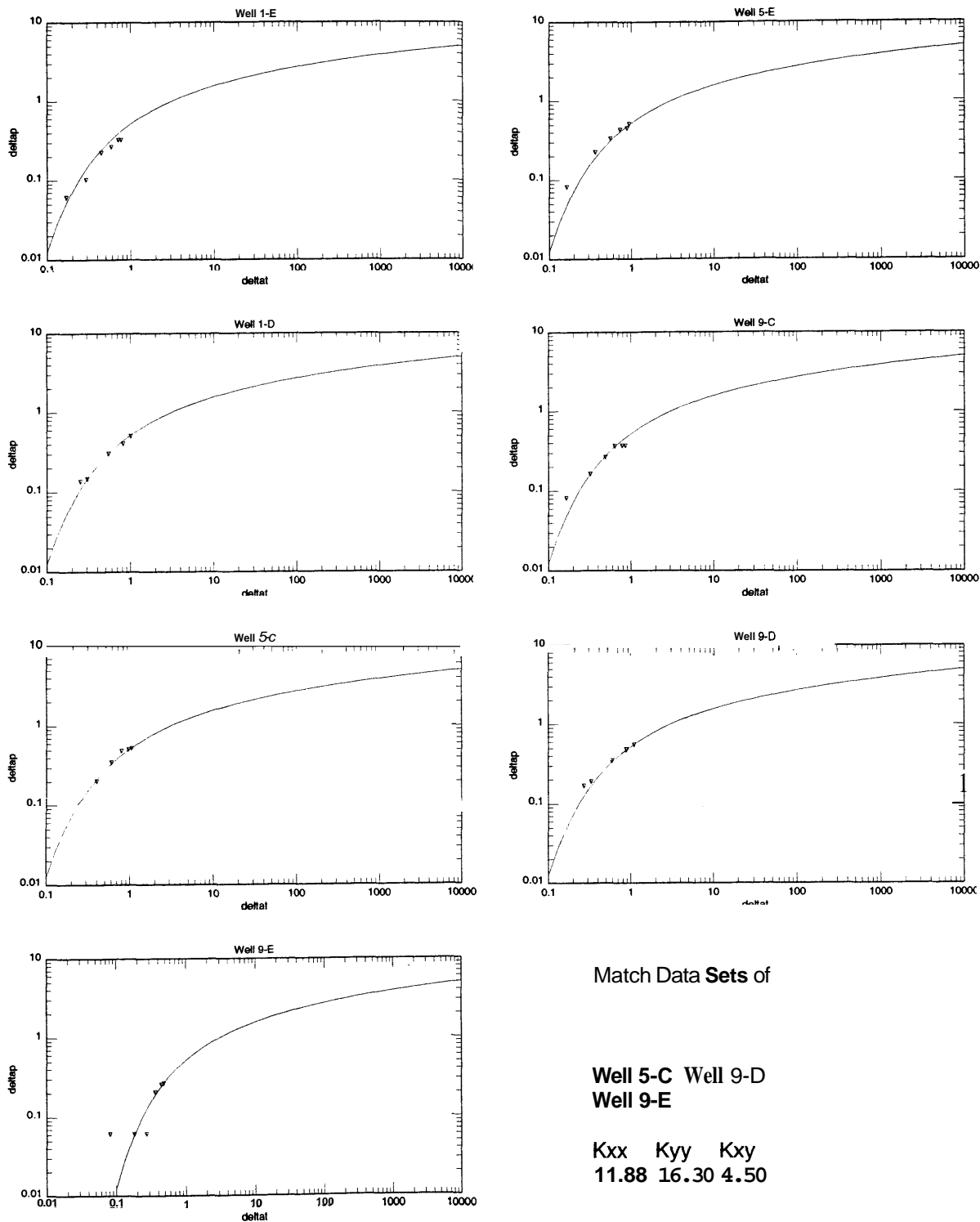


Figure 2.4: Using another three sets of pressure data in an anisotropic reservoir example

## 2.2 Heterogeneity of the Circular Discontinuity Type

Interference testing in geothermal fields is usually designed to estimate the mobility-thickness product and the reservoir thickness-porosity-compressibility product (also referred to as transmissivity and storativity, respectively), and to locate hydrological heterogeneities, for instance, no-flow boundaries or different property subregions. Heterogeneities in the hydrology of geothermal reservoirs can be caused by mineral deposition, by changes of heat in the system, by crustal movements, by changes in fluid compositions or by exploitation. The main disadvantage of interference testing is that the magnitude of the pressure changes decreases as the observation well is located farther away from the source well. When the pressure changes are small, especially at the early-time, noises such as earth tide and barometric pressure fluctuations may play a significant role and might lead to uncertainties in the estimation of reservoir parameters.

If the history of the noise is known, the effect of noise may be reduced by correcting the pressure data. An attractive and more practical alternative might be to use multiwell data to increase the tolerance of the procedure to noise in pressure data and decrease the uncertainty in parameter estimation.

The exponential integral solution introduced by *Theis (1935)* based on heat-transfer analogy can be used for a reservoir with homogeneous properties. However, if one treats the formation more elaborately, one may consider different property subregions within the reservoir. Such subregions may take various geometric shapes as in the case resulting from steam zones in geothermal reservoirs or shale lenses in oil reservoirs. In this section the subregion will be represented as a circular discontinuity in order to make mathematical consideration easier.

Many studies have appeared in the literature about composite reservoir systems with circular discontinuities since the related work of heat conduction in composite materials by *Jaeger (1941 and 1944)*. *Sageev (1983)*, also *Grader and Home (1988)* investigated discontinuities that either have constant pressure (equivalent to infinite

permeability of the model here) or have no-flow boundaries (equivalent to zero permeability of the model here). A more recent study by *Rosa* (1991) developed theoretical solutions without wellbore storage effect to both internal and external circular discontinuities though the numerical calculation of the pressure response was not robust.

This section focuses on the application of the composite model with and without wellbore storage to the interpretations of multiwell pressure data through nonlinear regression. The motivation was to examine the feasibility of estimating geometric parameters as a function of the number of different locations at which the pressure transients are maintained. This study formed a preliminary part of a broader study to investigate the matching of multiple data streams of different types (for example, pressure transient and tracer data).

### 2.2.1 Discontinuity Without Wellbore Storage

The pressure distribution in a reservoir with an external or internal discontinuity was obtained by *Rosa* (1991). With a simpler approach of the two cases being handled together and using the notation in Fig. 2.5, the solution function can be written for first discontinuous region ( $r < a$ ) as

$$\bar{v}_1 = \begin{cases} \frac{1}{2\pi\eta_1} \left[ K_0(z_1R) + \sum_{n=0}^{\infty} \varepsilon_n \frac{\Omega_n}{\Psi_n} I_n(z_1r') I_n(z_1r) \cos(\theta - \theta') \right] & \text{if } a \geq r' \\ \frac{\lambda_2}{2\pi a \eta_2} \sum_{n=0}^{\infty} \varepsilon_n \frac{K_n(z_2r') I_n(z_1r)}{\Psi_n} \cos(\theta - \theta') & \text{if } a < r' \end{cases} \quad (2.10)$$

and for second region ( $r \geq a$ ) as

$$\bar{v}_2 = \begin{cases} \frac{1}{2\pi\eta_1} \left[ K_0(z_2R) + \sum_{n=0}^{\infty} \varepsilon_n \frac{\Phi_n}{\Psi_n} K_n(z_2r') IC_n(z_2r) \cos(\theta - \theta') \right] & \text{if } a \leq r' \\ \frac{\lambda_1}{2\pi a \eta_1} \sum_{n=0}^{\infty} \varepsilon_n \frac{I_n(z_1r') K_n(z_2r)}{\Psi_n} \cos(\theta - \theta') & \text{if } a > r' \end{cases} \quad (2.11)$$

where

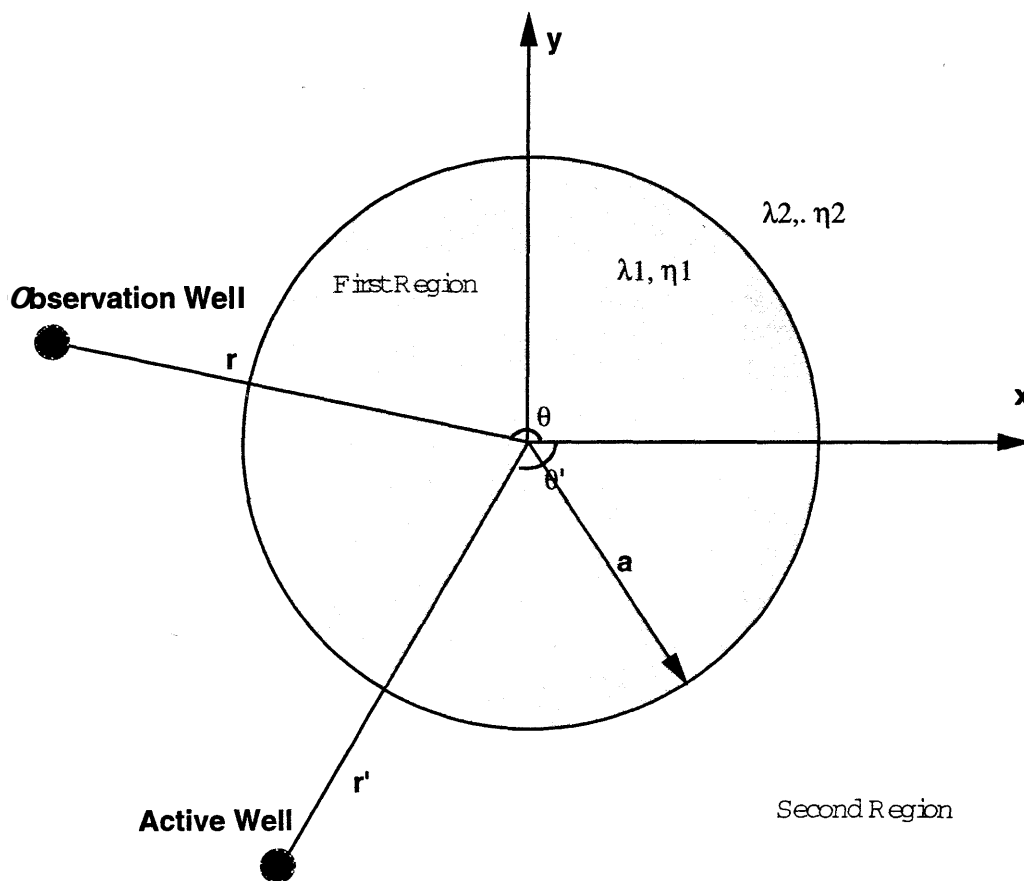


Figure 2.5: Infinite reservoir with a circular discontinuity



$$\begin{aligned}
\varepsilon_0 &= 1, \\
\varepsilon_n &= 2 \quad (n > 0), \\
\lambda_1 &= \frac{k_1}{\mu_1}, \\
\lambda_2 &= \frac{k_2}{\mu_2}, \\
\eta_1 &= \frac{k_1}{\phi \mu_1 c_{t1}}, \\
\eta_2 &= \frac{k_2}{\phi \mu_2 c_{t2}}, \\
z_1 &= \sqrt{\frac{z}{\eta_1}}, \\
z_2 &= \sqrt{\frac{z}{\eta_2}}, \\
R^2 &= r^2 + r'^2 - 2rr' \cos(\theta - \theta'), \\
\Omega_n &= \lambda_2 z_2 K_n(z_1 a) K'_n(z_2 a) - \lambda_1 z_1 K'_n(z_1 a) K_n(z_2 a), \\
\Phi_n &= \lambda_2 z_2 I'_n(z_2 a) I_n(z_1 a) - \lambda_1 z_1 I_n(z_2 a) I'_n(z_1 a), \\
\Psi_n &= \lambda_1 z_1 K_n(z_2 a) I'_n(z_1 a) - \lambda_2 z_2 K'_n(z_2 a) I_n(z_1 a).
\end{aligned}$$

The pressure drop for a constant surface flow rate  $q$  (without wellbore storage) in Laplace space is

$$\overline{\Delta p}(r, \theta, z) = \frac{qB}{\phi h c_t} \frac{1}{z} \overline{v}(r, \theta, z). \quad (2.12)$$

A computer program to evaluate the pressure drop was developed using the Stehfest's algorithm (Stehfest, 1970) to calculate the Laplace transformed expression. Since  $K_n$  and  $I_n$  appear together as a product, and since the product becomes of type  $(0 \cdot \infty)$  when the argument or the order goes to infinity, it is not practical to evaluate  $K_n$  and  $I_n$  directly. In order to avoid the overflow and underflow of  $K_n$  and  $I_n$ ,  $e^{-x} I_n(x)$  and  $e^x K_n(x)$  are calculated in the program when  $n$  is not too large or  $x$  is not so small. The convergence of the series was checked by the asymptotic expansions for large orders of Bessel functions. It turns out that the summation of 50 terms of the series is sufficient in practical calculation.

Figs. 2.6 to 2.12 show how the pressure drop responds as the parameters vary. For some parameters, the pressure drop changes a great deal, which means it is easier to estimate these parameters from pressure data. On the other hand, if the pressure drop does not change much as the parameters vary, as in the case of the pressure response of an observation well located in second region versus the compressibility of the first region, it means that pressure response is not sensitive to this parameter

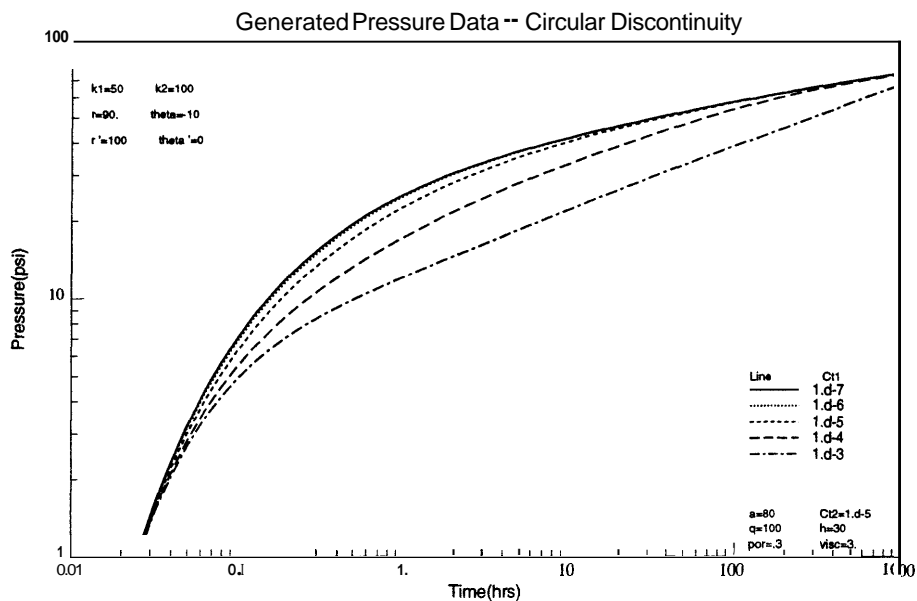


Figure 2.6: Pressure response versus compressibility of first region

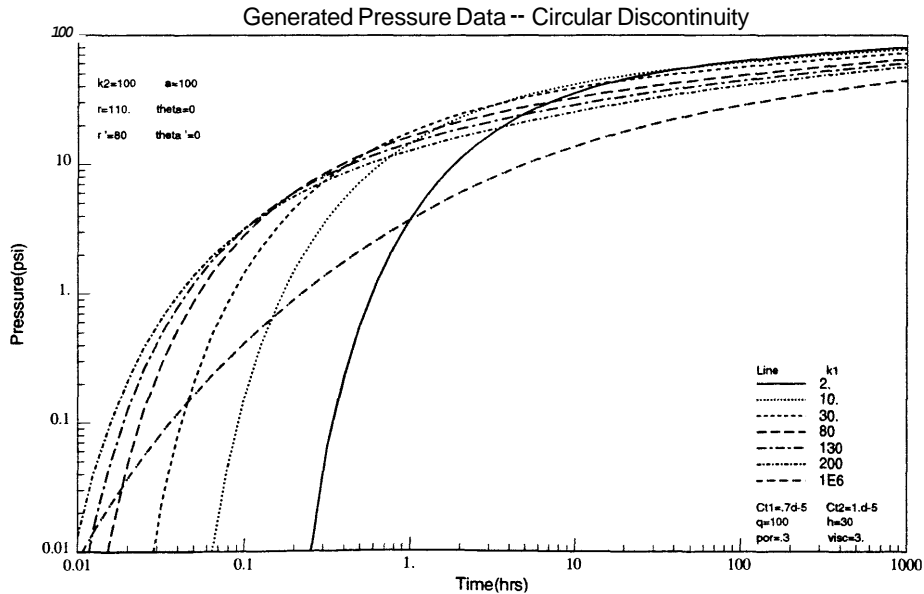


Figure 2.7: Pressure response versus permeability of first region

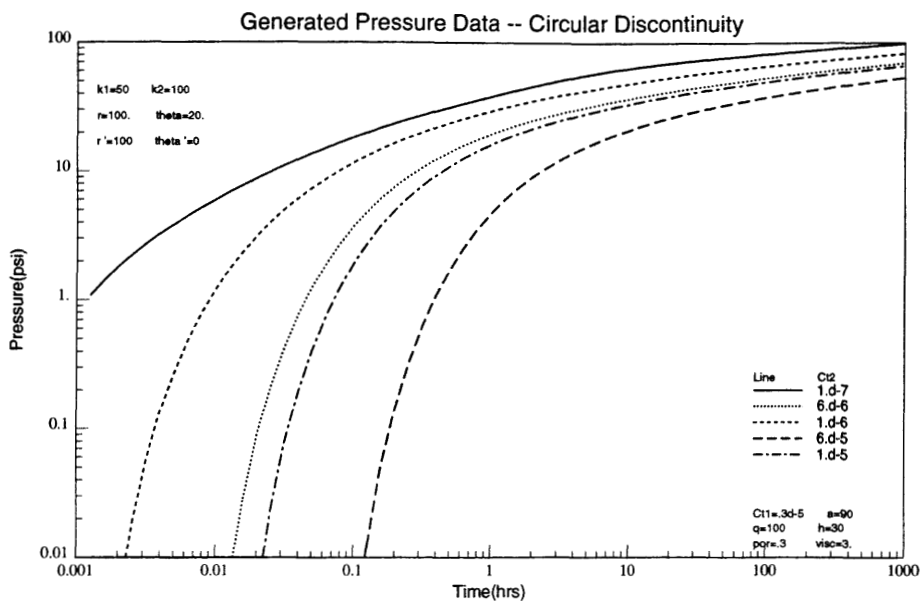


Figure 2.8: Pressure response versus compressibility of second region

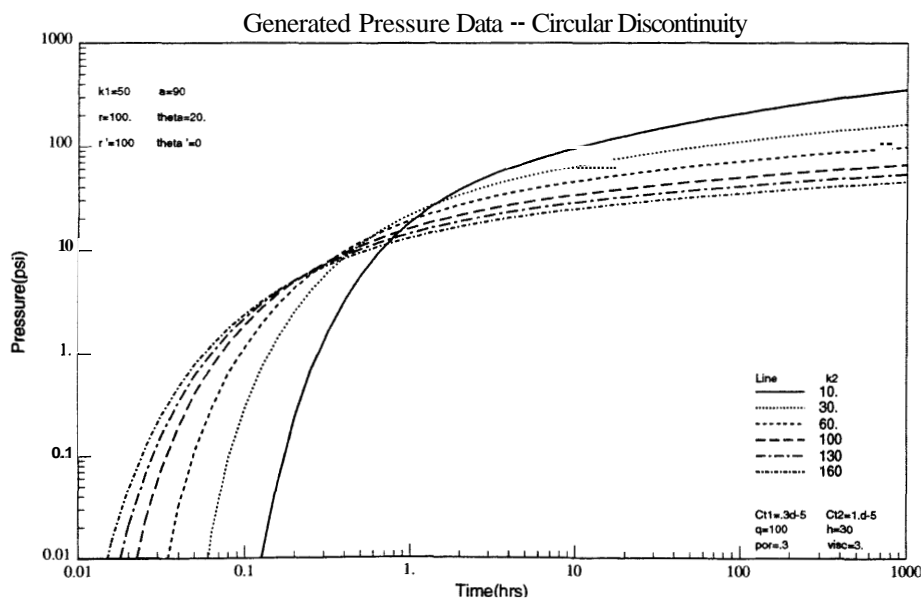


Figure 2.9: Pressure response versus permeability of second region

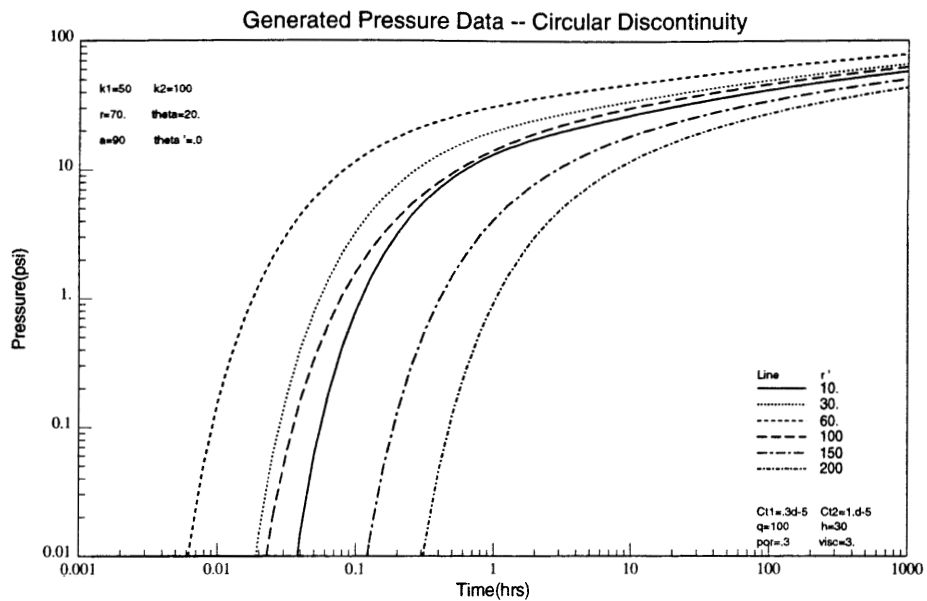


Figure 2.10: Pressure response versus position of active well (distance)

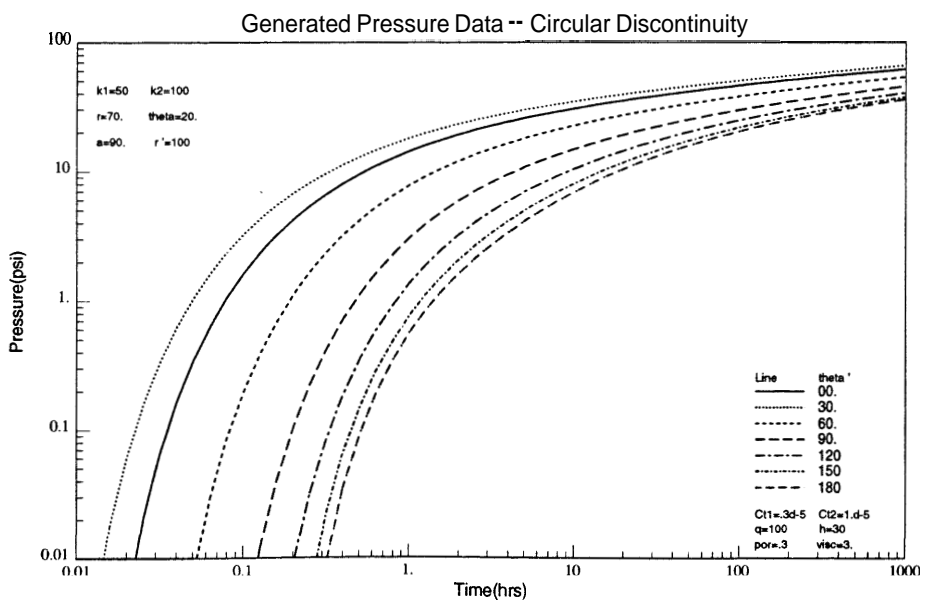


Figure 2.11: Pressure response versus position of active well (angle)

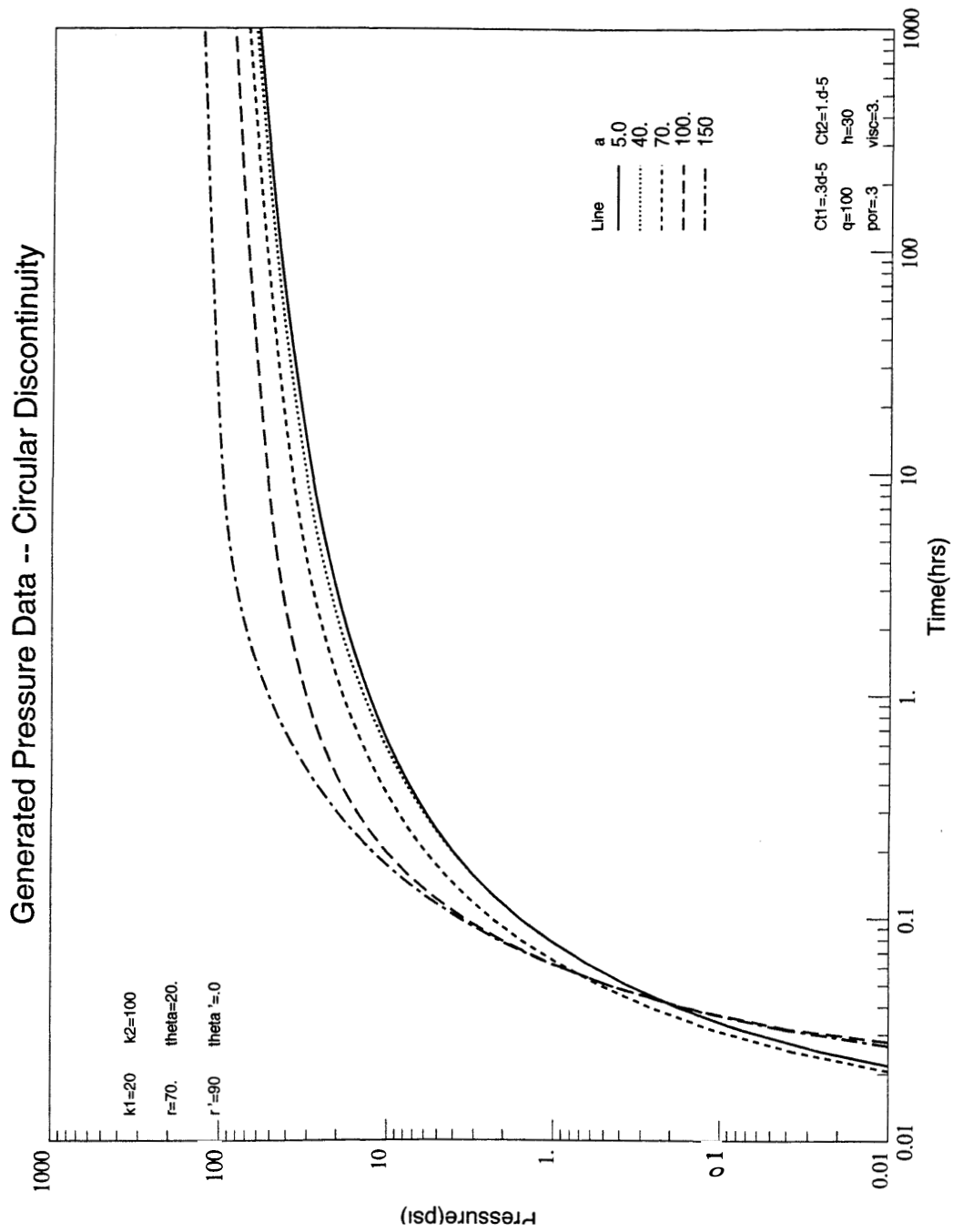


Figure 2.12: Pressure response versus radius of discontinuity

and the parameter would not be well determined in a well test. This is likely to be a problem in the interpretation of pressure data when the pressure data measured include noise larger than five percent.

## 2.2.2 Discontinuity with Wellbore Storage

When the wellbore storage effect at the active well is considered, the sandface flow rate  $q_{sf}$  is no longer constant even though the surface flow rate  $q$  is constant. These two flow rates are related by wellbore storage coefficient  $C$ ,

$$q_{sf}(t) = q + C \frac{dp(r_w, t)}{dt} = q - C \frac{d\Delta p(r_w, t)}{dt} \quad (2.13)$$

Hence

$$\bar{q}_{sf}(z) = \frac{q}{z} - Cz \bar{\Delta p}(r_w, z) \quad (2.14)$$

in Laplace space. The pressure drop caused by  $q_{sf}(t)$  is obtained by superposition (*Gringarten and Ramey, 1973*)

$$\Delta p(t) = \frac{1}{\phi C_t h} \int_0^t q_{sf}(t - \tau) \nu(r, r', \theta, \theta', \tau) d\tau. \quad (2.15)$$

Taking the Laplace transformation, the above equation becomes

$$\bar{\Delta p}(r, r', \theta, \theta', z) = \frac{1}{\phi C_t h} \bar{q}_{sf}(z) \bar{\nu}(r, r', \theta, \theta', z) \quad (2.16)$$

$$\bar{q}_{sf}(z) = \frac{q}{z} \frac{1}{1 + \frac{Cz}{\phi C_t h} \bar{\nu}(r, r', \theta, \theta')|_{r=r'+r_w}} \quad (2.17)$$

$$\bar{\Delta p}(r, r', \theta, \theta', z) = \frac{q}{\phi C_t h z} \frac{\bar{\nu}(r, r', \theta, \theta', z)}{1 + \frac{Cz}{\phi C_t h} \bar{\nu}(r, r', \theta, \theta')|_{r=r'+r_w}} \quad (2.18)$$

where  $\nu(r, r', \theta, \theta', t)$  is the Green's function for the composite model,

$$\bar{\nu} = \begin{cases} \bar{\nu}_1 & r < a \\ \bar{\nu}_2 & r \geq a \end{cases} \quad (2.19)$$

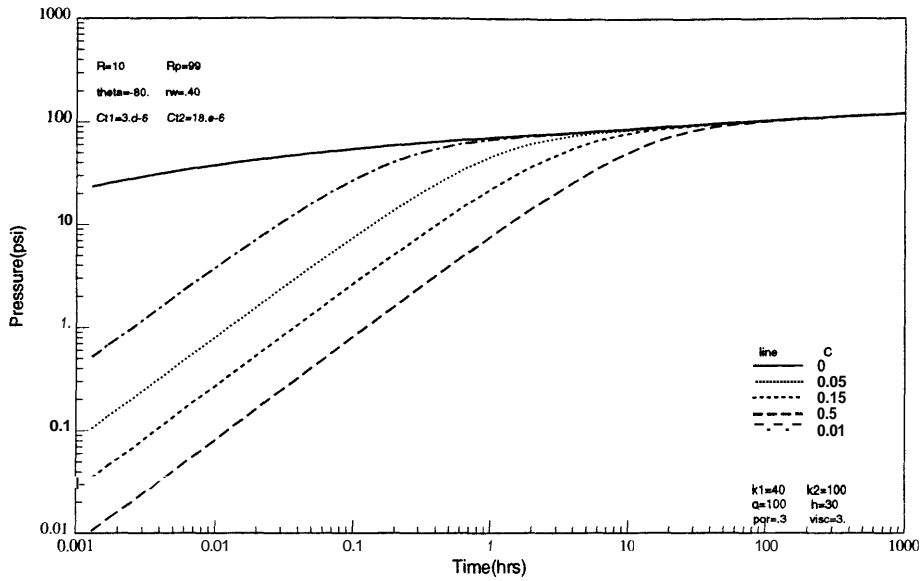


Figure 2.13: Comparison of pressure response in active well with or without wellbore storage

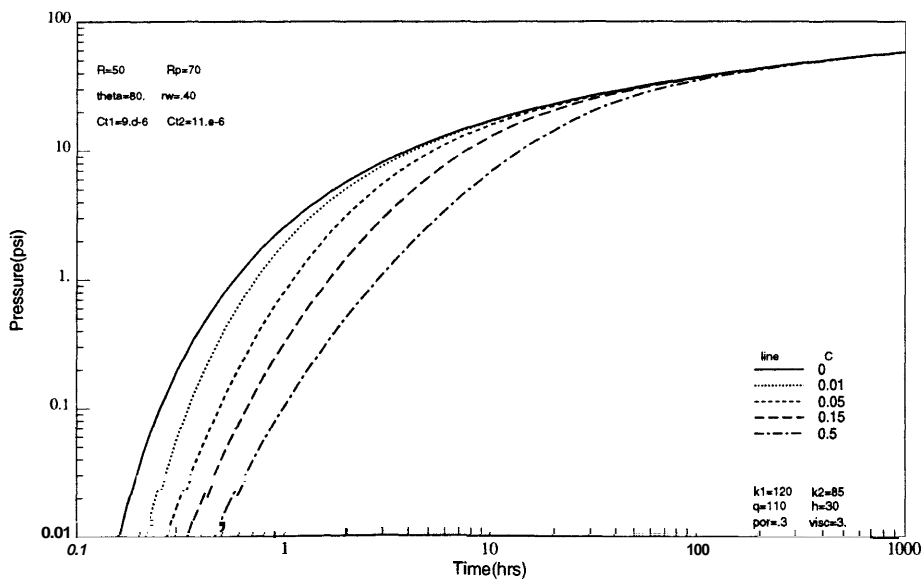


Figure 2.14: Comparison of pressure response in observation well with or without wellbore storage

and  $\bar{v}_1, \bar{v}_2$  are shown in Eq. 2.10 and Eq. 2.11. Fig. 2.13 shows the pressure response as a function of time in an active well with the wellbore storage coefficient  $C$  being increased from zero to  $0.5 \text{ bbl/psi}$ . Wellbore storage affects the pressure response at early time. These differences decrease with increasing time but may still be about  $5 \text{ psi}$  at  $10 \text{ hours}$  for  $C = 0.15 \text{ bbl/psi}$ .

Fig. 2.14 shows the pressure change at an observation well versus time for the cases of  $C = 0$  to  $0.5 \text{ bbl/psi}$ . The observation well is located  $100 \text{ feet}$  away from the active well. Neglecting the effect of wellbore storage at the active well will cause an underestimation of the permeability of the reservoir.

### 2.2.3 Transformation of Coordinate System

All the equations discussed above are based on a coordinate system that has the center of the circular discontinuity as the origin. However, when pressure data are analyzed, the position of the discontinuity is unknown; it is among the parameters to be obtained as part of the analysis. When field data are collected, the locations of the observation wells are therefore given relatively to the position of the active well. In other words, the locations of observation wells are represented in a Cartesian coordinate system with the active well as the origin. In order to calculate the pressure response in a reservoir of circular discontinuity, well locations need to be transferred to the coordinate system used in the solution expressions.

The relationship between two coordinate systems is straightforward as shown in Fig. 2.15, where  $(x_1, y_1)$  represents the field coordinate system and  $(x_2, y_2)$  represents the coordinate system of the circular discontinuity. Assuming that the active well is  $r'$  away from the center of discontinuity and is in  $\theta'$  direction, its Cartesian coordinates in  $(x_2, y_2)$  are

$$\begin{cases} x_{2ActWell} = r' \cdot \cos \theta' \\ y_{2ActWell} = r' \cdot \sin \theta'. \end{cases} \quad (2.20)$$

If the coordinates of an observation well given in the real data system is  $(x_1, y_1)$ , its Cartesian coordinates in system of circular discontinuity will be



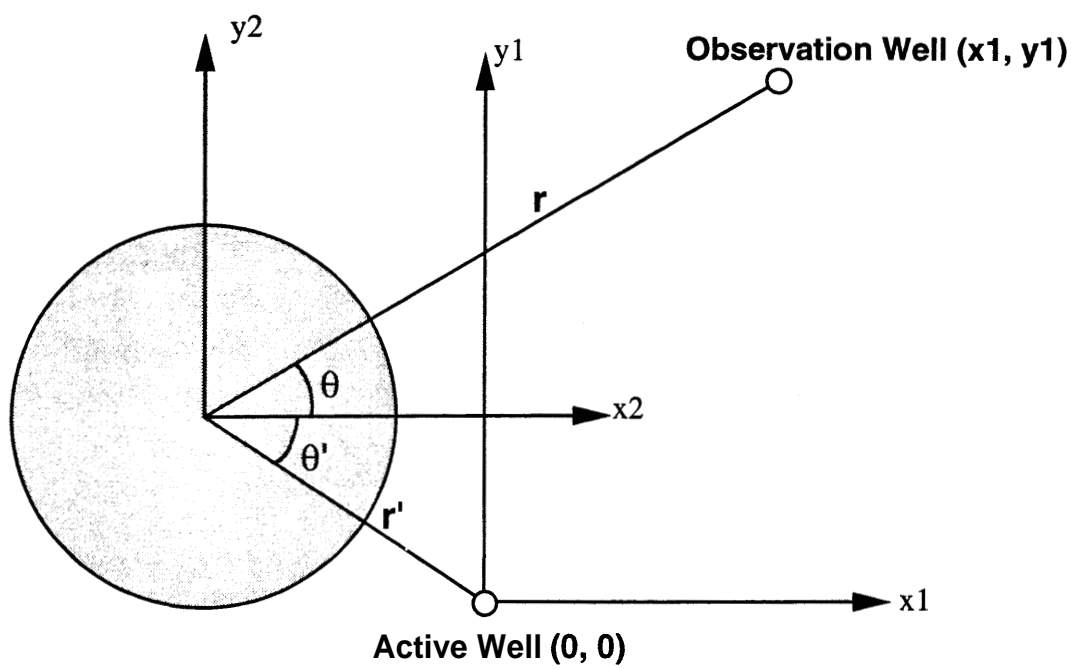


Figure 2.15: Transformation of two coordinate systems

Table 2.2: Configuration of the formation

$k_1(md)$	50	$k_2(md)$	100	$c_{t1}(psi^{-1})$	8.d-6	$c_{t2}(psi^{-1})$	11.d-6
$q(STB/D)$	110	$h(ft)$	60	$\mu(cp)$	3.	$\phi$	.3
$r'(ft)$	90	$\theta'(^\circ)$	.0	$a(ft)$	50		

$$\begin{cases} x_2 = x_{2ActWell} + x_1 = x_1 + r' \cdot \cos \theta' \\ y_2 = y_{2ActWell} + y_1 = x_1 + r' \cdot \sin \theta'. \end{cases} \quad (2.21)$$

Thus, from the coordinates of the observation well  $(x_1, y_1)$ , its polar coordinates  $(r, \theta)$  used in the solution expression can be obtained from the following equations

$$\begin{cases} r^2 = (r' \cdot \cos \theta' + x_1)^2 + (r' \cdot \sin \theta' + y_1)^2 \\ \theta = \arctan \left( \frac{y_1 + r' \cdot \sin \theta'}{x_1 + r' \cdot \cos \theta'} \right). \end{cases} \quad (2.22)$$

## 2.2.4 Objective Function

The estimation of reservoir parameters from multiwell observation responses can be posed as to a nonlinear regression problem (*Barua et al.*, 1988). In this study, a weighted least squares method is employed. The objective function is the weighted sum of squares of differences between the observed responses and the reservoir estimated model responses:

$$E = \sum_{i=1}^n \omega_i [\Delta p_i - \Delta p(\vec{\alpha}, At_i, x_i, y_i)]^2 \quad (2.23)$$

where  $(At_i, \Delta p_i)$  are a set of  $n$  time-pressure data from observation wells located at  $(x_i, y_i)$ ,  $\vec{\alpha}$  is a set of unknown reservoir parameters such as  $k_1$ ,  $k_2$ ,  $c_{t1}$ ,  $c_{t2}$ ,  $r'$ ,  $\theta'$ ,  $a$  or  $C$ , and  $\omega_i$  are the weighting set which emphasize the early time pressure data or small magnitude pressure data. In this formulation,  $\omega_i = \frac{\sum_{j=1}^n \Delta p_j}{\Delta p_i}$ .

Fig. 2.17, Fig. 2.18, Fig. 2.19 and Fig. 2.20 show the shapes of the objective function  $E$  as a function of  $r'$  and  $\theta'$ , with the the reservoir configuration shown in Table 2.2. It can be seen that as more and more observation wells are used, the shape of the objective function includes more character. So the minimum is easier to obtain and local minimum can be avoided. Actually, if the data of two observation

Distributions of Active Well and Observation Wells

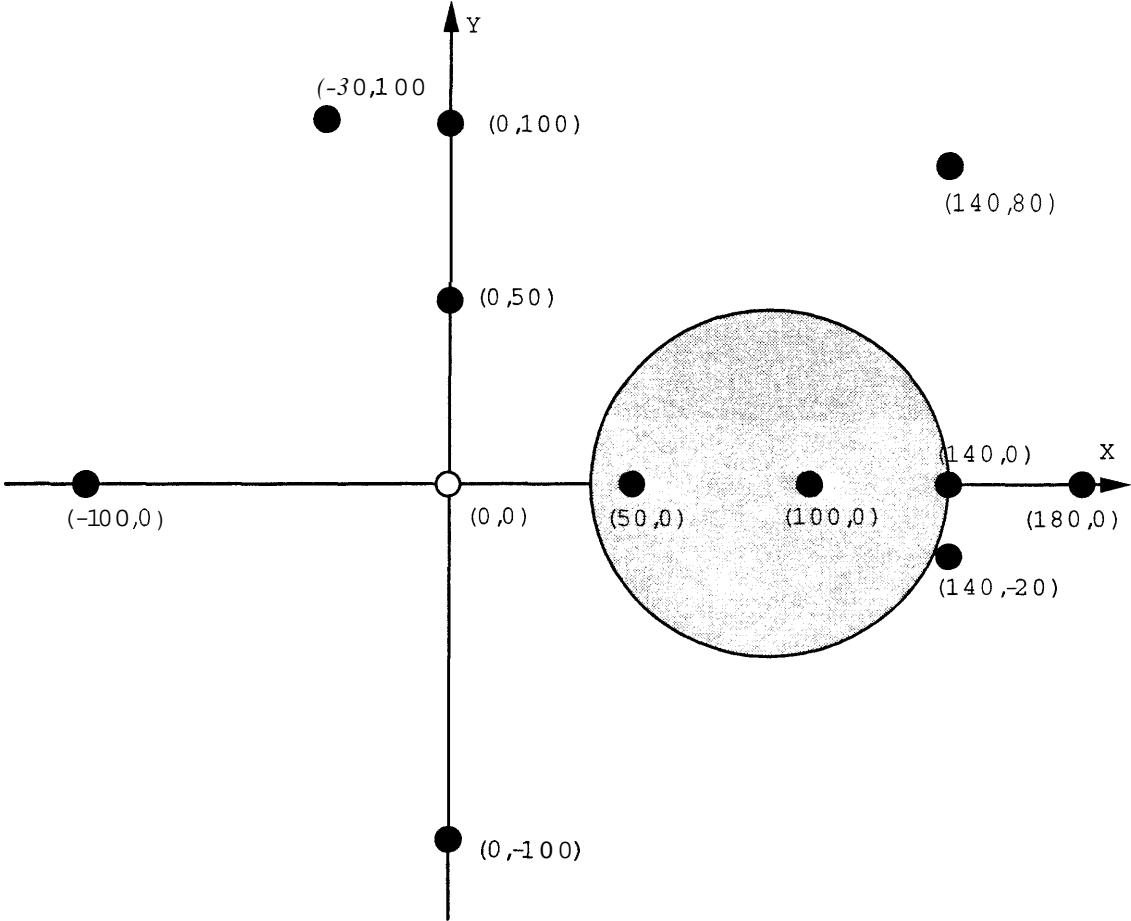


Figure 2.16: Well pattern for an infinite reservoir with a circular discontinuity

Surface Shape of the Objective Function

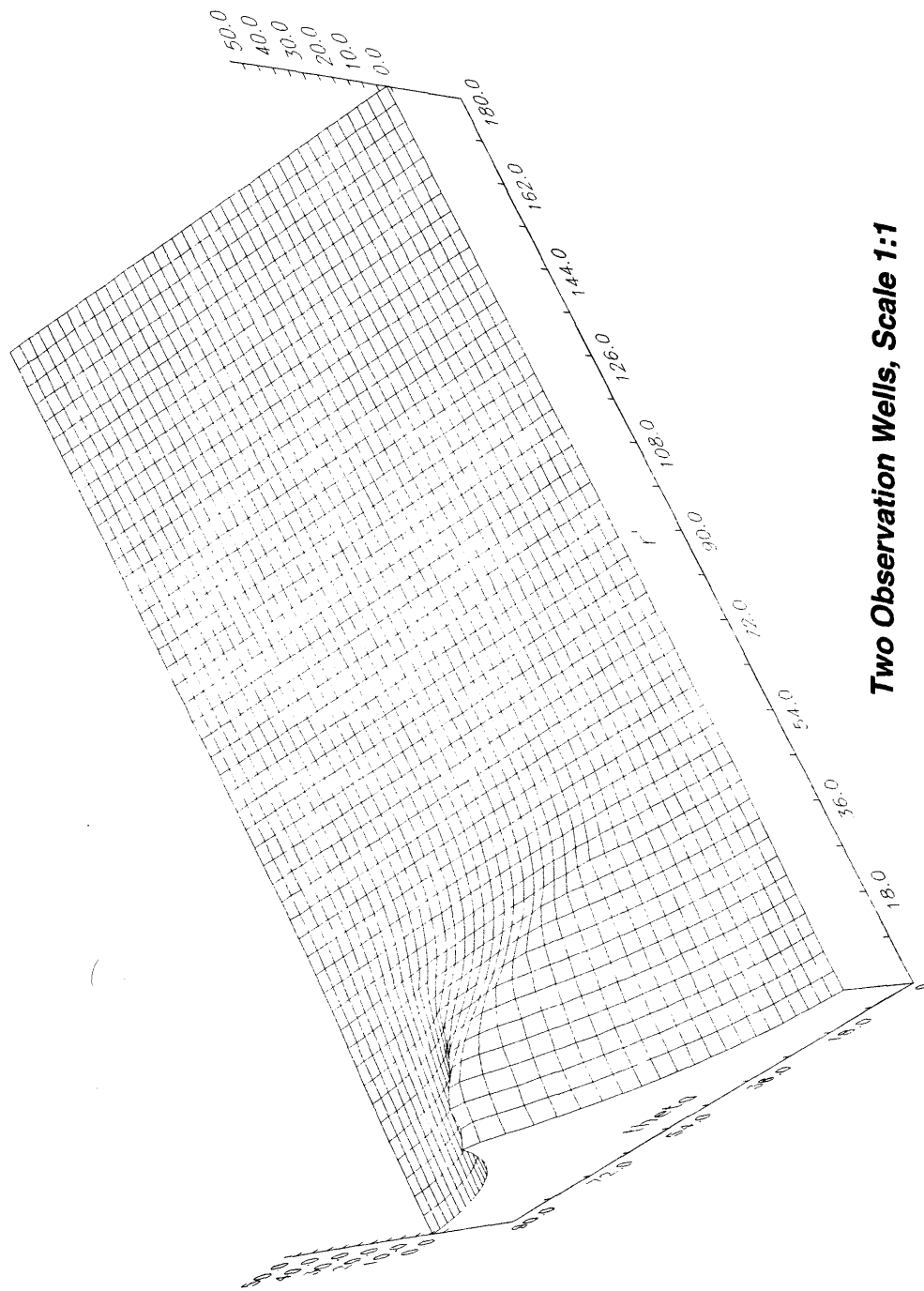


Figure 2.17: Objective function versus various position of active well

Surface Shape of the Objective Function

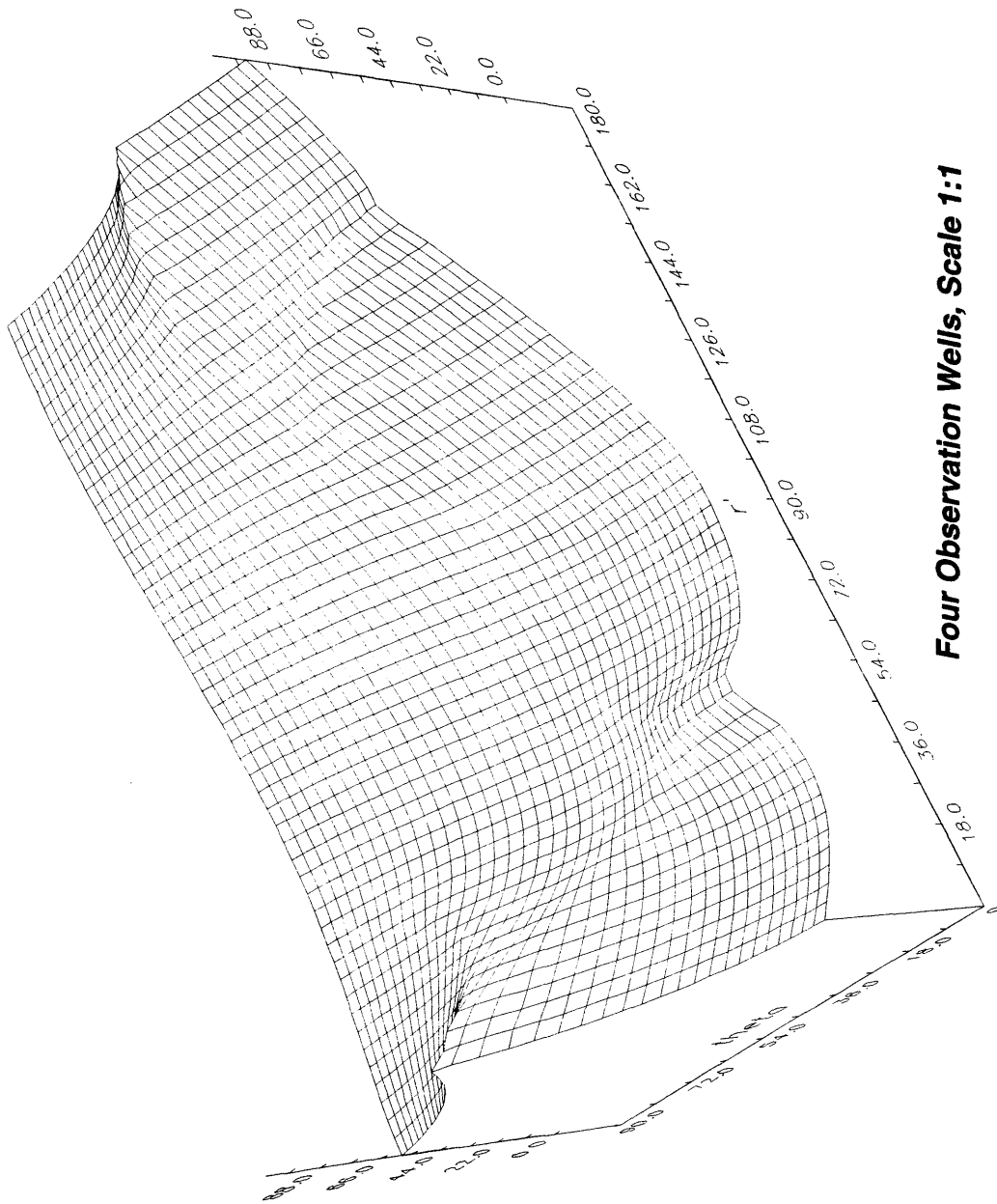


Figure 2.18: Objective function versus various position of active well

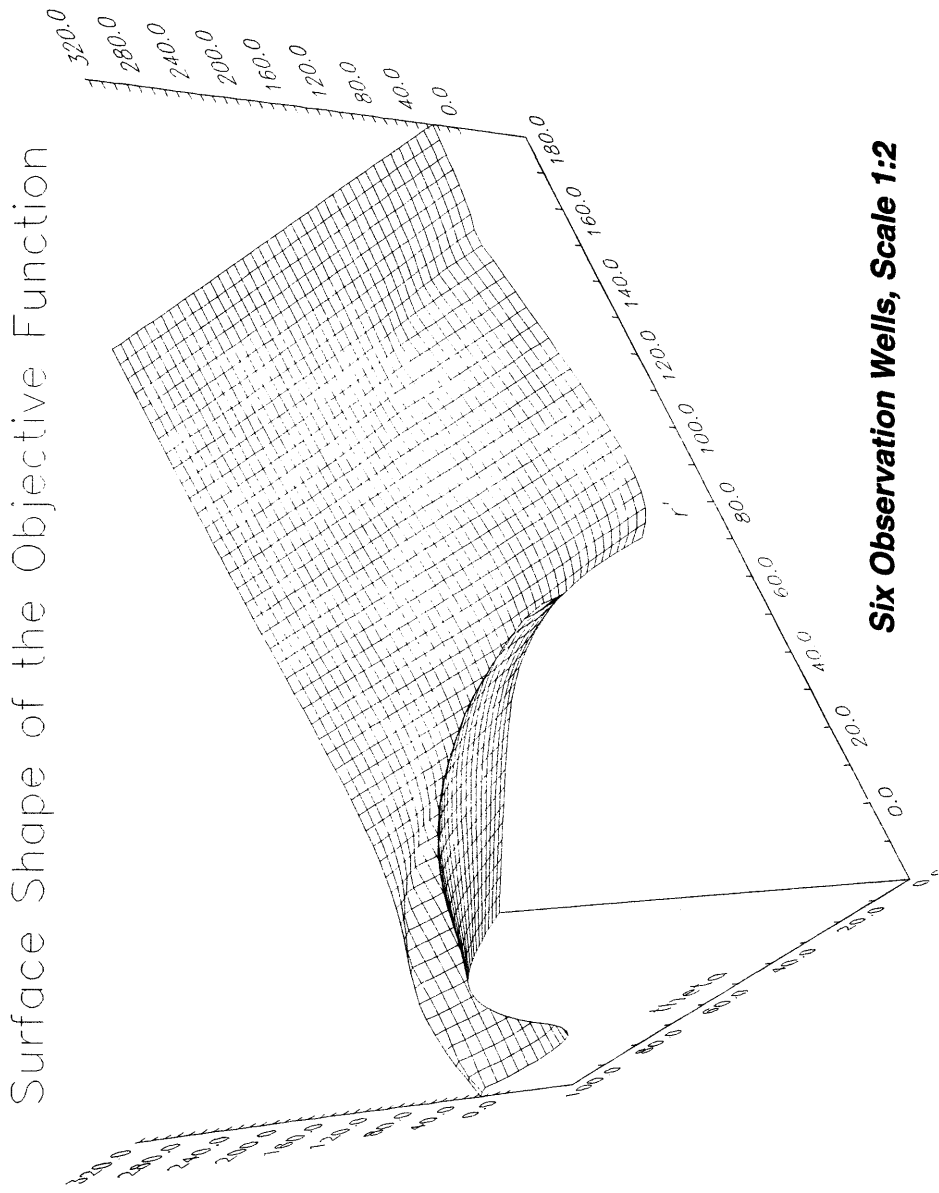


Figure 2.19: Objective function versus various position of active well

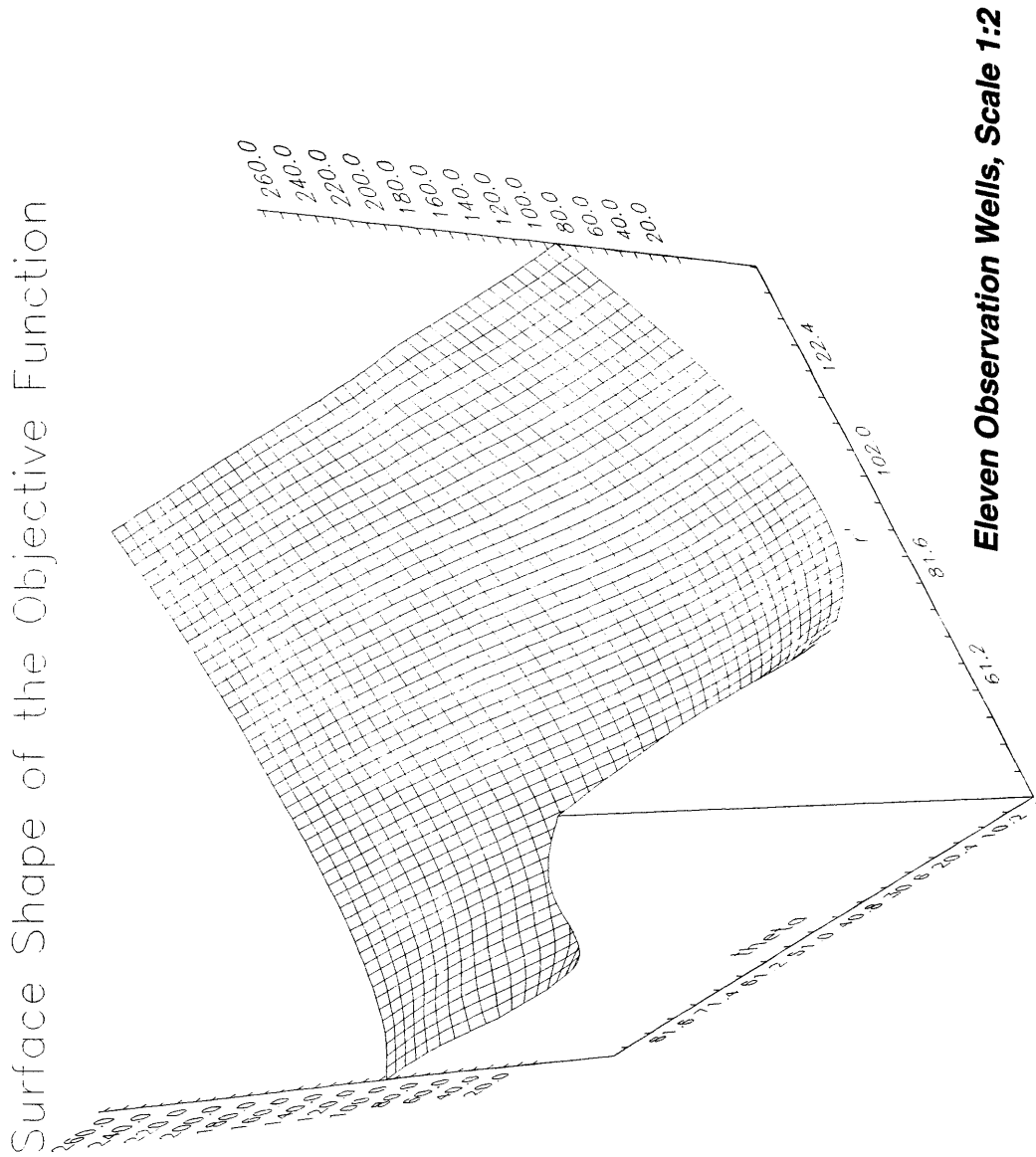


Figure 2.20: Objective function versus various position of active well

wells are used, one located at  $(r = 5, \theta = 0)$ , and the other located at  $(r = 125, \theta = 0)$ , there will be more than one local minimum value. For any fixed  $\theta'$  between  $(-50^\circ, 50^\circ)$ ,  $r'$  has three local minimum values, one lying in  $(0, 50)$ , one located in  $(50, 130)$  and one beyond  $130(\infty)$ , which stands for the homogeneous reservoir without discontinuity. This brings a restriction on the initial guess of  $r'$  because if the guess lies outside of  $(60, 130)$ , the global minimum cannot be reached by nonlinear regression. In this case, three or more initial guesses need to be tried before the search process reached the correct minimum.

There have been some powerful algorithms described in the literature for solving nonlinear least square problems. In this implementation, a modified algorithm is applied. The algorithm is based on a method proposed by *Fletcher* (1971). Let

$$f_i = \omega_i [\Delta p_i - \Delta p(\vec{\alpha}, \Delta t_i, x_i, y_i)] \quad (2.24)$$

$$f = (f_1, f_2, \dots, f_n)^T \quad (2.25)$$

the algorithm is as follows:

1. From an initial guess  $\vec{\alpha}_0$  and a damping factor  $U$ , calculate  $Df$ ,  $f$ ,  $Df^T Df$  and  $Df^T f$ , where  $D$  is the differential operator with respect to  $\vec{\alpha}$ .
2. Calculate  $E = f^T f$ . If  $E < \epsilon$ , stop the iteration. In order to avoid false convergence, some requirements can be put on the parameter change  $\|DX\|$  or on the number of iterations;
3. Solve equation system

$$(Df^T \cdot Df + UI)DX = -Df^T \cdot f$$

to obtain  $DX$ ;

4. Calculate the value of  $E$  as  $E_1$  at  $\vec{\alpha}_0 + DX$ ;
5. Calculate

$$R = \frac{E - E_1}{DX^T(-Df^T \cdot f) + UDX^T DX}$$



- o If  $R > .75$ , let  $U = \frac{U}{2}$  and if  $U < .001$ , let  $U = 0$ . Go to 6,
- o If  $.25 \leq R \leq .75$ , go to 6,
- o If  $R > .25$ , then  $U = 10^{-3}$  if  $U = 0$ , else  $U = U \cdot V$  where
  - $V = 2$  if  $V1 = 2 + \frac{E_1 - E}{DX^T(-Df^T.f)} < 2$ ,
  - $V = 10$  if  $V1 > 10$  and
  - $V = V1$  if  $2 \leq V1 \leq 10$ .

Then go to **3** if  $E_1 > E$ ; go to **6** if  $E_1 \leq E$ ;

6. Substitute  $\alpha_0$  with  $\alpha_0 + DX$ , go to 2.

The matrix of derivatives  $DX$  is obtained by numerical differentiation with relative step 0.001 and the initial value of damping factor  $U$  is 0.01.

It is easier to obtain estimates of the parameters of the second region  $k_2, c_{t2}$  because the objective function is a strong function of the two parameters. The same is true in the case of  $k_1, c_{t1}$  if there is one or more observation wells in the first region. However, it is not possible to know the location of the discontinuity in advance in practice as the position of the discontinuity is a unknown parameter.

It can be seen that the pressure data from the active well and one observation well are not sufficient to estimate the position of the discontinuity; at least two observation wells are needed in the example. Mathematically speaking, the more observation wells, the more information about the discontinuity that may be included. Notice that the active well and the observation wells should not be on a straight line, otherwise, the estimates based on the pressure data are not unique.

## 2.2.5 Examples

Pressure data were generated artificially with random noise to see how the non-linear least square approach would work and to determine which parameters can be estimated successfully.

**Example 1: Unknowns**  $k_2, r', \theta', a, c_{t2}, C$

Table 2.3 includes the pressure data generated with one percent noise and the known reservoir properties used are shown in Table 2.4. The initial guess and the

Positions (x, y)			(0, 100)	(0, -100)	(100, 0)	(-100, 0)
At;	$\Delta p_i$	$\Delta t_i$	$\Delta p_i$	$\Delta p_i$	$\Delta p_i$	$\Delta p_i$
0.0013	0.0457	0.1148	0.0001	0.0002	0.0002	0.0002
0.0016	0.0585	0.1318	0.0003	0.0003	0.0004	0.0004
0.0020	0.0743	0.1514	0.0004	0.0005	0.0005	0.0005
0.0025	0.0949	0.1738	0.0006	0.0007	0.0007	0.0007
0.0032	0.1208	0.1995	0.0008	0.0010	0.0011	0.0011
0.0040	0.1533	0.2291	0.0010	0.0017	0.0017	0.0017
0.0050	0.1942	0.2630	0.0014	0.0031	0.0031	0.0031
0.0063	0.2467	0.3020	0.0022	0.0059	0.0059	0.0059
0.0079	0.3134	0.3467	0.0040	0.0109	0.0110	0.0110
0.0100	0.3965	0.3981	0.0079	0.0199	0.0202	0.0199
0.0126	0.4970	0.4571	0.0155	0.0347	0.0353	0.0348
0.0158	0.6290	0.5248	0.0291	0.0585	0.0595	0.0591
0.0200	0.7982	0.6026	0.0525	0.0949	0.0966	0.0958
0.0251	1.0079	0.6918	0.0890	0.1481	0.1523	0.1508
0.0316	1.2693	0.7943	0.1453	0.2253	0.2324	0.2299
0.0398	1.5889	0.9120	0.2280	0.3325	0.3433	0.3392
0.0501	2.0089	1.0471	0.3427	0.4796	0.4949	0.4872
0.0631	2.5366	1.2023	0.4991	0.6723	0.6890	0.6851
0.0794	3.1567	1.3804	0.7086	0.9188	0.9504	0.9380
0.1000	3.9647	1.5849	0.9742	1.2365	1.2651	1.2689
0.1259	4.9781	1.8197	1.3029	1.6383	1.6744	1.6587
0.1585	6.2005	2.0893	1.7158	2.1156	2.1485	2.1515
0.1995	7.7146	2.3988	2.2126	2.6860	2.7238	2.7065
0.2512	9.5244	2.7542	2.7680	3.3449	3.3924	3.3905
0.3162	11.7947	3.1623	3.4309	4.0913	4.1293	4.1167
0.3981	14.4375	3.6308	4.1656	4.9047	4.9511	4.9638
0.5012	17.7034	4.1687	4.9930	5.8682	5.8711	5.9024
0.6310	21.3863	4.7863	5.8761	6.8062	6.8165	6.8714
0.7943	25.9568	5.4954	6.7674	7.9208	7.8794	7.9188
1.0000	30.9352	6.3096	7.7381	8.9722	8.9130	8.9863
1.2589	36.2503	7.2444	8.7613	10.1510	10.0283	10.1487

Active well		Observation Wells				
$\Delta t_i$	$\Delta p_i$	$At_i$	$\Delta p_i$	$\Delta p_i$	$\Delta p_i$	$\Delta p_i$
1.9953	48.7194	9.5499	10.9054	12.3914	12.2931	12.3826
2.5119	55.2196	10.9648	11.9544	13.5561	13.4564	13.5806
3.1623	61.6283	12.5893	13.0069	14.6518	14.5340	14.6424
3.9811	67.2365	14.4544	14.0602	15.7939	15.6419	15.7799
5.0119	72.5952	16.5959	15.0836	16.9317	16.8066	16.8296
6.3096	77.0253	19.0546	16.1059	18.0142	17.7633	17.8972
7.9433	81.1865	21.8776	17.2182	19.1974	18.8317	18.9823
12.5893	87.3582	28.8403	19.3435	21.1629	20.9977	21.0232
15.8489	89.9176	33.1131	20.2165	22.2034	22.0172	22.1025
19.9526	92.2144	38.0189	21.2108	23.3209	23.1296	23.1424
25.1189	94.2082	43.6516	22.3442	24.3604	24.0744	24.2053
31.6228	95.7760	50.1187	23.2092	25.2624	25.0429	25.2406
39.8107	98.2806	57.5440	24.3699	26.4343	26.0535	26.1485
50.1187	99.5769	66.0693	25.3674	27.3163	27.1172	27.1443
63.0957	101.0565	75.8578	26.1800	28.5421	28.0381	28.1081
79.4328	102.8120	87.0964	27.1859	29.3354	29.0095	29.3468
100.0000	104.5314	100.0000	28.3910	30.2947	30.2034	30.2314

Table 2.4: Properties of the reservoir in Example 1

$q$	<b>4</b>	$r_w$	$\mu$	$h$	$k_1$	$c_{t1}$
110 <i>bbl/day</i>	0.3	0.4 <i>ft</i>	3.0	30 <i>ft</i>	50 <i>md</i>	8.e-6 <i>1/psi</i>

Table 2.5: Initial guess, matching result and true value

	$k_2$ <i>md</i>	$r'$ <i>ft</i>	$\theta$ $^\circ$	$a$ <i>ft</i>	$c_{t2}$ (1/ <i>psi</i> )	$C$ ( <i>bbl/psi</i> )
Initial Guess	50	50	50	50	$8. \times 10^{-6}$	.05
Matching Result	110.0	79.8	81.5	49.1	11.E-6	0.0998
True Values	110	80	80	50	11.E-6	.1

matching result are listed in Table 2.5. The matching started from the initial guess of a homogeneous model  $k_1 = k_2 = 50(\text{md})$  and  $c_{t1} = c_{t2} = 8 \times 10^{-6}(1/\text{psi})$ . The residual of weighted squares was 0.357 and iteration number reached 40 to achieve the absolute and relative errors for each parameter less than  $10^{-8}$ . In this example, there is one observation well located in the discontinuity and the noise is only one percent, so the result is encouraging. However if  $k_1$  and  $c_{t1}$  were unknown, the initial guess  $k_1 = k_2 = r' = a = \theta = 70$ ,  $c_{t1} = c_{t2} = 1. \times 10^{-6}$ ,  $C = 0.05$  resulted in incorrect estimated values of  $k_1 = 159$ ,  $k_2 = 104$ ,  $r' = 83$ ,  $\theta = 125$ ,  $a = 58$ ,  $c_{t1} = 10.4 \times 10^{-6}$ ,  $c_{t2} = 11.2 \times 10^{-6}$ ,  $C = 0.1$  with the residual 38.0 after 11 iterations.

**Example 2: Unknowns**  $k_1, k_2, r', \theta, a, c_{t1}, c_{t2}, C$

This example also has one observation well located in the discontinuity region, and the noise added in pressure data is 3 percent.

Table 2.6 and Table 2.7 include the pressure data and the property data of the reservoir, respectively. The initial guess, matching result and the true parameter values are shown in Table 2.8. The absolute and relative errors of each parameter are within  $10^{-8}$  after 14 iterations, which gives 1.94 as the residual of the weighted squares.

## 2.2.6 A Special Case – Concentric Active Well

If  $r' = 0$ , the active well is concentrically located in the discontinuous region. The pressure drop in Laplace space can be simplified to be

$$\overline{\Delta p} = \begin{cases} \frac{141.2qB\mu_1}{k_1 h z} \left[ K_0(z_1 r) + \frac{\lambda_1 z_1 K_1(a z_1) K_0(a z_2) - \lambda_2 z_2 K_0(a z_1) K_1(a z_2)}{\lambda_1 z_1 I_1(a z_1) K_0(a z_2) + \lambda_2 z_2 I_0(a z_1) K_1(a z_2)} I_0(z_1 r) \right] & r \leq a \\ \frac{141.2qB\mu_1 \lambda_1}{k_1 h a z} \frac{K_0(z_2 r)}{\lambda_1 z_1 I_1(a z_1) K_0(a z_2) + \lambda_2 z_2 I_0(a z_1) K_1(a z_2)} & r > a. \end{cases} \quad (2.26)$$

Active Well		Observation Wells				
Positions (x, y)		(0, 100)	(0, -100)	(100, 0)	(-100, 0)	
$\Delta t_i$	$\Delta P_i$	$\Delta t_i$	$\Delta P_i$	$AP_i$	$\Delta P_i$	$AP_i$
0.0013	0.0114	0.1148	0.0001	0.0000	0.0001	0.0001
0.0016	0.0146	0.1318	0.0001	0.0001	0.0001	0.0001
0.0020	0.0184	0.1514	0.0001	0.0001	0.0001	0.0001
0.0025	0.0238	0.1738	0.0002	0.0001	0.0002	0.0002
0.0032	0.0304	0.1995	0.0002	0.0002	0.0003	0.0004
0.0040	0.0385	0.2291	0.0004	0.0004	0.0004	0.0006
0.0050	0.0486	0.2630	0.0008	0.0008	0.0008	0.0012
0.0063	0.0621	0.3020	0.0015	0.0015	0.0015	0.0022
0.0079	0.0794	0.3467	0.0028	0.0027	0.0029	0.0039
0.0100	0.1005	0.3981	0.0051	0.0050	0.0053	0.0066
0.0126	0.1238	0.4571	0.0089	0.0086	0.0092	0.0111
0.0158	0.1574	0.5248	0.0149	0.0145	0.0154	0.0182
0.0200	0.2020	0.6026	0.0246	0.0234	0.0249	0.0285
0.0251	0.2560	0.6918	0.0379	0.0362	0.0396	0.0439
0.0316	0.3224	0.7943	0.0578	0.0555	0.0608	0.0662
0.0398	0.3998	0.9120	0.0867	0.0822	0.0903	0.0966
0.0501	0.5123	1.0471	0.1244	0.1205	0.1319	0.1384
0.0631	0.6560	1.2023	0.1760	0.1708	0.1830	0.1969
0.0794	0.8072	1.3804	0.2475	0.2358	0.2597	0.2727
0.1000	1.0257	1.5849	0.3373	0.3261	0.3474	0.3829
0.1259	1.3091	1.8197	0.4490	0.4501	0.4781	0.5088
0.1585	1.6415	2.0893	0.6031	0.6010	0.6265	0.6910
0.1995	2.0670	2.3988	0.8006	0.7955	0.8259	0.8938
0.2512	2.5662	2.7542	1.0177	1.0347	1.0751	1.1898
0.3162	3.2503	3.1623	1.3158	1.3264	1.3588	1.5002
0.3981	4.0275	3.6308	1.6669	1.6618	1.7037	1.9229
0.5012	5.0944	4.1687	2.1124	2.1444	2.1412	2.4485
0.6310	6.2746	4.7863	2.6261	2.6071	2.6113	3.0241
0.7943	8.0072	5.4954	3.1618	3.3025	3.2418	3.7343
1.0000	9.9207	6.3096	3.8377	3.9685	3.8791	4.5257
1.2589	12.0264	7.2444	4.6438	4.8734	4.6848	5.5402

Active Well		Observation Wells				
$\Delta t_i$	$\Delta P_i$	$\Delta t_i$	$\Delta P_i$	$\Delta P_i$	$\Delta P_i$	$\Delta P_i$
1.5849	15.1704	8.3176	5.6226	5.7772	5.5340	6.4860
1.9953	18.3564	9.5499	6.6476	6.7930	6.6091	7.7252
2.5119	22.4510	10.9648	7.7459	7.9858	7.7805	9.1468
3.1623	27.3059	12.5893	8.9455	9.1699	8.9129	10.4160
3.9811	32.2894	14.4544	10.2400	10.5519	10.2032	11.9558
5.0119	38.3868	16.5959	11.5512	12.0340	11.7111	13.3947
6.3096	44.6571	19.0546	12.9272	13.4882	12.8658	14.9518
7.9433	52.1126	21.8776	14.5845	15.2493	14.3186	16.6145
10.0000	59.4432	25.1189	16.1505	16.7536	15.9403	18.3905
12.5893	66.6974	28.8403	17.7758	17.9402	17.4309	19.6863
15.8489	73.8492	33.1131	18.8632	19.4461	18.8634	21.3972
19.9526	80.4117	38.0189	20.2719	21.1601	20.5391	22.9837
25.1189	85.8640	43.6516	22.0724	22.6550	21.7625	24.6182
31.6228	89.5990	50.1187	23.0581	23.7405	23.0253	26.1421
39.8107	95.4497	57.5440	24.9066	25.5720	24.3816	27.2351
50.1187	97.3391	66.0693	26.2379	26.5427	25.8681	28.5692
63.0957	99.3742	75.8578	26.9678	28.5011	26.9258	29.7714
79.4328	101.9808	87.0964	28.2723	29.1563	28.1063	31.8347
100.0000	104.3303	100.0000	30.1881	30.2841	29.9239	32.7357

$q$ bbl/day	porosity	$r_w$ ft	viscosity	thickness
110.0000	0.3000	0.4000	3.0000	30.0000

Table 2.8: Initial guess, matching result and true value

	$k_1$ md	$k_2$ md	$r'$ ft	$\theta'$ °	$a$ ft	$c_{t1}$	$c_{t2}$ 1/psi	$C$
Initial	50	50	50	50	50	5.E-6	5.E-6	.1
Match	238.66	100.35	79.51	197.63	61.02	18.6E-6	10.E-6	0.4
True	250	100	80	200	60	19.E-6	10.E-6	.4

From the approximate expressions for modified Bessel functions of small arguments:

$$\begin{aligned} K_0(x) &\approx -\ln x, \\ K_1(x) &\approx \frac{1}{x}, \\ I_1(x) &\approx \frac{x}{2}, \\ I_0(x) &\approx 1, \\ (x &\approx 0), \end{aligned}$$

it follows that for  $a \cdot z \approx 0$

$$\begin{aligned} &\frac{\lambda_1}{\lambda_1 a z_1 K_0(a z_2) I_1(a z_1) + \lambda_2 a z_2 K_1(a z_2) I_0(a z_1)} \approx \\ &\frac{\lambda_1}{\lambda_1 a z_1 \cdot (-\ln a z_2) \cdot \frac{a z_1}{2} + \lambda_2 a z_2 \cdot \frac{1}{a z_2} \cdot 1} \approx \frac{\lambda_1}{\lambda_2}, \end{aligned} \quad (2.27)$$

$$\begin{aligned} K_0(z_1 r) + \frac{\lambda_1 z_1 K_1(a z_1) K_0(a z_2) - \lambda_2 z_2 K_0(a z_1) K_1(a z_2)}{\lambda_1 z_1 I_1(a z_1) K_0(a z_2) + \lambda_2 z_2 I_0(a z_1) K_1(a z_2)} I_0(z_1 r) \approx \\ \frac{\lambda_1}{\lambda_2} K_0(z_2 r) + (1 - \frac{\lambda_1}{\lambda_2}) \ln \frac{a}{r}. \end{aligned} \quad (2.28)$$

So for small radius  $a$  and large time (small  $z$ ), the pressure drop becomes

$$\overline{\Delta p}(r, z) = \begin{cases} \frac{141.2qB\mu_2}{k_2 h z} [K_0(z_2 r) + (\frac{\lambda_2}{\lambda_1} - 1) \ln \frac{a}{r}] & r \leq a \\ \frac{141.2qB\mu_2}{k_2 h z} K_0(z_2 r) & r > a \end{cases} \quad (2.29)$$

and its Laplace transformation inversion is easy to obtain. From Eq. 2.29, it can be seen that the pressure drop outside the discontinuity is the same as the line source solution (exponential integral solution) and the pressure drop inside discontinuity should be the line source solution plus  $\frac{141.2qB\mu_2}{k_2 h} (\frac{\lambda_2}{\lambda_1} - 1) \ln \frac{a}{r}$ . Therefore, a composite reservoir with a centered source well can be treated in convention as a homogeneous reservoir without the first region by introducing a skin factor

$$S = (\frac{\lambda_2}{\lambda_1} - 1) \ln \frac{a}{r}. \quad (2.30)$$

However, this simplification is true only when the radius of the first region is not very large and the time considered is not very small. Fig. 2.21 and Fig. 2.22 provide an idea what  $a$  and  $t$  should be. For  $a = 50$  (feet),  $t \leq 1$  (hour), using the skin factor approach will result in incorrect results as shown in Fig. 2.21.

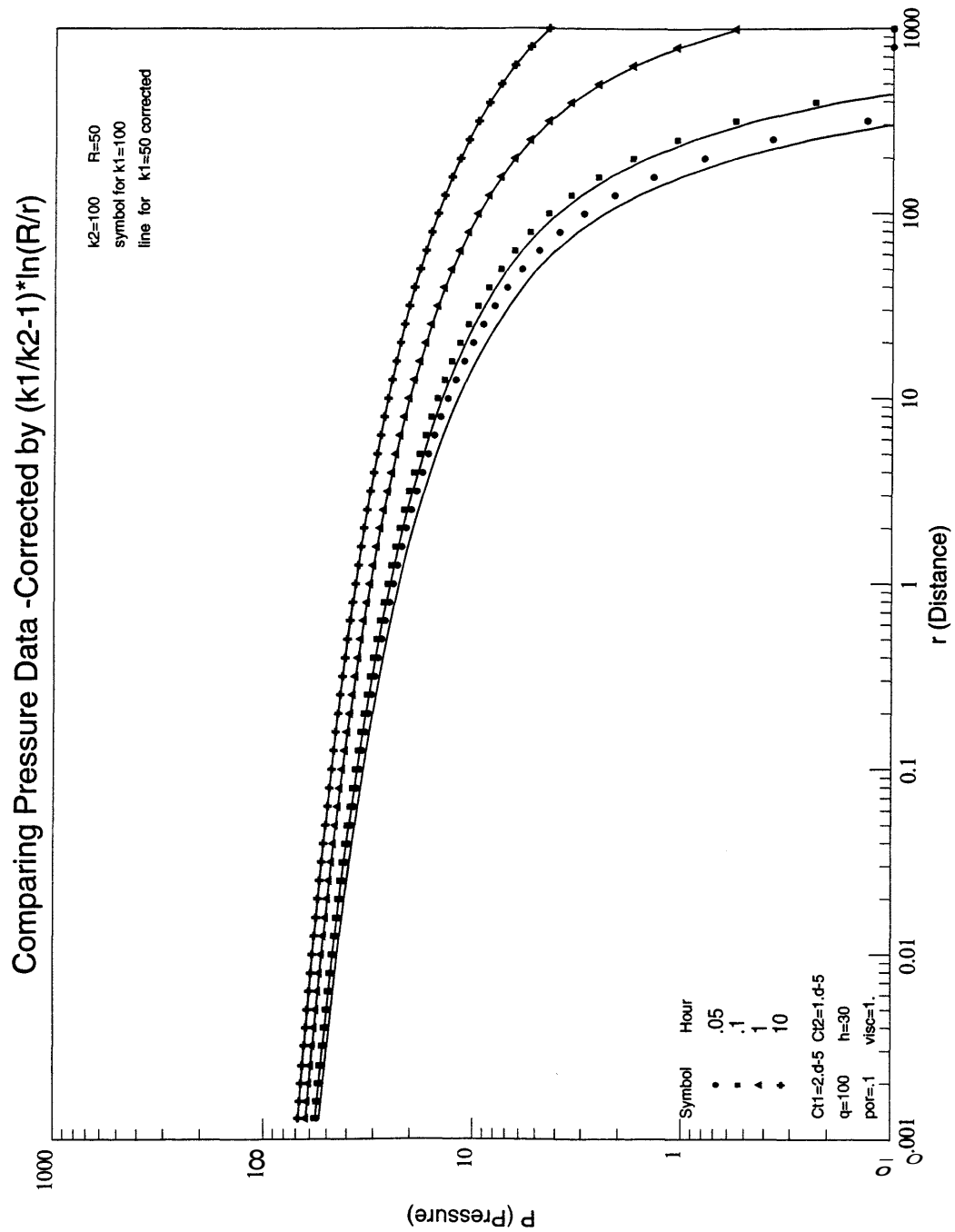


Figure 2.21: Comparison of pressure responses between skin factor approach and discontinuity approach



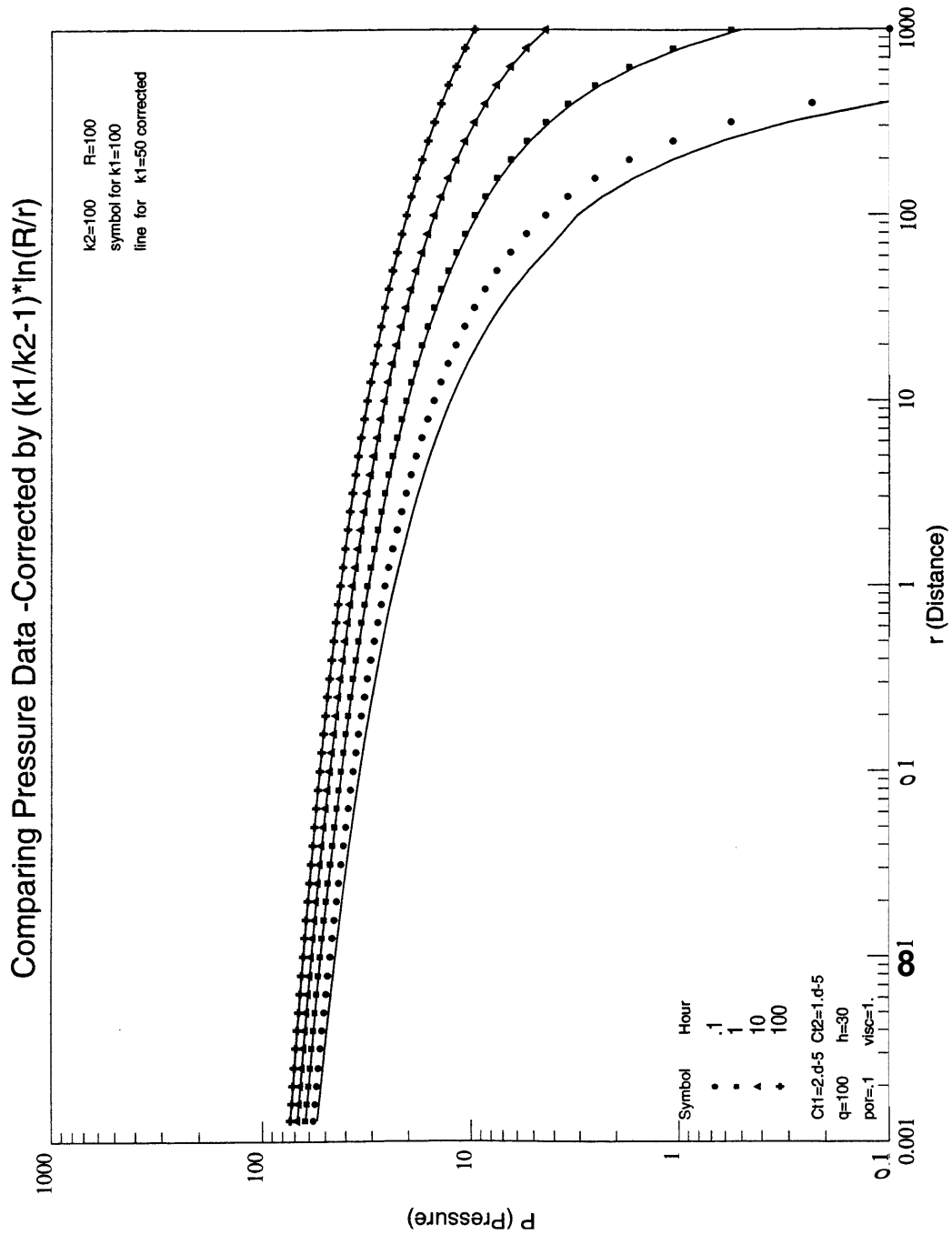


Figure 2.22: Comparison of pressure responses between skin factor approach and discontinuity model approach

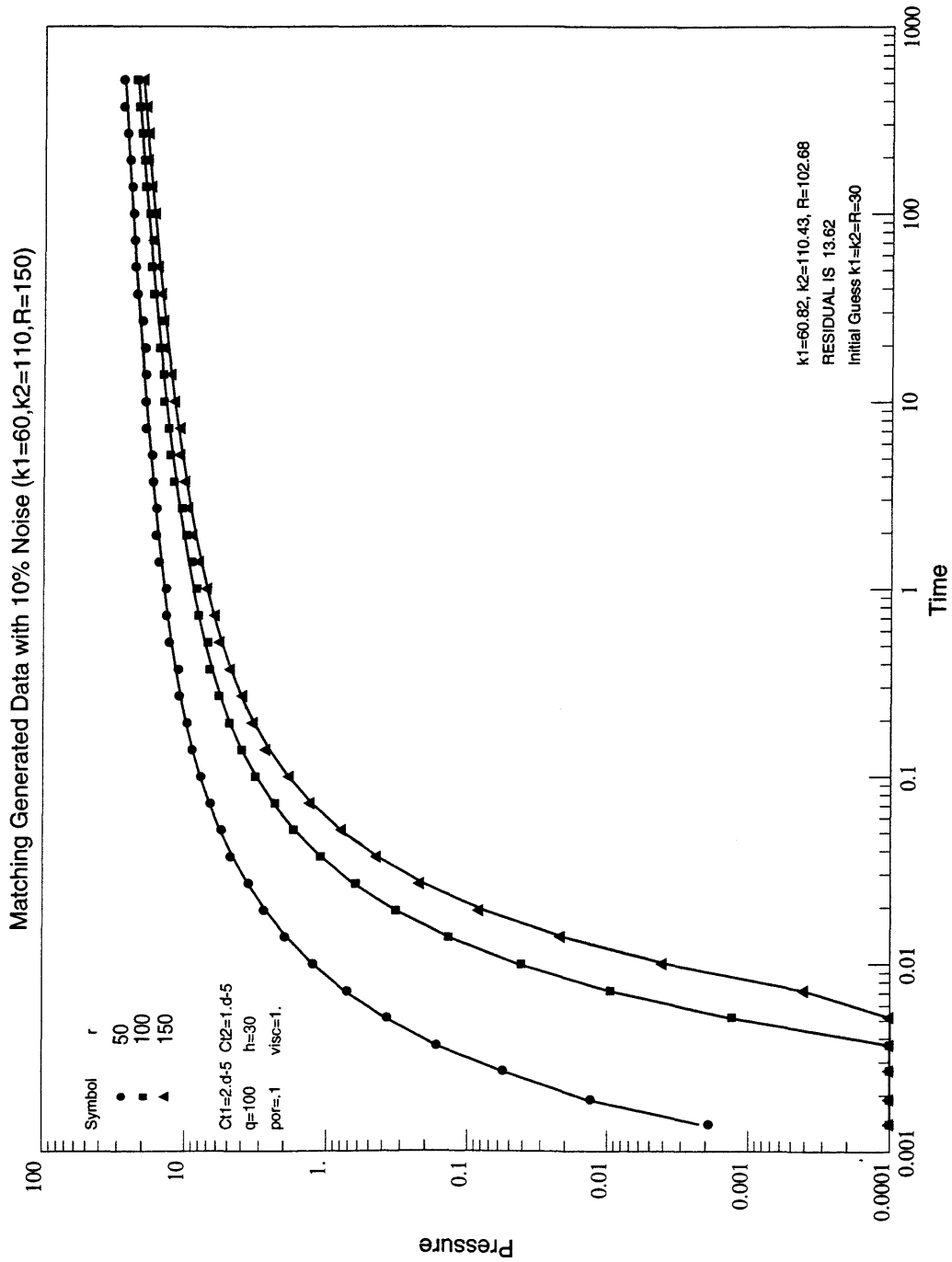


Figure 2.23: Matching result for concentric model

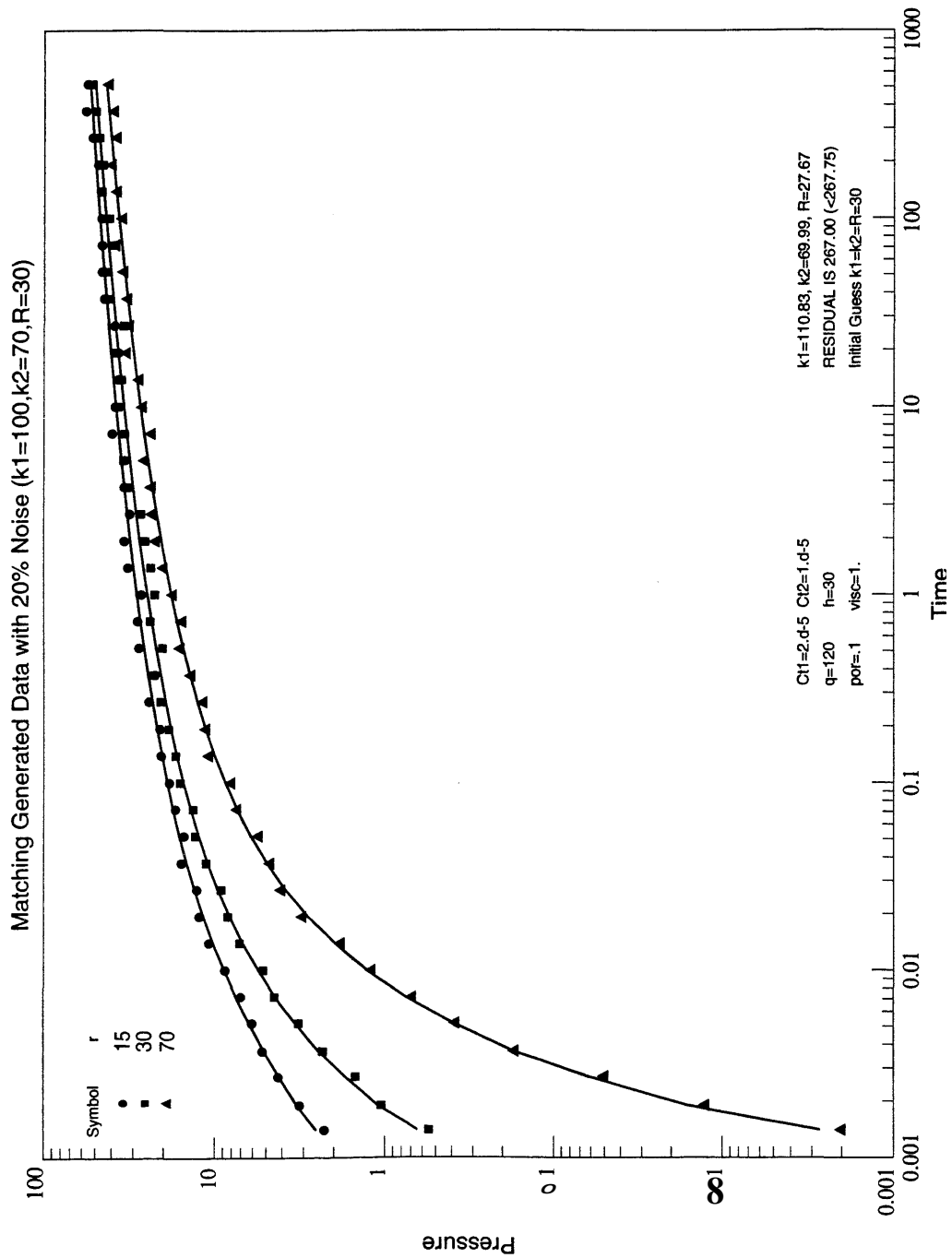


Figure 2.24: Matching result for concentric model

The same thing happens in Fig. 2.22 where  $a = 100$  feet,  $t \leq 10$  hours. For the general concentric composite reservoir where the simplified skin factor approach does not apply, the solution presented in Eq. 2.26 runs faster and is more suitable than the solution presented in Eqs. 2.10 and 2.11 in finding the unknown parameters such as  $k_1, k_2$  and  $a$  as shown in Fig. 2.23 and Fig. 2.24.

In summary, for circular discontinuities, parameters such as permeability, compressibility in both regions can be obtained in addition to the location and the range of the discontinuous region if the noise in the pressure data are not large. The more data that are used, the higher tolerance for noise that may be allowed in pressure data for parameter identification. The wellbore storage coefficient in the active well can also be estimated. If the active well is located in the center of the discontinuous region, a skin factor may replace an explicit representation of the discontinuous region under some restrictions.

## 2.3 Analysis of Drawdown-Buildup Pressure Data in Multiwell Systems

This section focuses on how the producing neighbor wells affect the buildup pressure data in the testing well. The investigation started with the development of the solutions in Laplace space and covered the system of both finite number of wells and infinite number of wells. The system of an infinite number of wells can be used to simulate the behavior of transient pressure in rectangular reservoirs.

Consider an infinite homogeneous reservoir with  $n + 1$  wells. All wells are labeled with an integer. Well 0 is the observation well, well 1 is the testing well producing at a constant flow rate  $q$  at the beginning and at constant rate 0 after  $t_{pD}$ , while wells  $n$  ( $n > 1$ ) are the neighbor wells producing at constant rate  $q$  at any time. The producing neighbor wells in this configuration will have impact on the pressure buildup on the observation well. The pressure data from shut-in test of well 1 cannot be analyzed correctly without studying the effect of neighbor wells.

If the wellbore storage effect is taken into account, the pressure solution in Laplace space for the multiwell system of finite number of wells can be obtained by superposing finite sources in time and space,

$$\bar{p}_D(r_{1D}, r_{2D}, \dots, r_{nD}, t_{pD}, s) = \frac{(1 - e^{-st_{pD}})K_0(r_{1D}\sqrt{s}) + K_0(r_{2D}\sqrt{s}) + K_0(r_{3D}\sqrt{s}) + \dots + K_0(r_{nD}\sqrt{s})}{s^{\frac{3}{2}}(K_1(\sqrt{s}) + C_D\sqrt{s}K_0(\sqrt{s}))}, \quad (2.31)$$

or basing the time scale on  $\frac{t_D}{r_{eD}^2}$  and using  $\frac{t_{pD}}{r_{eD}^2}$  as the parameter,

$$\bar{p}_D(r_{1D}, r_{2D}, \dots, r_{nD}, t_{pD}, z) = \frac{r_{eD}[(1 - e^{-zt_{pD}/r_{eD}^2})K_0(r_{1D}\sqrt{z}/r_{eD}) + K_0(r_{2D}\sqrt{z}/r_{eD}) + K_0(r_{3D}\sqrt{z}/r_{eD}) + \dots + K_0(r_{nD}\sqrt{z}/r_{eD})]}{z^{\frac{3}{2}}(K_1(\sqrt{z}/r_{eD}) + C_D\sqrt{z}/r_{eD}K_0(\sqrt{z}/r_{eD}))} \quad (2.32)$$

where  $C_D$  is the wellbore storage coefficient, and  $r_{iD}$  is the distance between observation well 0 and well  $i$ .

When  $n = 1$ , this solution represents the interference case with one active well and one observation well in an infinite homogeneous reservoir. The type curves for

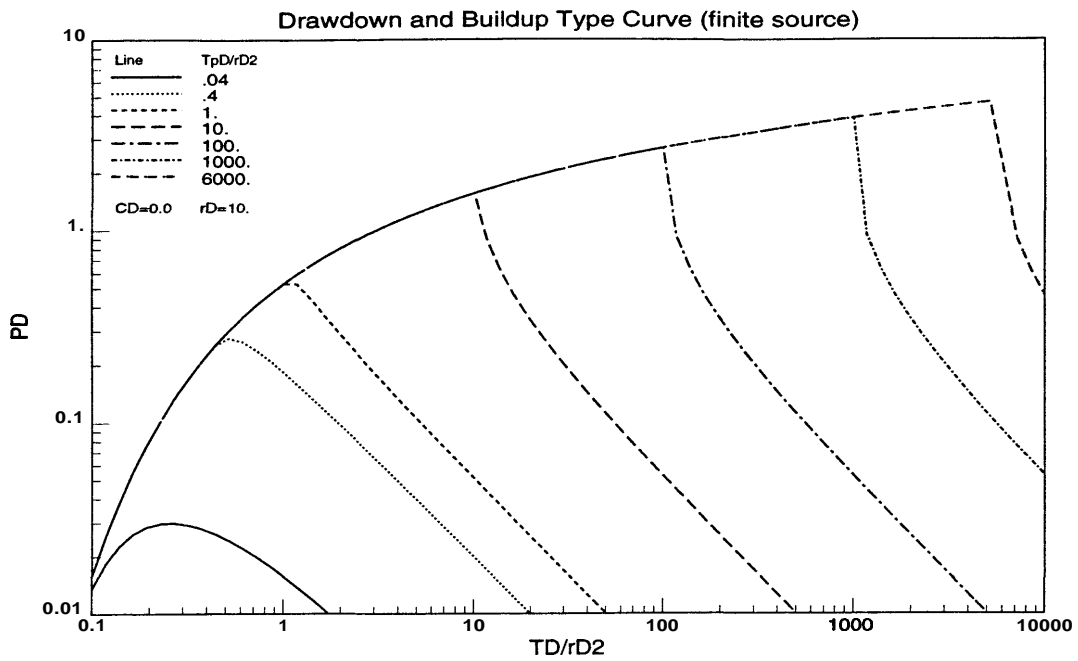
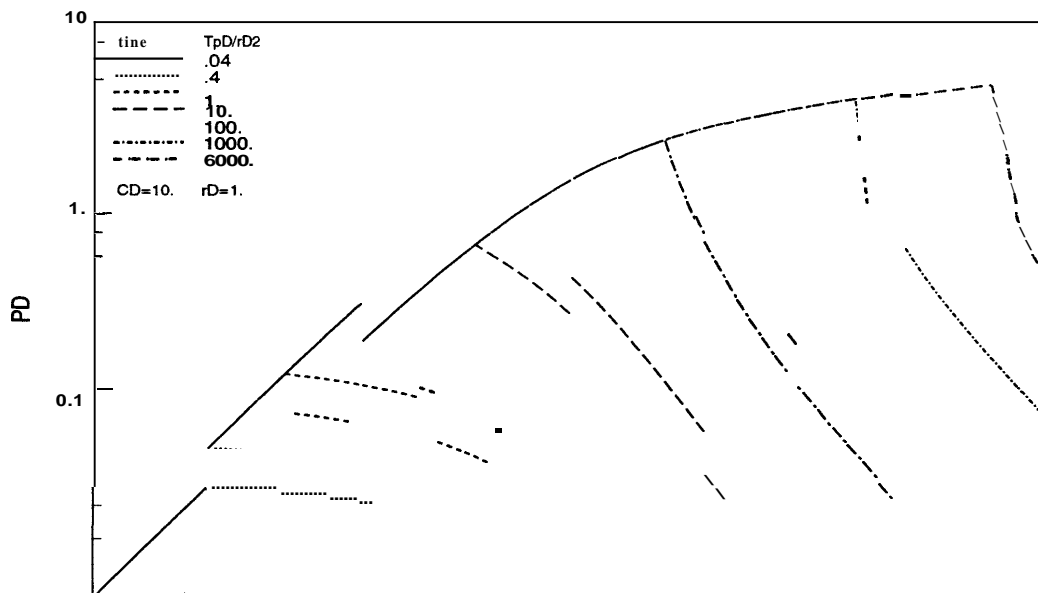


Figure 2.25: Interference pressure response versus production time



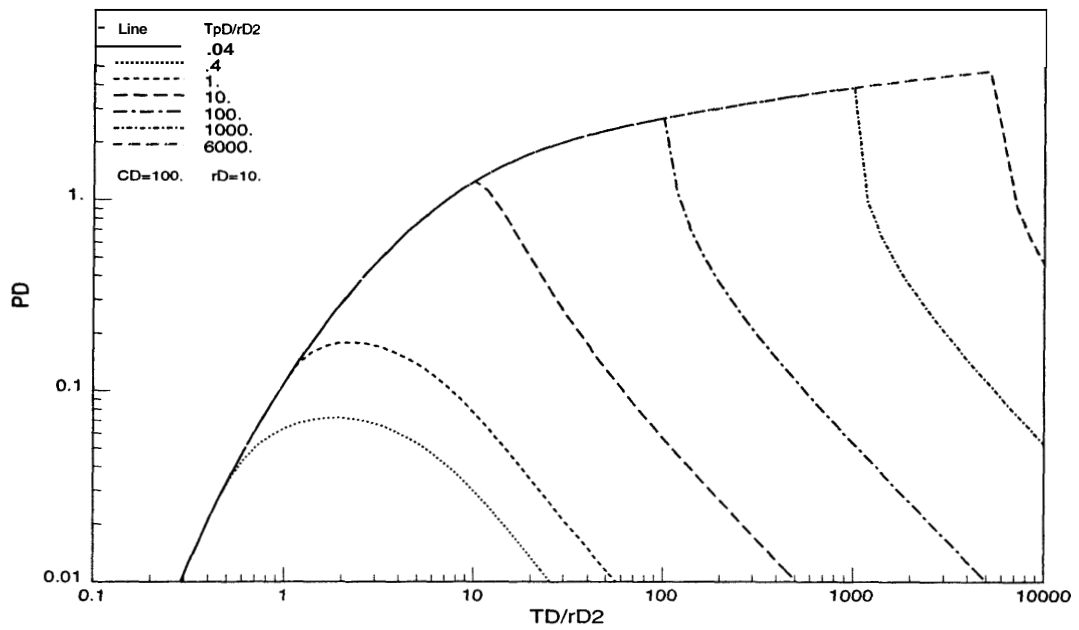


Figure 2.27: Pressure response versus production time and wellbore storage effect

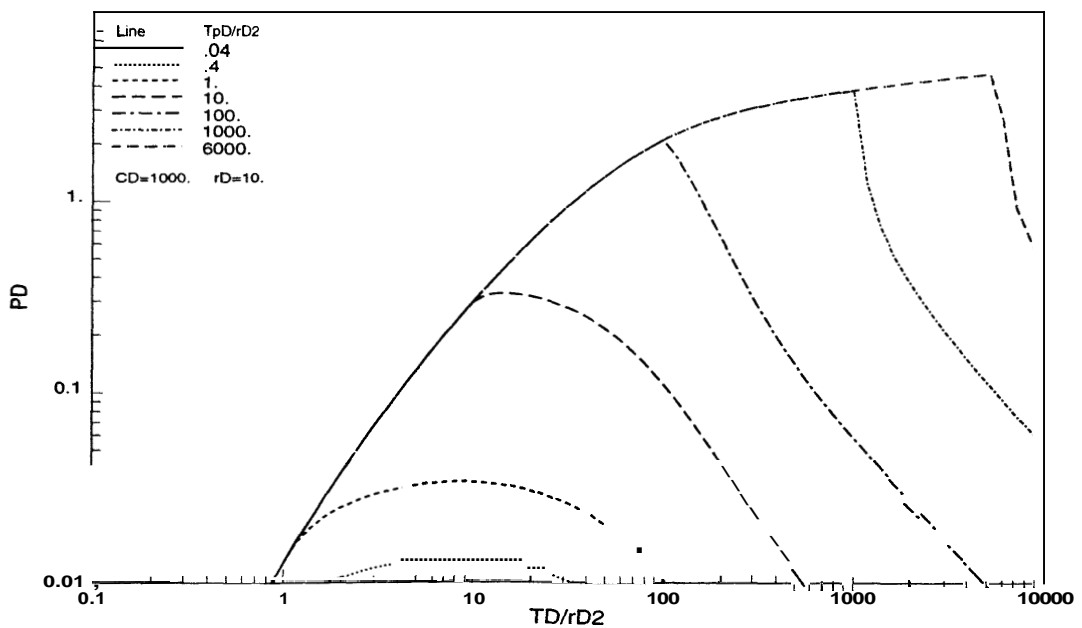


Figure 2.28: Pressure response versus production time and wellbore storage effect

drawdown and buildup without wellbore storage are provided by Ramey (1981) as shown in Fig. 2.25. In this special case, the pressures at any place are the same except at early time if  $p_D$  is plotted vs.  $\frac{t_D}{r_D^2}$  with  $\frac{t_{pD}}{r_D^2}$  as a parameter ( $r_{eD} = r_{1D} = r_D$ ). As can be seen from Fig. 2.26, Fig. 2.27 and Fig. 2.28, the pressure responses depend greatly on the distance between testing well and observation well if wellbore storage is considered.

Fig. 2.29 and Fig. 2.30 show the pressure drawdown and buildup for a six-well system, where the testing well is also the observation well. All the production wells contribute to the drawdown curve. When the testing well is shut in, the buildup curve eventually follows the curve corresponding to the production of all the neighboring wells.

Fig. 2.31 and Fig. 2.32 show the buildup parts for the same system. For a fixed shut-in time,  $p_D$  will become larger than  $p(t_{pD})$  at late time, so each curve reaches below zero at some time. The shut-in time affects the buildup pressure data very much as well as the wellbore storage effect as can be seen from Fig. 2.31.

If there are infinite number of wells, well 0 is the observation well, well 1 is the testing well producing at constant rate  $q$  first and at constant rate 0 after  $t_{pD}$ , if all the other neighboring wells are producing at the constant rate  $q$  all the time, and if the wellbore storage effect is included, the pressure solution in Laplace space for the infinite system can be written as

$$\bar{p}_D(r_{1D}, r_{2D}, \dots, t_{pD}, z) = \frac{r_{eD}(1 - e^{-zt_{pD}/r_{eD}^2})K_0(r_{1D}\sqrt{z}/r_{eD}) + \sum_{n=2}^{\infty} K_0(r_{nD}\sqrt{z}/r_{eD})}{z^{\frac{3}{2}}(K_1(\sqrt{z}/r_{eD}) + C_D\sqrt{z}/r_{eD}K_0(\sqrt{z}/r_{eD}))} \quad (2.33)$$

where  $r_{nD}$  is the distance between observation well 0 and well  $n$ .

To compare the effect of number of wells on the drawdown and buildup curves, a six-well system and an infinite-well system shown in Fig 2.33 are considered as an example, where the distances in  $x$  direction and  $y$  direction between any two neighboring wells are  $500ft$ , and the testing well and observation well are located at  $(0,0)$ . The pressure response due to the production of infinite neighboring wells is



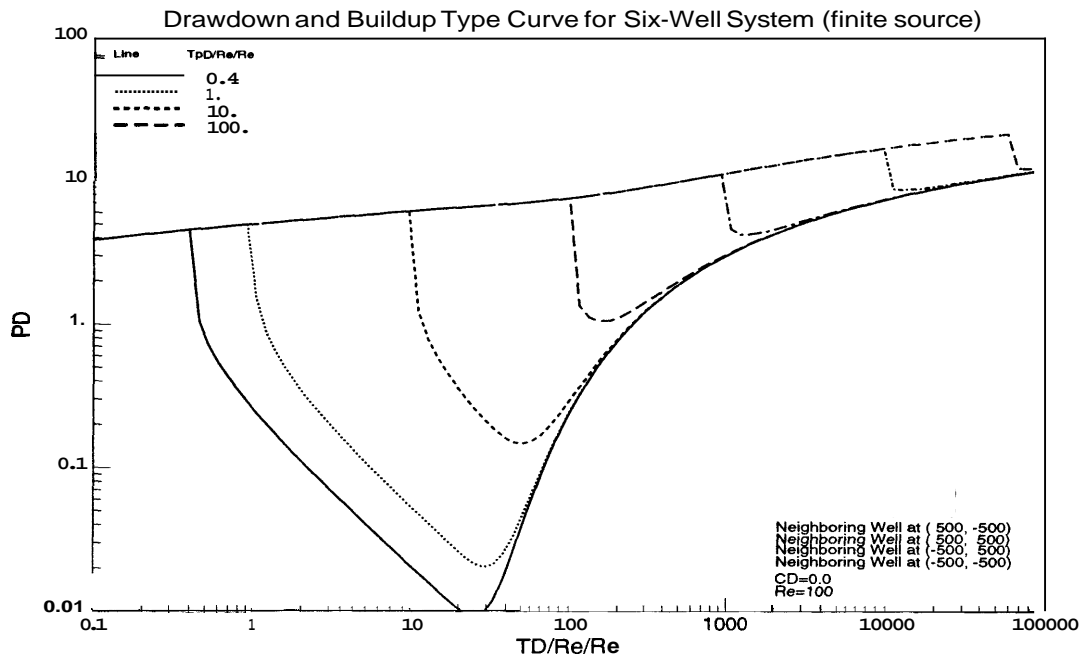


Figure 2.29: Pressure response versus production time

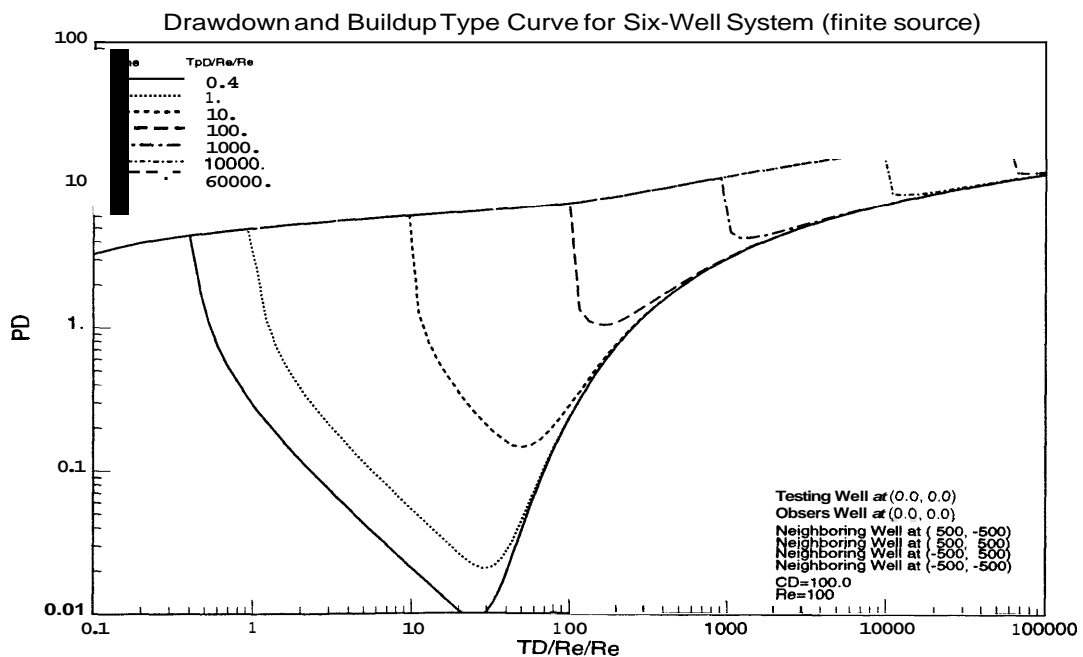


Figure 2.30: Pressure response versus production time and wellbore storage effect

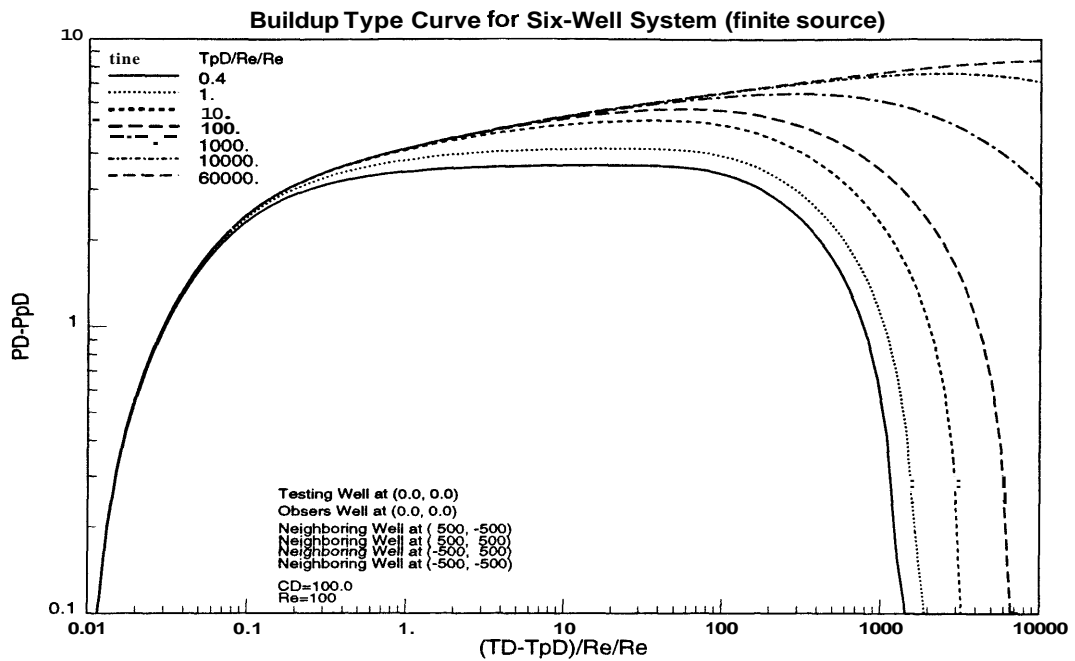


Figure 2.31: Pressure buildup response versus time after shut-in

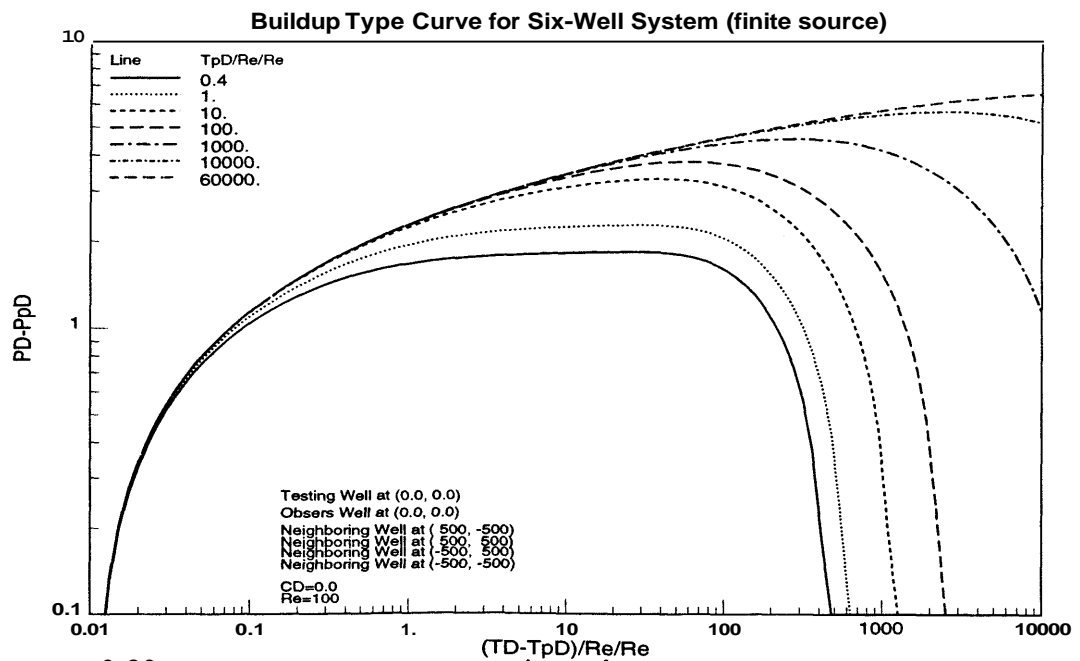
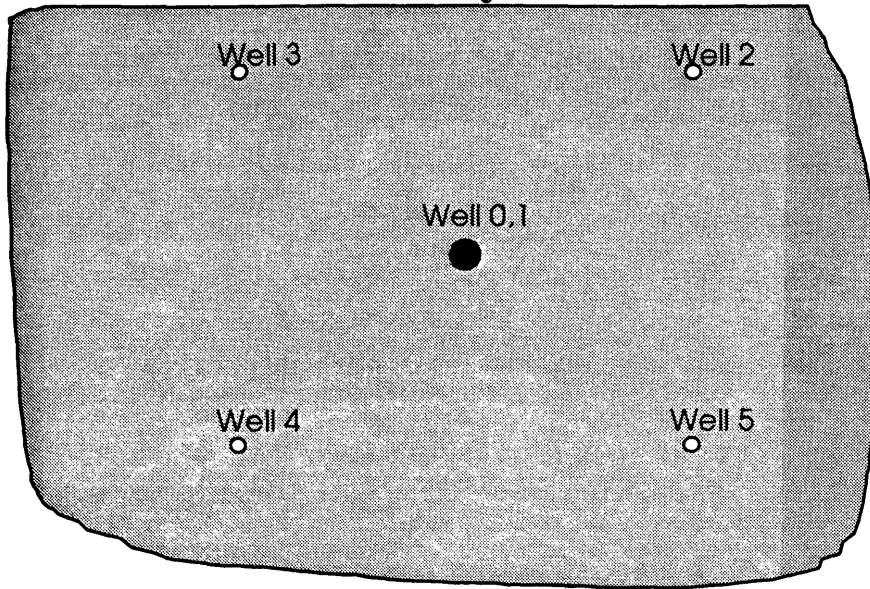


Figure 2.32: Pressure buildup versus time after shut-in and wellbore storage effect

### Six-well System



### Infinite-well System

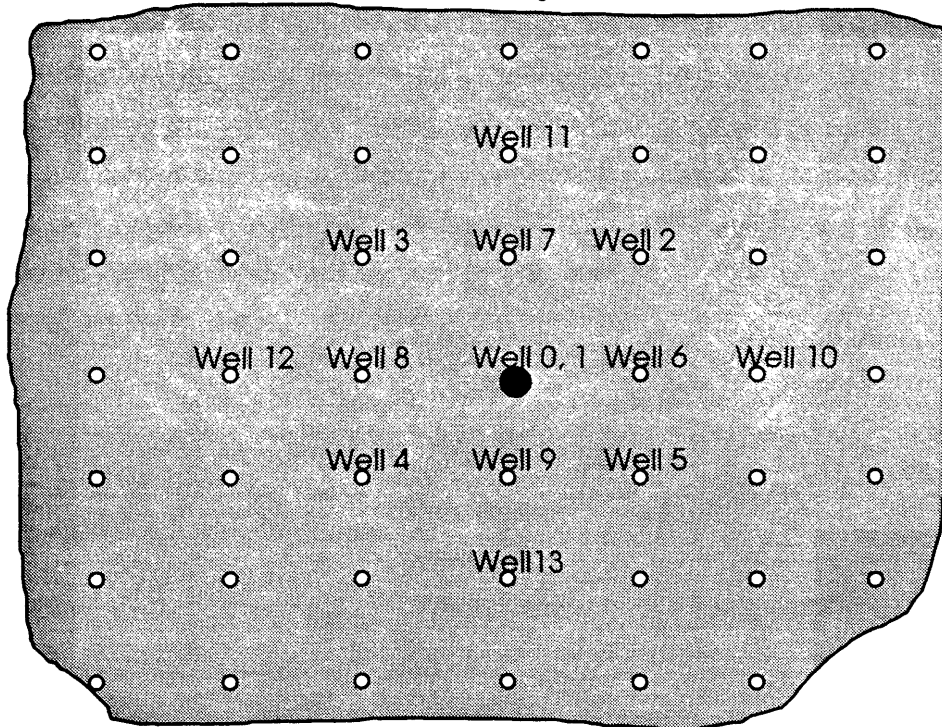


Figure 2.33: Configuration of six-well and infinite-well systems

$$\sum_{m=1}^{\infty} \sum_{n=1}^{\infty} [f(r_{m,n}) + f(r_{m,-n}) + f(r_{-m,n}) + f(r_{-m,-n})] \\ + \sum_{m=1}^{\infty} [f(r_{m,0}) + f(r_{-m,0}) + f(r_{0,m}) + f(r_{0,-m})]$$

where

$$f(r_{m,n}) = \frac{K_0(r_{m,n}\sqrt{z}/r_{eD})}{z^{\frac{3}{2}}(K_1(\sqrt{z}/r_{eD}) + C_D\sqrt{z}/r_{eD}K_0(\sqrt{z}/r_{eD}))}$$

and

$$r_{m,n} = \sqrt{(ma - x_w)^2 + (nb - y_w)^2} \frac{1}{r_w}.$$

With  $a = b = 500.0 \text{ ft}$ ,  $x_w = y_w = 0.0 \text{ ft}$  and  $r_w = 0.3 \text{ ft}$  as an example, Fig. 2.34 and Fig. 2.35 show the difference of drawdown and buildup curves between the two systems with and without wellbore storage effect, while Fig. 2.36 and Fig. 2.37 show only the buildup part of the response. The pressure in the infinite-well system drops more rapidly at long time, indicating a higher rate of depletion.

The solution for a well in a closed rectangular reservoir is equivalent to that of the infinite number of wells in an infinite reservoir. Eq. 2.32 can be extended to express the pressure response (drawdown or drawdown and buildup) for a well in a rectangle with closed boundary or constant pressure boundary.

For the drawdown case

$$\bar{p}_D(r_{1D}, r_{2D}, \dots, C_D, s) = \frac{(1 - e^{-st_{pD}}) \sum_{n=0}^{\infty} K_0(r_{nD}\sqrt{s})}{s^{\frac{3}{2}}(K_1(\sqrt{s}) + C_D\sqrt{s}K_0(\sqrt{s}))}. \quad (2.34)$$

For the drawdown and buildup case

$$\bar{p}_D(r_{1D}, r_{2D}, \dots, t_{pD}, C_D, z) = \frac{r_{eD}(1 - e^{-zt_{pD}/r_{eD}^2}) \sum_{n=0}^{\infty} K_0(r_{nD}\sqrt{z}/r_{eD})}{z^{\frac{3}{2}}(K_1(\sqrt{z}/r_{eD}) + C_D\sqrt{z}/r_{eD}K_0(\sqrt{z}/r_{eD}))}, \quad (2.35)$$

where  $r_{0D}$  is the distance between the testing well and the observation well, and  $r_{nD}$  represents the distance between the observation well and any image well or neighboring well. A similar expression could be written for a partial penetrating well in a

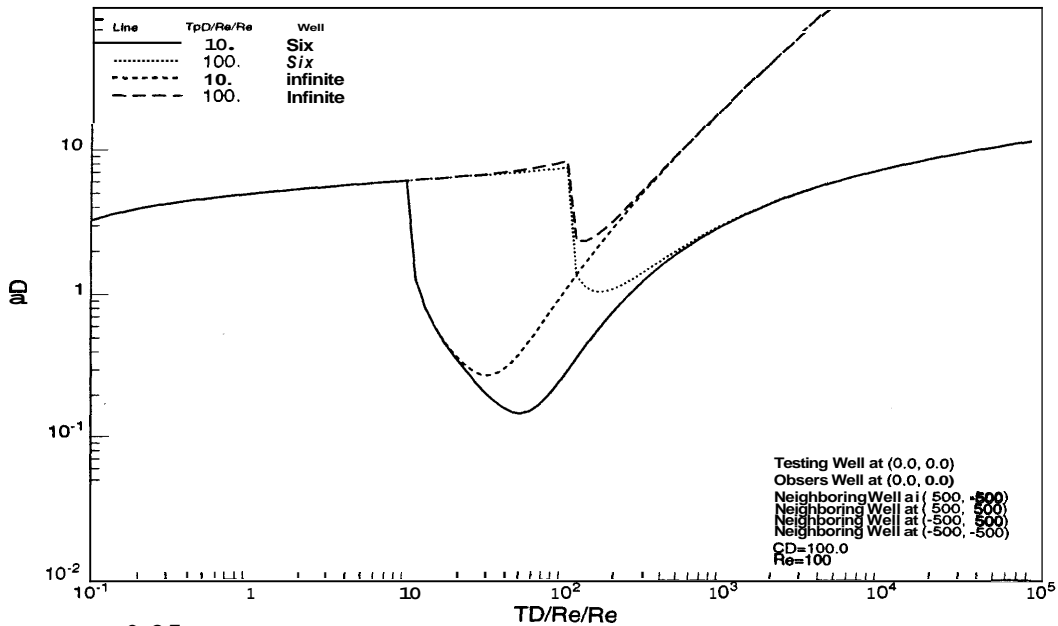
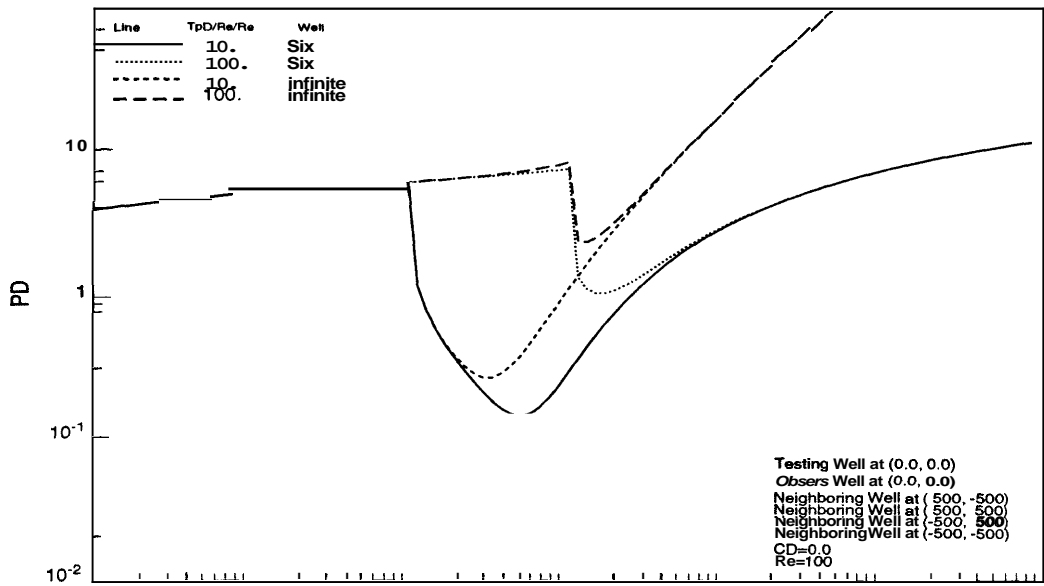


Figure 2.35: Pressure response versus production time and wellbore storage effect

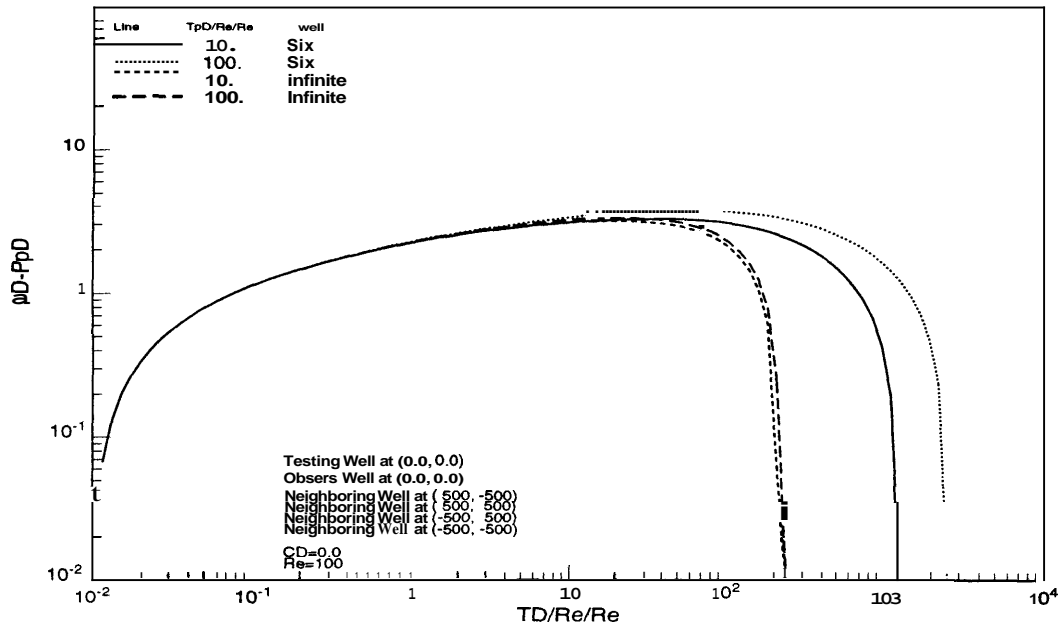


Figure 2.36: Pressure buildup response versus time after shut-in

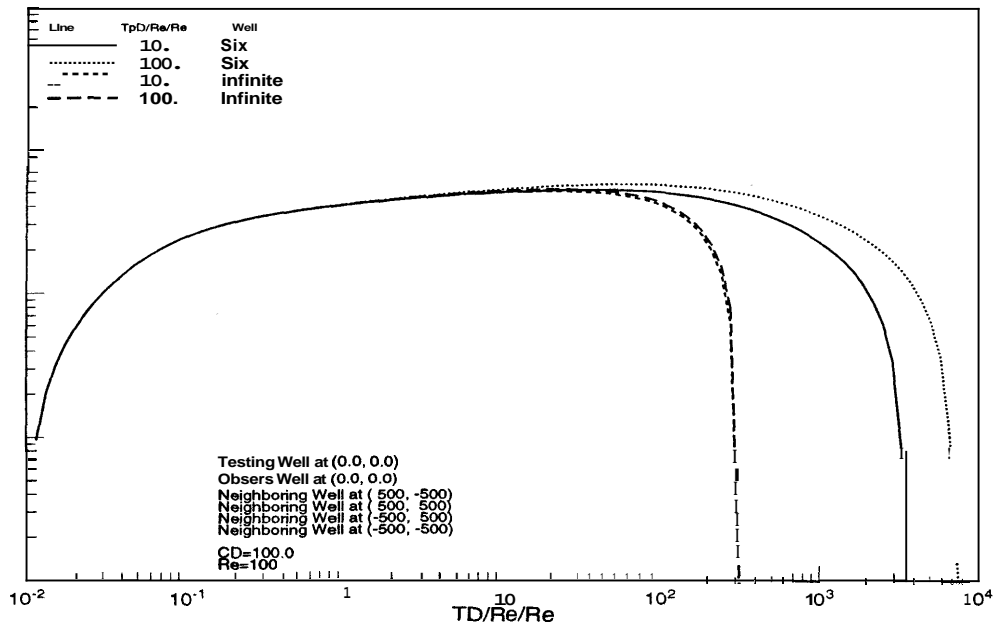


Figure 2.37: Pressure buildup versus time after shut-in and wellbore storage effect

reservoir with no flow or constant pressure boundary where superposition by imaging is applicable. As an example, the pressure responses are calculated in Fig. 2.38 and Fig. 2.39 for a rectangular reservoir of  $800\text{ft} \times 500\text{ft}$ , thickness  $50\text{ft}$ , permeability  $100\text{md}$  in radial direction and  $z$  direction. The testing well and observation well are located at  $(100\text{ft}, 100\text{ft})$  with well radius  $0.3\text{ft}$ . The well penetrates the upper 60% of the formation thickness and the pressure is measured both at the bottom of the well and at the top of the completion interval. The difference in pressure responses between the partial penetration and full penetration is noticeable in Fig. 2.38 and Fig. 2.39 from early time through late time. In well test analysis, if the partial penetration effect is not considered, the permeability of the reservoir will not be correctly interpreted.

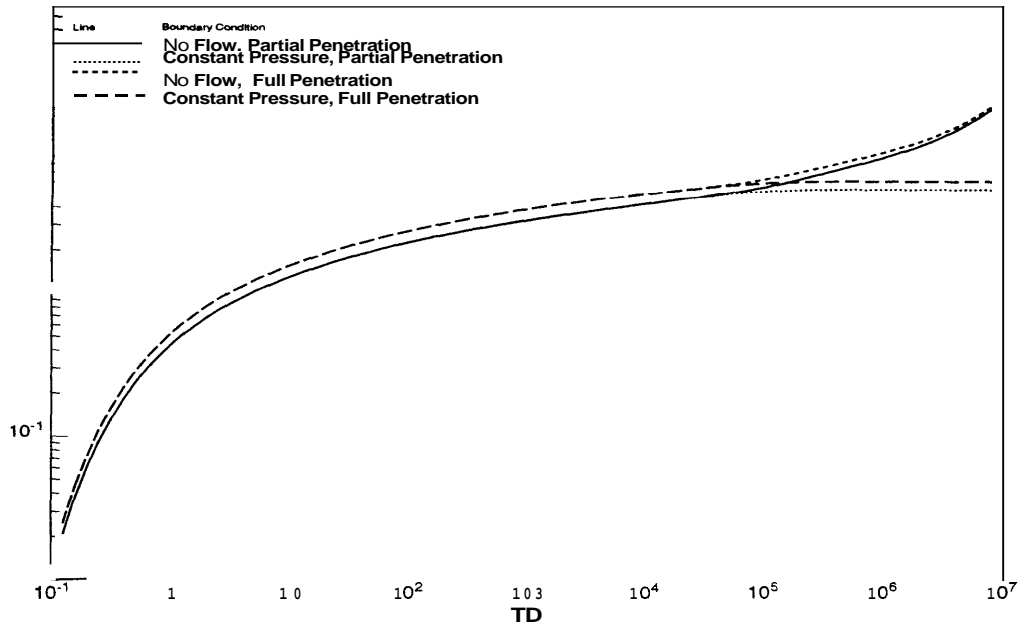


Figure 2.38: Drawdown pressure response versus production time

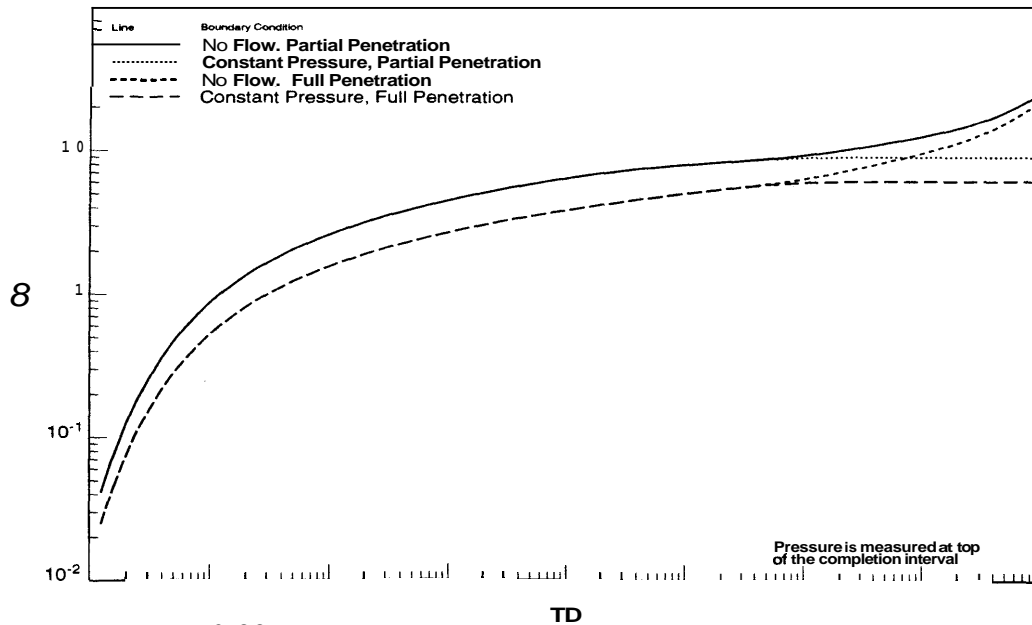


Figure 2.39: Drawdown pressure response versus production time



## 2.4 No-Flow Linear Boundary

For an infinite homogeneous reservoir with a linear no-flow boundary of infinite length, one method of locating the no-flow boundary is the *Inference Ellipse* method developed by Vela (1977). The *Inference Ellipse* method requires exactly two sets of interference data to determine the position of the no-flow boundary. If more than two sets of well pressure data are collected, as in most interference testing, using the inference ellipse method can only provide rough estimates about the location of the no-flow boundary and the result depends on which two sets of data are chosen. In this section, the pressure expression is formulated in consideration of applying multiple sets of the pressure data to locate the no-flow boundary position. The approach will be applied to the field pressure data in following section.

If the wellbore storage effect is included at the active well, the pressure solution in Laplace space would be

$$\begin{aligned} \bar{p}_D(r_{1D}, r_{2D}, z) = & \frac{r_{1D}(1 - e^{-zt_{pD}/r_{1D}^2})K_0(\sqrt{z})}{z^{\frac{3}{2}}(K_1(\sqrt{z}/r_{1D}) + C_D\sqrt{z}/r_{1D}K_0(\sqrt{z}/r_{1D}))} \\ & + \frac{r_{2D}(1 - e^{-zt_{pD}/r_{2D}^2})K_0(\sqrt{z})}{z^{\frac{3}{2}}(K_1(\sqrt{z}/r_{2D}) + C_D\sqrt{z}/r_{2D}K_0(\sqrt{z}/r_{2D}))} \end{aligned} \quad (2.36)$$

Consider a reservoir configured as in Fig. 2.40, where one active well and three observation wells are present. The shapes of the least square residual objective function are shown in Fig. 2.41 and Fig. 2.42. Pressure data, from two wells are used in Fig. 2.41 and the objective function has two local minima, leaving the interpretation result nonunique. However, if more than two sets of pressure data are used, there will be only one global minimum as in Fig. 2.42. This indicates that using multiwell interference pressure data simultaneously is necessary in locating the position of the no-flow boundary as well as in estimating permeability and storativity. The wellbore storage in the interference test is not important except when  $C_D/r_D^2$  becomes larger than 10. It can be seen from Eq. 2.36 that small  $r_D$  will contribute to the enlargement of the wellbore storage effect.

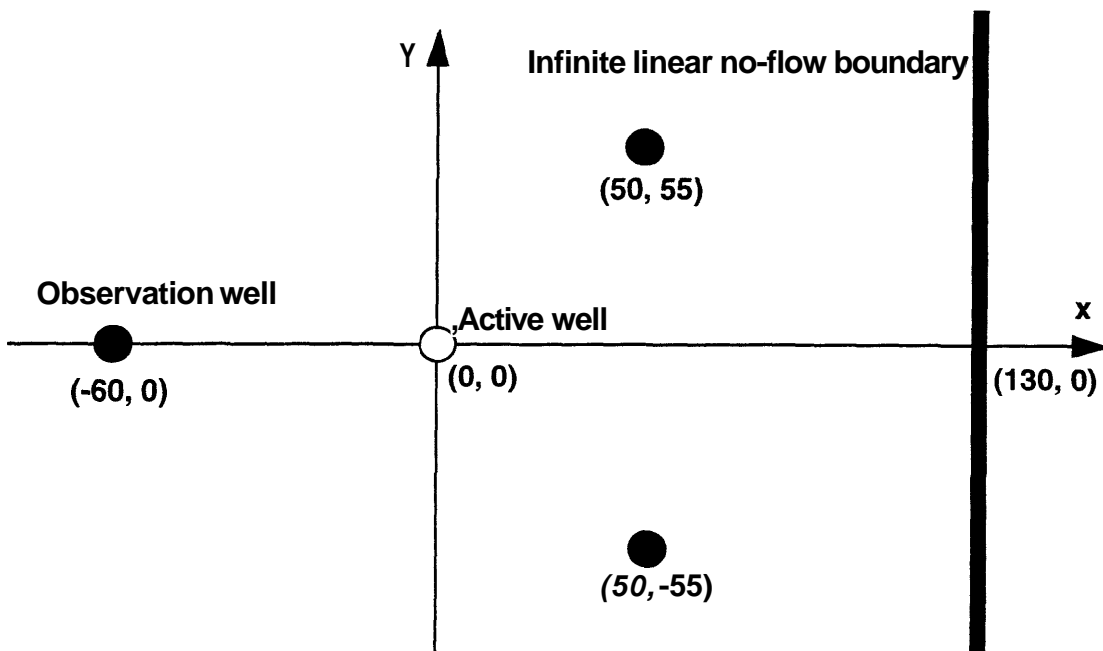


Figure 2.40: Well pattern for an infinite reservoir with a linear no-flow boundary

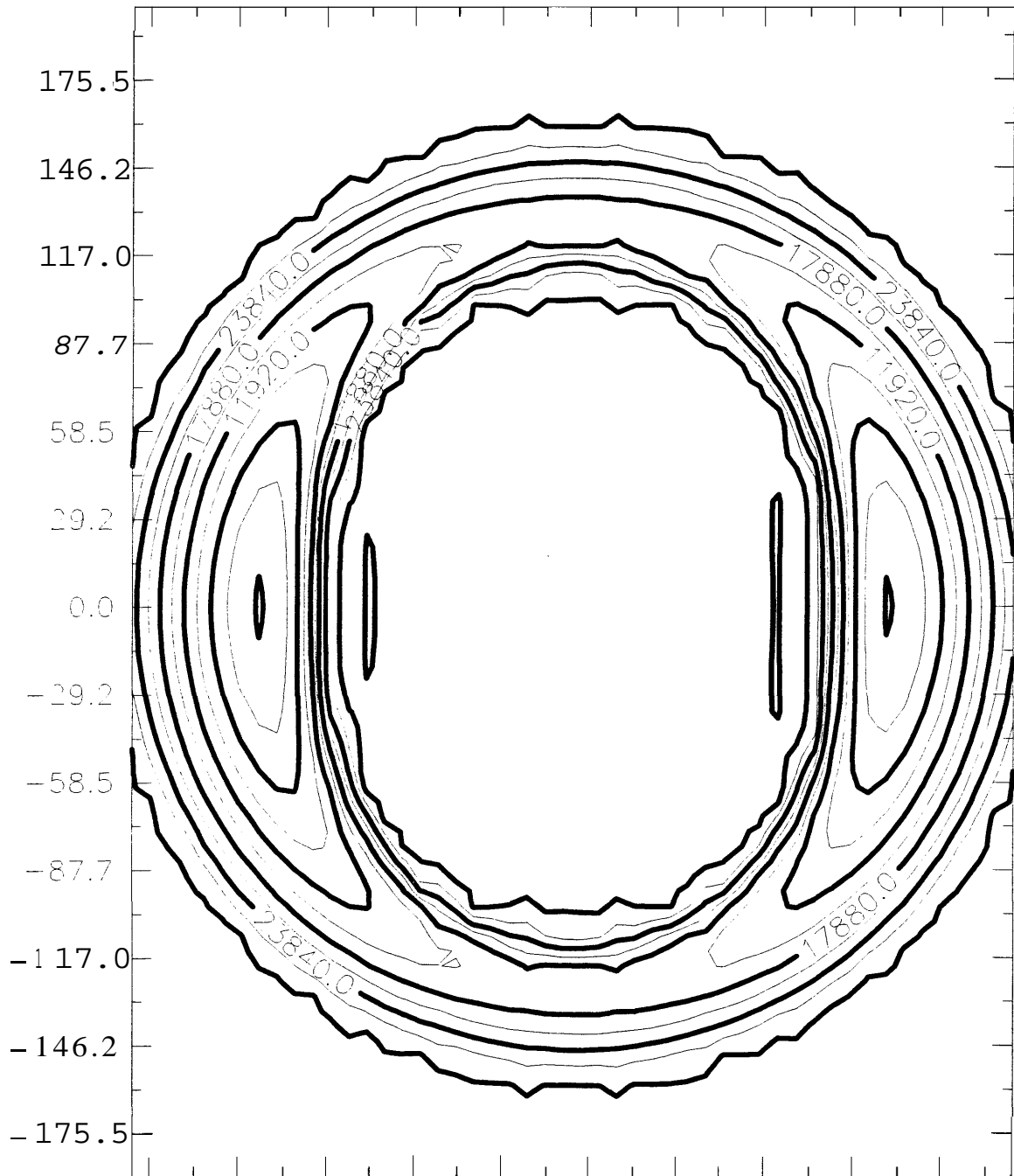


Figure 2.41: Contour of objective function using two sets of pressure data

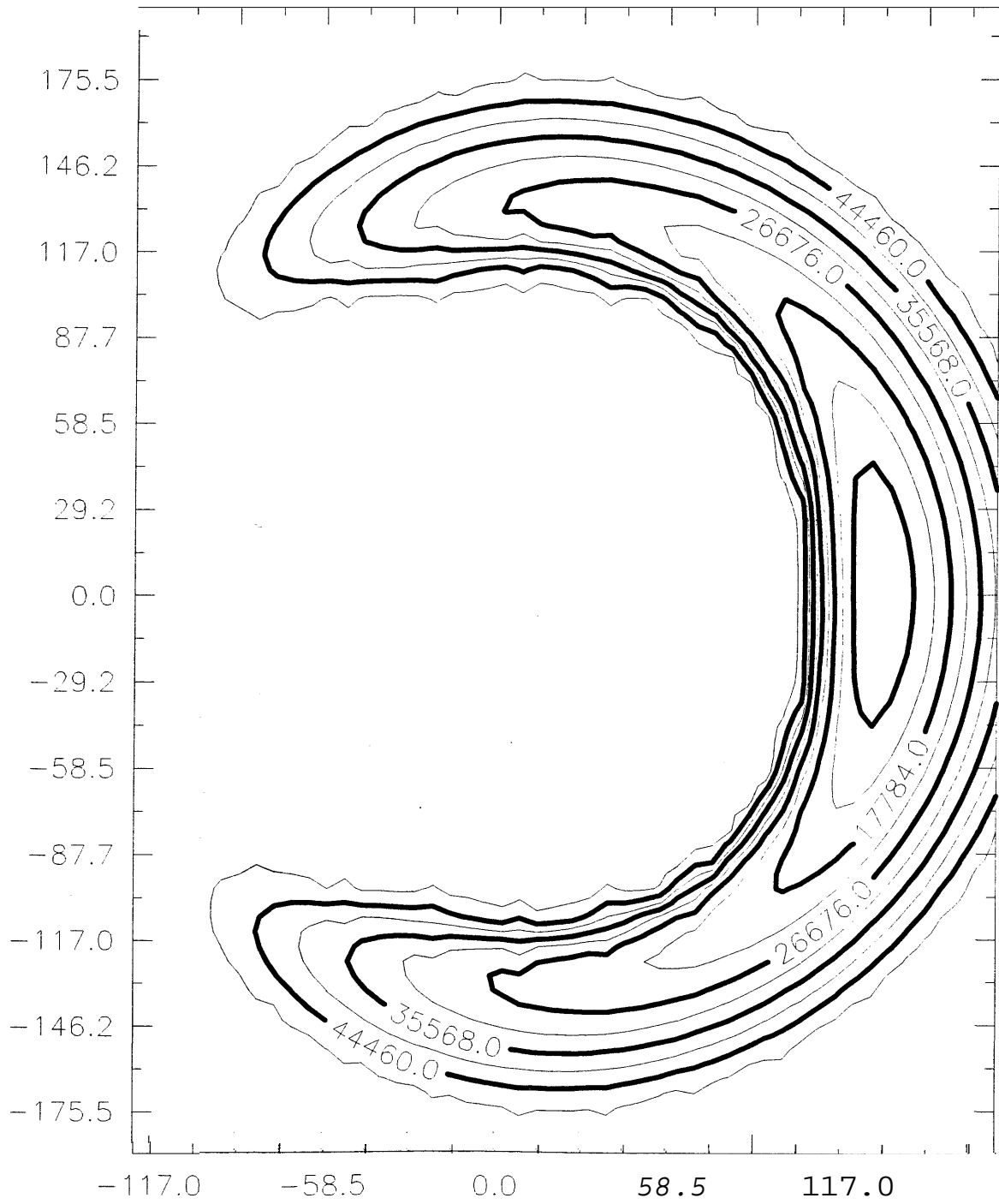


Figure 2.42: Contour of objective function using three sets of pressure data

## 2.5 Interpreting Multiwell Pressure Data of Ohaaki Geothermal Field

This section shows the interpretation of a set of interference data from Ohaaki geothermal field using nonlinear regression. Multiple sets of pressure data were used. The purpose was to identify how the no-flow boundary affects the result.

Using interference testing to evaluate reservoir heterogeneity and average transmissivity and storativity is a convenient and common method in geothermal fields. Twelve interference tests were conducted in the Ohaaki geothermal field among six wells at different times. *Leaver et al* (1988) analyzed these tests in an effort to identify a no-flow linear boundary using the inference ellipse method by *Vela* (1977). The pressure data sets were matched only one pair at a time. The results were dominated by the local transmissivity and storativity between or around the two wells; each match gave a different local average. It is hard to determine which value can be used as the average for the whole reservoir. Furthermore, the inference ellipse method carries some uncertainty in deciding the location of linear boundary, since two pairs of data provide two inference ellipses that are sufficient to determine the location of linear boundary. A better approach is to match all the pairs simultaneously to give consistent results.

The parameters matched were bulk transmissivity  $kh/\mu$ , storativity  $\phi_{ct}h$ , the location of linear boundary (two coordinate variables) and the initial pressures of each active well. There are twelve sets of interference pressure data available, which means we have sixteen parameters to be matched in our model. The theoretical drawdown and buildup curves used in our analysis were similar to those developed by *Eipper* (1985), but the linear boundary effect has been included in the curves in order to regress on all the parameters together. To make this possible, a Cartesian coordinate was created with *BR20* as the origin, so the location of each well is represented by a pair of numbers  $(x, y)$  as follows:

**BR23** (0.0, 0.0)

**BR13** (-1079.9, -1977.3)

**BR23** (-527, -1230.31)

**BR31** (-1757.5, -878.8)

**BR34** (-2680.3, -2636.4)

**BR19** (-1318, -659.1)

We represented the linear boundary by another pair of  $(x, y)$ , the coordinates of one point on the boundary that are nearest to the origin of our Cartesian coordinates. The algorithm used to solve this nonlinear regression problem is the same modified *Fletcher* (1971) method discussed in Section 2.2.4.

The results from *Leaver et al* (1988) are presented in Fig. 2.43 and listed as follows with an average set of values:

$$kh = 250.0 \text{ d ft} \quad \phi_{c_t}h = 80.0 \text{ ft/psi} \times 10^4 \quad x_b = -1494.0 \text{ ft} \quad y_b = 2724.0 \text{ ft}.$$

This interpretation gives a residual of  $1.999 \text{ psi}^2$  per data point (there are 1969 data points for all 12 wells). Starting from this result as an initial guess, after 11 iterations, the algorithm found a solution as shown in Fig. 2.44:

$$kh = 547.92477 \quad \phi_{c_t}h = 119.91531 \quad x_b = -1981.07651 \quad y_b = -1631.12899,$$

which gave an average residual of  $1.4366 \text{ psi}^2$  per point. Notice that tests B7 and B8 are worse than before, because they have fewer points and contribute less to the residual.

Adding the twelve initial pressures of the active wells as parameters, we were able to reduce the residual to  $0.97 \text{ psi}^2$  per data point as shown in Fig. 2.45 with estimated parameter values as follows:

$$\begin{aligned} kh &= 584.96150 & \phi_{c_t}h &= 47.34690 & x_b &= -3031.12267, & y_b &= -2076.63377 \\ p_i^{B1} &= -7.11689 & p_i^{B2} &= -10.50041 & p_i^{B3} &= -53.15206 & p_i^{B4} &= 14.30722 \\ p_i^{B6} &= -9.13517 & p_i^{B7} &= -117.83430 & p_i^{B8} &= -67.89931 & p_i^{B9} &= 297.20062 \\ p_i^{B10} &= -32.76060 & p_i^{C1} &= 3.36854 & p_i^{C2} &= -24.25505 & p_i^{C3} &= -6.17686 \end{aligned}$$

From Fig. 2.45, we see that four sets of data B6, B7, B8 and B9 are not well-behaved. Excluding these four sets, we performed the matching again with the remaining eight sets of pressure data. Fig. 2.46 is the matching result without initial pressures as parameters but with weights to emphasize the early data. The result is

$$kh = 734.75503 \quad \phi c_t h = 52.16619 \quad x_b = -1663.09485 \quad y_b = -2883.21636$$

With initial pressures as parameters without emphasis on early data, we have (Fig. 2.47):

$$\begin{aligned} kh &= 659.31439 & \phi c_t h &= 32.35258 & x_b &= -5067.12074 & y_b &= 18.74405 \\ p_i^{B1} &= -4.88181 & p_i^{B2} &= -2.75039 & p_i^{B3} &= -54.73846 & p_i^{B4} &= 14.38455 \\ p_i^{B10} &= -29.48337 & p_i^{C1} &= 12.12687 & p_i^{C2} &= -14.24363 & p_i^{C3} &= 14.83868 \end{aligned}$$

With weights and initial pressures as parameters, we end up with

$$\begin{aligned} kh &= 630.98879 & \phi c_t h &= 33.71702 & x_b &= -1506.85394 & y_b &= 2749.59898 \\ p_i^{B1} &= -4.41652 & p_i^{B2} &= 0.37996 & p_i^{B3} &= -61.96414 & p_i^{B4} &= 17.10718 \\ p_i^{B10} &= -34.01868 & p_i^{C1} &= 5.96005 & p_i^{C2} &= -28.81102 & p_i^{C3} &= 17.35140 \end{aligned}$$

as shown in Fig. 2.48. All the results were calculated with  $h = 2297.0 \text{ ft}$  and  $\mu = 0.34 \text{ cp}$ . Notice that in B3 of Fig. 2.46 we see the calculated type curve parallel above the actual data and we can not shift the curve vertically without sacrificing other matches. All the data affect each other here. When the initial pressures are allowed to vary, the actual data of B3 are increased by the same amount, resulting in the early data having a big jump in the log-log graphs as in Fig. 2.47 and Fig. 2.46.

The location of the linear boundary is sensitive to the sets of data used. It is more likely that there is a northwest/southeast trend of faults, and we always had a higher estimate of average permeability than the value  $110 \text{ md}$  as suggested by *Leaver et al* (1988).

Type-curve Match for Multi-well Pressure Data of Ohaaki Geothermal Field

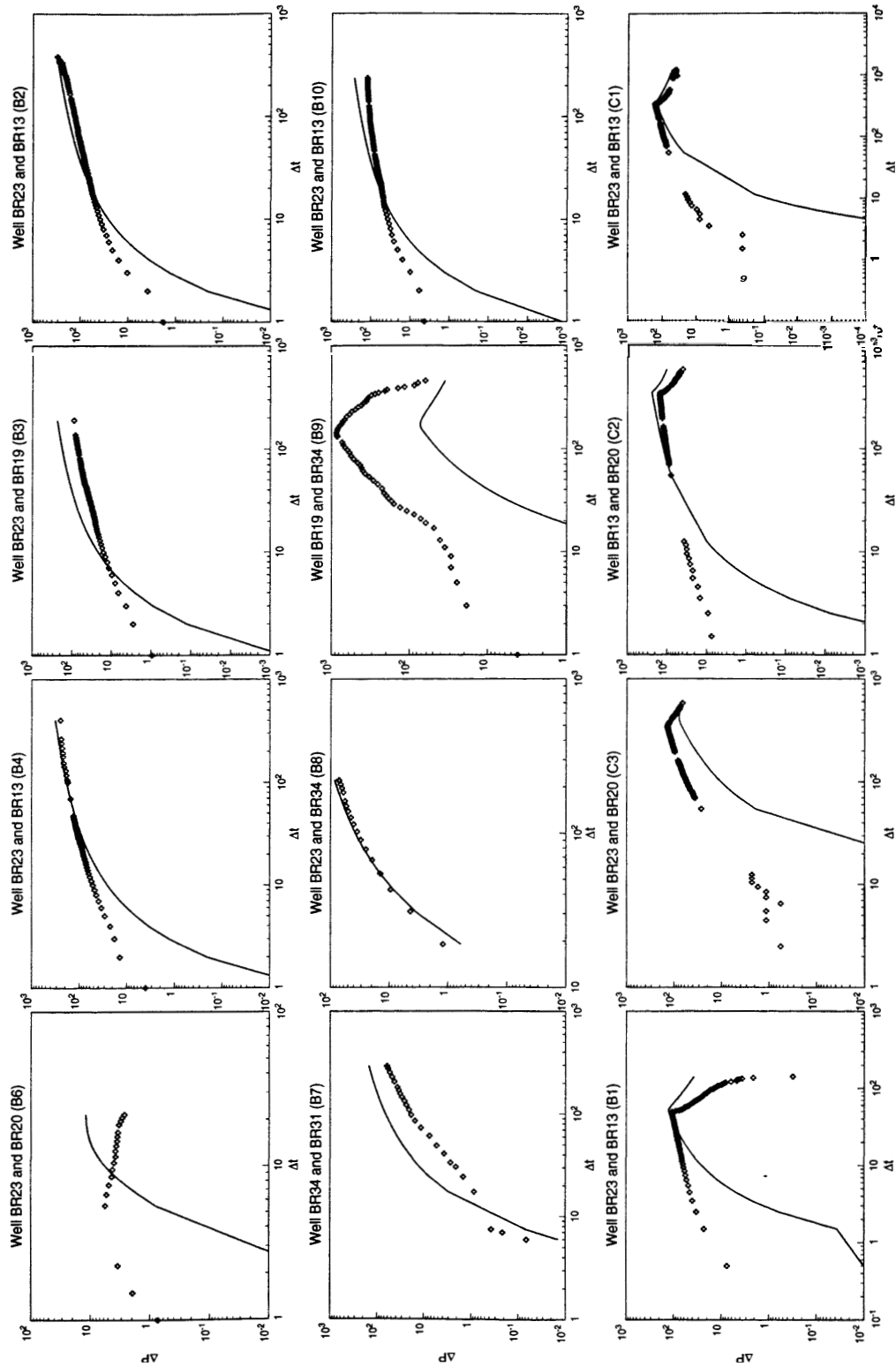


Figure 2.43: Approximate matching results from *Leaver et al* (1988)



Type-curve Match for Multi-well Pressure Data of Ohaaki Geothermal Field

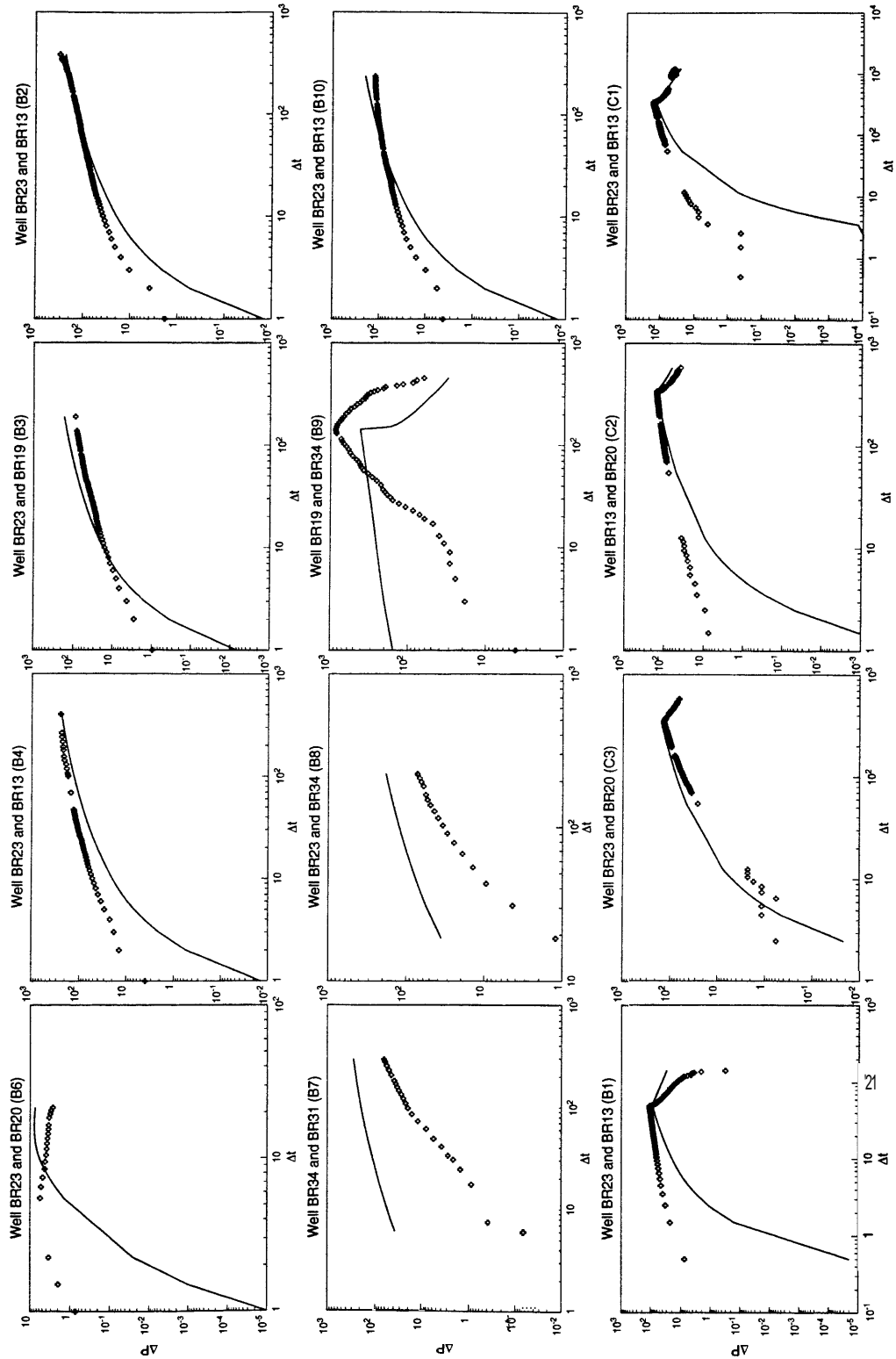


Figure 2.44: Matching results without weights and initial pressures as parameters

Type-curve Match for Multi-well Pressure Data of Chaaki Geothermal Field

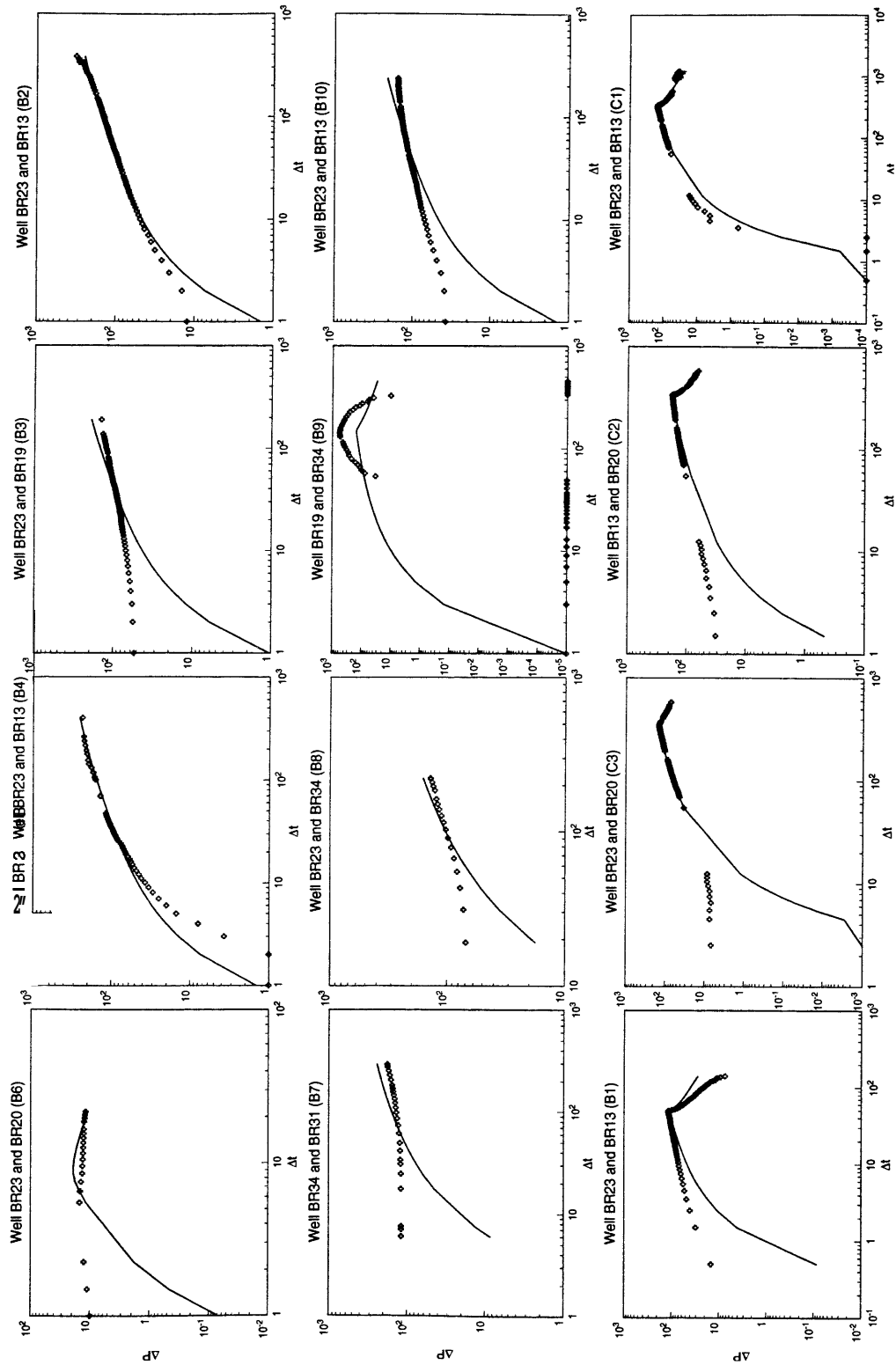


Figure 2.45: Matching results with initial pressures as parameters

Type-curve Match for Multi-well Pressure Data of Ohaaki Geothermal Field

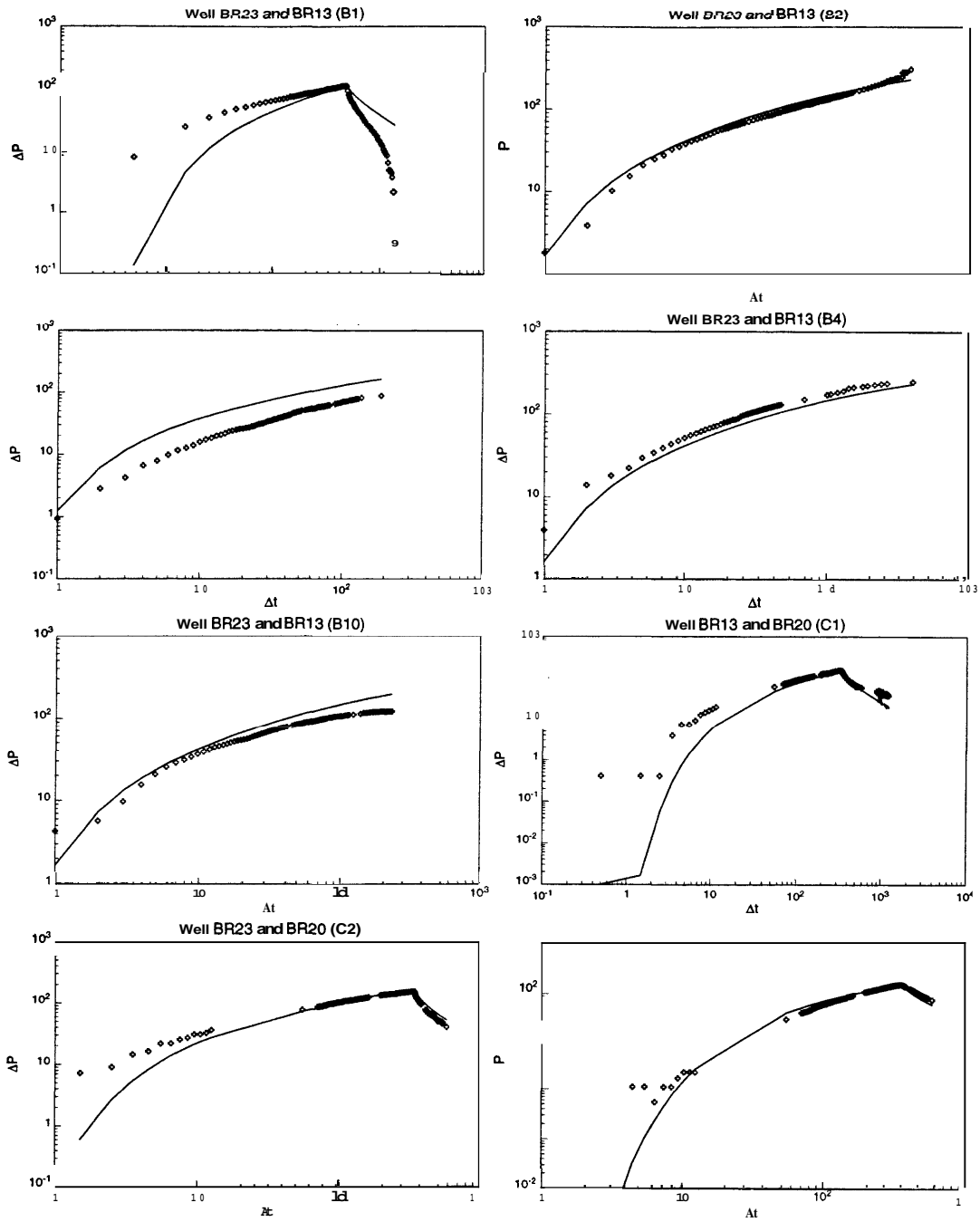


Figure 2.46: Matching results with weights emphasizing early data

Type-curve Match for Multi-well Pressure Data of Ohaaki Geothermal Field

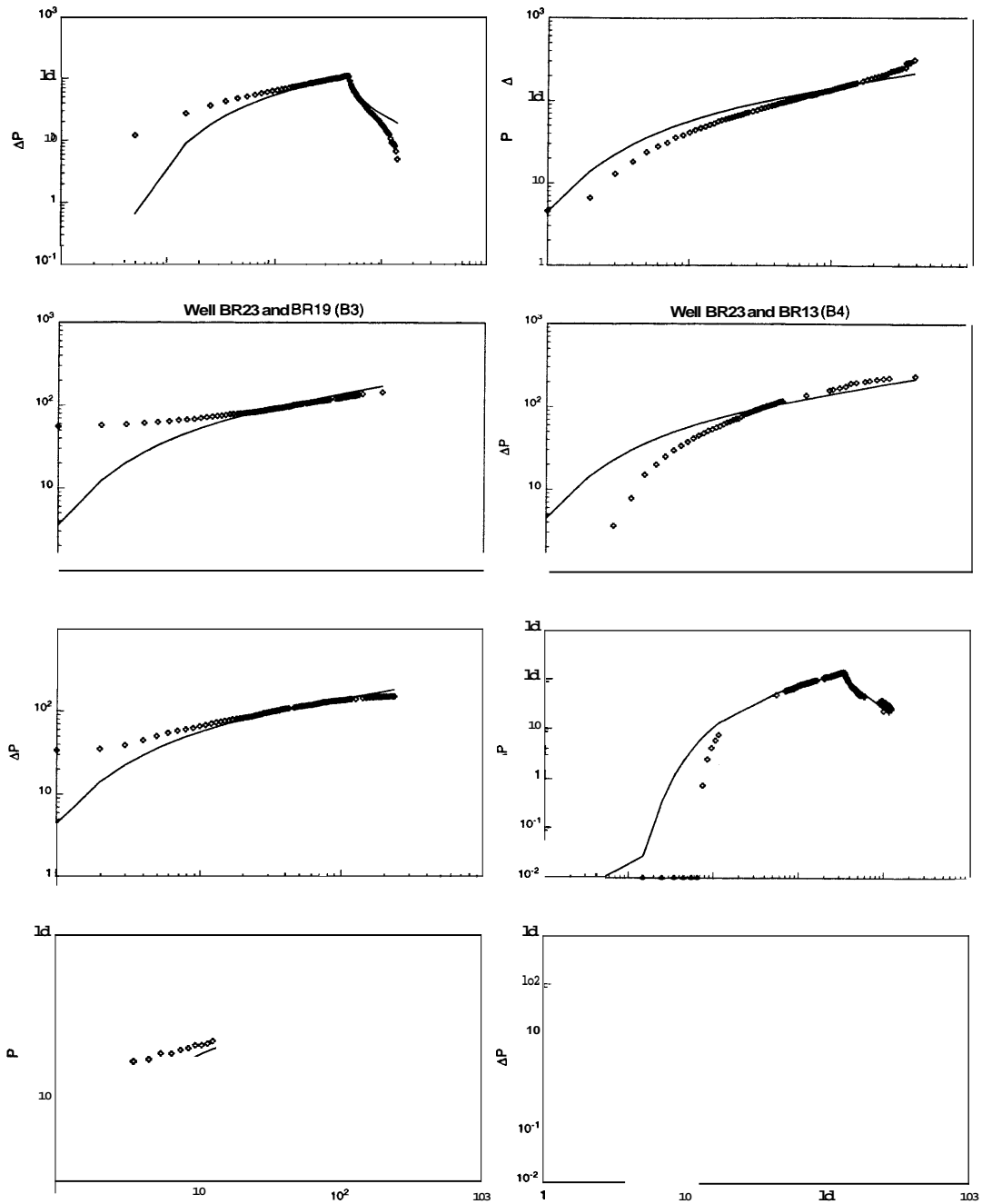


Figure 2.47: Matching results with initial pressures as parameters

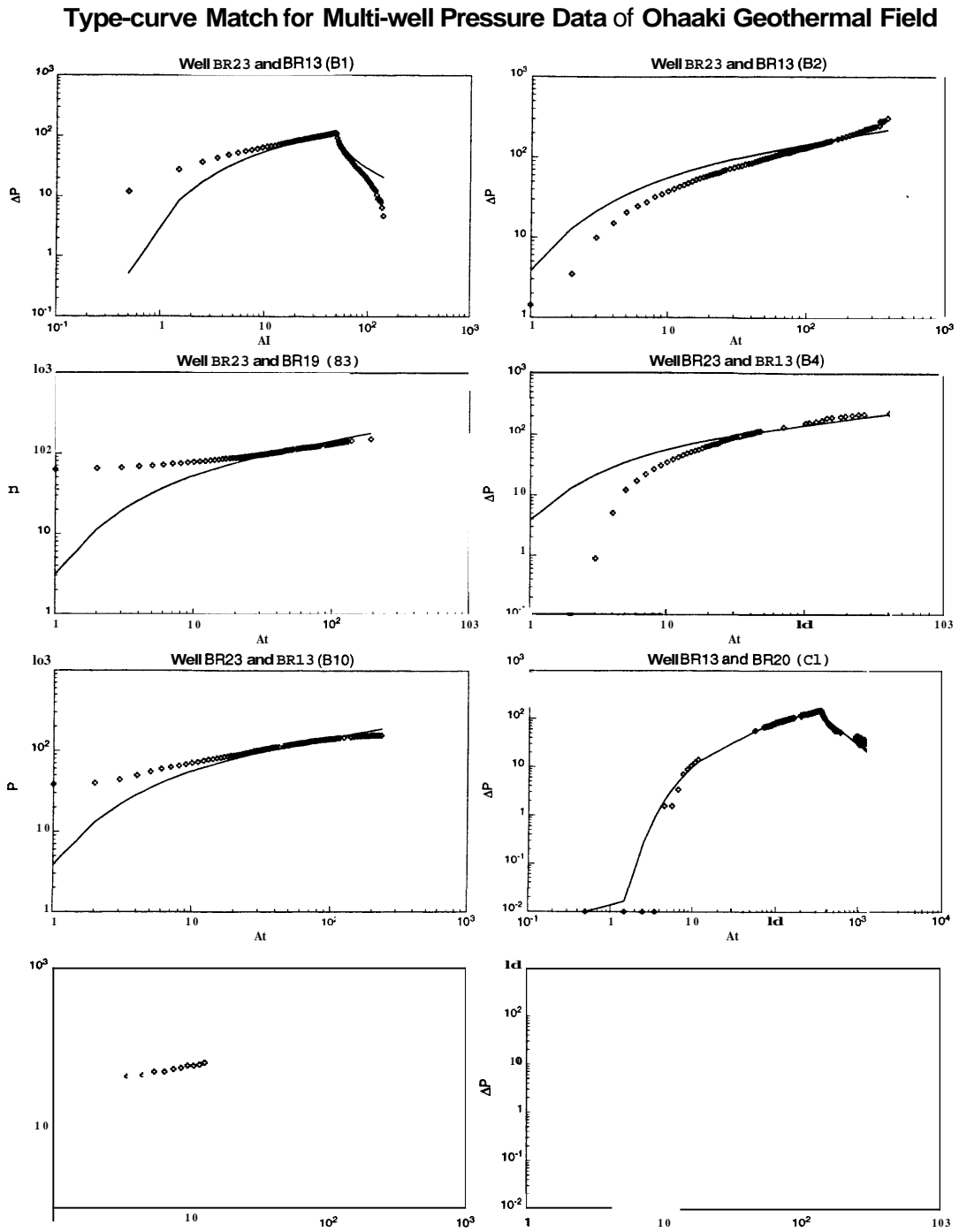


Figure 2.48: Matching results with weights and initial pressures as parameters

## Chapter 3

# Green's Functions and the Reciprocity Principle in Heterogeneous Media

This chapter starts with the definition of the Green's function for heterogeneous reservoirs and the discussion of its properties. The general expression to represent pressure in terms of Green's functions is presented. Through some examples, it is shown that the Green's function method is still a helpful tool in finding analytical pressure solutions for heterogeneous reservoirs even though it loses the useful Newman product property.

The Principle of reciprocity is discussed next. The effect of wellbore storage and skin on reciprocity is also included. Finally, using Green's functions in tracer flow problems is briefly discussed.

### 3.1 Definition of Green's Functions

For pressure transient calculations in a homogeneous formation, the Green's function is usually defined as the pressure response at  $(x, y, z)$  at time  $t$  due to an instantaneous point source of unit strength generated at point  $(x', y', z')$  at time  $\tau$ , with the reservoir being initially at a constant pressure  $p_i$ , and the boundary being kept without flow

or at the same constant pressure  $p_i$ . So, the Green's function  $G(x, y, z, x', y', z', t - \tau)$  is the solution to the following equation,

$$\frac{\partial^2 G}{\partial x^2} + \frac{\partial^2 G}{\partial y^2} + \frac{\partial^2 G}{\partial z^2} \equiv \frac{\phi \mu c_t}{k} \frac{\partial G}{\partial t} \quad (3.1)$$

$$G(x, y, z, x', y', z', 0) = \delta(x - x')\delta(y - y')\delta(z - z') \quad (3.2)$$

where  $\delta(x)$  is the Dirac function, which is handled algebraically as if it were an ordinary function with the following properties,

$$\delta(x) = 0 \text{ for } x \neq 0$$

$$\int_{-\infty}^{\infty} \delta(x) dx = 1$$

$$\int_{-\infty}^{\infty} f(x)\delta(x) dx = f(0)$$

and

$$\int_{-\infty}^{\infty} f(y)\delta(x - y) dy = f(x)$$

for every arbitrary continuous function  $\phi(x)$ . However this definition of Green's function can not be used directly for heterogeneous reservoirs, since the coefficients of the flow equation for heterogeneous reservoir are not constant.

There are two ways to define the Green's function for heterogeneous formations. One treats the instantaneous source still as an initial condition and the time range involved is  $[0, \infty]$ :

$$\begin{aligned} & \frac{\partial}{\partial x} \frac{k(x, y, z)}{\mu(x, y, z)} \frac{\partial G}{\partial x} + \frac{\partial}{\partial y} \frac{k(x, y, z)}{\mu(x, y, z)} \frac{\partial G}{\partial y} + \frac{\partial}{\partial z} \frac{k(x, y, z)}{\mu(x, y, z)} \frac{\partial G}{\partial z} \\ & = \phi(x, y, z) c_t(x, y, z) \frac{\partial G}{\partial t} \end{aligned} \quad (3.3)$$

$$G(x, y, z, x', y', z', 0) = \frac{\delta(x - x')\delta(y - y')\delta(z - z')}{\phi(x', y', z') c_t(x', y', z')} \quad (3.4)$$

Another way treats the instantaneous source as a source with strength concentrated at time  $\tau$ , the time range as  $(-\infty, \infty)$  and restricts the solution to be zero for  $t < \tau$ . So  $G(x, y, z, x', y', z', t - \tau)$  is a solution of the following equation:

$$\frac{\partial}{\partial x} \left( \frac{k(x, y, z)}{\mu(x, y, z)} \frac{\partial G}{\partial x} \right) + \frac{\partial}{\partial y} \left( \frac{k(x, y, z)}{\mu(x, y, z)} \frac{\partial G}{\partial y} \right) + \frac{\partial}{\partial z} \left( \frac{k(x, y, z)}{\mu(x, y, z)} \frac{\partial G}{\partial z} \right) = \phi(x, y, z) c_t(x, y, z) \frac{\partial G}{\partial t} - \delta(x - x') \delta(y - y') \delta(z - z') \delta(t - \tau) \quad (3.5)$$

$$G(x, y, z, x', y', z', t) = 0 \text{ for } t < \tau. \quad (3.6)$$

$k, \mu, \phi$  and  $c_t$  above are all functions of  $(x, y, z)$ , continuous throughout the reservoir, or continuous within several subdomains of the reservoir and discontinuous on the subdomains' boundaries along which additional conditions of continuous pressure and material balance are maintained.

These two definitions are equivalent in some sense. Assume  $G_1$  and  $G_2$  are Green's functions from the first and the second definitions respectively, then

$$G_2(x, y, z, x', y', z', t - \tau) = G_1(x, y, z, x', y', z', t - \tau) H(t - \tau) \quad (3.7)$$

where

$$H(t - \tau) = \begin{cases} 1 & \text{if } t \geq \tau \\ 0 & \text{otherwise} \end{cases} \quad (3.8)$$

If  $G_1$  satisfies Eqs. 3.3 and 3.4, then

$$\frac{\partial}{\partial x_i} \left( \frac{k}{\mu} \frac{\partial G_2}{\partial x_i} \right) = \frac{\partial}{\partial x_i} \left( \frac{k}{\mu} \frac{\partial G_1}{\partial x_i} \right) \cdot H(t - \tau) = \phi c_t \frac{\partial G_1}{\partial t} H(t - \tau)$$

$$\phi c_t \frac{\partial G_1}{\partial t} H(t - \tau) = \phi c_t \frac{\partial [G_1 H(t - \tau)]}{\partial t} - \phi c_t G_1(0) \delta(t - \tau)$$

so  $G_2$  satisfies Eqs. 3.5 and 3.6. We chose the first approach which is easier to understand and has more obvious physical meaning. It defines the Green's function as the pressure response due to an instantaneous source of a strength related to the storativity at the source location, rather than due to an always unit strength as in the homogeneous case.



## 3.2 Properties of Green's Functions

From the definition, some properties can be inferred for Green's functions in heterogeneous reservoirs. Those properties will be applied to derive the expression for the general pressure response in terms of Green's function.

1. Principle of reciprocity:

$$G(x, y, z, x', y', z', t - \tau) = G(x', y', z', x, y, z, t - \tau) \quad (3.9)$$

Proof is included in Appendix C. Once we have this reciprocity for a Green's function due to an instantaneous point source, it is not difficult to derive the conditions of reciprocity for the general pressure due to any kind of source.

2.  $G(x, y, z, x', y', z', t - \tau)$  as a function of  $(x', y', z', \tau)$  satisfies:

$$\begin{aligned} \frac{\partial}{\partial x'} \frac{k(x', y', z')}{\mu(x', y', z')} \frac{\partial G}{\partial x'} + \frac{\partial}{\partial y'} \frac{k(x', y', z')}{\mu(x', y', z')} \frac{\partial G}{\partial y'} + \\ \frac{\partial}{\partial z'} \frac{k(x', y', z')}{\mu(x', y', z')} \frac{\partial G}{\partial z'} = -\phi c_t(x', y', z') \frac{\partial G}{\partial \tau} \end{aligned} \quad (3.10)$$

3. The initial condition gives:

$$\begin{aligned} \lim_{t \rightarrow \tau^+} \iiint_{\Omega} \phi c_t(x', y', z') f(x', y', z') \\ G(x, y, z, x', y', z', t - \tau) dx' dy' dz' = f(x, y, z) \end{aligned} \quad (3.11)$$

4. If the outer boundary of domain  $\Omega$  is closed or no-flow, then for  $t > \tau$ :

$$\int_{\Omega} \phi(x', y', z') c_t(x', y', z') G(x, y, z, x', y', z', t - \tau) d\Omega = 1 \quad (3.12)$$

The Newman's product theorem presented by *Newman (1936)* does not hold in heterogeneous reservoirs. This is a major limitation on the use of Green's functions for heterogeneous problems. The Green's functions have to be found individually, instead of being constructed from existing easier solutions. This restriction comes from the fact that the domain can not be decomposed as in the homogeneous case, for instance, a cubic region (three-dimensional) is no longer the product of three one-dimensional intervals.

### 3.3 Pressure in Terms of Green's Functions

The Green's function is the pressure response due to an instantaneous point source in the reservoir with homogeneous boundary conditions. With that, we can derive the pressure response due to any kind of source in the reservoir and with any non-homogeneous boundary condition. Suppose that the distribution of pressure in the reservoir is initially  $g(x, y, z)$ , and the source in the reservoir is  $f(x, y, z, t)$  at point  $(x, y, z)$ , at time  $t$  with a unit *volume rate of injection per unit volume of reservoir*, then the pressure can be expressed in terms of the Green's function:

$$p(x, y, z, t) = \int_0^t \int_{S_e} \frac{k}{\mu} \left( G \frac{\partial p}{\partial n} + p \frac{\partial G}{\partial n} \right) dS_e d\tau - \int_0^t \int_{\Omega} G \cdot f dx' dy' dz' d\tau + \int_{\Omega} \phi c_t G(t) \cdot g dx' dy' dz' \quad (3.13)$$

The detailed derivation is included in Appendix B.

### 3.4 Examples of Green's Functions

Without the Newman product scheme it is more difficult to find the Green's function for a heterogeneous region. Appropriate mathematical method is needed for the method to be successful in heterogeneous reservoirs. In this section, several mathematical methods are presented with examples in finding Green's functions for some interesting and practical distributions of permeability and porosity.

#### 3.4.1 Case 1: Separation of Variables

In a one-dimensional finite region, usually the time variable  $t$  and the space variable  $x$  can be separated. Consider the problem in region  $0 < x < 1$ , with  $\frac{k(x)}{\mu(x)} = e^x$ ,  $\phi(x)c_t(x) = e^x$  and a constant pressure boundary. We need to find the solution to:

$$\frac{\partial}{\partial x} \left( e^x \frac{\partial G}{\partial x} \right) = e^x \frac{\partial G}{\partial t} \quad 0 < x < 1, \quad t > 0 \quad (3.14)$$

$$G(x, x', 0) = \frac{\delta(x - x')}{e^{x'}} \quad (3.15)$$

$$G(0, x', t) = G(1, x', t) = 0 \quad t > 0. \quad (3.16)$$

The corresponding Sturm-Liouville problem is:

$$\frac{d}{dx} \left( e^x \frac{dX}{dx} \right) + \lambda e^x X = 0 \quad (3.17)$$

$$X(0) = X(1) = 0. \quad (3.18)$$

The equivalent equation

$$X'' + X' + \lambda X = 0 \quad (3.19)$$

gives

$$X(x) = \begin{cases} C_1 e^{\frac{1}{2}(-1+\sqrt{1-4\lambda})x} + C_2 e^{\frac{1}{2}(-1-\sqrt{1-4\lambda})x} & \text{if } \lambda \leq \frac{1}{4} \\ e^{-\frac{1}{2}x} [C_1 \cos(\frac{\sqrt{4\lambda-1}}{2}x) + C_2 \sin(\frac{\sqrt{4\lambda-1}}{2}x)] & \text{if } \lambda > \frac{1}{4} \end{cases} \quad (3.20)$$

where  $C_1$ ,  $C_2$  and  $\lambda$  are decided from the boundary condition (Eq. 3.18),

$$\lambda = n^2\pi^2 + \frac{1}{4}, \quad n = 1, 2, \dots \quad (3.21)$$

with  $C_1 = 0$  and eigenfunction:

$$G_n(x, t) = C_n e^{-(n^2\pi^2+1/4)t-x/2} \sin n\pi x \quad (3.22)$$

Using the initial condition, multiplying by  $e^{\frac{x}{2}} \sin n\pi x$ , then  $C_n = 2e^{-\frac{x'}{2}} \sin n\pi x'$ , and the Green's function is:

$$G(x, x', t) = 2e^{-\frac{x'+x}{2}-\frac{t}{4}} \sum_{n=1}^{\infty} e^{-n^2\pi^2 t} \sin n\pi x' \sin n\pi x \quad (3.23)$$

With the approach of variable separation, Green's functions can be found for one-dimensional flow problems with the following distributions of mobilities and storativities, where either could be scaled by a constant:

- $k(x)/\mu(x) = x$ ,  $\phi(x)C_t(x) = x$  in region  $[-1, 1]$ .
- $k(x)/\mu(x) = 1 - x^2$ ,  $\phi(x)C_t(x) = 1$  in region  $[-1, 1]$ .
- $k(x)/\mu(x) = e^{-x^2}$ ,  $\phi(x)C_t(x) = e^{-x^2}$  in region  $(-\infty, \infty)$ .

- $k(x)/\mu(x) = xe^{-x}$ ,  $\phi(x)C_t(x) = e^{-x}$  in region  $[0, \infty)$ .
- $k(x)/\mu(x) = (1-x)^{p-q+1}x^q$ ,  $\phi(x)C_t(x) = (1-x)^{p-q}x^{q-1}$  where  $q \geq 1, p-q \geq 0$  in region  $[-1, 1]$ .
- $k(x)/\mu(x) = a(x-b)^2$ ,  $\phi(x)C_t(x) = 1$  in region  $[0, \infty)$ .
- $k(x)/\mu(x) = a(x-b)^3$ ,  $\phi(x)C_t(x) = x-b$  in region  $[0, \infty)$ .

Special functions are involved in those solutions. Notice that we can not specify a boundary condition at a place where mobility vanishes.

### 3.4.2 Case 2: Fourier Transformation

When the eigenvalue problem resulted from the separation of variables has a continuous spectrum, Fourier transformation is a good choice.

Let us try to find the Green's function in a two-dimensional infinite reservoir with a plane interface at  $x = 0$  which separates the reservoir into two regions with different properties of storativity and mobility.

Assume that the mobility and storativity are  $\lambda_1$  and  $\eta_1$  respectively for the half space  $x > 0$  and  $\lambda_2$  and  $\eta_2$  respectively for the other half  $x < 0$ . Without loss of generality, the position of the instantaneous source can be taken to be at  $(x', 0)$ .

The free space Green's function in Laplace space is

$$\bar{u}_1 = \frac{1}{2\pi\eta_1} K_0(z_1 \sqrt{(x-x')^2 + y^2}) \quad (3.24)$$

Assume in region 1 that  $G = u_1 + w$  and in region 2 that  $G = v$ , then in Laplace space we need to solve:

$$\frac{\partial^2 \bar{w}}{\partial x^2} + \frac{\partial^2 \bar{w}}{\partial y^2} - z_1^2 \bar{w} = 0 \quad \text{for } x > 0 \quad (3.25)$$

$$\frac{\partial^2 \bar{v}}{\partial x^2} + \frac{\partial^2 \bar{v}}{\partial y^2} - z_2^2 \bar{v} = 0 \quad \text{for } x < 0 \quad (3.26)$$

with boundary conditions:

$$\bar{u}_1 + \bar{w} = \bar{v} \quad \text{at } x = 0 \quad (3.27)$$

$$\lambda_1 \left( \frac{\partial \bar{u}_1}{\partial x} + \frac{\partial \bar{w}}{\partial x} \right) = \lambda_2 \frac{\partial \bar{v}}{\partial x} \quad \text{at } x = 0 \quad (3.28)$$

where  $z_1 = \sqrt{\frac{z}{\eta_1}}$  and  $z_2 = \sqrt{\frac{z}{\eta_2}}$ .

Separation of variables  $x$  and  $y$  gives a continuous spectrum for this eigenvalue problem, which suggests that a Fourier integral replace the eigenfunction expansion theorem. An equivalent way is to use the Fourier transformation.

After Fourier transformation:

$$\frac{\partial^2 \bar{w}}{\partial x^2} - (s^2 + z_1^2) \bar{w} = 0 \quad \text{for } x > 0 \quad (3.29)$$

$$\frac{\partial^2 \bar{v}}{\partial x^2} - (s^2 + z_2^2) \bar{v} = 0 \quad \text{for } x < 0 \quad (3.30)$$

with  $\bar{v} = 0$  when  $x \rightarrow -\infty$  we see that:

$$\bar{w} = A e^{-\sqrt{s^2 + z_1^2} x} \quad (3.31)$$

$$\bar{v} = B e^{\sqrt{s^2 + z_2^2} x} \quad (3.32)$$

$A$  and  $B$  can be decided by the boundary conditions:

$$\bar{u}_1 + \bar{w} = \bar{v} \quad \text{at } x = 0 \quad (3.33)$$

$$\lambda_1 \left( \frac{\partial \bar{u}_1}{\partial x} + \frac{\partial \bar{w}}{\partial x} \right) = \lambda_2 \frac{\partial \bar{v}}{\partial x} \quad \text{at } x = 0 \quad (3.34)$$

Substituting  $\bar{u}_1 = \frac{1}{2\sqrt{2\pi\eta_1}} \frac{e^{-|x-x'|\sqrt{s^2+z_1^2}}}{\sqrt{s^2+z_1^2}}$  gives

$$A = \frac{(\lambda_1 \sqrt{s^2 + z_1^2} - \lambda_2 \sqrt{s^2 + z_2^2}) e^{-\sqrt{s^2 + z_1^2} x'}}{2\sqrt{2\pi\eta_1} \sqrt{s^2 + z_1^2} (\lambda_1 \sqrt{s^2 + z_1^2} + \lambda_2 \sqrt{s^2 + z_2^2})} \quad (3.35)$$

$$B = \frac{\lambda_1 \sqrt{s^2 + z_1^2} e^{-\sqrt{s^2 + z_1^2} x'}}{\sqrt{2\pi\eta_1} (\lambda_1 \sqrt{s^2 + z_1^2} + \lambda_2 \sqrt{s^2 + z_2^2})} \quad (3.36)$$

so

$$\bar{G} = e^{-\sqrt{s^2 + z_1^2} |x-x'|} + \frac{1}{2\sqrt{2\pi\eta_1} \sqrt{s^2 + z_1^2}}$$

$$\frac{(\lambda_1\sqrt{s^2+z_1^2}-\lambda_2\sqrt{s^2+z_2^2})e^{-\sqrt{s^2+z_1^2}(x+x')}}{\lambda_1\sqrt{s^2+z_1^2}+\lambda_2\sqrt{s^2+z_2^2}} \quad (3.37)$$

for  $x > 0$ , and

$$\bar{\bar{G}} = \frac{\lambda_1 e^{\sqrt{s^2+z_2^2}x - \sqrt{s^2+z_1^2}x'}}{\sqrt{2\pi}\eta_1(\lambda_1\sqrt{s^2+z_1^2}+\lambda_2\sqrt{s^2+z_2^2})} \quad (3.38)$$

for  $x < 0$ . In Laplace space, the Green's function is

$$\bar{G}(x, y, x', z) = \sqrt{\frac{2}{\pi}} \int_0^\infty \bar{\bar{G}}(x, s, x', z) \cos(ys) ds \quad (3.39)$$

### 3.4.3 Case 3: Working in Laplace Space

For infinite reservoirs, working in Laplace space is a good idea since we can focus on spatial variables without worrying about the time variable or the initial condition. There are effective numerical methods that invert the solutions in Laplace space to real space conveniently.

A good example is the pressure solution for an infinite homogeneous reservoir with a circular discontinuity in properties as shown in Fig. 2.5. For this problem, it is easier to work in Laplace space. In Laplace space, a function extended from the homogeneous Green's function was obtained by *Rosa* (1991). The key idea is a kind of perturbation; adding a to-be-decided function to the already known solution for the homogeneous reservoir without the discontinuity. The solution is assumed to be  $u_i + v_i$  for region  $i$  ( $i = 1, 2$ ), where  $u_i$  is the solution of homogeneous reservoir with the same properties as region  $i$  and  $v_i$  is the function to be decided. This idea was applied to composite media for heat transfer by *Carslaw and Jaeger* (1959). In their approach, the Green's function was defined due to a unit strength source. This definition makes the Green's function lose the reciprocity property in heterogeneous reservoirs, and is quite inconvenient when applied to continuous sources. In our definition, the Green's function in Laplace space for the first region ( $r < a$ ) is

$$\bar{v}_1 = \begin{cases} \frac{1}{2\pi\lambda_1} \left[ \sum_{n=0}^{\infty} \varepsilon_n \frac{\Omega_n}{\Psi_n} I_n(z_1 r') I_n(z_1 r) \cos(\theta - \theta') \right. \\ \quad \left. + K_0(z_1 R) \right] & \text{if } a \geq r' \\ \frac{1}{2\pi a} \sum_{n=0}^{\infty} \varepsilon_n \frac{K_n(z_2 r') I_n(z_1 r)}{\Psi_n} \cos(\theta - \theta') & \text{if } a < r' \end{cases} \quad (3.40)$$

For the second region ( $r \geq a$ ), it is

$$\bar{v}_2 = \begin{cases} \frac{\eta_2}{2\pi\lambda_1\eta_1} \left[ \sum_{n=0}^{\infty} \varepsilon_n \frac{\Phi_n}{\Psi_n} K_n(z_2 r') K_n(z_2 r) \cos(\theta - \theta') \right. \\ \quad \left. + K_0(z_2 R) \right] & \text{if } a \leq r' \\ \frac{1}{2\pi a} \sum_{n=0}^{\infty} \varepsilon_n \frac{I_n(z_1 r') K_n(z_2 r)}{\Psi_n} \cos(\theta - \theta') & \text{if } a > r' \end{cases} \quad (3.41)$$

where

$$\begin{aligned} \varepsilon_0 &= 1, \\ \varepsilon_n &= 2 \quad (n > 0), \\ \lambda_1 &= \frac{k_1}{\mu_1}, \\ \lambda_2 &= \frac{k_2}{\mu_2}, \\ \eta_1 &= \frac{k_1}{\phi\mu_1 c_{t1}}, \\ \eta_2 &= \frac{k_2}{\phi\mu_2 c_{t2}}, \\ z_1 &= \sqrt{\frac{z}{\eta_1}}, \\ z_2 &= \sqrt{\frac{z}{\eta_2}}, \\ R^2 &= r^2 + r'^2 - 2rr' \cos(\theta - \theta'), \\ \Omega_n &= \lambda_2 z_2 K_n(z_1 a) K'_n(z_2 a) - \lambda_1 z_1 K'_n(z_1 a) K_n(z_2 a), \\ \Phi_n &= \lambda_2 z_2 I'_n(z_2 a) I_n(z_1 a) - \lambda_1 z_1 I_n(z_2 a) I'_n(z_1 a), \\ \Psi_n &= \lambda_1 z_1 K_n(z_2 a) I'_n(z_1 a) - \lambda_2 z_2 K'_n(z_2 a) I_n(z_1 a). \end{aligned}$$

Notice that the two equations presented above are different from Eq. 2.10 and Eq. 2.11 because Eq. 2.10 and Eq. 2.11 are not actually Green's function for the circular discontinuity problem.

The pressure drop for a constant surface flow rate  $q$  in Laplace space is

$$\overline{\Delta P}(r, \theta, z) = \frac{qB}{\pi r_w^2 h} \frac{1}{z} \bar{v}(r, \theta, z). \quad (3.42)$$

where

$$\bar{v}(r, \theta, z) = \begin{cases} \bar{v}_1 & r < a \\ \bar{v}_2 & r \geq a \end{cases}$$

### 3.4.4 Case 4: Decomposition

We do not have Newman's product theorem for Green's functions in heterogeneous reservoirs, so generally we can not decompose a higher dimensional problem into several lower dimensional problems that are easier to solve, except in some very special cases, for example, when mobility and storativity have the same distributions and are functions of only one of  $x, y$  or  $z$ .

Consider a closed rectangular reservoir in two dimensions with mobility and storativity varying linearly in the  $x$  direction only, as shown in Fig. 3.4.4. The Green's function for this problem satisfies:

$$\frac{\partial}{\partial x} [(ax + b) \frac{\partial G}{\partial x}] + \frac{\partial}{\partial y} [(ax + b) \frac{\partial G}{\partial y}] = (ax + b) \frac{\partial G}{\partial t} \quad (3.43)$$

which, after transformation with any constant  $c$ ,

$$\begin{cases} x' = ax + b \\ y' = ay + c \\ t' = a^2 t \end{cases} \quad (3.44)$$

is equivalent to the following problem:

$$\frac{1}{s} \frac{\partial}{\partial x} (x \frac{\partial G}{\partial x}) + \frac{\partial^2 G}{\partial y^2} - \frac{\partial G}{\partial t} \quad (3.45)$$

with  $0 \leq a \leq x \leq \text{band}$  and  $0 \leq y \leq l$ .

$$G(x, x', y, y', 0) = \frac{\delta(x - x') \delta(y - y')}{x'} \quad (3.46)$$

This two-dimensional problem can be decomposed into two one-dimensional problems by assuming

$$G(x, x', y, y', t) = G_1(x, x', t) G_2(y, y', t).$$

Substituting into Eq. 3.45, we obtain two subproblems,



- Closed rectangular reservoir in two dimensions
- Mobility and storativity vary linearly in  $x$  direction

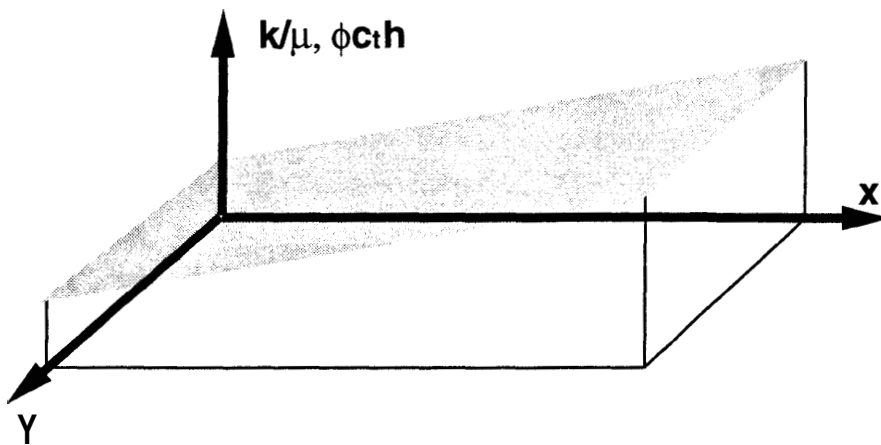


Figure 3.1: Distribution of mobility and storativity

$$\frac{1}{x} \frac{\partial}{\partial x} \left( x \frac{\partial G_1}{\partial x} \right) = \frac{\partial G_1}{\partial t} \quad (3.47)$$

with  $0 \leq a \leq x \leq b$  and  $G_1(x, x', 0) = \frac{\delta(x-x')}{2lx'x^2}$ , and

$$\frac{\partial^2 G_2}{\partial y^2} = \frac{dG_2}{dt} \quad (3.48)$$

with  $0 \leq y \leq l$  and  $G_2(y, y', 0) = \delta(y - y')$ .

The Green's function for Eq. 3.47 is

$$G_1(x, x', t) = \left\{ \frac{2}{b^2 - a^2} + \sum_{n=1}^{\infty} \frac{\pi^2 \alpha_n^2 Y_1^2(\alpha_n b) e^{-\alpha_n^2 t} y_n(x) y_n(x')}{2[Y_1^2(\alpha_n a) - Y_1^2(\alpha_n b)]} \right\} \quad (3.49)$$

where  $y_n(x) = J_1(\alpha_n a) Y_0(\alpha_n x) - Y_1(\alpha_n a) J_0(\alpha_n x)$ . Detailed derivation for this solution is in Appendix D.

Eq. 3.48 represents a one-dimensional homogeneous reservoir with a Green's function presented by *Gringarten and Ramey (1973)*

$$G_2(y, y', t) = \frac{1}{l} \left( 1 + 2 \sum_{n=1}^{\infty} e^{-\frac{n^2 \pi^2 t}{l^2}} \cos \frac{n \pi y}{l} \cos \frac{n \pi y'}{l} \right). \quad (3.50)$$

Therefore, the Green's function for our two-dimensional problem is

$$G(x, x', y, y', t) = \frac{1}{l} \left( 1 + 2 \sum_{n=1}^{\infty} e^{-\frac{n^2 \pi^2 t}{l^2}} \cos \frac{n \pi y'}{l} \cos \frac{n \pi y}{l} \right) \left\{ \frac{2}{b^2 - a^2} + \sum_{n=1}^{\infty} \frac{\pi^2 \alpha_n^2 Y_1^2(\alpha_n b) e^{-\alpha_n^2 t} y_n(x) y_n(x')}{2[Y_1^2(\alpha_n a) - Y_1^2(\alpha_n b)]} \right\}. \quad (3.51)$$

If we have one active well with production rate  $q(t)$  at position  $(x', y')$ , then the pressure response is

$$p_i - p(x, y, t) = \int_0^t \frac{q(\tau)}{\pi r_w^2 h} G(x, x', y, y', t - \tau) d\tau \quad (3.52)$$

### 3.5 Anisotropic and Heterogeneous Reservoirs

The general pressure equation for an anisotropic and heterogeneous reservoir can be written as:

$$\begin{aligned} \frac{\partial}{\partial x} \frac{k_x(x, y, z)}{\mu_x(x, y, z)} \frac{\partial p}{\partial x} + \frac{\partial}{\partial y} \frac{k_y(x, y, z)}{\mu_y(x, y, z)} \frac{\partial p}{\partial y} + \frac{\partial}{\partial z} \frac{k_z(x, y, z)}{\mu_z(x, y, z)} \frac{\partial p}{\partial z} = \\ \phi(x, y, z) c_t(x, y, z) \frac{\partial p}{\partial t}. \end{aligned} \quad (3.53)$$

Generally speaking, Green's functions are not good for this kind of complicated problem. We will look at the problem with the following restriction,

$$\begin{aligned} \frac{k_x(x, y, z)}{\mu_x(x, y, z)} &= \frac{k_x(x)}{\mu_x(x)}, \\ \frac{k_y(x, y, z)}{\mu_y(x, y, z)} &= \frac{k_y(y)}{\mu_y(y)}, \\ \frac{k_z(x, y, z)}{\mu_z(x, y, z)} &= \frac{k_z(z)}{\mu_z(z)} \end{aligned}$$

and

$$\phi(x, y, z) c_t(x, y, z) = \phi c_t.$$

In such a case, this three-dimensional problem can be decomposed into three one-dimensional problems provided that the domain of the three-dimensional problem can be represented by the product of three one-dimensional intervals.

Suppose  $p_1(x, t)$  is the solution of

$$\frac{\partial}{\partial x} \frac{k_x(x)}{\mu_x(x)} \frac{\partial p_1}{\partial x} = \phi c_t \frac{\partial p_1}{\partial t}, \quad (3.54)$$

$p_2(y, t)$  is the solution of

$$\frac{\partial}{\partial y} \frac{k_y(y)}{\mu_y(y)} \frac{\partial p_2}{\partial y} = \phi c_t \frac{\partial p_2}{\partial t} \quad (3.55)$$

and  $p_3(z, t)$  is the solution of

$$\frac{\partial}{\partial z} \frac{k_z(z)}{\mu_z(z)} \frac{\partial p_3}{\partial z} = \phi c_t \frac{\partial p_3}{\partial t} \quad (3.56)$$

over the corresponding decomposed intervals, then it is true that

$$p(x, y, z) = p_1(x, t) p_2(y, t) p_3(z, t) \quad (3.57)$$

is the solution of the three-dimensional problem.

### 3.6 Principle of Reciprocity

Once we know that reciprocity holds for the Green's function, we can start to investigate under which conditions the pressure response is reciprocal. Suppose there are two wells, well **A** produces at some rate, which causes a pressure response at well **B**. Under which conditions, will the pressure response at well **A** be the same if well **B** is produced at that rate? The pressure can be represented in terms of Green's function as:

$$p(x, y, z, t) = \int_0^t \int_{S_e} \frac{k}{\mu} \left( G \frac{\partial p}{\partial n} + p \frac{\partial G}{\partial n} \right) dS_e d\tau - \int_0^t \int_{\Omega} G \cdot f dx' dy' dz' d\tau + \int_{\Omega} \phi c_t G(t) \cdot g dx' dy' dz' \quad (3.58)$$

where  $f(x, y, z, t)$  is the source distribution and  $g(x, y, z)$  is the initial pressure.

In order to satisfy reciprocity, the second and last terms on the right hand side have to be zero, i.e. the initial pressure is zero everywhere and boundary is no-flow or kept at constant zero pressure. From this, considering the pressure drop instead of the pressure response itself, we see that reciprocity also holds for the pressure response if the initial pressure is uniform and the boundary is kept at the initial pressure or the boundary is no-flow. For infinite reservoirs, the boundary terms disappear, and only the uniform initial pressure condition is required. Notice that these conditions are also necessary conditions. So if the initial pressure distribution is not uniform, or when there is a boundary at which the pressure is not kept at initial pressure, then we do not have reciprocal pressure responses.

### 3.7 Effects of Wellbore Storage and Skin

The skin factor does not change reciprocity, since the reservoir is treated as a composite reservoir when skin is present. From the discussion above, we know that reciprocity holds for the composite reservoir which is a special case of heterogeneity.

The wellbore storage coefficient is related to the sandface flow rate by

$$q_{sf}(t) = Q + C \frac{dp_w}{dt} \quad (3.59)$$

$$q_{sfD}(t_D) = 1 + C_D \frac{dp_{wD}}{dt_D} \quad (3.60)$$

In Laplace space, it is

$$\overline{q_{sfD}}(s) = \frac{1}{s} + C_D s \overline{p_{wD}} \quad (3.61)$$

The derivation is true for any dimension, but we will show it only in two dimensions as an example. Suppose there are two positions  $(x_1, y_1)$  and  $(x_2, y_2)$  and two corresponding Green's functions  $G_1(x_D, y_D, x_{1D}, y_{1D}, t_D - \tau_D)$  and  $G_2(x_D, y_D, x_{2D}, y_{2D}, t_D - \tau_D)$ . From the principle of reciprocity, we know that:

$$G_1(x_{2D}, y_{2D}, x_{1D}, y_{1D}, t_D) = G_2(x_{1D}, y_{1D}, x_{2D}, y_{2D}, t_D) \quad (3.62)$$

$$\begin{aligned} p_{1D}(x_D, y_D, x_{1D}, y_{1D}, t_D) = \\ \int_0^{t_D} q_{sfD}(t_D) G_1(x_D, y_D, x_{1D}, y_{1D}, t_D - \tau_D) d\tau_D \end{aligned} \quad (3.63)$$

In Laplace space,

$$\overline{p_{1D}}(x_D, y_D, x_{1D}, y_{1D}, s) = \overline{q_{sfD}}(s) \overline{G_1}(x_D, y_D, x_{1D}, y_{1D}, s) \quad (3.64)$$

$$\overline{q_{sfD}}(s) = \frac{1}{s} + C_D s \overline{G_1}(x_{rD}, y_{rD}, x_{1D}, y_{1D}, s) \quad (3.65)$$

so

$$\overline{q_{sfD}}(s) = \frac{1}{s[1 + C_D s \overline{G_1}(x_{rD}, y_{rD}, x_{1D}, y_{1D}, s)]} \quad (3.66)$$

$$\begin{aligned} \overline{p_{1D}}(x_D, y_D, x_{1D}, y_{1D}, s) = \\ \frac{\overline{G_1}(x_D, y_D, x_{1D}, y_{1D}, s)}{s[1 + C_D s \overline{G_1}(x_{1rD}, y_{1rD}, x_{1D}, y_{1D}, s)]}. \end{aligned} \quad (3.67)$$

Similarly,

$$\begin{aligned} \overline{p_{2D}}(x_D, y_D, x_{2D}, y_{2D}, s) = \\ \frac{\overline{G_2}(x_D, y_D, x_{2D}, y_{2D}, s)}{s[1 + C_D s \overline{G_2}(x_{2rD}, y_{2rD}, x_{2D}, y_{2D}, s)]}. \end{aligned} \quad (3.68)$$

Thus in order to make

$$\overline{p_{1D}}(x_{2D}, y_{2D}, x_{1D}, y_{1D}, s) = \overline{p_{2D}}(x_{1D}, y_{1D}, x_{2D}, y_{2D}, s)$$

we need

$$\overline{G}_1(x_{1rD}, y_{1rD}, x_{1D}, y_{1D}, s) = \overline{G}_2(x_{2rD}, y_{2rD}, x_{2D}, y_{2D}, s). \quad (3.69)$$

if  $C_D$  is not zero.

In infinite homogeneous reservoirs, this can always be satisfied since

$$\overline{G}(x_D, y_D, x_{1D}, y_{1D}, s) = \overline{G}(x_D - x_{1D}, y_D - y_{1D}, s). \quad (3.70)$$

For other cases, even in homogeneous reservoirs, the wellbore storage may invalidate the reciprocity as shown by the following example.

For a one-dimensional homogeneous reservoir, with a no-flow boundary at  $x = 0$  and  $x = x_e$ , its Green's function is

$$G(x, x', t - \tau) = \frac{1}{x_e} \left[ 1 + 2 \sum_{n=1}^{\infty} e^{-\frac{n^2 \pi^2 \eta t}{x_e^2}} \cos \frac{n\pi x'}{x_e} \cos \frac{n\pi x}{x_e} \right]$$

For reciprocity to hold we require

$$G(x_{1w}, x_1, t) = G(x_{2w}, x_2, t)$$

or

$$\cos \frac{n\pi x_{1w}}{x_e} \cos \frac{n\pi x_1}{x_e} = \cos \frac{n\pi x_{2w}}{x_e} \cos \frac{n\pi x_2}{x_e}$$

Assuming  $x_{1w} = x_1 + x_w$ , and  $x_{2w} = x_2 + x_w$ , then we would need:

$$\cos \frac{n\pi(x_1 + x_w)}{x_e} \cos \frac{n\pi x_1}{x_e} = \cos \frac{n\pi(x_2 + x_w)}{x_e} \cos \frac{n\pi x_2}{x_e}$$

which is not true, hence reciprocity does not hold for this no-flow boundary reservoir.

### 3.8 Green's Functions for Tracer Flow Problems

This section considers the application of the Green's function method in convection-dispersion tracer problems.

Considering one-phase flow through a homogeneous porous media, the general convection-dispersion equation is

$$\frac{\partial}{\partial t}(\phi x_i \rho) + \nabla(\rho \vec{v} x_i) - \nabla(\phi D_i \rho \nabla x_i) = 0 \quad i = 1, \dots, n_c \quad (3.71)$$

Assuming no volume change on mixing, then  $\sum_{i=1}^{n_c} \frac{\rho x_i}{\rho_i^0} = 1$ . Denoting  $c_i = \frac{\rho x_i}{\rho_i^0}$ , we have

$$\frac{\partial}{\partial t}(\phi c_i) + \nabla(\vec{v} c_i) - \nabla(\phi D_i \nabla c_i) = 0 \quad i = 1, \dots, n_c \quad (3.72)$$

if  $\nabla(\phi D_i \frac{x_i}{\rho_i^0} \nabla \rho)$  is neglected. For one dimension and two components:

$$\phi(x) \frac{\partial c}{\partial t} + [v - \frac{d(\phi D)}{dx}] \frac{\partial c}{\partial x} - \phi D \frac{\partial^2 c}{\partial x^2} + \frac{\partial v}{\partial x} c = 0. \quad (3.73)$$

Multiplying on both sides by  $\xi(x)$  which is yet to be determined:

$$\xi(x) \phi(x) \frac{\partial c}{\partial t} + \xi(x) [v(x) - \frac{d(\phi D)}{dx}] \frac{\partial c}{\partial x} - \xi(x) \phi(x) D \frac{\partial^2 c}{\partial x^2} + \xi(x) \frac{\partial v}{\partial x} c = 0. \quad (3.74)$$

We want to have:

$$\xi(x) [v(x) - \frac{d(\phi D)}{dx}] = -\frac{d}{dx} [\xi(x) \phi(x) D(x)]$$

$$\xi(x) [v(x) - (\phi D)'] = -\xi'(x) \phi(x) D(x) - \xi(x) (\phi D)'$$

So the requirement is

$$\frac{\xi'}{\xi} = -\frac{v}{\phi D} \quad (3.75)$$

$$\xi(x) = e^{-\int \frac{v(x)}{\phi(x) D(x)} dx} \quad (3.76)$$

which gives

$$\frac{\partial}{\partial x} [\xi(x) \phi(x) D(x) \frac{\partial c}{\partial x}] - \xi \frac{\partial v}{\partial x} c = \xi(x) \phi(x) \frac{\partial c}{\partial t}. \quad (3.77)$$

If  $v$  is constant, the convection-dispersion problem

$$\frac{\partial}{\partial x} [\xi(x) \phi(x) D(x) \frac{\partial c}{\partial x}] = \xi(x) \phi(x) \frac{\partial c}{\partial t} \quad x > 0 \quad (3.78)$$

with conditions  $c(x, 0) = c_1$  and  $c(0, t) = c_2$  is the same as the pressure problem in one dimension:

$$\frac{\partial}{\partial x} \left[ \frac{k(x)}{\mu(x)} \frac{\partial p}{\partial x} \right] = \phi(x) c_t(x) \frac{\partial p}{\partial t} \quad x > 0 \quad (3.79)$$

with conditions  $p(x, 0) = p_1$  and  $p(0, t) = p_2$ . Thus the Green's function also can be used for the convection-dispersion equation in one dimension, or even for the convection-dispersion equation with adsorption in a homogeneous reservoir.

For two-dimensional or three-dimensional dispersion problems, the Green's function method can be applied too, but it will not so powerful as it is for pressure problems. The difference comes from the fact that for dispersion problem, we usually have fixed concentrations at wells that are kinds of boundary conditions rather than source constraints, and the Green's function for boundary problems is more complicated to derive analytically.



# Chapter 4

## Analytical Solutions to Tracer Flow

Solving tracer problems analytically is challenging **work**. A classical analytical solution found by *Aronofsky and Heller (1957)* is the complementary error function for a semiinfinite linear flow in a homogeneous reservoir:

$$c(\xi, \tau) = \frac{1}{2} \operatorname{erfc}\left(\frac{\sqrt{P_e}(\xi - \tau)}{2\sqrt{\tau}}\right) + \frac{1}{2} e^{P_e \xi} \operatorname{erfc}\left(\frac{\sqrt{P_e}(\xi + \tau)}{2\sqrt{\tau}}\right) \quad (4.1)$$

where  $c$  is the dimensionless normalized concentration,  $P_e = \frac{vL}{\phi D}$  is the Peclet number,  $D$  is dispersion coefficient,  $v$  is the Darcy velocity, and  $L$  is the length of the flow. The second term is small and usually is neglected in application except at very early time. A general convection-dispersion equation in two dimensions is:

$$\frac{\partial c}{\partial t} = \frac{\partial}{\partial x} \left( D_{xx} \frac{\partial c}{\partial x} + D_{xy} \frac{\partial c}{\partial y} \right) + \frac{\partial}{\partial y} \left( D_{yx} \frac{\partial c}{\partial x} + D_{yy} \frac{\partial c}{\partial y} \right) - v_x \frac{\partial c}{\partial x} - v_y \frac{\partial c}{\partial y} - \frac{c_1 q}{\phi h} \quad (4.2)$$

where the velocities  $v_x$  and  $v_y$  are related to pressure distribution,  $D_{ij}$  are the components of the hydrodynamic dispersion coefficients,  $c_1$  is the concentration of the source/sink, and  $q$  is the rate of injection and/or withdrawal in volume flux per unit area.

The reasons this convection-dispersion equation is difficult to solve analytically include:

- o The phase velocity  $(v_x, v_y)$  appears as a coefficient in the convection-diffusive equation.
- o The velocity is determined by the pressure distribution and depends on the well pattern.
- o Analytical expressions for velocity usually are complicated in two dimensions.

Even though the Green's function method can be extended for convection-dispersion equations as for the diffusive equations in heterogeneous reservoirs, the method is not as effective because the condition at the injection well is a constant concentration and a constant concentration can not be described as a source. On the other hand, if the injection condition is treated as a constant boundary condition, the mathematical domain becomes more complex and makes it virtually impossible to find the Green's function.

Due to these restrictions, analytical solutions for convection-dispersion equation can be obtained only in some simplified situations. In this chapter, some of these cases are discussed. The concentration expression in a one-dimensional composite region with different constant dispersivities will be shown. Also shown is the solution to linear tracer flow with linearly changing dispersivity. One-dimensional problems are always easier to handle in seeking the analytical solution. Moving from one dimension to two dimensions requires more simplifications. A two-dimensional example included in this chapter is the analytical solution to radial tracer flow that actually is solved as a one-dimensional problem. At the end, a streamline semianalytic solution based on characteristic method is presented for an infinite reservoir with a circular discontinuity.

## 4.1 Convection-Dispersion Equation with Linearly Changing Dispersivity

Denoting the fluid Darcy velocity by  $v$ , porosity by  $\phi$  and dispersion coefficient by  $D$ , for two-component, one-phase linear flow in a semiinfinite region, the tracer concentration can be expressed in Laplace space as

$$\bar{C}(s, x) = \frac{1}{s} e^{\frac{v(x-a)}{2\phi D} - (x-a)\sqrt{\frac{v^2}{4\phi^2 D^2} + \frac{s}{D}}} \quad (4.3)$$

This solution can be inverted analytically to real space.

For a one-dimensional system with linearly varying dispersion coefficient  $D(x) = \frac{v_0}{\phi}x$ , in a semiinfinite domain, the concentration equation is

$$\frac{\partial C}{\partial t} = \frac{a}{ax} \frac{v_0 x}{\phi} \frac{\partial C}{\partial x} - \frac{v}{\phi ax} \frac{\partial C}{\partial x} \quad (4.4)$$

with initial condition  $C(x, 0) = 0 (x > a)$ , boundary conditions  $C(a, t) = 1 (t > 0)$ ,  $C(\infty, t) = O(t > 0)$ . Taking the Laplace transform, it becomes

$$s\bar{C} = \frac{v_0 x}{\phi} \frac{d^2 \bar{C}}{dx^2} - \left( \frac{v}{\phi} - \frac{v_0}{\phi} \right) \frac{d\bar{C}}{dx} \quad (4.5)$$

$$\bar{C}(x, 0) = 0 \quad (x > a) \quad (4.6)$$

$$\bar{C}(a, s) = \frac{1}{s} \quad (4.7)$$

$$\bar{C}(\infty, s) = 0 \quad (4.8)$$

The solution for this equation was worked out in Laplace space as

$$\bar{C}(s, x) = \frac{1}{s} \left( \frac{x}{a} \right)^{\frac{v}{2v_0}} \frac{K_\nu \left( 2\sqrt{\frac{\phi s x}{v_0}} \right)}{K_\nu \left( 2\sqrt{\frac{\phi s a}{v_0}} \right)} \quad (4.9)$$

where  $\nu = \frac{v}{v_0}$ .

Using the Stehfest algorithm to invert the solution to real space will not yield the correct answer. As can be seen in Fig. 4.1, numerical errors similar to Gibb's phenomena are present on two sides of the front zone indicating that the Stehfest

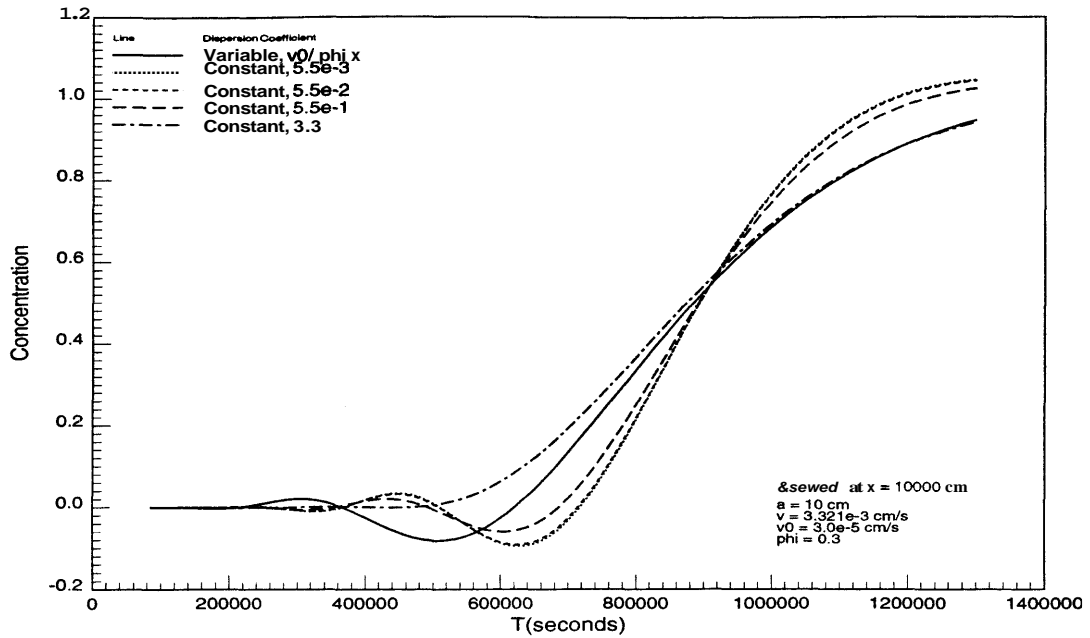
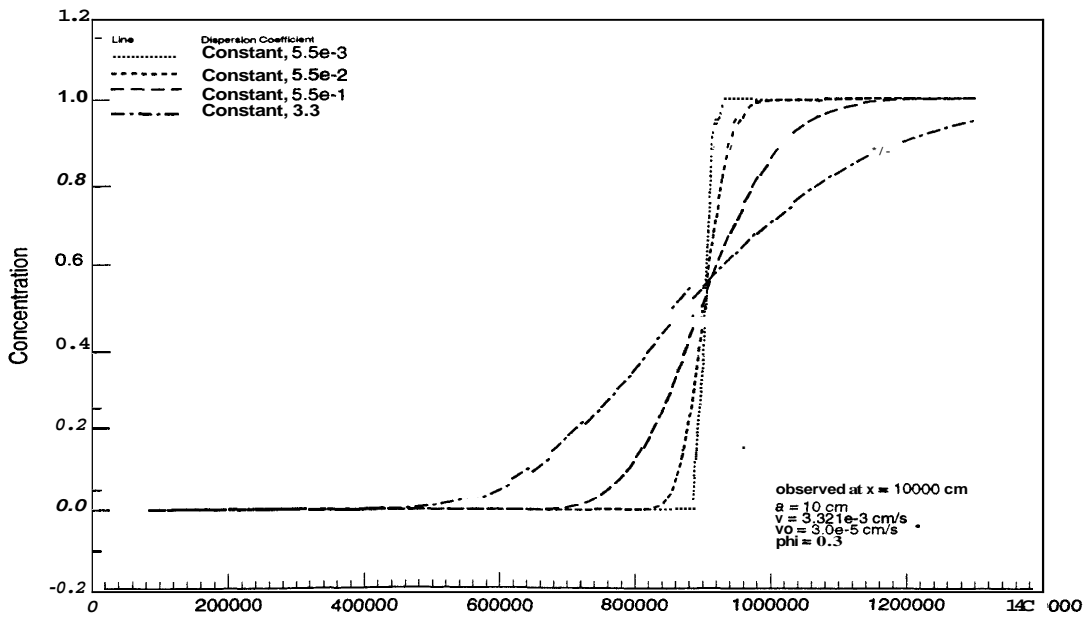


Figure 4.1: Tracer responses(incorrect) calculated by Stehfest algorithm



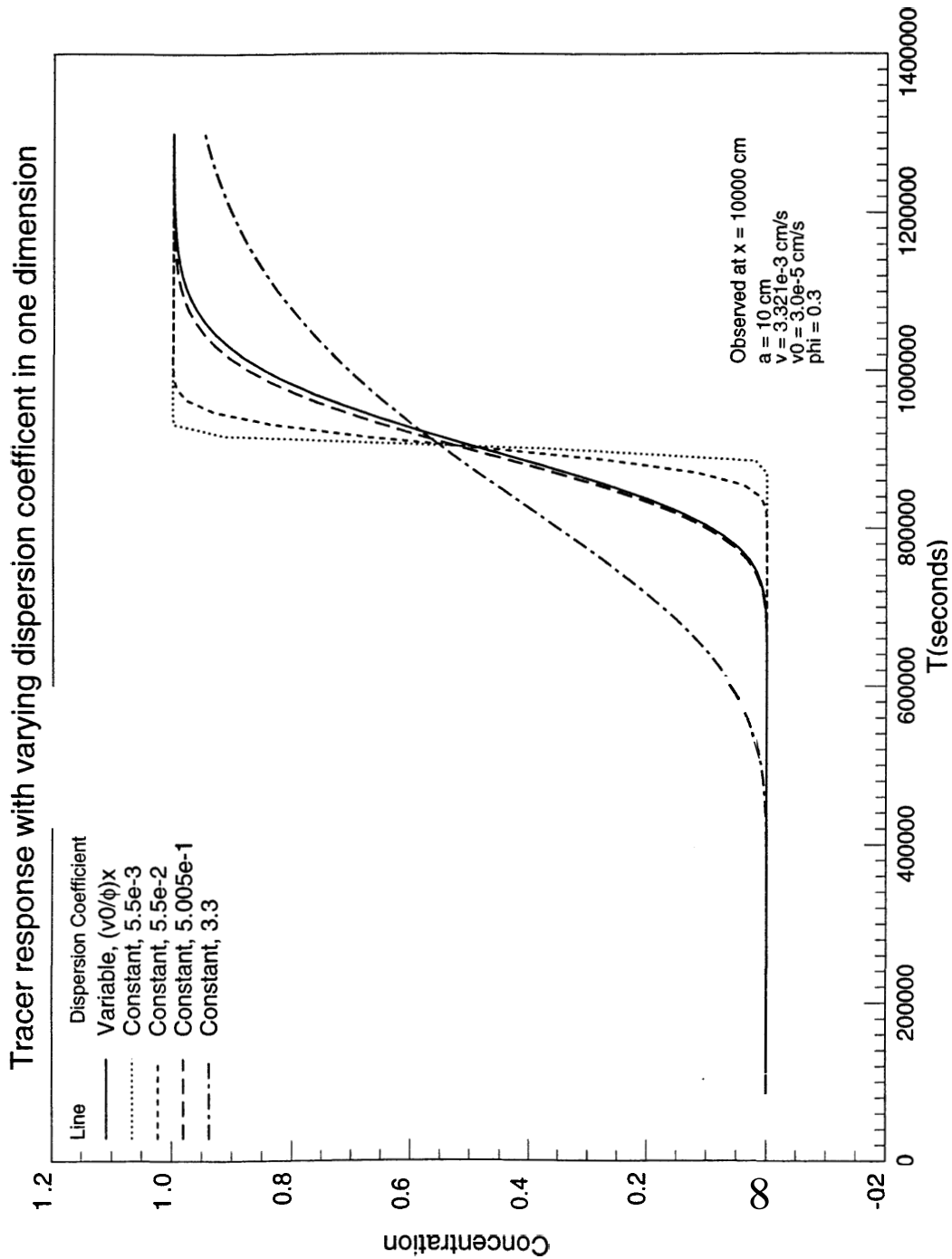


Figure 4.3: Comparison of constant dispersivity and linearly changing dispersivity

algorithm is not applicable here. A better approach for Laplace inversion in the tracer problem is the algorithm developed by *Crump (1976)*. Fig. 4.2 shows the corresponding correct tracer concentrations recalculated by the Crump algorithm.

As a contrast to constant dispersivity, Fig. 4.3 shows the concentration profiles at fixed points with different dispersivities in the media. The differences between constant dispersivity and linearly changing dispersivity solutions are not large though the concentration of the latter cannot be matched well using the concentration from the constant dispersivity solution. This implies that the concentration profile does carry the nonconstant dispersivity information even though it is not reflected strongly.

## 4.2 Linear Tracer Flow in a Composite Reservoir

Consider a linear flow in a reservoir that has two regions of different dispersivities  $D_1$  and  $D_2$  as shown in Fig. 4.4. The two regions contact at  $x = a$ . Since the flow is linear?the phase velocities in two regions are the same  $v$ .

$$\frac{\partial C_1}{\partial t} = D_1 \frac{\partial^2 C_1}{\partial x^2} - \frac{v}{\phi_1} \frac{\partial C_1}{\partial x} \quad 0 < x < a \quad (4.10)$$

$$\frac{\partial C_2}{\partial t} = D_2 \frac{\partial^2 C_2}{\partial x^2} - \frac{v}{\phi_2} \frac{\partial C_2}{\partial x} \quad x > a \quad (4.11)$$

with initial condition  $C(x, 0) = 0$  ( $x > 0$ ) and two boundary conditions  $C_1(0, t) = 1$  ( $t > 0$ ),  $C_2(\infty, t) = 0$  ( $t > 0$ ). In order to completely define the problem, we need two other conditions at  $x = a$ . One has to be the material balance at  $x = a$ , that flux in due to convection and dispersion should be equal to flux out due to convection and dispersion,

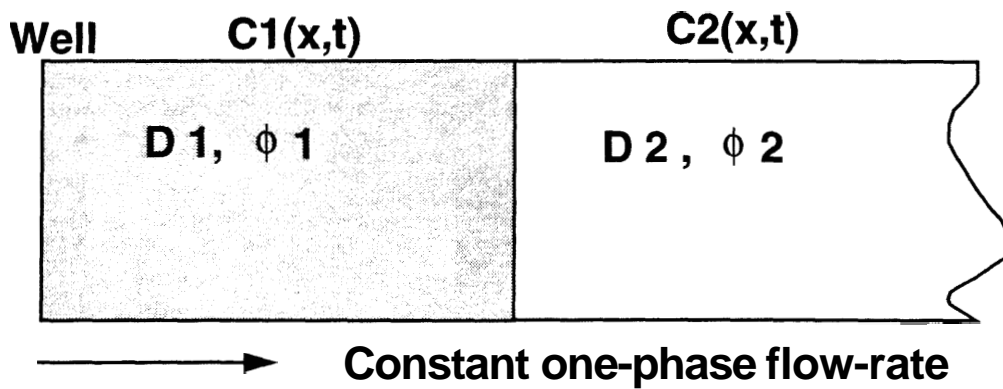
$$C_1 - \frac{\phi_1 D_1}{v} \frac{\partial C_1}{\partial x} \Big|_{x=a} = C_2 - \frac{\phi_2 D_2}{v} \frac{\partial C_2}{\partial x} \Big|_{x=a} \quad (4.12)$$

The other condition can be posed to require continuity of concentration across  $x = a$ ,

$$C_1(a, t) - C_2(a, t) = 0 \quad (4.13)$$

The solutions in Laplace space are

$$\bar{C}_1(x, s) = A_1 e^{\lambda_{11} x} + B_1 e^{\lambda_{12} x} \quad (4.14)$$



**Two conditions at the interface:**

- 1 Material balance**
- 2 Continuity of concentration**

Figure 4.4: Linear tracer flow in composite region

with  $\lambda_{11} = \frac{v}{2\phi_1 D_1} + \sqrt{\frac{v^2}{4\phi_1^2 D_1^2} + \frac{s}{D_1}}$  and  $\lambda_{12} = \frac{v}{2\phi_1 D_1} - \sqrt{\frac{v^2}{4\phi_1^2 D_1^2} + \frac{s}{D_1}}$   
and

$$\bar{C}_2(x, s) = A_2 e^{\lambda_{21}x} + B_2 e^{\lambda_{22}x} \quad (4.15)$$

with  $\lambda_{21} = \frac{v}{2\phi_2 D_2} + \sqrt{\frac{v^2}{4\phi_2^2 D_2^2} + \frac{s}{D_2}}$  and  $\lambda_{22} = \frac{v}{2\phi_2 D_2} - \sqrt{\frac{v^2}{4\phi_2^2 D_2^2} + \frac{s}{D_2}}$ .

Applying boundary conditions to  $\bar{C}_1$  and  $\bar{C}_2$ , we obtain:

$$A_1 + B_1 = \frac{1}{s} \quad (4.16)$$

$$A_2 = 0 \quad (4.17)$$

$$\frac{e^{\lambda_{11}a}}{s} + B_1(e^{\lambda_{12}a} - e^{\lambda_{11}a}) = B_2 e^{\lambda_{22}a} \quad (4.18)$$

$$\begin{aligned} & \frac{e^{\lambda_{11}a}}{s} + B_1(e^{\lambda_{12}a} - e^{\lambda_{11}a}) - \frac{\phi_1 D_1 \lambda_{11} e^{\lambda_{11}a}}{vs} - \frac{\phi_1 D_1 B_1}{v} (\lambda_{12} e^{\lambda_{12}a} - \lambda_{11} e^{\lambda_{11}a}) \\ & = B_2 e^{\lambda_{22}a} - \frac{\phi_2 D_2 B_2 \lambda_{22}}{v} e^{\lambda_{22}a} \end{aligned} \quad (4.19)$$

This linear equation system gives:

$$A_1 = \frac{e^{\lambda_{12}a}}{s} \frac{-\frac{\phi_1 D_1}{v} \lambda_{12} + \frac{\phi_2 D_2}{v} \lambda_{22}}{(\frac{\phi_1 D_1}{v} \lambda_{11} - \frac{\phi_2 D_2}{v} \lambda_{22}) e^{\lambda_{11}a} - (\frac{\phi_1 D_1}{v} \lambda_{12} - \frac{\phi_2 D_2}{v} \lambda_{22}) e^{\lambda_{12}a}} \quad (4.20)$$

$$B_1 = \frac{e^{\lambda_{11}a}}{s} \frac{\frac{\phi_1 D_1}{v} \lambda_{11} - \frac{\phi_2 D_2}{v} \lambda_{22}}{(\frac{\phi_1 D_1}{v} \lambda_{11} - \frac{\phi_2 D_2}{v} \lambda_{22}) e^{\lambda_{11}a} - (\frac{\phi_1 D_1}{v} \lambda_{12} - \frac{\phi_2 D_2}{v} \lambda_{22}) e^{\lambda_{12}a}} \quad (4.21)$$

$$B_2 = \frac{e^{(\lambda_{11} + \lambda_{12} - \lambda_{22})a}}{s} \frac{\frac{\phi_1 D_1}{v} (\lambda_{11} - \lambda_{22})}{(\frac{\phi_1 D_1}{v} \lambda_{11} - \frac{\phi_2 D_2}{v} \lambda_{22}) e^{\lambda_{11}a} - (\frac{\phi_1 D_1}{v} \lambda_{12} - \frac{\phi_2 D_2}{v} \lambda_{22}) e^{\lambda_{12}a}} \quad (4.22)$$

Therefore, we obtained tracer solutions in Laplace space for the composite one-dimensional problem:

$$\begin{aligned} \bar{C}_1(x, s) &= \frac{(\phi_1 D_1 \lambda_{11} - \phi_2 D_2 \lambda_{22}) e^{\lambda_{11}a + \lambda_{12}x} - (\phi_1 D_1 \lambda_{12} - \phi_2 D_2 \lambda_{22}) e^{\lambda_{12}a + \lambda_{11}x}}{s[(\phi_1 D_1 \lambda_{11} - \phi_2 D_2 \lambda_{22}) e^{\lambda_{11}a} - (\phi_1 D_1 \lambda_{12} - \phi_2 D_2 \lambda_{22}) e^{\lambda_{12}a}]} \\ \bar{C}_2(x, s) &= \frac{\phi_1 D_1 (\lambda_{11} - \lambda_{22}) e^{(\lambda_{11} + \lambda_{12} - \lambda_{22})a + \lambda_{22}x}}{s[(\phi_1 D_1 \lambda_{11} - \phi_2 D_2 \lambda_{22}) e^{\lambda_{11}a} - (\phi_1 D_1 \lambda_{12} - \phi_2 D_2 \lambda_{22}) e^{\lambda_{12}a}]} \end{aligned} \quad (4.23)$$



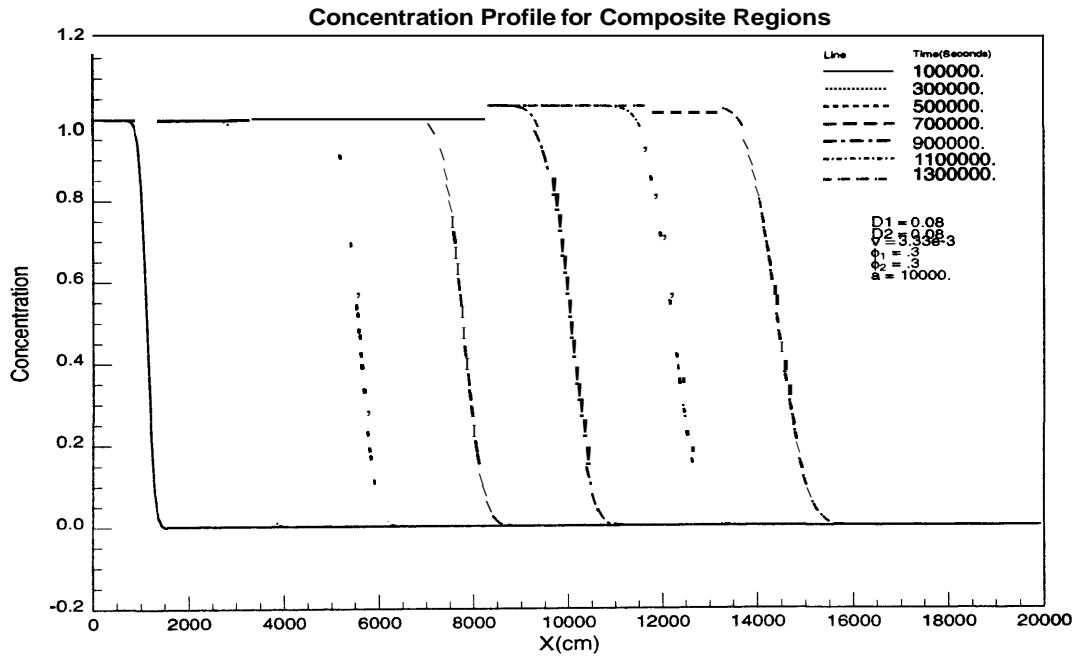


Figure 4.5: Tracer profile in one dimensional uniform region

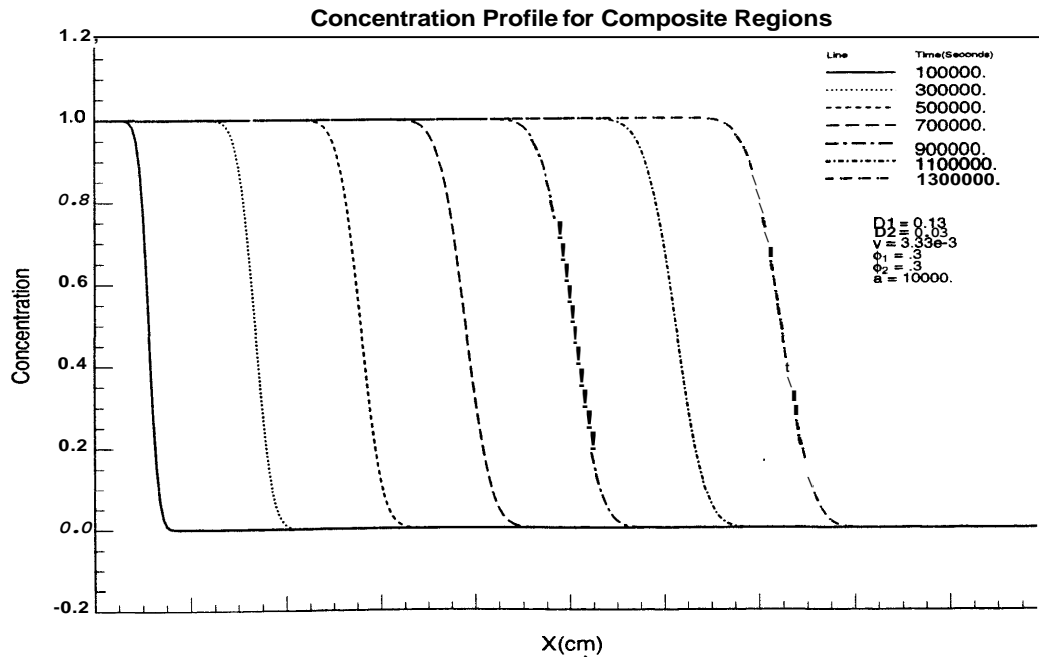


Figure 4.6: Tracer profile in one dimension with two different dispersivities

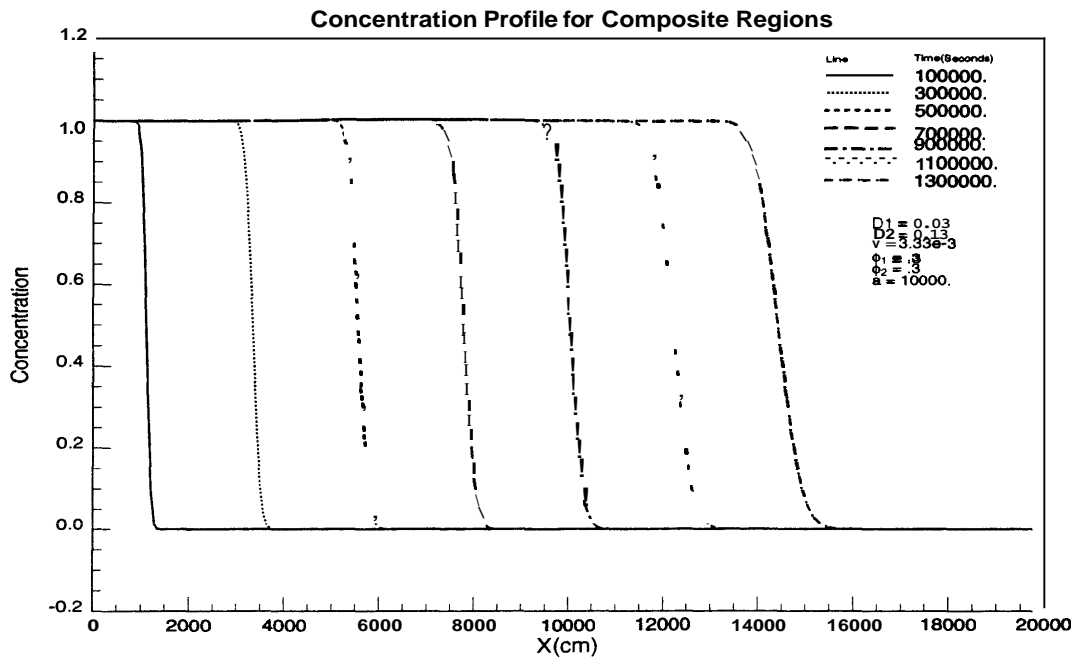


Figure 4.7: Tracer profile in one dimension with two different dispersivities

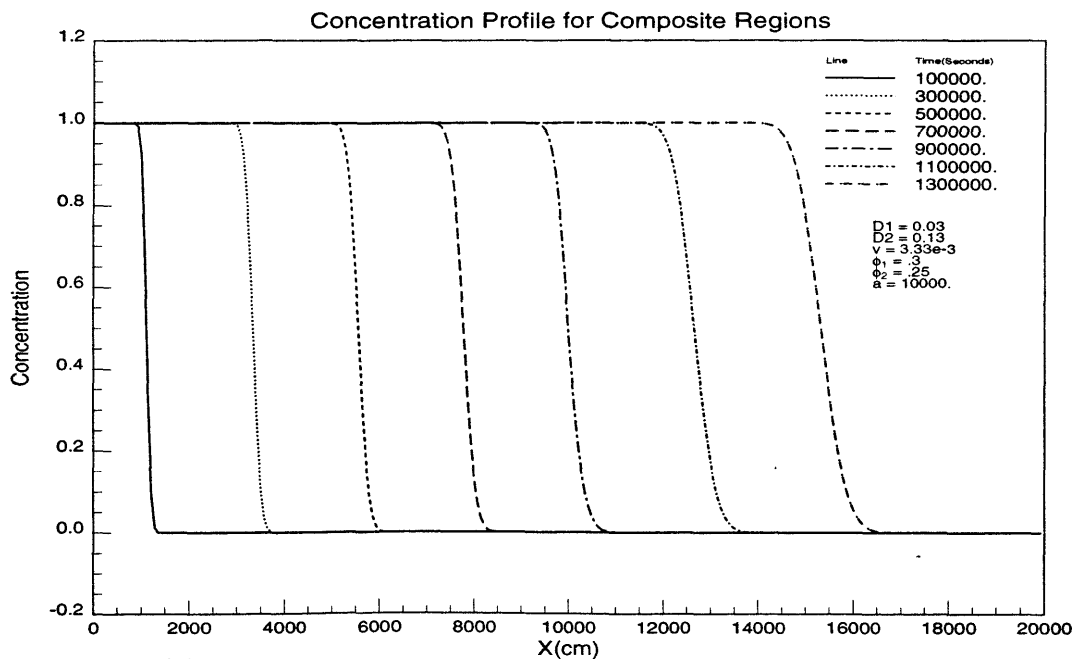


Figure 4.8: Tracer profile in one dimension with two different porosities

This solution, again, cannot be inverted into real space correctly using the Stehfest algorithm. Some profile curves are calculated by the Crump algorithm as shown in Figs. 4.5-4.8. The change in dispersivities in the two regions affects the curves. The differences between the figures are not so obvious, but are there and can contribute significantly to the breakthrough curves.

Now let us consider a linear flow in a reservoir which has two regions of different properties, with very small dispersion in one or both regions. This is a special case of the convection-dispersion equation with some of the dispersion coefficients equal to zero. However, the solution expressed in Eq. 4.23 does not apply to this special case because  $D_1$  and  $D_2$  appear in the denominator of  $\lambda$ 's. All other conditions are set as before, namely: two regions contact at  $x = a$ ; initial condition  $C(x, 0) = 0 (x > 0)$ ; boundary conditions  $C_1(0, t) = 1 (t \geq 0)$ ,  $C_2(\infty, t) = 0 (t > 0)$ ; continuous concentration  $C_1(a, t) - C_2(a, t) = 0$ ; and material balance

$$C_1 - \frac{\phi_1 D_1}{v} \frac{\partial C_1}{\partial x} \Big|_{x=a} = C_2 - \frac{\phi_2 D_2}{v} \frac{\partial C_2}{\partial x} \Big|_{x=a}.$$

There are three cases possible.

## 1. Dispersion in Both Regions Neglected

If dispersion coefficients in both regions are set to zero, then we have

$$\begin{aligned} \frac{\partial C_1}{\partial t} + \frac{v}{\phi_1} \frac{\partial C_1}{\partial x} &= 0 \quad 0 < x < a \\ \frac{\partial C_2}{\partial t} + \frac{v}{\phi_2} \frac{\partial C_2}{\partial x} &= 0 \quad x > a \end{aligned} \quad (4.24)$$

The solution in Laplace space is

$$\bar{C}_1(x, s) = \frac{1}{s} e^{-\frac{\phi_1 x}{v} s} \quad (4.25)$$

$$\bar{C}_2(x, s) = \frac{1}{s} e^{-\frac{(\phi_1 - \phi_2)a + \phi_2 x}{v} s} \quad (4.26)$$

These solutions can be inverted back to real space as

$$C_1(x, t) = \begin{cases} 0 & t < \frac{\phi_1 x}{v} \\ 1 & t > \frac{\phi_1 x}{v} \end{cases} \quad (4.27)$$

$$C_2(x, t) = \begin{cases} 0 & t < \frac{(\phi_1 - \phi_2)a + \phi_2 x}{v} \\ 1 & t > \frac{(\phi_1 - \phi_2)a + \phi_2 x}{v} \end{cases} \quad (4.28)$$

The tracer front moves at velocity  $\frac{v}{\phi_1}$  in the first region, and at velocity  $\frac{v}{\phi_2}$  in the second region.

## 2. Dispersion in the First Region Neglected

For this case, the equations governing the tracer flow in two regions are:

$$\frac{\partial C_1}{\partial t} = -\frac{v}{\phi_1} \frac{\partial C_1}{\partial x} \quad 0 < x < a \quad (4.29)$$

$$\frac{\partial C_2}{\partial t} = D_2 \frac{\partial^2 C_2}{\partial x^2} - \frac{v}{\phi_2} \frac{\partial C_2}{\partial x} \quad x > a \quad (4.30)$$

The solutions for this case can be worked out in Laplace space as

$$\bar{C}_1(x, s) = \frac{1}{s} e^{-\frac{\phi_1 x}{v} s}$$

$$\bar{C}_2(x, s) = \frac{1}{s} e^{-\frac{\phi_1 a}{v} s} e^{\frac{v(x-a)}{2\phi_2 D_2} - (x-a) \sqrt{\frac{v^2}{4\phi_2^2 D_2^2} + \frac{s}{D_2}}},$$

and both of these can be inverted analytically into real space.

## 2. Dispersion in the Second Region Neglected

The second region has a very small dispersion coefficient  $D_2 \approx 0$ ,

$$\frac{\partial C_1}{\partial t} = D_1 \frac{\partial^2 C_1}{\partial x^2} - \frac{v}{\phi_1} \frac{\partial C_1}{\partial x} \quad 0 < x < a \quad (4.31)$$

$$\frac{\partial C_2}{\partial t} = -\frac{v}{\phi_2} \frac{\partial C_2}{\partial x} \quad x > a \quad (4.32)$$

with the material balance condition  $C_1 - \frac{\phi_1 D_1}{v} \frac{\partial C_1}{\partial x} \Big|_{x=a} = C_2$ . Transforming into Laplace space, we have:

$$s\bar{C}_1 - D_1 \frac{d^2 \bar{C}_1}{dx^2} + \frac{v}{\phi_1} \frac{d\bar{C}_1}{dx} \quad 0 < x < a$$

$$s\bar{C}_2 + \frac{v}{\phi_1} \frac{d\bar{C}_1}{dx} \quad x > a$$

The general solutions are

$$\bar{C}_1(x, s) = A_1 e^{\lambda_{11}x} + B_1 e^{\lambda_{12}x}$$

$$\bar{C}_2(x, s) = A_2 e^{-\frac{\phi_2 x}{v} s}$$

Applying boundary conditions

$$\bar{C}_1(0, s) = \frac{1}{s},$$

$$\bar{C}_1(a, s) = \bar{C}_2(a, s)$$

and

$$\bar{C}_1(a, s) - \frac{\phi_1 D_1}{v} \frac{d\bar{C}_1}{dx} = \bar{C}_2$$

or

$$\left. \frac{d\bar{C}_1}{dx} \right|_{x=a} = 0,$$

then

$$A_1 + B_1 = \frac{1}{s} \tag{4.33}$$

$$A_1 e^{\lambda_{11}a} + B_1 e^{\lambda_{12}a} = A_2 e^{-\frac{\phi_2 a}{v} s} \tag{4.34}$$

$$A_1 \lambda_{11} e^{\lambda_{11}a} + B_1 \lambda_{12} e^{\lambda_{12}a} = 0 \tag{4.35}$$

Solving linear equations Eq. 4.33, Eq. 4.34, and Eq. 4.35 to determine the coefficients gives

$$A_1 = -\frac{1}{s} \frac{\lambda_{12} e^{\lambda_{12}a}}{\lambda_{11} e^{\lambda_{11}a} - \lambda_{12} e^{\lambda_{12}a}}$$

$$B_1 = \frac{1}{s} \frac{\lambda_{11} e^{\lambda_{11}a}}{\lambda_{11} e^{\lambda_{11}a} - \lambda_{12} e^{\lambda_{12}a}}$$

$$A_2 = \frac{1}{s} \frac{(\lambda_{11} - \lambda_{12})e^{(\lambda_{11} + \lambda_{12})a + \frac{\phi_2 a}{v}s}}{\lambda_{11}e^{\lambda_{11}a} - \lambda_{12}e^{\lambda_{12}a}}$$

So, the solutions of tracer concentration in Laplace space for this case are

$$\bar{C}_1(x, s) = \frac{1}{s} \frac{\lambda_{11}e^{\lambda_{11}a + \lambda_{12}x} - \lambda_{12}e^{\lambda_{12}a + \lambda_{11}x}}{\lambda_{11}e^{\lambda_{11}a} - \lambda_{12}e^{\lambda_{12}a}} \quad (4.36)$$

$$\bar{C}_2(x, s) = \frac{1}{s} \frac{(\lambda_{11} - \lambda_{12})e^{(\lambda_{11} + \lambda_{12})a + \frac{\phi_2(a-x)}{v}s}}{\lambda_{11}e^{\lambda_{11}a} - \lambda_{12}e^{\lambda_{12}a}} \quad (4.37)$$

where

$$\lambda_{11} = \frac{v}{2\phi_1 D_1} + \sqrt{\frac{v^2}{4\phi_1^2 D_1^2} + \frac{s}{D_1}}$$

and

$$\lambda_{12} = \frac{v}{2\phi_1 D_1} - \sqrt{\frac{v^2}{4\phi_1^2 D_1^2} + \frac{s}{D_1}}$$

These solutions cannot be inverted to real space analytically, so a numerical inversion method like Crump algorithm should be used.

### 4.3 Radial Convection-Dispersion Tracer Flow in Homogeneous Reservoir

This section deals with the tracer problem for radial flow in homogeneous reservoirs. Denote the Peclet number by  $P_e = \frac{vL}{\phi D}$  where  $v$  is the Darcy velocity,  $L$  is the length of the flow)  $\phi$  is the porosity and  $D$  is the diffusion coefficient. For two-component, one phase linear flow, the solution has been obtained by solving the following convection-diffusion equation,

$$\frac{\partial C}{\partial t} + \frac{v}{\phi} \frac{\partial C}{\partial x} - D \frac{\partial^2 C}{\partial x^2} = 0. \quad (4.38)$$

The governing equation of tracer flow in the two-dimensional infinite domain is

$$\frac{\partial C}{\partial t} + \frac{v_x \partial C}{\partial x} + \frac{v_y \partial C}{\partial y} - \frac{\partial}{\partial x} \left( D \frac{\partial C}{\partial x} \right) - \frac{\partial}{\partial y} \left( D \frac{\partial C}{\partial y} \right) = 0 \quad (4.39)$$

Starting from **Eq. 4.39**, the equation for a radial system that satisfies

$$\begin{cases} v_x = r \cos \theta \\ v_y = r \sin \theta \end{cases}$$

can be derived as

$$\frac{\partial C}{\partial t} + \frac{1}{r} \frac{\partial C}{\partial r} - \frac{1}{P_e} \frac{\partial^2 C}{\partial r^2} = 0, \quad (4.40)$$

Consider a model with simple initial condition and boundary conditions as an example

$$\begin{cases} C(r, 0) = 0 \\ C(1, t) = 1 \\ \lim_{r \rightarrow \infty} C(r, t) = 0 \end{cases}$$

The tracer solution to this model in Laplace space can be expressed in terms of modified Bessel functions of real orders

$$\bar{C}(r, s) = r^p \frac{I_p(\sqrt{P_e} sr) - I_{-p}(\sqrt{P_e} sr)}{s[I_p(\sqrt{P_e} s) - I_{-p}(\sqrt{P_e} s)]} \quad (4.41)$$

where  $p = \frac{1+P_e}{2}$ .

After the superposition for the convection-dispersion equation in two-dimensional tracer flow was investigated and found not to be true, it was realized that the concentration distribution of tracer in multiwell system cannot be obtained by superposing the separate radial flow solutions. The superposition is not true due to the specification of concentration at each injection well that serves as a boundary condition.

## 4.4 Streamlines in an Infinite Reservoir with a Circular Discontinuity

This section introduces a semianalytic method for generating streamlines in an infinite two-dimensional heterogeneous reservoir, where the local heterogeneity is approximated by a circular region with permeability and porosity different than the rest of the reservoir. This semianalytic solution can serve as a basis to verify the general numerical method that solves the tracer flow in reservoirs with blocks of heterogeneity. In this semianalytic method, the pressure equation is solved first, the velocity

fields are obtained from the pressure distributions, and then the streamline is calculated. Following enough number of streamlines from injection well to production well simulates the tracer flowing between wells and will give the tracer concentration in the production well, i.e., tracer return profile. It is believed that heterogeneity has more effect on tracer flowing than dispersion. The dispersion effect, therefore, is assumed to be very small in this discussion. With the dispersion effect neglected, the tracer convection-dispersion equation

$$\frac{\partial C}{\partial t} - \frac{\partial}{\partial x}(D_{xx} \frac{\partial C}{\partial x}) + \frac{\partial}{\partial y}(D_{yy} \frac{\partial C}{\partial y}) + \frac{\partial}{\partial x}(D_{xy} \frac{\partial C}{\partial y}) + \frac{\partial}{\partial y}(D_{yx} \frac{\partial C}{\partial x}) - \frac{\partial(v_x C)}{\partial x} - \frac{\partial(v_y C)}{\partial y} - \frac{C'q}{\phi h} \quad (4.42)$$

can be simplified to a first order equation

$$\frac{\partial C}{\partial t} + v_x \frac{\partial C}{\partial x} + v_y \frac{\partial C}{\partial y} = 0 \quad (4.43)$$

where the velocity  $v_x$  and  $v_y$  are determined by pressure equation. The streamline is calculated according to

$$\frac{dx}{v_x} = \frac{dy}{v_y} = \frac{dt}{1} = \frac{C}{0}. \quad (4.44)$$

The pressure distribution for a reservoir with circular discontinuity can be obtained exactly from the Green's function with superposition of the effects of the injection wells and production wells. Fig. 4.9 shows the pressure distribution in a configuration of one injection well and one production well in an infinite reservoir with a circular discontinuity between the two wells. Streamlines in Fig. 4.10 are for the reservoir without the discontinuity, while Figs. 4.11 and 4.12 show the streamlines for different permeabilities in the discontinuity, lower than the reservoir in Fig. 4.11 and higher than the reservoir in Fig. 4.12. The example has just one production well and one injection well. The scheme is applicable directly to multiwell system when the pressure distribution is superposed using all wells.

The circular discontinuity does affect the shape of the streamlines. What is the effect on the tracer breakthrough? To answer this, the tracer return profile should be calculated. Following sufficient streamlines from the tracer injection well to the



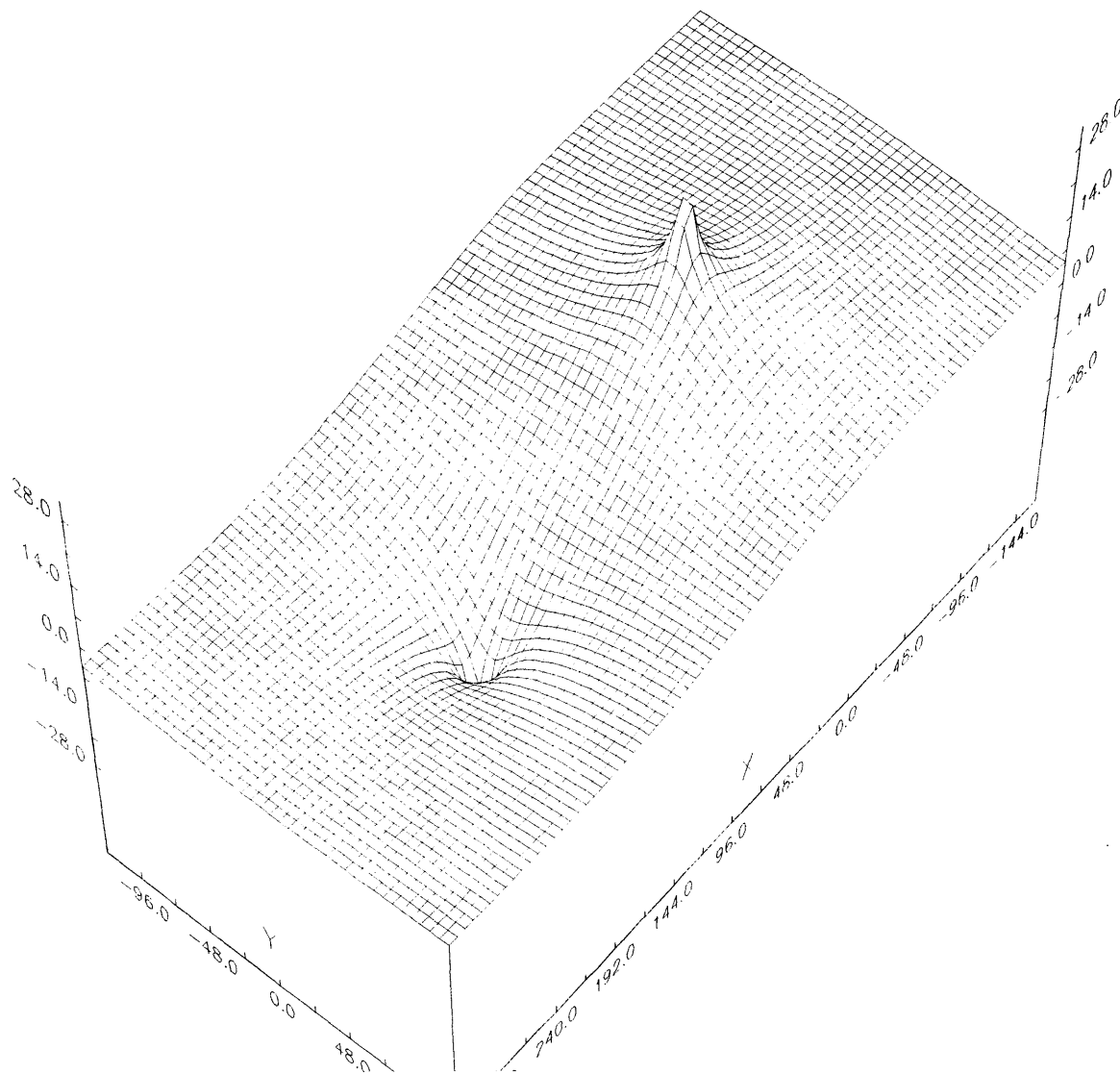


Figure 4.9: Pressure distribution of two wells in discontinuous reservoir

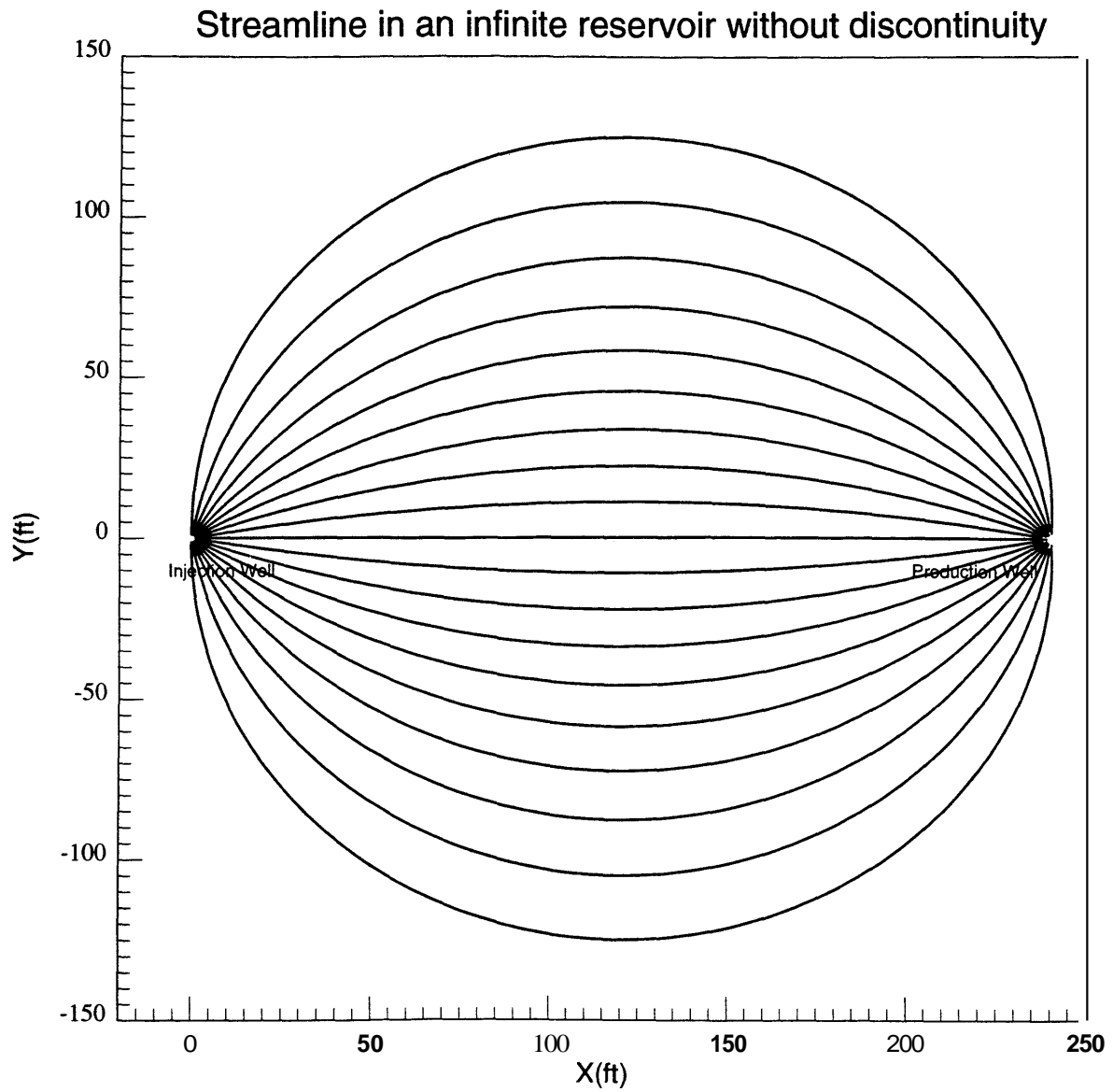


Figure 4.10: Streamlines of two wells in a homogeneous reservoir

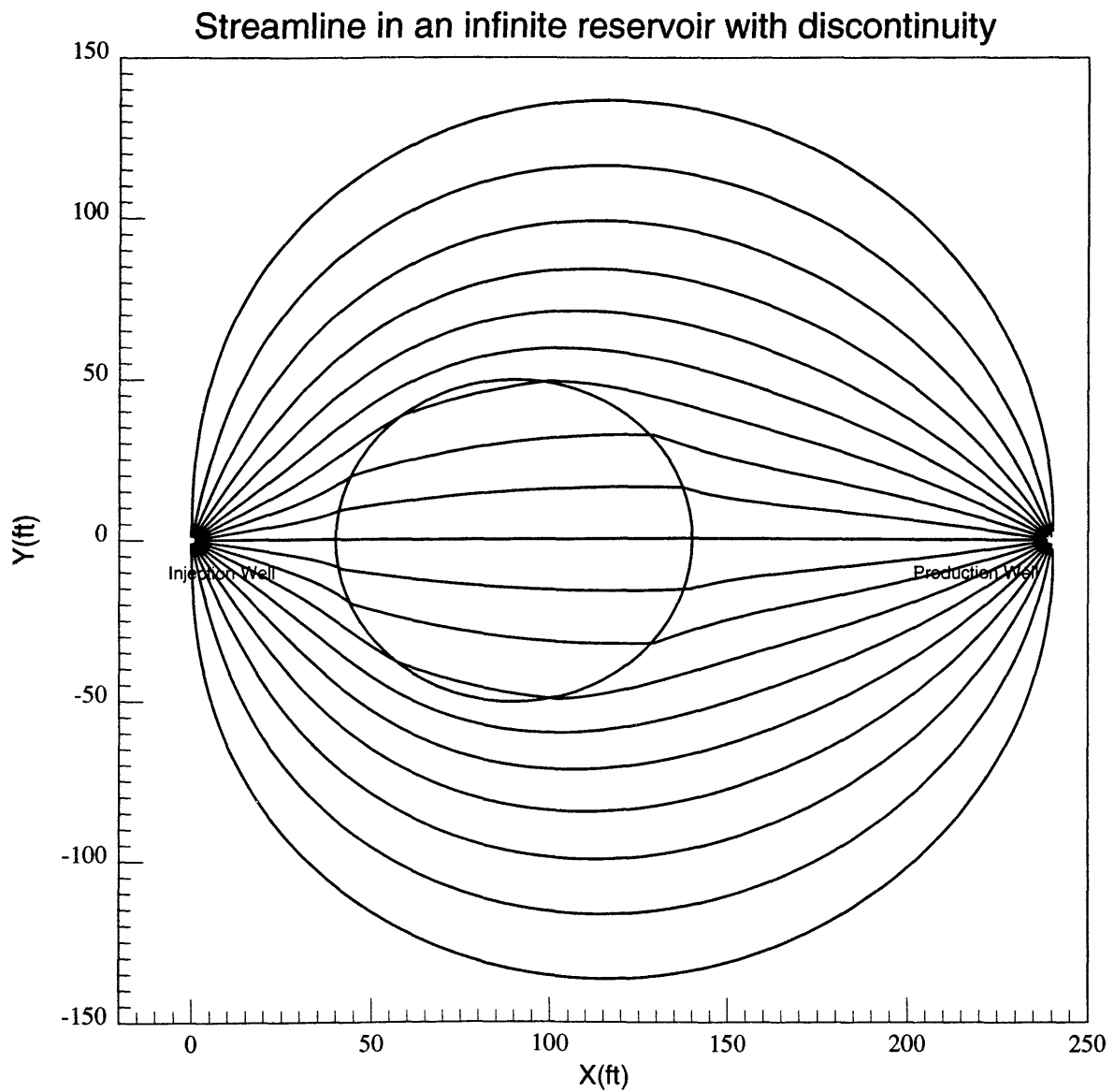


Figure 4.11: Streamlines of two wells with a discontinuity of lower permeability

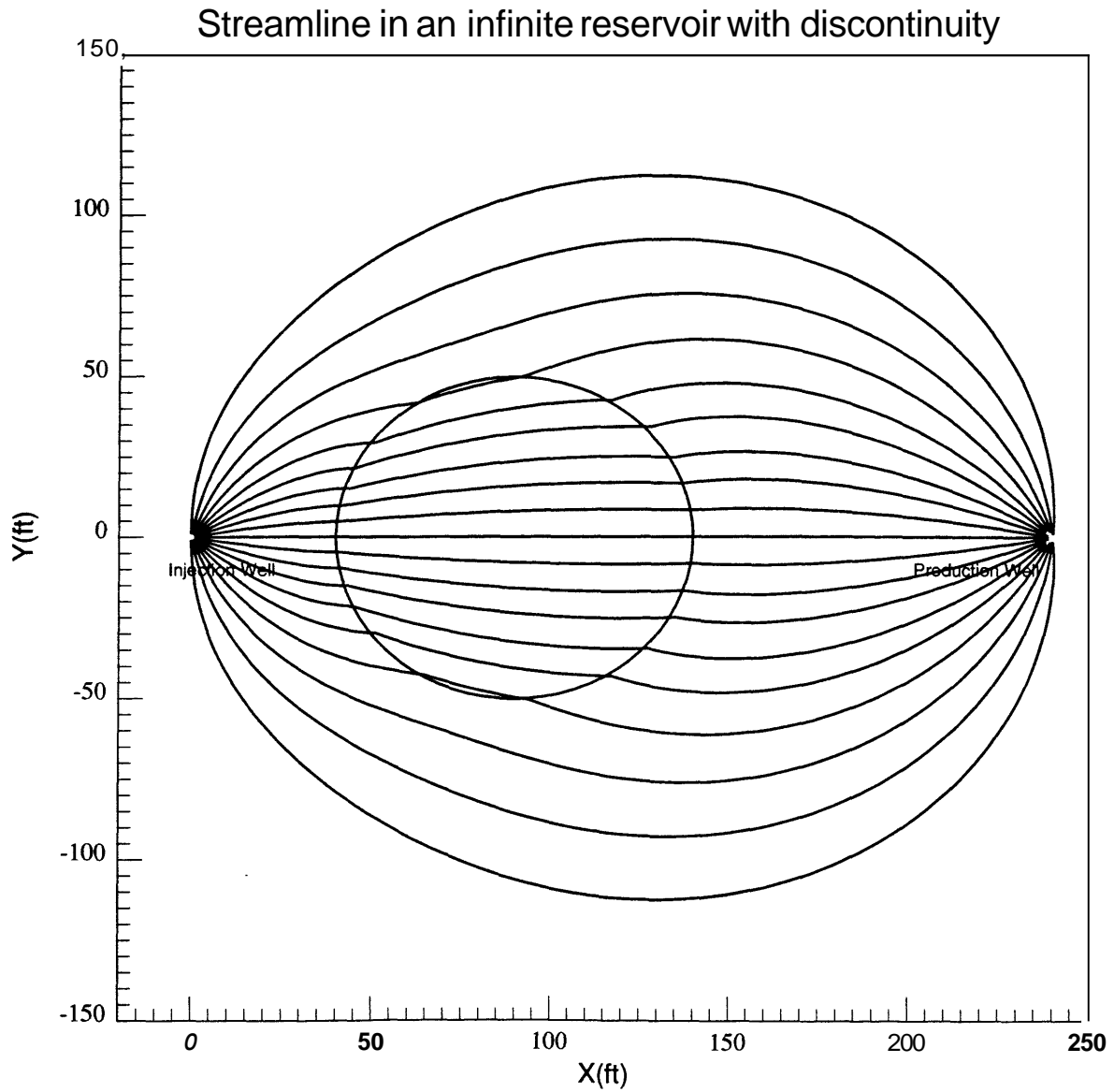


Figure 4.12: Streamlines of two wells with a discontinuity of higher permeability

tracer production well is an effective way to calculate the tracer concentration in the production well or tracer profile. Weighting each streamline according to its velocity upon the breakthrough time generates the solution to the tracer flow problem. The implementation is a numerical method of characteristics.

Fig. 4.13 and Fig. 4.14 compare the tracer return profiles for three permeabilities of the circular disk. The locations of the circular disks in the two figures are different; one lies between two wells ( $0^\circ$ ), 90 ft away from the injection well and the other lies  $45^\circ$ , 90 ft away from the injection well. In both figures, the system with the discontinuity of smaller permeability has later breakthrough. This is easy to understand with a physical explanation that the presence of the small permeability zone blocks the flowing channel. The curves are distinguishable from each other, so a small area of heterogeneity does yield different concentration profiles at the production well. On the other hand, the difference present between curves probably is not large enough to determine the permeability of circular discontinuity with confidence. More data would be needed to reduce the ambiguity, for example, by combining pressure data with the tracer data.

The tracer return profiles in both figures are calculated by following 500 streamlines from the injection well to the production well. Each streamline is assigned a weight proportional to its in-flux, where the sum of the 500 weights is 1. When a streamline breaks through, its weight is counted into the contribution of the tracer concentration at the production well.

The streamlines actually are the projection of three-dimensional characteristic curves defined in Eq. 4.44 onto the x-y plane. Along each characteristic curve, the concentration  $C(t, x, y)$  is a constant equal to the concentration  $C_0$  at the injection well. Each characteristic curve starts from the injection well, and eventually reaches into the production well. The time at which a characteristic curve intersects with the production well is its breakthrough time.

In calculation of the streamlines, the time step for each iteration should be chosen carefully so that the advances of tracer fronts during the time step along all the streamlines are no more than a given distance. The time step should not be calculated based on the average velocity at the current time, which causes problems because the

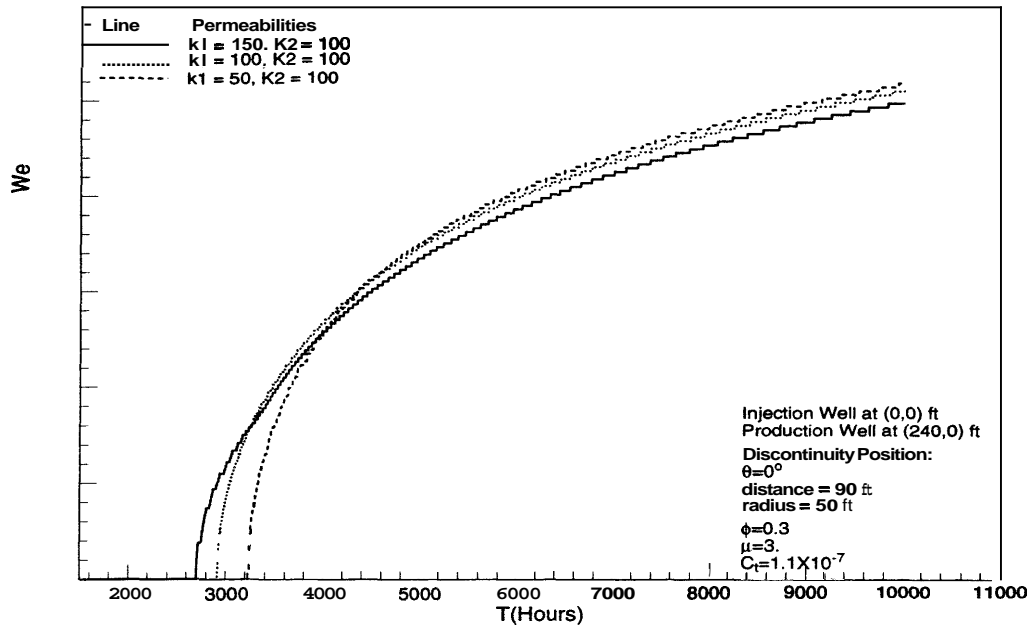


Figure 4.13: Tracer profile in a doublet system of infinite reservoir

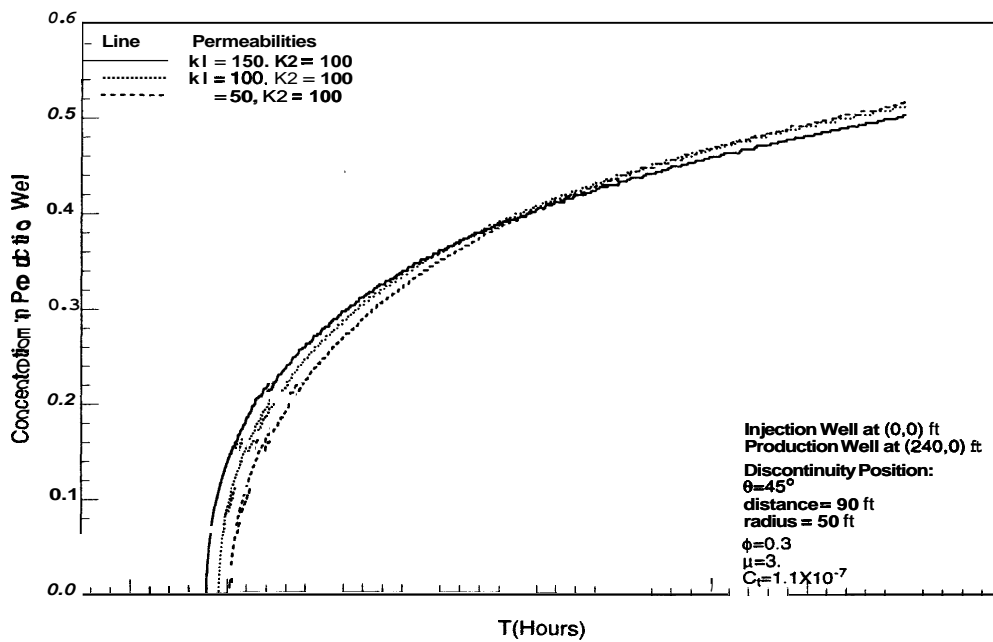


Figure 4.14: Tracer profile in a doublet system of infinite reservoir

advance of the fastest tracer front might be larger than the diameter of the production well, and the front could escape from the detection of the breakthrough condition.

In this example, the velocity at the start point of each time step was used in computing streamlines along a characteristic curve. Using the velocity at the start point is just a first approximation. To be more accurate, a second approximation can be applied. In the second approximation, the velocities are replaced by known mean values over the advance arc along the characteristic curve. This second procedure can be repeated iteratively until successive iterates agree to a specified number of decimal places, and will usually yield a much better approximation.

# Chapter 5

## Using Tracer and Pressure Data Simultaneously

The nonlinear least square regression method is an indirect method to obtain reservoir properties from observed data. It has been applied widely in well test analysis, especially for interpreting transient pressure data. Based on the difference between observed and calculated pressure data, the estimates of the parameters are adjusted until the calculated response is sufficiently close to that of observations. This method works for limited observations and is most successful if the objective function is convex or has few local minima. However, as the number of observations increases, as in the case of data from multiple wells, the calculation in the indirect method becomes inefficient. Another disadvantage is that the optimization may converge to a local minimum and hence the estimated result becomes dependent on the initial guess of the parameters.

### 5.1 Dispersivity and Permeability Correlation

It has long been considered that heterogeneity is one of the causes of the dispersion effect and the coefficients of dispersion should be a function of permeability. *Harleman et al. (1963)* conducted an experiment for uniform media and formulated expressions relating intrinsic permeability and longitudinal dispersivity. **Bear (1979)**



showed that the dispersivity of an isotropic porous medium can be defined by two constants, the longitudinal dispersivity of the medium and the transverse dispersivity of the medium. A more detailed study by *Arya and Hewett* (1988) introduced the concepts of macroscopic dispersion and megascopic dispersion, and investigated how the dispersions vary with heterogeneity, aspect ratio, and diffusion coefficient.

Including the molecular diffusion effect, a commonly used formula for dispersion coefficients, is

$$(D_{ij}(x, \mathbf{u})) = \phi d_m I + \frac{1}{|\mathbf{u}|} \begin{pmatrix} (d_l + d_t)u_1^2 & (d_l - d_t)u_1u_2 \\ (d_l - d_t)u_1u_2 & (d_l + d_t)u_2^2 \end{pmatrix} \quad (5.1)$$

where  $\mathbf{u} = (u_1, u_2) = -\frac{k}{\mu} \nabla p$  is the Darcy velocity,  $|\mathbf{u}| = \sqrt{u_1^2 + u_2^2}$ ,  $d_m$  is the molecular diffusion coefficient, and  $d_l$  and  $d_t$  are the magnitudes of longitudinal and transverse dispersion. Since

$$|\mathbf{u}| = \sqrt{u_1^2 + u_2^2} = \frac{k}{\mu} \sqrt{\left(\frac{\partial p}{\partial x}\right)^2 + \left(\frac{\partial p}{\partial y}\right)^2},$$

dispersion coefficients can be expressed in term of permeability and pressure

$$(D_{ij}(k)) = \phi d_m I + \frac{d_l k}{|\nabla p| \mu} A + \frac{d_t k}{|\nabla p| \mu} B \quad (5.2)$$

where matrices  $A$  and  $B$  are just of functions of pressure:

$$A = \begin{pmatrix} \left(\frac{\partial p}{\partial x}\right)^2 & \frac{\partial p}{\partial x} \frac{\partial p}{\partial y} \\ \frac{\partial p}{\partial x} \frac{\partial p}{\partial y} & \left(\frac{\partial p}{\partial y}\right)^2 \end{pmatrix}$$

$$B = \begin{pmatrix} \left(\frac{\partial p}{\partial x}\right)^2 & -\frac{\partial p}{\partial x} \frac{\partial p}{\partial y} \\ -\frac{\partial p}{\partial x} \frac{\partial p}{\partial y} & \left(\frac{\partial p}{\partial y}\right)^2 \end{pmatrix}$$

This expression transforms the convection-diffusion equation to an equation with  $k$  as coefficient instead of  $D_{ij}$ , which is the basis of the integrating tracer and pressure data.

## 5.2 Integrating Tracer and Pressure Data in Heterogeneous Reservoirs

Consider two-dimensional single phase flow in an isotropic reservoir, the pressure governing equation at steady state is given by

$$\frac{\partial}{\partial x} \left( k \frac{\partial p}{\partial x} + k \frac{\partial p}{\partial y} \right) + \frac{\partial}{\partial y} \left( k \frac{\partial p}{\partial x} + k \frac{\partial p}{\partial y} \right) = \frac{q\mu}{h}, \quad (5.3)$$

and an example of a transport dominated convection-diffusion equation is given by

$$\begin{aligned} \frac{\partial c}{\partial t} = & \frac{\partial}{\partial x} \left( D_{xx} \frac{\partial c}{\partial x} + D_{xy} \frac{\partial c}{\partial y} \right) + \frac{\partial}{\partial y} \left( D_{yx} \frac{\partial c}{\partial x} + D_{yy} \frac{\partial c}{\partial y} \right) \\ & - \frac{\partial}{\partial x} v_x c - \frac{\partial}{\partial y} v_y c - \frac{c_1 q}{\phi h}, \end{aligned} \quad (5.4)$$

where the velocities

$$v_x = -\frac{k}{\phi\mu} \frac{\partial p}{\partial x}$$

and

$$v_y = -\frac{k}{\phi\mu} \frac{\partial p}{\partial y}$$

are interstitial velocities, related to pressure distribution,  $D_{ij}$  are the components of dispersion coefficients as expressed in Eqs. 5.1 and 5.2,  $c_1$  is the concentration of the source/sink, and  $q$  is the rate of injection and/or withdrawal in volume flux per unit area.

The following are the steps in the direct approach for integrating tracer and pressure data:

1. According to the data measured at multiple wells, generate tracer and pressure distributions at various time on the whole reservoir by an interpolation scheme such as spline or kriging.
2. After the pressure as a function of  $x, y$  is known, Eq. 5.3 becomes a first order partial differential equation for  $k(x, y)$ .

3. Apply a relationship between dispersion coefficients and permeability, so that tracer equation has permeability as coefficients, too. The relationship could be the correlation from the experiment.

Eq. 5.4 at this step becomes a first-order hyperbolic equation for  $k(x, y)$ .

4. Discretize both first-order hyperbolic equations. They have permeabilities as unknowns after discretization, and are solved by numerical methods to obtain  $k_{ij}$ .

This scheme favors the multiwell data. When there are more observation wells, the reconstruction of the pressure distribution and tracer distribution becomes more accurate. Another useful feature of this approach is that including data from more wells will not increase the amount of computation, which differs from the nonlinear regression scheme of matching pressure data.

On the other hand, there are two steps of approximation in the approach. The first approximation comes from the reconstruction of the pressure and tracer distributions, which can be reduced by applying more data from more wells. The second approximation comes from the numerical error introduced in solving the first-order equations.

Other important factors need to be taken into consideration. For examples, how to pose boundary conditions for the permeability in the discretized pressure equation.

This approach generally is not applicable to three dimensional problems because the pressure and tracer data are not collected for different locations in the vertical direction and so pressure or tracer data cannot be interpolated vertically.

### 5.3 Ill-posedness

The process of solving a partial differential equation numerically usually ends **up** as the solution to a system of linear equations, such as

$$Ak = u, \tag{5.5}$$

where  $A$  is a matrix and  $k$  and  $u$  are vectors. The problem of determining  $k$  from  $u$  is called well-posed if it satisfies the following three conditions:

- o for each  $u$ , there exists a solution  $k$
- the solution is unique and
- the solution depends continuously on  $u$  (it is stable against small variations of  $u$ ).

If one of the above conditions is not satisfied, then the problem is called ill-posed. As an example of numerical demonstration for ill-posedness, look at the following system of equations:

$$\begin{pmatrix} 1 & 1 \\ 1 & 1.01 \end{pmatrix} \begin{pmatrix} k_{xx} \\ k_{yy} \end{pmatrix} = \begin{pmatrix} 1 \\ 1 \end{pmatrix} \quad (5.6)$$

The solution of the system is  $k_{xx} = 1, k_{yy} = 0$ .

Now, let us introduce one percent error into the right hand side as in measurement, and see what effect the small error has on the solution. Solving

$$\begin{pmatrix} 1 & 1 \\ 1 & 1.01 \end{pmatrix} \begin{pmatrix} k_{xx} \\ k_{yy} \end{pmatrix} = \begin{pmatrix} 1 \\ 1.01 \end{pmatrix} \quad (5.7)$$

yields  $k_{xx} = 0, k_{yy} = 1$ . A small change in the right hand side has dramatically changed the permeability solution.

The system of simultaneous equations that come up in performing inverse analyses during parameter identification is often ill-posed. Basically, for the case of nonuniqueness, there is no mathematical method that can do much in overcoming the difficulty. The only way is to add more limitation or constraint to the solution, e.g. range, smoothness. However, for instability, various mathematical methods have been introduced. For example, the inverse problem of mathematical physics can be well-posedly formulated based on the introduction of additional information about the sought-for solution; the regularization method studied by *Kravaris* and *Seinfeld* (1985) can yield stable approximate solutions to ill-posed problems in accordance with the accuracy of the data.

The solution for the direct method of pressure equation is theoretically unique under appropriate conditions provided that the pressure related terms are given exactly anywhere. These appropriate conditions have been studied by *Richter* (October, 1981) for the steady state diffusion equation.

As an example of ill-posed permeability identification, whose boundary conditions are not appropriately posed, consider a rectangular reservoir of  $0 < x < a$ ,  $0 < y < b$  that has reached steady-state,

$$\frac{\partial}{\partial x}(k(x, y)\frac{\partial p}{\partial x}) + \frac{\partial}{\partial y}(k(x, y)\frac{\partial p}{\partial y}) = 0 \quad (5.8)$$

with boundary conditions

$$\begin{cases} p(x, 0) = 100 & 0 < x < a \\ p(0, y) = 100 & 0 < y < b \\ \frac{\partial p}{\partial y}|_{y=b} = 0 & 0 < x < a \\ \frac{\partial p}{\partial x}|_{x=a} = 0 & 0 < y < b. \end{cases} \quad (5.9)$$

Furthermore, the pressure data are measured at any location in the reservoir as

$$p(x, y) = 100 \quad 0 < x < a, \quad 0 < y < b. \quad (5.10)$$

The permeability identification is not well-posed for the given boundary conditions and the measured data because the permeability coefficient could take any value. Since no fluid flow occurs in the reservoir, the measured pressure data do not carry any information about the reservoir.

Ill-posedness is not a property of the direct method. It is associated with the parameter identification problem itself. Ill-posedness could also exist in the nonlinear least square regression approach; including noise in the pressure data can change the nonlinear least square solution dramatically or introduce more local minima to the objective function.

## 5.4 Permeability Constraints

**Eq. 5.3** with permeability as the unknown is a first order hyperbolic equation. To solve it, permeability should be specified on a curve that intersects with each characteristic curve as discussed by *Nelson* (1962). The following one-dimensional problem will help understand the inverse nature of permeability.

Consider a finite section of linear flow bounded by  $x = 0$  and  $x = 1$  with a source distribution  $q(x)$ ,  $0 < x < 1$  such that  $\int_0^1 q(x)dx = 0$ ,

$$\frac{d}{dx} \frac{k(x)}{\mu} \frac{dp}{dx} = q(x) \quad 0 < x < 1 \quad (5.11)$$

with the boundary conditions

$$\begin{cases} -\frac{k(0)}{\mu} p'(0) = v_0 \\ -\frac{k(1)}{\mu} p'(1) = v_1. \end{cases} \quad (5.12)$$

For such a one-dimensional problem, pressure  $p(x)$  as the unknown can be solved easily as a function of  $k(x)$ . It is also easy to obtain  $k(x)$  as a result of interpretation from the given  $p(x)$ ,  $q(x)$  and the boundary conditions in Eq. 5.12 if  $v_0 \neq 0$  and  $v_1 \neq 0$ . Will it be as easy if the boundary condition is changed to a no-flow boundary, e.g.  $v_0 = v_1 = 0$ ? In this case, we have

$$\frac{d}{dx} \frac{k(x)}{\mu} \frac{dp}{dx} = q(x) \quad 0 < x < 1 \quad (5.13)$$

with boundary conditions

$$\begin{cases} p'(0) = 0 \\ p'(1) = 0 \end{cases} \quad (5.14)$$

Suppose the pressure distribution  $p(x)$  satisfying conditions  $p'(0) = p'(1) = 0$  has been solved or measured, can we infer  $k(x)$  uniquely from  $p(x)$ ? Since it is a one-dimensional equation, taking an integral of  $x$  on both sides will yield

$$\frac{k(x)}{\mu} \frac{dp(x)}{dx} = \int_0^x q(x) dx \quad (5.15)$$

so at  $x$  where  $p'(x) \neq 0$ ,  $k(x)$  can be obtained explicitly as

$$k(x) = \frac{\mu}{p'(x)} \int_0^x q(x) dx \quad (5.16)$$

The observation from this discussion is that discretization and solution of Eq. 5.13 do not require any boundary condition for  $k(x)$  at  $x = 0$  or  $x = 1$ .

However, if the boundary condition is constant pressure  $p(0) = p(1) = 0$ , the same discretized equation itself will not be sufficient to give  $k(x)$ . A permeability value specified anywhere makes the equation solvable uniquely. What is going on, is  $k(x)$  not uniquely determined by  $p(x)$ ? It is generally believed that different  $k(x)$  will result in a different pressure distribution. To answer this question, it is helpful to have a look at the analytical derivation. Treating  $p(x)$  as known, measured or solved, solve for  $k(x)$  from Eq. 5.13 by integration

$$\frac{k(x)}{\mu} \frac{dp(x)}{dx} = \int_0^x q(x) dx + C \quad (5.17)$$

where  $C$  is a constant. This constant is not free, however, it is related to the constant pressure boundary condition.

$$p(x) = \int_0^x \frac{\mu}{k(x)} \left( \int_0^x q(x) dx + C \right) dx + C_1 \quad (5.18)$$

To satisfy  $p(0) = p(1) = 0$ , we have

$$C_1 = 0 \quad (5.19)$$

and

$$\int_0^1 \frac{\mu}{k(x)} \left( \int_0^x q(x) dx + C \right) dx = 0 \quad (5.20)$$

so

$$C = \frac{\int_0^1 \frac{\mu}{k(x)} \int_0^x q(\alpha) d\alpha dx}{\int_0^1 \frac{\mu}{k(x)} dx} \quad (5.21)$$

Therefore,

$$\frac{k(x)}{\mu} \frac{dp(x)}{dx} = \int_0^x q(x) dx + \frac{\int_0^1 \frac{\mu}{k(x)} \int_0^x q(\alpha) d\alpha dx}{\int_0^1 \frac{\mu}{k(x)} dx} \quad (5.22)$$

Eq. 5.22 is an integral equation, which suggests that permeability can not be obtained by a simple finite difference method even though permeability is determined uniquely. In this case, constraining permeability at any given point as suggested by *Nelson* (1962) will make the finite difference method work. Similar discussion can be extended to infinite linear flow and the flow in higher dimensions provided that permeability is of value larger than zero. *Richter* (April, 1981) developed a modified upwind difference method to solve for permeability directly from the first order hyperbolic equation. When certain conditions are met, this method has first order convergence.

## 5.5 Direct Method for Tracer Data

A traditional approach of interpreting field tracer data involves a history matching procedure based on the nonlinear least square method, which in many cases is time-consuming and may result in a nonunique solution. In this section, a direct method is investigated for tracer data provided that the tracer distribution has been reconstructed correctly. There are various schemes to reconstruct the concentration distribution at any location in the reservoir at any time from the tracer data at production wells and observation wells, such as cubic spline, finite difference, Lagrange interpolations and kriging. Kriging interpolation is an exact method. *Pan* (1995) studied kriging algorithm as an multivariate interpolation method. The smoothness of the interpolated function was controlled by the highest degree of the representative polynomials in Kriging algorithm. *Pan* (1995) found that kriging interpolation is more accurate than least square interpolation in capturing the optimal values of the interpolated function.

In the following discussion, it is assumed that dispersion effect is small enough to be neglected. The one-dimensional problem is studied first and then the two-dimensional.

For the one-dimensional tracer equation without dispersion, the phase of fluid carrying concentration  $c$  moves at a constant average velocity  $u$ ,

$$\frac{\partial c}{\partial t} + \frac{u}{\phi(x)} \frac{\partial c}{\partial x} = 0 \quad (5.23)$$

where  $x$  is distance,  $t$  is time and  $\phi$  is a non-constant porosity. As an easy example, for

$$\phi(x) = \begin{cases} \phi_1 & 0 < x < a \\ \phi_2 & x > a \end{cases} \quad (5.24)$$

where  $\phi_1$  and  $\phi_2$  are constant, the solution for the boundary condition that a constant concentration  $c_0$  is maintained at  $x = 0$ , is

$$c(x, t) = \begin{cases} c_0 & ut - \phi_1 x > 0 \\ 0 & ut - \phi_1 x < 0 \end{cases} \quad (5.25)$$

for the region  $0 < x < a$ , and



$$c(x, t) = \begin{cases} c_0 & ut - \phi_1 a - \phi_2(x - a) > 0 \\ 0 & ut - \phi_1 a - \phi_2(x - a) < 0 \end{cases} \quad (5.26)$$

for the region  $x > a$ .

This solution represents a piston-like displacement with a concentration discontinuity varying from 0 to  $c_0$  that propagates forward as shown in Fig. 5.1. This solution will facilitate the understanding of the following recovery method for  $\frac{u}{\phi}$ .

Now, assume that the solution is given numerically, i.e., either there is a function or a table to tell the concentration  $c$  at any  $x > 0$  and any  $t > 0$ , how to obtain  $\frac{u}{\phi}$  for any  $x$  from this information? The most important information is the concentration discontinuity position, at what time  $t$  the discontinuity reaches at position  $x$ . After that time, the concentration at  $x$  will always be  $c_0$ . The concentration at  $x$  before that time is always 0. These values do not contribute to the recovery of  $\frac{u}{\phi}$  at all. Through the given table or function, the time at which the discontinuity reaches  $x_1$  can be obtained

$$t_1 = f(x_1). \quad (5.27)$$

So the time for  $x_2 = x + dx$  is

$$t_2 = f(x_2). \quad (5.28)$$

With  $t_1, t_2, x_1$  and  $x_2$  available, then  $\frac{u}{\phi}$  can be calculated,

$$\frac{u}{\phi} = \frac{x_2 - x_1}{t_2 - t_1}. \quad (5.29)$$

This expression actually is the difference form of the characteristic equation

$$\frac{dx}{dt} = \frac{u}{\phi}.$$

A similar scheme can be developed for two-dimensional tracer problem

$$\frac{\partial c}{\partial t} + v_x \frac{\partial c}{\partial x} + v_y \frac{\partial c}{\partial y} = 0. \quad (5.30)$$

The characteristic curve for this first order hyperbolic equation is determined by

$$\frac{dx}{v_x} = \frac{dy}{v_y} = \frac{dt}{1} \quad (5.31)$$

If the concentration distribution is reconstructed by the measured tracer data, then  $v_x$  and  $v_y$  can be recovered as

$$\begin{cases} v_x = \frac{\Delta x}{t(x+\Delta x, y) - t(x, y)} = \frac{\Delta x}{\Delta t_x} \\ v_y = \frac{\Delta y}{t(x, y+\Delta y) - t(x, y)} = \frac{\Delta y}{\Delta t_y}, \end{cases} \quad (5.32)$$

where  $t(x, y)$  is the time at which the concentration discontinuity reaches at location  $(x, y)$ .

As an example, consider the radial flow around an injection well in an infinite reservoir. The injection flow rate is a constant  $q$ . With the coordinates origin set at injection well, the average phase velocity at  $(x, y)$  can be derived,

$$\begin{cases} u_x = \frac{qx}{\pi h \sqrt{(x^2 + y^2)^3}} \\ u_y = \frac{qy}{\pi h \sqrt{(x^2 + y^2)^3}}. \end{cases} \quad (5.33)$$

The tracer equation for this radial flow model without dispersion is

$$\frac{\partial c}{\partial t} + \frac{qx}{\pi h \phi \sqrt{(x^2 + y^2)^3}} \frac{\partial c}{\partial x} + \frac{qy}{\pi h \phi \sqrt{(x^2 + y^2)^3}} \frac{\partial c}{\partial y} = 0. \quad (5.34)$$

The solution to this equation with an injection well maintained at a constant concentration  $c_0$  starting at  $t = 0$  and a zero initial concentration can be obtained by the characteristic method,

$$c(x, y, t) = \begin{cases} c_0 & 3\pi h \phi t - 2q\sqrt{(x^2 + y^2)^3} > 0 \\ 0 & 3\pi h \phi t - 2q\sqrt{(x^2 + y^2)^3} < 0 \end{cases} \quad (5.35)$$

The surface consisting of all the characteristic curves originating from  $x = 0, y = 0$  and  $t = 0$  in space  $(x, y, t)$  is plotted in Fig. 5.2. The equation defining this surface is

$$t(x, y) = \frac{2q}{3\pi h \phi} \sqrt{(x^2 + y^2)^3},$$

which, actually, turns out to be the time function that plays an important role in recovering  $u_x, u_y$  or  $\phi$ .

Once the pressure distribution is known and the velocity field is obtained, the permeability distribution can be calculated by applying Darcy's law. Notice that there is no boundary difficulty in interpreting tracer data, which is different to the direct interpretation of pressure data.

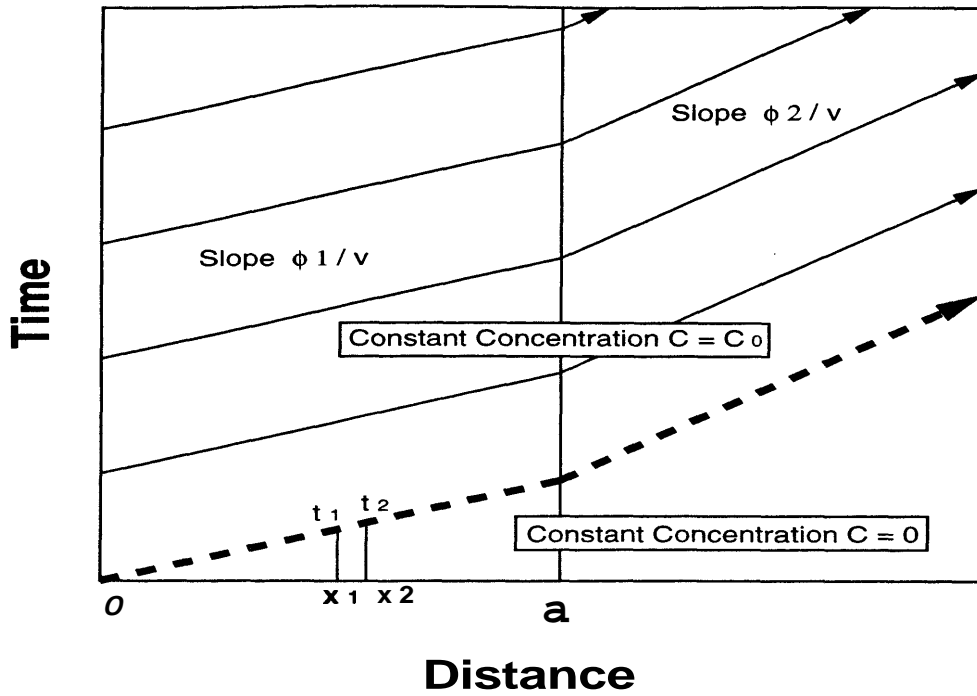


Figure 5.1: Propagation of concentration of discontinuity at  $x = 0$

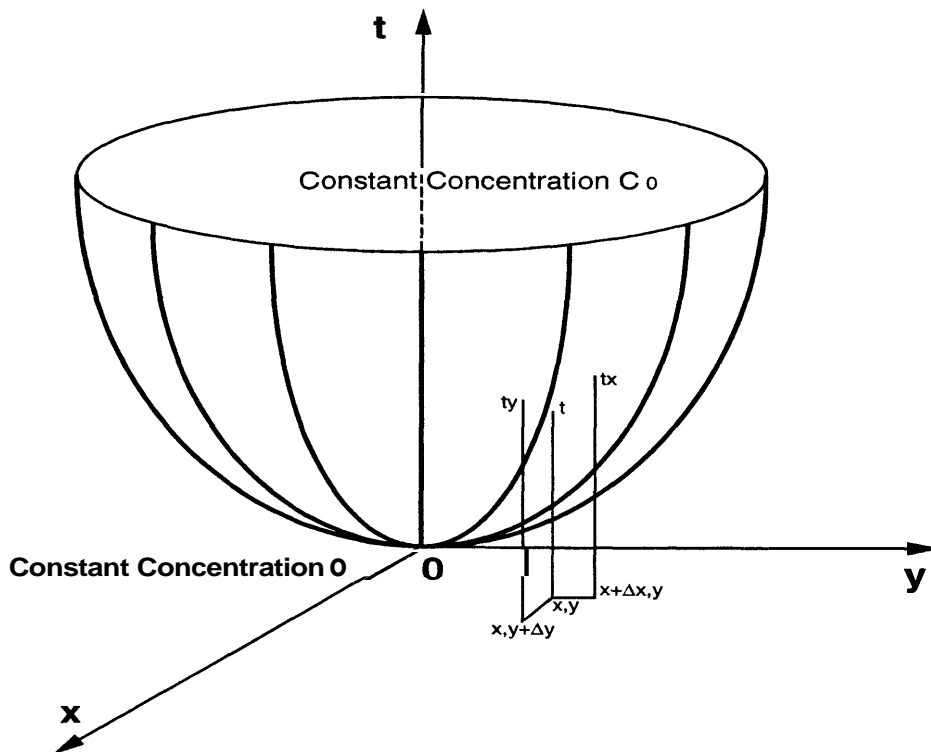


Figure 5.2: x-y-t diagram showing characteristic surface for the concentration of radial flow

In the above discussion it was assumed that tracer flow has negligible dispersion effect. In the case in which significant dispersion prevails, it remains true that the concentration front data has more weight in contributing to the recovery of the areal permeabilities.

## 5.6 Example

Consider a multiple well system in an infinite isotropic reservoir with a local region of heterogeneity that can be approximated by a circular disk of different permeability and porosity. The center of the circular discontinuity is chosen to be the origin of coordinates system in order to make the pressure expression simple. Assume the permeability of the circular discontinuity is

$$k_1 = 50 \text{ md}$$

and its radius is

$$a = 50,$$

and the rest of the reservoir has permeability of

$$k_2 = 100 \text{ md}.$$

There is an injection well located at  $(-100, 0)$  with injection rate  $q = 400$ . Four production wells are located at

- $(100, 0)$  with production rate  $q = 150$
- $(-300, 0)$  with production rate  $q = 50$
- $(-100, 200)$  with production rate  $q = 100$
- $(-100, -200)$  with production rate  $q = 100$

Furthermore, assume that the system has been in injection and production for a long time. The solution for the pressure change for such a multiple well system can be obtained as shown in Appendix E by superposition. Fig. 5.3 shows the pressure distribution calculated from Eq. E.23 in Appendix E for this system, and Fig. 5.4 is the corresponding pressure contour.

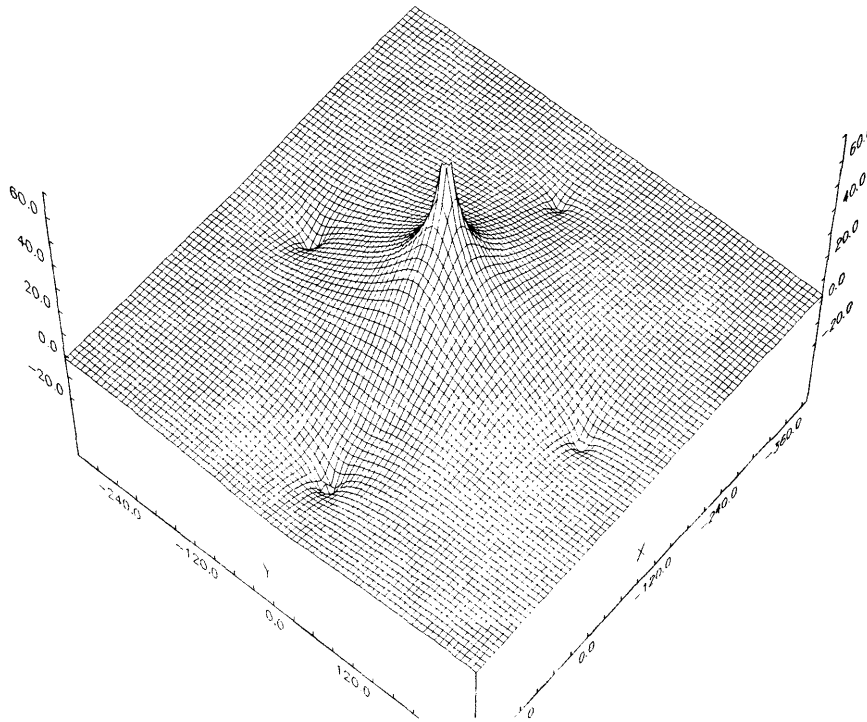


Figure 5.3: Pressure distribution of multiwell system with a circular discontinuity

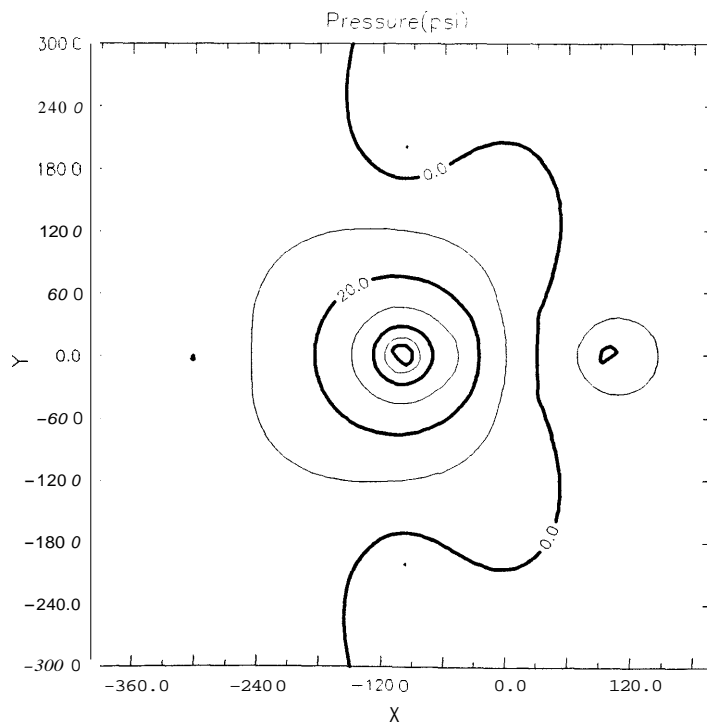


Figure 5.4: Pressure contour of multiwell system with a circular discontinuity

To obtain the concentration semianalytically, assume that the dispersion effect is small enough to neglect. With this assumption, convection-diffusion Eq. 5.4 becomes Eq. 5.30, so the characteristic method can be applied here to show the idea.

As discussed in the previous chapter, the streamlines are actually the projection of three dimensional characteristic curves defined in Eq. 5.31 onto the  $x$ - $y$  plane. Fig. 5.5 includes some streamlines for the multiple well example with the circular discontinuity. As a comparison, Fig. 5.6 shows all the corresponding streamlines in the homogeneous reservoir where the permeability of circular region is equal to  $100\text{ md}$ .

The concentration front at each time step can be computed together with the streamlines. Fig. 5.7 shows the shape of concentration fronts at various time for the heterogeneous system while Fig. 5.8 shows the shape for the corresponding homogeneous reservoir. However, in order to obtain the velocity as expressed in Eq. 5.32, it is necessary to determine the time function of  $(x, y)$  at which the concentration front reaches the location  $(x, y)$ . In real application, the time function is reconstructed from the observed concentration data. Fig. 5.9 is an example of the three-dimensional plot of this time function and Fig. 5.10 is the two-dimensional contour of the time function. Once this time function is available, the velocity at each location can be obtained and therefore the permeability is derived from applying Darcy's law as pressure distribution is known. In a little more details, the recovery of permeability follows these steps:

1. To obtain the permeability distribution, first the pressure distribution is generated by interpolation from observation wells, so the pressure gradient  $(\frac{\partial p}{\partial x}, \frac{\partial p}{\partial y})$  can be calculated for any location  $(x, y)$ ;
2. Reconstruct the front time function  $t(x, y)$  at each location  $(x, y)$  from the observed concentration data; so the time  $t(x, y)$  for tracer front to reach  $(x, y)$  can be found;
3. Move a small distance  $dd$  along the opposite direction of pressure gradient  $(\frac{\partial p}{\partial x}, \frac{\partial p}{\partial y})$  and find another time  $t_{dd}$  tracer front takes to reach by interpolation;
4. Then, a formula that is derived from Eq. 5.32

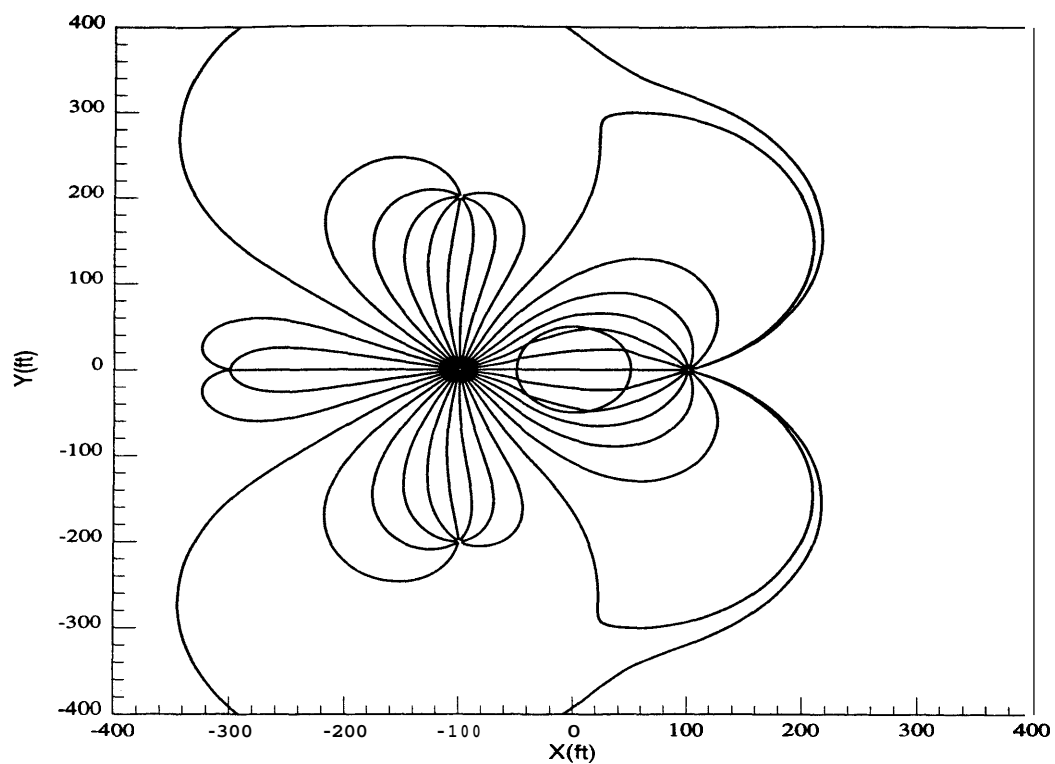


Figure 5.5: Streamline of multiwell system with a circular discontinuity

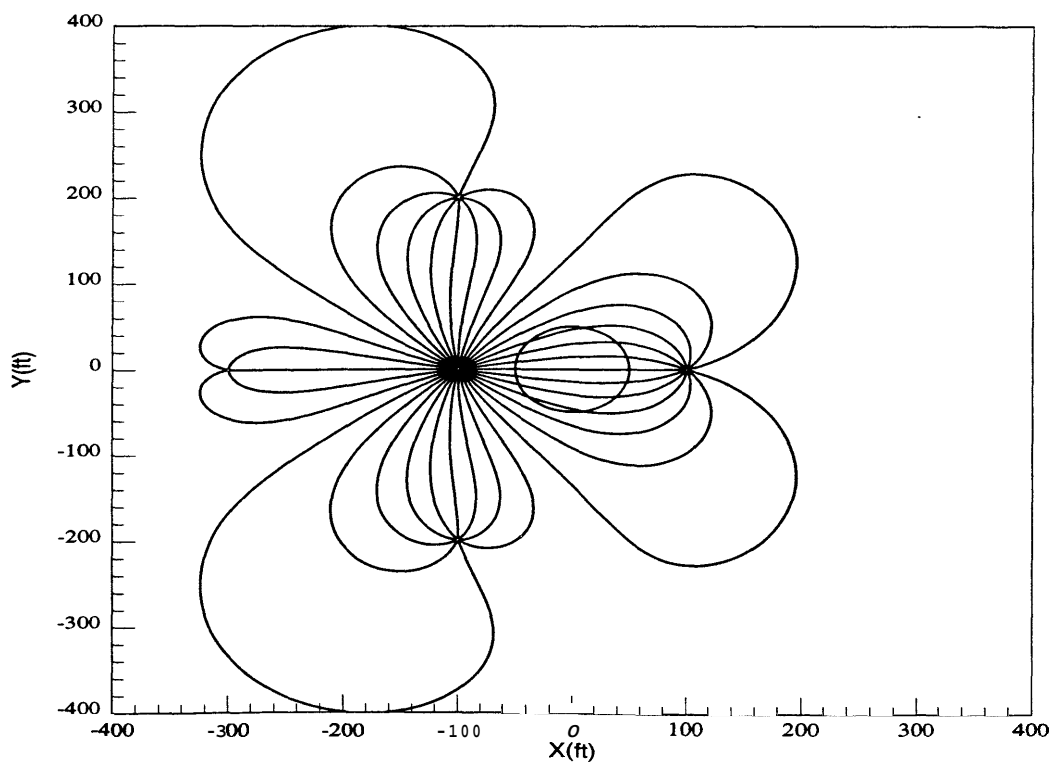


Figure 5.6: Streamline of multiwell system but without the circular discontinuity

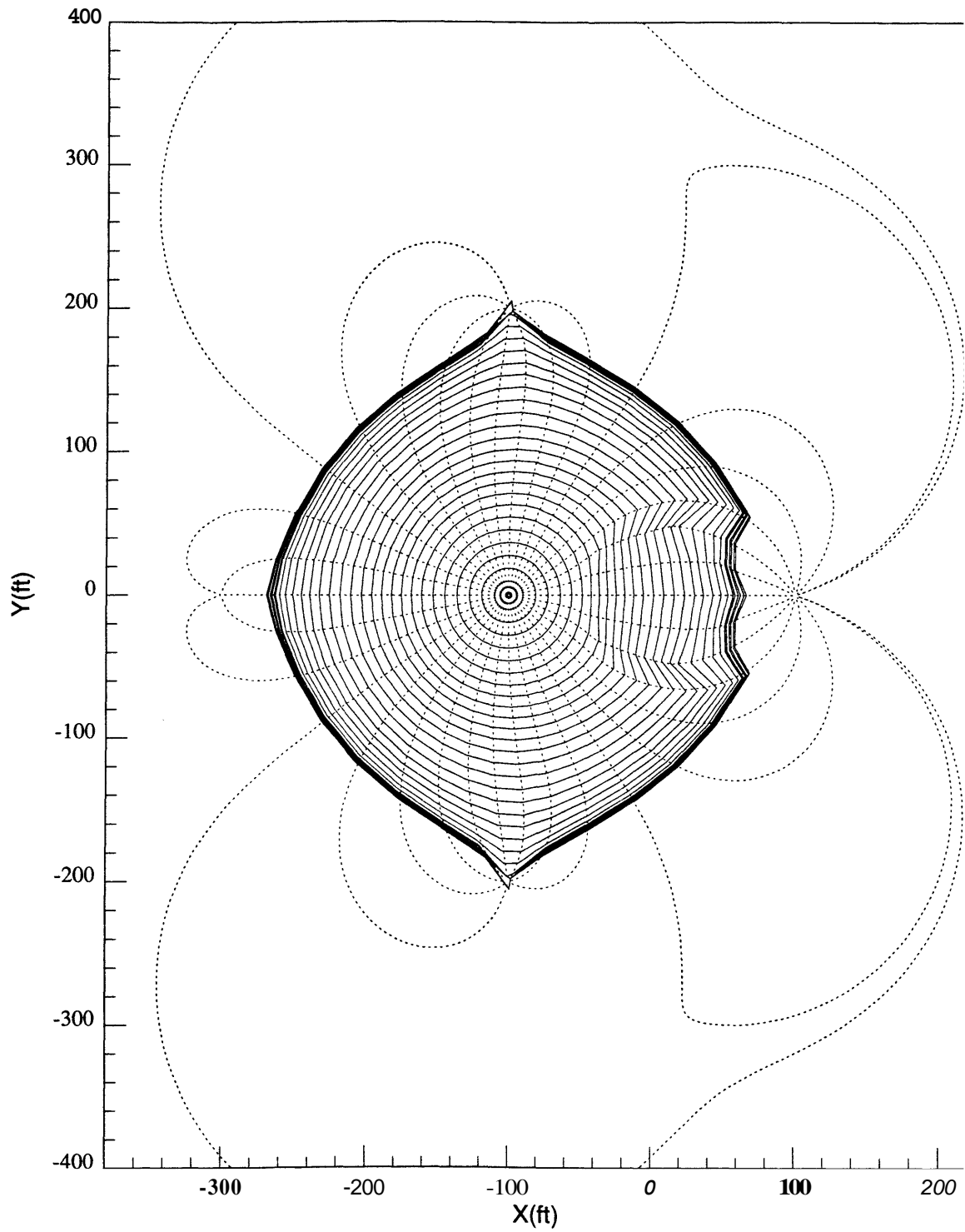


Figure 5.7: Concentration front in the multiwell system with a circular discontinuity



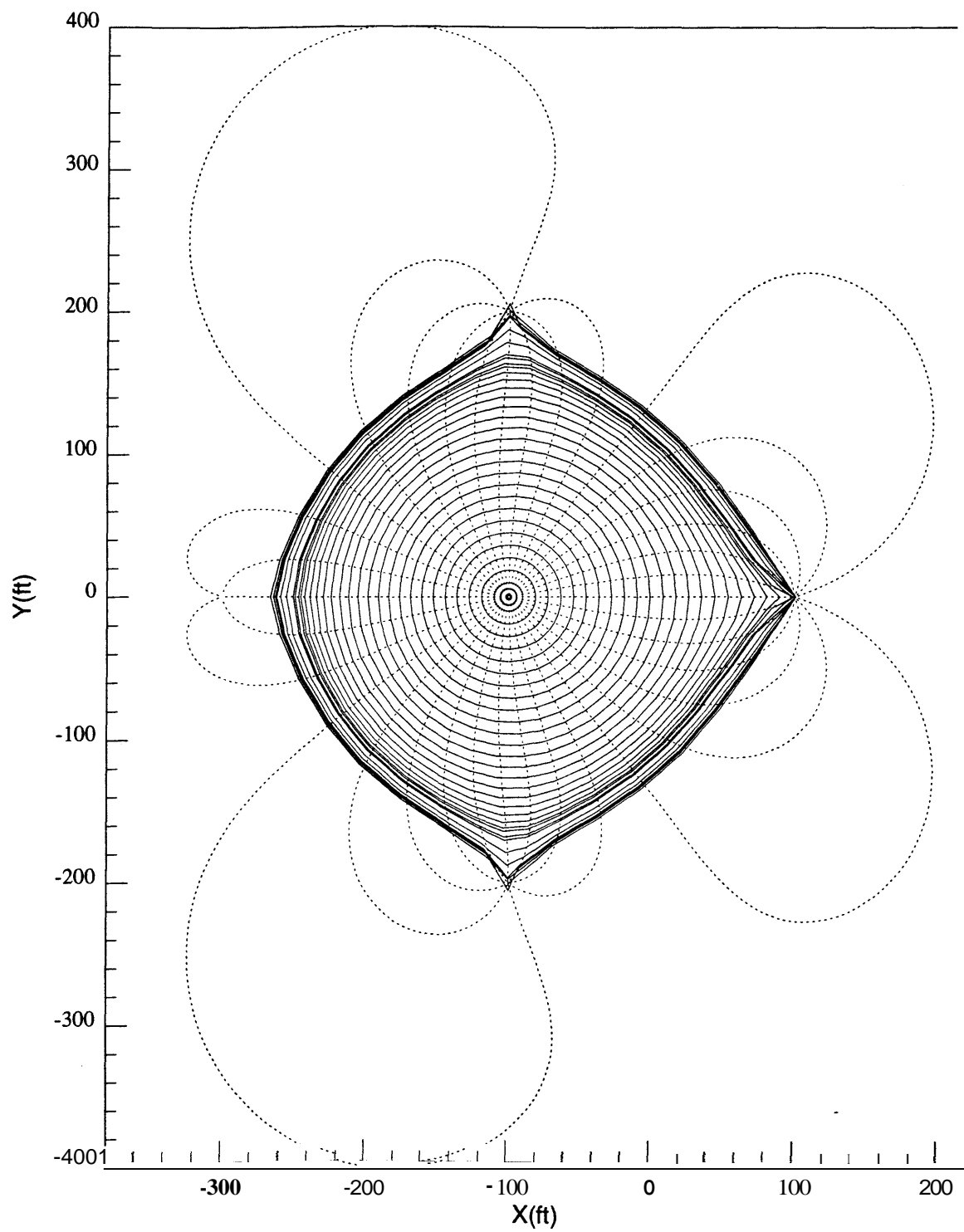


Figure 5.8: Concentration front in the multiwell system without the circular discontinuity

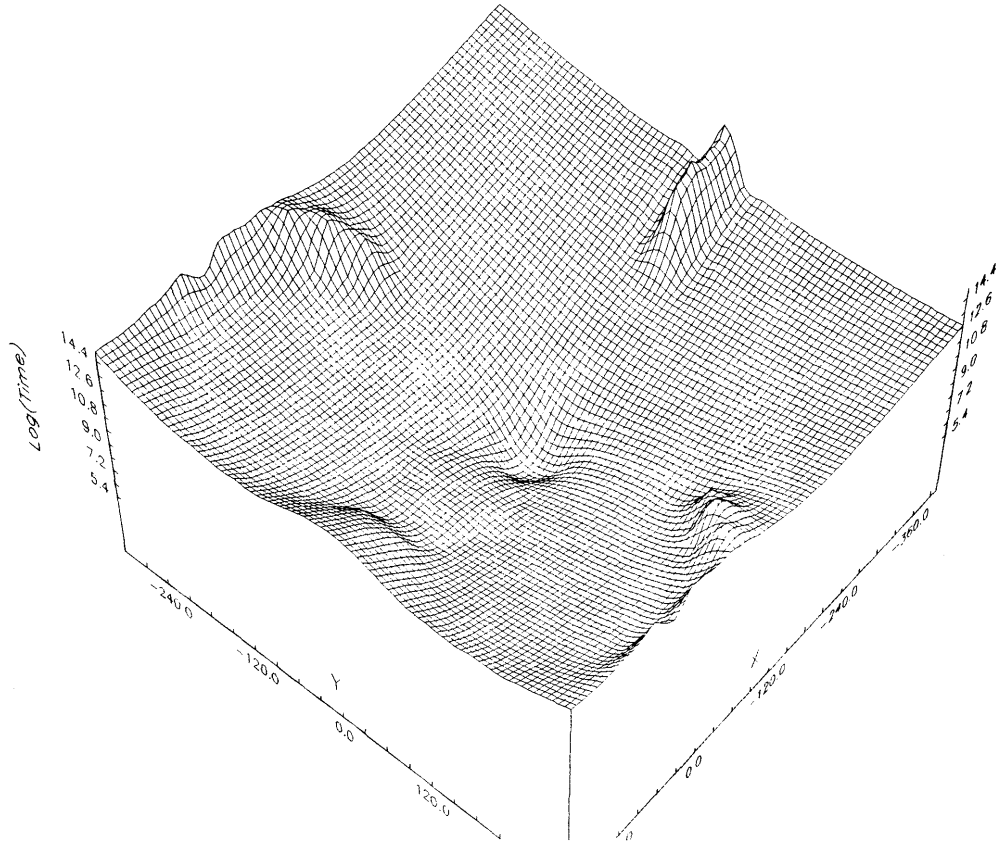


Figure 5.9: x-y-t diagram showing the time at which the concentration front arrives as a function of  $(x, y)$

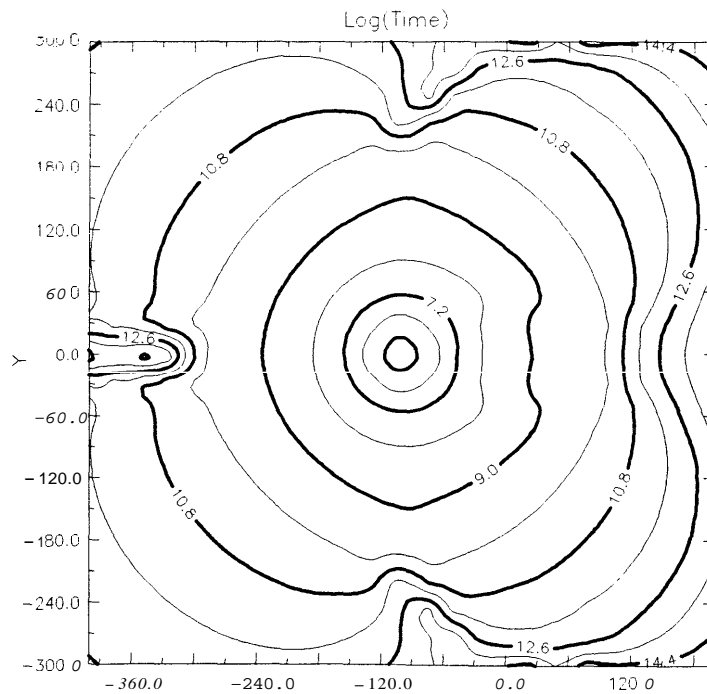


Figure 5.10: The time at which the concentration front arrives as a function of  $(x, y)$

$$v = \frac{dd}{t_{dd} - t(x, y)} \quad (5.36)$$

is applied to obtain velocity value;

5. Finally, Darcy's law

$$k = \mu \frac{v}{\sqrt{\left(\frac{\partial p}{\partial x}\right)^2 + \left(\frac{\partial p}{\partial y}\right)^2}} \quad (5.37)$$

is used to obtain permeability.

The results of this calculation procedure for different numbers of observation points for the example of circularly discontinuous reservoir are shown in Figs 5.11, 5.12 and 5.13. The number of observation points used in the three figures are **300x300**, **100x100** and **30x30**, respectively.

Since a tracer test usually measures the cumulative concentration vs. time at production well, it would be difficult to recover this entire permeability distribution from observations of tracer returns at a limited number of locations. However, the new technique of **4-D** seismology has the ability to track the moving front of steam or tracer in the reservoirs as discussed by *Nur* (1988) and *Brzostowski and McMechan* (1991). With the help of **4-D** seismology, the direct method using the time function will be a practical method in the near future.

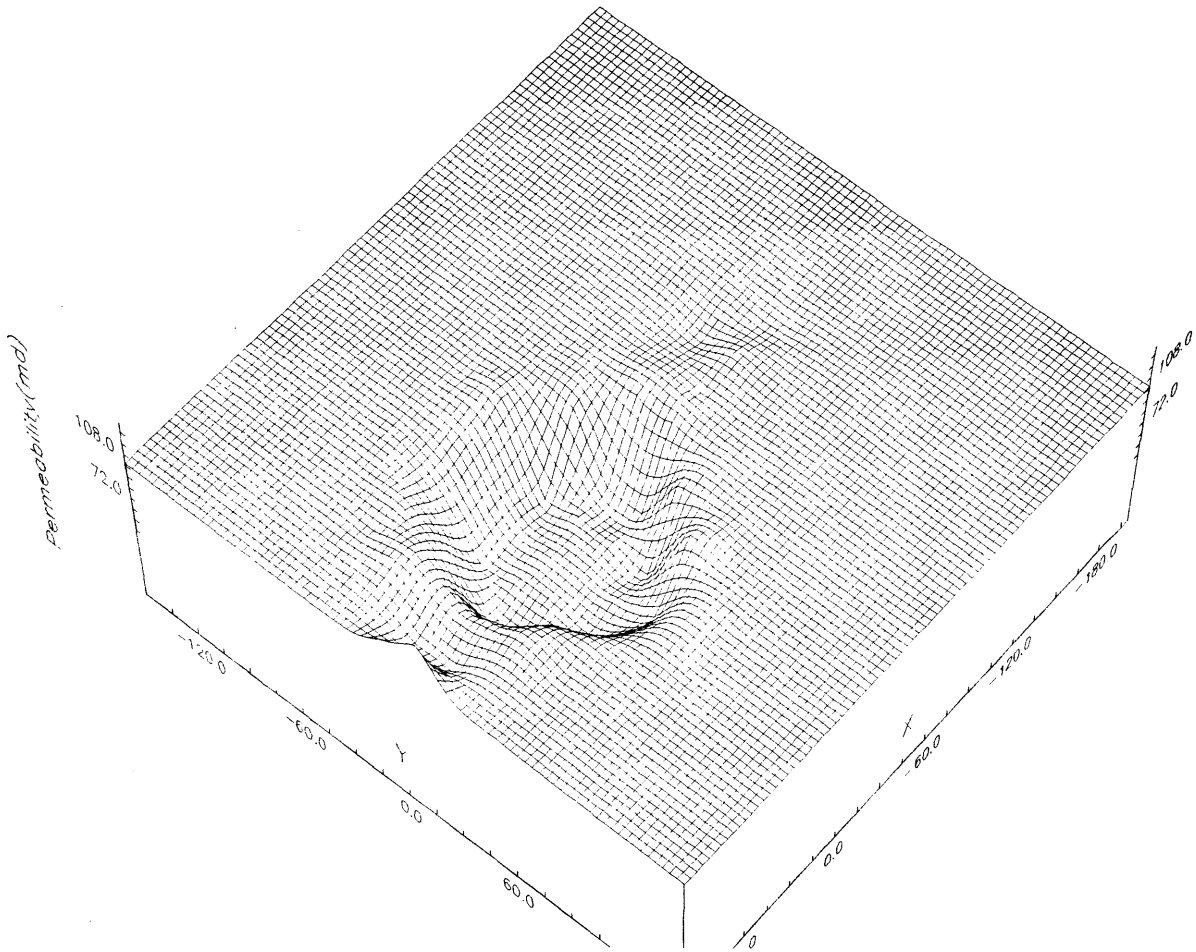


Figure 5.11: Permeability distribution calculated using pressure and tracer data from **300** by **300** observation points

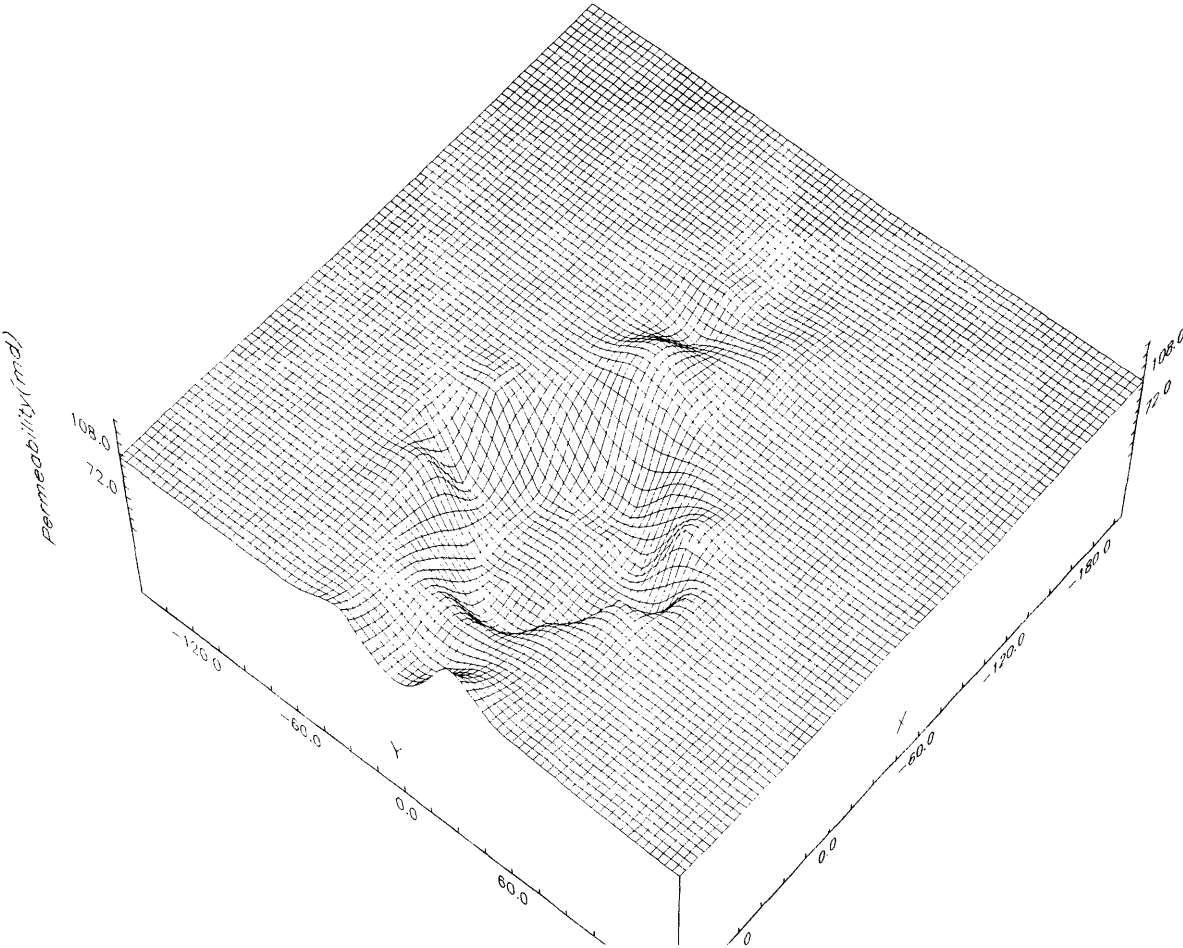


Figure 5.12: Permeability distribution calculated using pressure and tracer data from 100 by 100 observation points

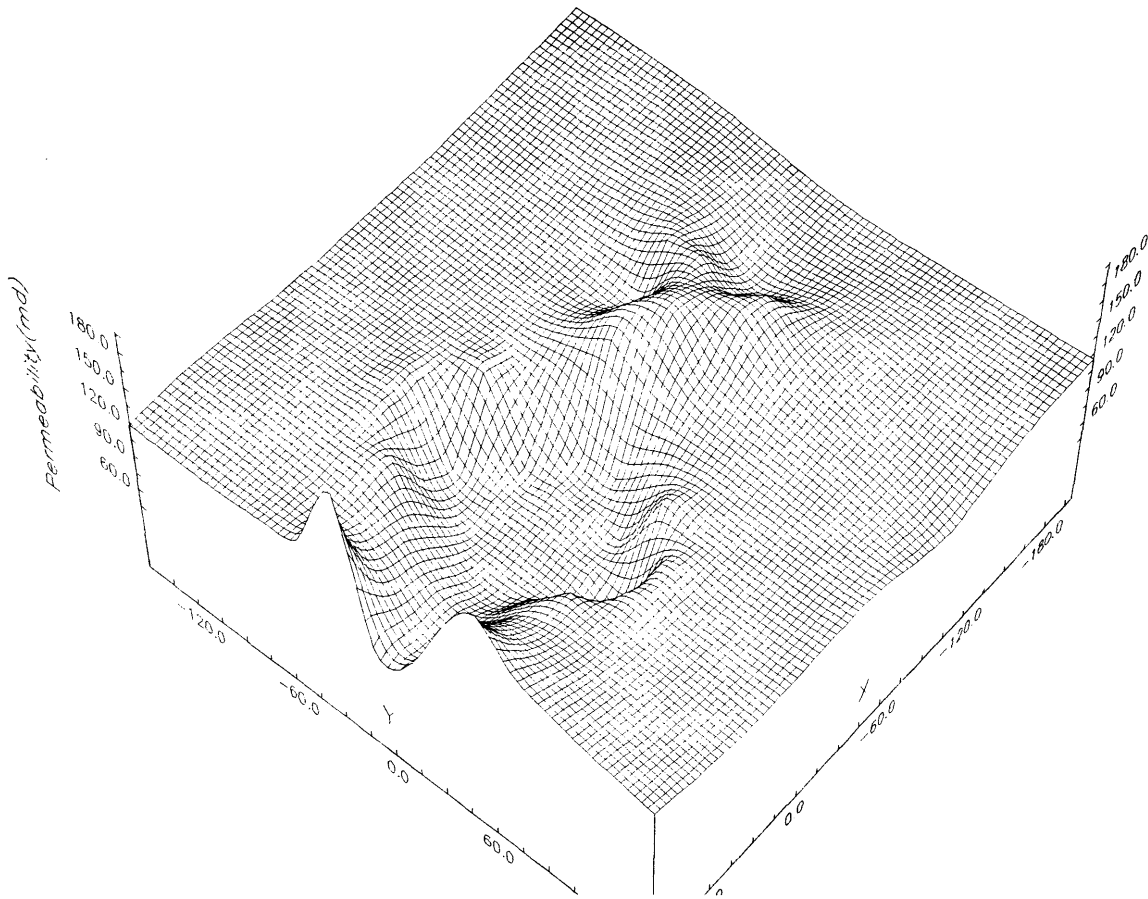


Figure 5.13: Permeability distribution calculated using pressure and tracer data from 30 by 30 observation points

# Chapter 6

## Conclusions

In this work, pressure test analysis and tracer test analysis in multiwell systems were studied first individually and then together. The main contribution of this work will be summarized in this chapter and the conclusions will be stated for each topic.

### 6.1 Analysis of Pressure Data from Multiple Wells

Several models were studied with an emphasis on how to use the pressure data from multiple wells. The objective functions were formulated to avoid using just a subset of the multiwell data. A nonlinear least square method was presented to find the optimal solutions to the objective functions.

In the analysis of multiwell interference tests for anisotropic reservoirs, the nonlinear regression method was proposed to utilize multiple sets of pressure data. A field example from an injection interference test was interpreted using the new approach. It can be concluded that:

- o The nonlinear least square approach is a practical method for estimating the anisotropic permeabilities – compared to the conventional approach, it makes use of all the pressure data, avoids inconsistent results and increases the confidence level of the estimates.
- o The solution presented by *Papadopoulos (1965)* is preferable to the one by *Collins (1961)* in formulating the objective function.

For the multiwell system whose heterogeneity is represented by a circular discontinuity, a robust procedure was developed to generate the pressure solution with wellbore storage. Pressure-time curves were plotted to show how the pressure varies with the parameters. Two coordinate systems were discussed to make nonlinear regression possible. A modified *Fletcher* (1971) method was presented for solving the nonlinear least square problems. The interpretation procedure was applied to some simulated examples. The effect of the noise and the number of observation wells were investigated. For this circular discontinuity model, the following conclusions can be stated:

- If wellbore storage is not significant and the noise in the measured pressure data is no greater than five percent, the transmissivity and storativity in both reservoir and the circular discontinuity can be estimated. The position and extent of the discontinuity are also obtainable.
- When wellbore storage effect is significant, all the properties for the circular discontinuity can be obtained by analyzing the pressure data from the active well and more than one observation well. However, the validity of the estimated properties of the discontinuity depends on the locations of the observation wells.
- The larger the noise in the pressure data, the less accurate are the estimates of the properties, the position and the range of the discontinuity.
- With more well data, the surface of the objective function is steeper and smoother, and the parameters are easier to estimate. Adding more observation wells can suppress the effect of noise in the pressure data.
- The skin factor approach for wellbore damage is applicable at the active well when the following two conditions are satisfied: the damage area is not very large and the measured data is not at very early time.
- Having some of the observation wells near or inside the discontinuity region can make the objective function more sensitive to the properties, the position and the extent of the discontinuity.



In a multiple well system, neighbor wells may have impact on the interference pressure behavior for a testing well if these neighbor wells continue production during the test. The solution to the homogeneous system of any number of neighboring wells was obtained through the application of the Laplace transformation and superposition. Type curves of drawdown and buildup were presented for both finite well systems and infinite well systems. The pressure solution for rectangular reservoirs was derived by using an infinite number of imaging wells. From the results of these investigations, the following conclusions can be reached:

- Pressure responses in drawdown and buildup tests depend greatly on the observation distance when wellbore storage is taken into consideration.
- In drawdown and buildup tests, the shut-in time and the wellbore storage effect have large influence on the buildup part of the pressure data.
- The buildup pressure in a reservoir in which other wells are producing eventually follows the pressure trend of the neighboring producing wells.
- Partial penetration effects need to be considered to make the pressure interpretation accurate for the rectangular reservoirs with no-flow or constant pressure boundaries.

The situation in identifying the position of a no-flow linear boundary in a homogeneous reservoir is similar to that of estimating permeabilities in an anisotropic reservoir. The identification problem is over-specified in the sense of utilizing the inference ellipse method. In order to apply multiple sets of pressure data, the nonlinear least square method was used with the general pressure solution developed in the Laplace space. Then the nonlinear regression was applied to interpret a real multiwell interference test in a geothermal field. From the study, we can conclude that:

- Theoretically, more than two sets of observation data are required to locate the position of a no-flow boundary uniquely.
- The wellbore storage effect is reduced in more distant observations. A closer observation well sees more wellbore storage effect in the pressure data.

- The Ohaaki geothermal field appears to have a northwest to southeast trend of faults when all the interference pressure data are considered simultaneously.

## 6.2 The Green's Function and Principle of Reciprocity in Heterogeneous Problems

The Green's function method, a powerful tool in finding analytical pressure transient solutions, was extended to heterogeneous reservoirs in this study. The properties of the Green's function were derived and their application were discussed. As the Newman's product cannot be used for heterogeneous reservoirs, Green's functions are more difficult to find for heterogeneous problems of high dimension. Therefore, some mathematical methods were presented through examples. The Green's function method is still attractive for heterogeneous problems because finding the Green's function means that a set of pressure problems with various boundary conditions, initial condition and well conditions are all solved. Even though the Green's function method can be applied to tracer problems, it is not as powerful since the fixed concentration at well is a boundary condition rather than a source constraint.

The reciprocal property is an interesting topic that turns out to be associated with the Green's function. With Green's function theory extended, the Principle of Reciprocity was investigated for practical cases in heterogeneous reservoirs including those with discontinuous mobility and storativity. The cases where the Principle of Reciprocity does not hold were also illustrated. In general, reciprocity holds for:

1. Heterogeneous reservoirs of uniform initial pressure with no-flow boundaries.
2. Heterogeneous reservoirs of uniform initial pressure with constant initial pressure boundaries.
3. Heterogeneous infinite reservoirs of uniform initial pressure.
4. Homogeneous infinite reservoirs with wellbore storage.

Reciprocity does not hold for:

1. Reservoirs of nonuniform initial pressure.

2. Reservoirs with nonzero flux across the outer boundary.
3. Reservoirs with wellbore storage where Eq. 3.69 is not true.

### 6.3 Analytical Solutions to the Convection-Dispersion Equation

The analytical solutions to the convection-dispersion equations of three simplified tracer flow systems in heterogeneous reservoirs were derived using the Laplace transformation approach. One of the objectives in developing these analytical solutions was to help understand more about the tracer flow in heterogeneous reservoirs. A semianalytic method was also discussed for calculating streamlines and tracer return profiles.

- o The Crump algorithm is more suitable than the Stehfest algorithm for inverting the analytical tracer solution from Laplace space.
- o Superposition does not apply to two-dimensional tracer flow. This means that the concentration distribution in a multiwell system cannot be obtained by superposing the solution of each single well system.
- o The time step in the semianalytic method should be selected so that the advance of the fastest tracer front will not be too big to escape from the detection of breakthrough condition.

### 6.4 Simultaneous Analysis of Pressure and Tracer Data

Pressure data and tracer data were studied together for characterizing heterogeneous reservoirs. The correlation between dispersion coefficients and permeabilities was discussed, and based on this correlation a scheme to integrate pressure data and tracer data was proposed. The technique presented can be used to obtain the permeability distribution as well as the storativity from interpreting tracer data and pressure data simultaneously, and can be used directly in practice for well test analysis of heterogeneous reservoirs with slight modification. The concept of ill-posedness was investigated for the direct method of permeability identification. The need to constrain permeability when using the direct method to interpret pressure data was examined. Finally, the direct method was demonstrated as an example in a steady-state

multiple well reservoir with a circular discontinuity. Tracer data and pressure data were generated artificially, and then successfully inverted to estimate the permeability distribution. The observations and conclusions reached from this study are:

- The direct method favors multiple well data.
- Permeability constraint is needed for the direct method to be applied to the pressure equation if the simple finite difference method is used even though the permeability is uniquely determined mathematically.
- The solution to the pressure equation from the direct method is unique under appropriate conditions including that flow occurs at all locations and that pressure can be estimated everywhere.
- No permeability constraint is required to apply the direct method to the tracer equation.
- For tracer data, the concentration front data are of greater importance in recovering the areal permeability distribution.
- Unless the pressure and tracer data are collected vertically over depth, the direct method is not applicable to three dimensional problems.
- The time function approach described here is a method by which 4-D seismic data can be interpreted together with pressure data to yield estimates of the permeability distribution.

# Appendix A

## Equivalence of two Anisotropic Solutions

This appendix shows the equivalence between two equations used by *Papadopoulos* (1965) and *Collins* (1961). The equation used by *Collins* (1961) will be derived from the equation used by *Papadopoulos* (1965).

Start with equation

$$k_{xx} \frac{\partial^2 p}{\partial x^2} + 2k_{xy} \frac{\partial^2 p}{\partial x \partial y} + k_{yy} \frac{\partial^2 p}{\partial y^2} = \phi \mu c_t \frac{\partial p}{\partial t} \quad (\text{A.1})$$

Rotate the  $(x, y)$  coordinates by  $\theta$  degree to a new coordinates  $(\xi, \eta)$ , where  $\theta$  will be determined later.

$$\begin{cases} \xi = x \cos \theta + y \sin \theta \\ \eta = -x \sin \theta + y \cos \theta \end{cases} \quad (\text{A.2})$$

Under the new coordinates, the pressure derivatives are

$$\frac{\partial p}{\partial x} = \frac{\partial p}{\partial \xi} \frac{\partial \xi}{\partial x} + \frac{\partial p}{\partial \eta} \frac{\partial \eta}{\partial x} = \frac{\partial p}{\partial \xi} \cos \theta - \frac{\partial p}{\partial \eta} \sin \theta \quad (\text{A.3})$$

$$\frac{\partial^2 p}{\partial x \partial y} = p_{\xi \xi} \sin \theta \cos \theta + p_{\xi \eta} \cos 2\theta - p_{\eta \eta} \sin 2\theta - p_{,\eta} \sin \theta \cos \theta \quad (\text{A.4})$$

$$\frac{\partial^2 p}{\partial x^2} = p_{\xi \xi} \cos^2 \theta - p_{\xi \eta} \cos \theta \sin \theta - p_{\eta \eta} \sin^2 \theta + p_{,\eta} \sin \theta \cos \theta \quad (\text{A.5})$$

$$\frac{\partial p}{\partial y} = \frac{\partial p}{\partial \xi} \frac{\partial \xi}{\partial y} + \frac{\partial p}{\partial \eta} \frac{\partial \eta}{\partial y} = \frac{\partial p}{\partial \xi} \sin \theta + \frac{\partial p}{\partial \eta} \cos \theta \quad (\text{A.6})$$

$$\frac{\partial^2 p}{\partial^2 y} - p_{\xi\xi} \sin^2 \theta + p_{\xi\eta} \cos \theta \sin \theta + p_{\eta\xi} \sin \theta \cos \theta + p_{\eta\eta} \cos^2 \theta \quad (\text{A.7})$$

Substituting the pressure derivatives into **Eq. A.1**,

$$\begin{aligned} & k_{xx} p_{\xi\xi} \cos^2 \theta - 2k_{xx} p_{\xi\eta} \sin \theta \cos \theta + k_{xx} \sin^2 \theta p_{\xi\eta} + 2k_{xy} p_{\xi\xi} \sin \theta \cos \theta \\ & + 2k_{xy} p_{\xi\eta} (\cos^2 \theta - \sin^2 \theta) - 2k_{xy} p_{\eta\eta} \sin \theta \cos \theta + k_{yy} p_{\xi\xi} \sin^2 \theta \\ & + 2k_{yy} p_{\xi\eta} \sin \theta \cos \theta + k_{yy} p_{\eta\eta} \cos^2 \theta = \phi \mu c_t \frac{\partial p}{\partial t} \end{aligned} \quad (\text{A.8})$$

or in a simpler form,

$$\begin{aligned} & (k_{xx} \cos^2 \theta + 2k_{xy} \sin \theta \cos \theta + k_{yy} \sin^2 \theta) p_{\xi\xi} + 2[(\cos^2 \theta - \sin^2 \theta) k_{xy} \\ & + (k_{yy} - k_{xx}) \sin \theta \cos \theta] p_{\xi\eta} + (k_{xx} \sin^2 \theta - 2k_{xy} \sin \theta \cos \theta + k_{yy} \cos^2 \theta) p_{\eta\eta} \\ & = \phi \mu c_t \frac{\partial p}{\partial t} \end{aligned} \quad (\text{A.9})$$

In order to find the principal axis direction, choose a value of  $\theta$  that makes the coefficient of  $p_{\xi\xi}$  disappear, i.e.

$$(\cos^2 \theta - \sin^2 \theta) k_{xy} + (k_{yy} - k_{xx}) \sin \theta \cos \theta = 0. \quad (\text{A.10})$$

Written in another form,

$$\frac{\cos \theta \sin \theta}{\cos^2 \theta - \sin^2 \theta} = \frac{k_{xy}}{k_{xx} - k_{yy}}. \quad (\text{A.11})$$

So  $\theta$  has to satisfy

$$\frac{\tan \theta}{1 - \tan^2 \theta} = \frac{1}{2} \tan 2\theta = \frac{k_{xy}}{k_{xx} - k_{yy}}. \quad (\text{A.12})$$

Denote  $\frac{k_{xy}}{k_{xx} - k_{yy}} = A$  as a known term, then  $\tan \theta$  can be solved first from

$$\frac{\tan \theta}{1 - \tan^2 \theta} = A. \quad (\text{A.13})$$

This is a quadratic equation,

$$A \tan^2 \theta + \tan \theta - A = 0 \quad (\text{A.14})$$

with solution

$$\tan \theta = \frac{-1 + \sqrt{1 + 4A^2}}{2A}, \quad (\text{A.15})$$

or

$$\tan \theta = \frac{k_{yy} - k_{xx} + \sqrt{(k_{xx} - k_{yy})^2 + 4k_{xy}^2}}{2k_{xy}} \quad (\text{A.16})$$

Now  $\cos \theta$  and  $\sin \theta$  can be expressed in terms of  $k_{xx}$ ,  $k_{xy}$  and  $k_{yy}$ . Denote  $B = \sqrt{(k_{xx} - k_{yy})^2 + 4k_{xy}^2}$ , then

$$\cos^2 \theta = \frac{1}{1 + \tan^2 \theta} = \frac{4k_{xy}^2}{4k_{xy}^2 + (k_{yy} - k_{xx} + B)^2}, \quad (\text{A.17})$$

$$\sin^2 \theta = \frac{(k_{yy} - k_{xx} + B)^2}{4k_{xy}^2 + (k_{yy} - k_{xx} + B)^2}. \quad (\text{A.18})$$

The coefficients of  $p_{\xi\xi}$  and  $p_{\eta\eta}$  can also be written in terms of  $k_{xx}$ ,  $k_{xy}$  and  $k_{yy}$  without  $\theta$ ,

$$\begin{aligned} & k_{xx} \cos^2 \theta + 2k_{xy} \sin \theta \cos \theta + k_{yy} \sin^2 \theta \\ &= \frac{4k_{xy}^2 k_{xx} + 2k_{xy}(k_{yy} - k_{xx} + B)2k_{xy} + (k_{yy} - k_{xx} + B)^2 k_{yy}}{4k_{xy}^2 + (k_{yy} - k_{xx} + B)^2} \\ &= \frac{2Bk_{yy} + 2k_{xy}^2 - 2k_{xx}k_{yy} + 4k_{xy}^2}{2(B + k_{yy} - k_{xx})} \\ &= \frac{2Bk_{yy} + B^2 - k_{xx}^2 + k_{yy}^2}{2(B + k_{yy} - k_{xx})} \\ &= \frac{(B + k_{yy} - k_{xx})(B + k_{yy} + k_{xx})}{2(B + k_{yy} - k_{xx})} \\ &= \frac{1}{2}(B + k_{yy} + k_{xx}) \\ &= k_{XX}. \end{aligned} \quad (\text{A.19})$$

$$\begin{aligned}
 & k_{xx} \sin^2 \theta - 2k_{xy} \sin \theta \cos \theta + k_{yy} \cos^2 \theta \\
 &= k_{xx} + k_{yy} - (k_{xx} \cos^2 \theta + 2k_{xy} \sin \theta \cos \theta + k_{yy} \sin^2 \theta) \\
 &= k_{xx} + k_{yy} - \frac{1}{2}(B + k_{yy} + k_{xx}) \\
 &= \frac{1}{2}(k_{yy} + k_{xx} - B) \\
 &= k_{yy}.
 \end{aligned} \tag{A.20}$$

Therefore, in the new coordinates, **Eq. A.9** becomes

$$k_{XX} \frac{\partial^2 p}{\partial \xi^2} + k_{YY} \frac{\partial^2 p}{\partial \eta^2} = \phi \mu c_t \frac{\partial p}{\partial t}. \tag{A.21}$$



# Appendix B

## Pressure Expression in Green's Function

Once the Green's function is worked out for the homogeneous equation, the solution to the equivalent nonhomogeneous equation with a nonhomogeneous initial condition and nonhomogeneous boundary conditions can be represented.

We start by defining a differential operator  $L$ :

$$L[p] = \frac{\partial}{\partial x} \left( \frac{k}{\mu} \frac{\partial p}{\partial x} \right) + \frac{\partial}{\partial y} \left( \frac{k}{\mu} \frac{\partial p}{\partial y} \right) + \frac{\partial}{\partial z} \left( \frac{k}{\mu} \frac{\partial p}{\partial z} \right) - \phi c_t \frac{\partial p}{\partial \tau}, \quad (\text{B.1})$$

Its adjoint operator is then

$$L^*[G] = \frac{\partial}{\partial x'} \left( \frac{k}{\mu} \frac{\partial G}{\partial x'} \right) + \frac{\partial}{\partial y'} \left( \frac{k}{\mu} \frac{\partial G}{\partial y'} \right) + \frac{\partial}{\partial z'} \left( \frac{k}{\mu} \frac{\partial G}{\partial z'} \right) + \phi c_t \frac{\partial G}{\partial \tau}. \quad (\text{B.2})$$

Suppose  $p(x, y, z, t)$  is the solution to

$$L[p] = f(x, y, z, t) \quad (\text{B.3})$$

$$p(x, y, z, 0) = g(x, y, z) \quad (\text{B.4})$$

with some well-posed boundary conditions and suppose that  $G(x, y, z, x', y', z', t - r)$  is the Green's function to the corresponding homogeneous equation with homogeneous boundary conditions, i.e.  $G(x, y, z, x', y', z', t - \tau)$  satisfies:

$$L[G] = 0 \quad (\text{B.5})$$

$$G(x, y, z, x', y', z', 0) = \frac{\delta(x - x', y - y', z - z')}{\phi(x', y', z')c_t(x', y', z')} \quad (\text{B.6})$$

$$G(x, y, z, x', y', z', t - \tau) = 0 \text{ or } \frac{\partial G}{\partial n} = 0 \quad (x, y, z) \in S_e \quad (\text{B.7})$$

where  $S_e$  denotes the boundary if there is. From Property 2 of the Green's function that is listed in Section 3.2,  $G(x, y, z, x', y', z', t - \tau)$  satisfies the adjoint equation as function of variables  $(x', y', z', \tau)$

$$L^*[G] = 0 \quad (\text{B.8})$$

$$G(x, y, z, x', y', z', 0) = \frac{\delta(x - x', y - y', z - z')}{\phi(x', y', z')c_t(x', y', z')} \quad (\text{B.9})$$

$$G(x, y, z, x', y', z', t - \tau) = 0 \text{ or } \frac{\partial G}{\partial n} = 0 \quad (x', y', z') \in S_e. \quad (\text{B.10})$$

Consider a general second order linear differential operator  $\mathcal{L}$

$$\mathcal{L} \equiv \sum_{i,j=1}^m a_{ij} \frac{\partial^2}{\partial x_i \partial x_j} + \sum_{i=1}^m b_i \frac{\partial}{\partial x_i} + c \quad (\text{B.11})$$

and its adjoint differential operator  $\mathcal{L}^*$

$$\mathcal{L}^*v \equiv \sum_{i,j=1}^m \frac{\partial^2}{\partial x_i \partial x_j} (a_{ij}v) - \sum_{i=1}^m \frac{\partial}{\partial x_i} (b_i v) + cv \quad (\text{B.12})$$

where  $a_{ij}$ ,  $b_i$ ,  $c$  are second order continuously differentiable functions of  $x_1, x_2, \dots, x_m$ .

The Green's formula for these operators is:

$$\int_{\Omega} (v\mathcal{L}u - u\mathcal{L}^*v) d\Omega = \int_{S_e} \sum_{i=1}^m p_i \cos(\mathbf{n}, \mathbf{e}_i) dS_e \quad (\text{B.13})$$

where  $S_e$  is the boundary of domain  $\Omega$ ,  $\mathbf{n}$  is the outward normal vector of  $S_e$ ,  $\mathbf{e}_i = (0, \dots, 0, 1, 0, \dots, 0)$  is the axis vector of  $x_i$ ,  $(n, e_i)$  represents the angle between vectors  $\mathbf{n}$  and  $\mathbf{e}_i$  and

$$p_i = \sum_{j=1}^m [va_{ij} \frac{\partial u}{\partial x_j} - u \frac{\partial}{\partial x_j} (a_{ij}v)] + b_i uv \quad (\text{B.14})$$

As for our operator  $L$  and its adjoint operator  $L^*$ ,

$$p_1 = vk \frac{du}{\partial x} - u \frac{\partial(kv)}{\partial x} + uv \frac{dk}{\partial x} \quad (\text{B.15})$$

$$p_2 = vk \frac{\partial u}{\partial y} - u \frac{\partial(kv)}{\partial y} + uv \frac{\partial k}{\partial y} \quad (\text{B.16})$$

$$p_3 = vk \frac{du}{\partial z} - u \frac{\partial(kv)}{\partial z} + uv \frac{dk}{\partial z} \quad (\text{B.17})$$

we can work out a Green's formula from the above

$$\int_{\Omega} (vLu - uL^*v) d\Omega = \int_{S_e} \left[ \frac{k}{\mu} \left( v \frac{\partial u}{\partial n} - u \frac{\partial v}{\partial n} \right) \right] dS_e - \int_{\Omega} \phi_{c_t} \frac{\partial(uv)}{\partial \tau} d\Omega \quad (\text{B.18})$$

Now let  $v = G(x, y, z, x', y', z', t - \tau)$ ,  $u = p(x', y', z', \tau)$ , then

$$L^*v = 0 \quad (\text{B.19})$$

and

$$Lu = f(x', y', z', \tau), \quad (\text{B.20})$$

so

$$\begin{aligned} \int_{\Omega} G \cdot f(x', y', z', \tau) dx' dy' dz' &= \int_{S_e} \frac{k}{\mu} \left( G \frac{\partial p}{\partial n} - p \frac{\partial G}{\partial n} \right) dS_e - \\ &\int_{\Omega} \phi_{c_t} \frac{\partial(pG)}{\partial \tau} dx' dy' dz'. \end{aligned} \quad (\text{B.21})$$

Integrating  $\tau$  from 0 to  $t$  gives:

$$\begin{aligned} \int_0^t \int_{\Omega} G \cdot f dx' dy' dz' d\tau &= \int_0^t \int_{S_e} \frac{k}{\mu} \left( G \frac{\partial p}{\partial n} - p \frac{\partial G}{\partial n} \right) dS_e d\tau + \\ &\int_{\Omega} \phi_{c_t} G(t) \cdot g dx' dy' dz' - p(x, y, z, t) \end{aligned} \quad (\text{B.22})$$

because of Eqs. B.4, B.9 and

$$\begin{aligned} \int_0^t \int_{\Omega} \phi_{c_t} \frac{\partial(pG)}{\partial \tau} dx' dy' dz' d\tau &= \\ \int_{\Omega} \phi_{c_t} [p(x', y', z', t)G(0) - p(x', y', z', 0)G(t)] dx' dy' dz'. \end{aligned} \quad (\text{B.23})$$

Therefore the solution can be written as

$$\begin{aligned}
p(x, y, z, t) &= \int_0^t \int_{S_e} \frac{k}{\mu} \left( G \frac{\partial p}{\partial n} + p \frac{\partial G}{\partial n} \right) dS_e d\tau \\
&\quad - \int_0^t \int_{\Omega} G \cdot f dx' dy' dz' d\tau + \int_{\Omega} \phi c_t G(t) \cdot g dx' dy' dz'
\end{aligned} \tag{B.24}$$

If the domain is infinite and has no boundary, then the first term in the right hand side will disappear.

Now we can apply this result to the production of a well at a flow rate  $q$ . Remember in the material balance equation, Eq. B.3, the source term  $f(x, y, z, t)$  has the unit **volume rate of injection per unit volume of reservoir**, so

$$f(x, y, z, t) = \begin{cases} \frac{q}{V_w} & \text{inside the well} \\ 0 & \text{outside the well} \end{cases} \tag{B.25}$$

if the source is uniform over the well volume. Assuming the boundary is no-flow, then

$$\begin{aligned}
p(x, y, z, t) &= \int_0^t \int_W \frac{q(\tau)}{\pi r_w^2 h} G(x, y, z, x', y', z', t - \tau) dx' dy' dz' d\tau \\
&\quad + \int_{\Omega} \phi c_t G(t) \cdot g dx' dy' dz',
\end{aligned} \tag{B.26}$$

where  $W$  is the region in the well, and  $\Omega$  is the domain of reservoir. Now if the initial pressure is constant  $p_i$  everywhere, we have

$$\begin{aligned}
p_i - p(x, y, z, t) &= \\
&\int_0^t \int_W \frac{q(\tau)}{\pi r_w^2 h} G(x, y, z, x', y', z', t - \tau) dx' dy' dz' d\tau
\end{aligned} \tag{B.27}$$

For three dimensions, if the well is approximated by a point source at position  $x', y', z'$ , the solution becomes

$$p_i - p(x, y, z, t) = \int_0^t \frac{q(\tau)}{\pi r_w^2 h} G(x, y, z, x', y', z', t - \tau) d\tau \tag{B.28}$$

For two dimensions, if the well is approximated by a line source at  $x', y'$ , the solution is

$$p_i - p(x, y, t) = \int_0^t \frac{q(\tau)}{\pi r_w^2 h} G(x, y, x', y', t - \tau) d\tau \tag{B.29}$$

For one dimension, if the well is approximated by a plane source at  $x'$ , the solution is then

$$p_i - p(x, t) = \int_0^t \frac{q(\tau)}{\pi r_w^2 h} G(x, x', t - \tau) d\tau. \tag{B.30}$$

# Appendix C

## Reciprocity of Green's Function

For one dimension, we can easily show that Green's function is symmetric to  $x$  and  $x'$ . According to the definition,  $G(x, x', t)$  is the solution to

$$\frac{\partial}{\partial x} \left[ \frac{k(x)}{\mu(x)} \frac{\partial G}{\partial x} \right] = \phi(x) c_t(x) \frac{\partial G}{\partial t} \quad a < x < b \text{ and } t > 0 \quad (\text{C.1})$$

$$G(x, x', 0) = \frac{\delta(x - x')}{\phi(x') c_t(x')} \quad (\text{C.2})$$

$$\alpha_1 G + \alpha_2 \frac{\partial G}{\partial x} = 0 \quad \text{at } x = a \quad (\text{C.3})$$

$$\beta_1 G + \beta_2 \frac{\partial G}{\partial x} = 0 \quad \text{at } x = b \quad (\text{C.4})$$

Assuming  $G(x, t) = T(t)X(x)$ , substituting into Eq. C.1, and separating variables, then:

$$\frac{[\frac{k(x)}{\mu(x)} X'(x)]'}{\phi(x) c_t(x) X(x)} = \frac{T'(t)}{T(t)} = -\lambda \quad (\text{C.5})$$

which gives two equations

$$T'(t) + \lambda T(t) = 0 \quad \text{or} \quad T(t) = b e^{-\lambda t} \quad (\text{C.6})$$

and

$$[\frac{k(x)}{\mu(x)} X'(x)]' + \lambda \phi(x) c_t(x) X(x) = 0 \quad (\text{C.7})$$

with boundary conditions:

$$\alpha_1 X + \alpha_2 \frac{dX}{dx} = 0 \quad \text{at } x = a \quad (\text{C.8})$$

$$\beta_1 X + \beta_2 \frac{dX}{dx} = 0 \quad \text{at } x = b \quad (\text{C.9})$$

which is a Sturm-Liouville boundary-value problem having eigenvalues  $\lambda_n$  and eigenfunctions  $X_n(x)$ . The solution can be written in terms of the eigenfunction expansion:

$$G(x, t) = \sum_{n=1}^{\infty} b_n e^{-\lambda_n t} X_n(x). \quad (\text{C.10})$$

The initial condition requires:

$$G(x, 0) = \frac{\delta(x - x')}{\phi(x')c_t(x')} = \sum_{n=1}^{\infty} b_n X_n(x).$$

Multiplying  $\phi(x)c_t(x)X_n(x)$  and integrating  $x$  from  $a$  to  $b$  leads to

$$b_n = \int_a^b \phi(x)c_t(x)X_n(x) \frac{\delta(x - x')}{\phi(x')c_t(x')} dx = X_n(x')$$

if we normalize  $X_n(x)$  to make  $\int_a^b \phi(x)c_t(x)X_n^2(x)dx = 1$ . Therefore, the Green's function is

$$G(x, x', t) = \sum_{n=1}^{\infty} e^{-\lambda_n t} X_n(x)X_n(x') \quad (\text{C.11})$$

which does have the symmetry for  $x$  and  $x'$ , and therefore assures the the principle of reciprocity.

For higher dimensional or discontinuous coefficients, we cannot apply Sturm-Liouville theory. However, the reciprocity for Green's function still holds, as can be shown from calculus of variations. The following argument applies to Green's function of any dimension, but for simplicity, we will consider the Green's function for a two dimensional domain  $\Omega$  with discontinuous mobility  $p(x, y)$  and storativity  $\rho(x, y)$  on  $\Omega$ . In order to write the equations for the Green's function on this domain  $\Omega$ , we need to divide the domain into several subdomains  $\Omega_1, \Omega_2, \Omega_3, \dots, \Omega_n$  such that  $p(x, y)$  and  $\rho(x, y)$  are continuous on each of the subdomains. On the boundary between any two subdomains, the Green's function and its derivative needs to be continuous because pressure and flux are continuous across any boundary. Denoting the boundaries among the subdomains by  $\Gamma_1, \Gamma_2, \dots, \Gamma_m$ , the Green's function satisfies

$$\frac{\partial}{\partial x}(p(x,y)\frac{\partial G}{\partial x}) + \frac{\partial}{\partial y}(p(x,y)\frac{\partial G}{\partial y}) = \rho(x,y)\frac{\partial G}{\partial t} \quad \text{on } \Omega_1, \dots, \Omega_n \quad (\text{C.12})$$

$$G(x,y,x',y',0) = \frac{\delta(x-x',y-y')}{\rho(x',y')} \quad (\text{C.13})$$

$$\frac{\partial G}{\partial n} + \sigma G = 0 \quad \text{or} \quad G = 0 \quad \text{on boundary } \Gamma \quad (\text{C.14})$$

and also conditions that guarantee function's continuity and material balance (flux continuity) along  $\Gamma_i$  ( $i = 1, \dots, m$ ). So the Green's function is continuous in  $\Omega$  and has piecewise continuous first derivatives in  $\Omega$ .

By assuming  $G(x,y,x',y',t) = u(x,y)\theta(t)$  and separating variables, we have an eigenvalue problem,

$$\begin{cases} (pu_x)_x + (pu_y)_y + \lambda \rho u = 0 & \text{on } \Omega_1, \Omega_2, \dots, \Omega_n \\ \text{function continuity equation} & \text{along } \Gamma_1, \Gamma_2, \dots, \Gamma_m \\ \text{flux continuity} & \text{along } \Gamma_1, \Gamma_2, \dots, \Gamma_m \\ \frac{\partial G}{\partial n} + \sigma G = 0 \quad \text{or} \quad G = 0 & \text{on boundary } \Gamma \end{cases} \quad (\text{C.15})$$

Reciprocity can be shown for the Green's function as in the one-dimensional case if the eigenvalues  $\lambda_i$  and associated complete eigenfunctions  $u_i$  for eigenvalue problem (C.15) exist. This existence is obtained from its variational counterpart.

The associated variational eigenvalue problem is to find  $\phi$  which minimizes the following quadratic functional expression

$$\mathcal{D}[\phi, \phi] = D[\phi, \phi] + \int_{\Gamma} p\sigma\phi^2 ds \quad (\text{C.16})$$

where

$$D[\phi, \phi] = \iint_{\Omega} p(\phi_x^2 + \phi_y^2) dx dy \quad (\text{C.17})$$

under the normal condition

$$H[\phi, \phi] = \iint_{\Omega} \rho\phi^2 dx dy = 1 \quad (\text{C.18})$$

and the orthogonality condition

$$H[\phi, u_i] = \iint_{\Omega} \rho\phi u_i dx dy = 0 \quad (i = 1, 2, \dots, \nu - 1) \quad (\text{C.19})$$

The existence of a solution to our minimum problem  $\phi$  is discussed by Morrey [1966] for piecewise continuous  $p(x, y)$  and  $\rho(x, y)$ . This  $\phi$  gives the next eigenfunction  $u_\nu$  of equation (C.15) with boundary condition  $\frac{\partial u_\nu}{\partial n} + \sigma u_\nu = 0$  on  $\Gamma$ ; the associated eigenvalue  $\lambda_\nu$  equals the minimum value  $\mathcal{D}[u_\nu]$ .

For the boundary condition  $u = 0$  on  $\Gamma$ , everything above applies except that one more boundary condition  $\phi = 0$  is added and  $\mathcal{D}[\phi, \phi]$  becomes  $D[\phi, 43]$ .

The proofs that those  $u_\nu$  are also eigenfunctions for the differential equation problem (Eq. C.15) and that they are complete are similar to the discussions made by *Courant and Hilbert* (1953), and so are omitted here.



## Appendix D

# Two-Dimensional Green's Functions in Problems with Variable Permeability

To obtain  $G_1(x, x', t)$  for the following equation,

$$\frac{1}{x} \frac{\partial}{\partial x} \left( x \frac{\partial G_1}{\partial x} \right) = \frac{\partial G_1}{\partial t} \quad (\text{D.1})$$

with  $0 \leq a \leq x \leq b$  and  $G_1(x, x', 0) = \frac{\delta(x-x')}{x'}$ , we try separating variables by assuming  $G_1 = X(x)T(t)$ , which in turns gives two equations. The first one is

$$T' + \alpha^2 T = 0 \quad (\text{D.2})$$

with solution  $T(t) = be^{-\alpha^2 t}$

The second equation is

$$X'' + \frac{X'}{x} + \alpha^2 X = 0 \quad (\text{D.3})$$

which is a Bessel equation with general solution

$$X(x) = c_1 J_0(\alpha x) + c_2 Y_0(\alpha x) \quad (\text{D.4})$$

Applying boundary conditions,

$$\begin{cases} c_1 J_1(a\alpha) + c_2 Y_1(a\alpha) = 0 \\ c_1 J_1(b\alpha) + c_2 Y_1(b\alpha) = 0 \end{cases} \quad (\text{D.5})$$

Denote  $\alpha_n$  ( $n = 1, 2, \dots$ ) as the roots of

$$J_1(a\alpha)Y_1(b\alpha) - J_1(b\alpha)Y_1(a\alpha) = 0 \quad (\text{D.6})$$

then the solutions to Eq. D.3 are  $X_0(x) = C_0$  and  $X_n(x) = C_n y_n$  ( $n = 1, 2, \dots$ ) where

$$y_n = J_1(a\alpha_n)Y_0(\alpha_n x) - J_0(\alpha_n x)Y_1(a\alpha_n) \quad (\text{D.7})$$

and  $C_n$  ( $n = 0, 1, 2, \dots$ ) are constants to be decided.

So the eigenfunctions for Eq. D.1 are

$$G_{10}(x, t) = C_0,$$

$$G_{1n}(x, t) = C_n e^{-\alpha_n^2 t} y_n(x)$$

and the Green's function we are looking for is

$$G_1(x, t) = C_0 + \sum_{n=1}^{\infty} C_n e^{-\alpha_n^2 t} y_n(x) \quad (\text{D.8})$$

where  $y_0(x) = 1$  and  $C_n$  ( $n = 0, 1, 2, \dots$ ) are determined by the initial condition

$$C_0 + \sum_{n=1}^{\infty} C_n y_n(x) = \frac{\delta(x - x')}{x'} \quad (\text{D.9})$$

We can obtain  $C_n$  by the orthogonality of  $y_n(x)$

$$\int_a^b x y_n(x) y_m(x) dx = 0 \quad m \neq n; \quad m, n = 0, 1, 2, \dots \quad (\text{D.10})$$

Multiplying by  $x y_m(x)$  on both sides of Eq. D.9 and integrating on  $(a, b)$ , we have

$$C_n = \frac{\int_a^b x y_n(x) \delta(x - x') dx}{x' \int_a^b x y_n^2(x) dx} = \frac{y_n(x')}{\int_a^b x y_n^2(x) dx}. \quad (\text{D.11})$$

$C_0$  can be worked out directly,

$$C_0 = \frac{1}{\int_a^b x dx} = \frac{2}{b^2 - a^2}. \quad (\text{D.12})$$

Therefore the Green's function is

$$G_1(x, t) = \frac{2}{b^2 - a^2} + \sum_{n=1}^{\infty} \frac{y_n(x')y_n(x)}{\int_a^b xy_n^2(x)dx} e^{-\alpha_n^2 t} \quad (\text{D.13})$$

We can further simplify  $\int_a^b xy_n^2(x)dx$  ( $n > 0$ ) by applying the following five equations:

$$\int_a^b xJ_0^2(\alpha x)dx = \frac{b^2}{2}[J_1^2(\alpha b) + J_0^2(\alpha b)] - \frac{a^2}{2}[J_1^2(\alpha a) + J_0^2(\alpha a)] \quad (\text{D.14})$$

$$\int_a^b xY_0^2(\alpha x)dx = \frac{b^2}{2}[Y_1^2(\alpha b) + Y_0^2(\alpha b)] - \frac{a^2}{2}[Y_1^2(\alpha a) + Y_0^2(\alpha a)] \quad (\text{D.15})$$

$$\begin{aligned} \int_a^b xY_0(\alpha x)J_0(\alpha x)dx &= \frac{b}{2}[Y_1(\alpha b)J_1(\alpha b) + Y_0(\alpha b)J_0(\alpha b)] \\ &- \frac{a}{2}[Y_1(\alpha a)J_1(\alpha a) + Y_0(\alpha a)J_0(\alpha a)] \end{aligned} \quad (\text{D.16})$$

$$J_1(x)Y_0(x) - J_0(x)Y_1(x) = \frac{2}{\pi x} \quad (\text{D.17})$$

$$J_1(\alpha_n a)Y_0(\alpha_n x) - Y_1(\alpha_n a)J_0(\alpha_n x) = 0 \quad (\text{D.18})$$

We first expand  $y_n^2(x)$  in the integral, then apply Eqs. D.14, D.15 and D.16. Through some algebraic manipulation, we get

$$\begin{aligned} \int_a^b xy_n^2(x)dx &= \frac{b^2}{2}[J_1(\alpha_n a)Y_0(\alpha_n b) - Y_1(\alpha_n a)J_0(\alpha_n b)]^2 \\ &- \frac{a^2}{2}[J_1(\alpha_n a)Y_0(\alpha a) - Y_1(\alpha_n a)J_0(\alpha_n a)]^2 \end{aligned}$$

Now, by Eq. D.17,

$$\begin{aligned} &\int_a^b xy_n^2(x)dx \\ &= \frac{b^2}{2}[J_1(\alpha_n a)Y_0(\alpha_n b) - Y_1(\alpha_n a)J_0(\alpha_n b)]^2 - \frac{2}{\pi^2 \alpha_n^2} \end{aligned}$$

and by Eq. D.18,

$$\int_a^b xy_n^2(x)dx = -\frac{2}{\pi^2 \alpha_n^2}$$

$$+ \frac{b^2 Y_1^2(\alpha_n a)}{2 Y_1^2(\alpha_n b)} [J_1(\alpha_n b) Y_0(\alpha_n b) - Y_1(\alpha_n b) J_0(\alpha_n b)]^2$$

The last step is to apply **Eq. D.16** again,

$$\int_a^b x y_n^2(x) dx = \frac{2}{\pi^2 \alpha_n^2} \left[ \frac{Y_1^2(\alpha_n a)}{Y_1^2(\alpha_n b)} - 1 \right]$$

Therefore, we end up with the Green's function as

$$G_1(x, t) = \frac{2}{b^2 - a^2} + \sum_{n=1}^{\infty} \frac{\pi^2 \alpha_n^2 Y_1^2(\alpha_n b) y_n(x') y_n(x)}{2 [Y_1^2(\alpha_n a) - Y_1^2(\alpha_n b)]} e^{-\alpha_n^2 t} \quad (\text{D.19})$$

# Appendix E

## Pressure and Tracer Solutions for a Multiwell Heterogeneous System

The pressure solution for a multiwell system in an infinite reservoir with a circular discontinuity can be obtained by its Green's function; the pressure change due to multiwell production/injection is the superposition of pressure change due to production/injection of each well. This transient pressure solution is costly to compute because of the series of Bessel functions. For the tracer problem, what is needed from this pressure expression is its late time solution, which is difficult to derive from the transient pressure expression. However, the late-time pressure solution for a multiwell system that has equal amounts of injection and production, can be closely approximated by superposing pressure change of each well in steady state. This appendix includes the derivation of the steady-state pressure solution for an infinite reservoir with a circular discontinuity.

Denote the permeability, porosity of the circular region  $k_1(x, y)$ ,  $\phi_1(x, y)$ , the permeability, porosity of the other region  $k_2(x, y)$ ,  $\phi_2(x, y)$ . The first step in the derivation is to find  $p_1(r, \theta)$  and  $p_2(r, \theta)$  that satisfy the following two equations

$$\frac{\partial^2 p_1}{\partial r^2} + \frac{1}{r} \frac{\partial p_1}{\partial r} + \frac{1}{r^2} \frac{\partial^2 p_1}{\partial \theta^2} = 0 \quad r < a \quad (\text{E.1})$$

$$\frac{\partial^2 p_2}{\partial r^2} + \frac{1}{r} \frac{\partial p_2}{\partial r} + \frac{1}{r^2} \frac{\partial^2 p_2}{\partial \theta^2} = 0 \quad r > a \quad (\text{E.2})$$

with the boundary conditions

$$p_1(a, \theta) = p_2(a, \theta) \quad (\text{E.3})$$

$$\lambda_1 \frac{\partial p_1}{\partial r} \Big|_{r=a} = \lambda_2 \frac{\partial p_2}{\partial r} \Big|_{r=a} \quad (\text{E.4})$$

and the condition posed by a single well with flow rate  $q$  at position  $(r', \theta')$ . Depending on the value of  $r'$ , there are two cases:

1. Source well inside of circular discontinuity  $r' < a$
2. Source well outside of circular discontinuity  $r' > a$ .

Assume

$$\begin{cases} p_1 = u_1 + v = \frac{q}{2\pi\lambda_1 h} \ln R + v \\ p_2 = w \end{cases} \quad (\text{E.5})$$

for Case 1 and

$$\begin{cases} p_1 = v \\ p_2 = u_2 + w = \frac{q}{2\pi\lambda_2 h} \ln R + w \end{cases} \quad (\text{E.6})$$

For Case 2, where  $R = \sqrt{r^2 + r'^2 - 2rr' \cos(\theta - \theta')}$ , while  $v$  and  $w$  are the functions to be determined accounting for the existence of circular discontinuity,  $u_1$  and  $u_2$  are the well-known pressure solutions to the homogeneous reservoirs of  $\lambda_1$  and  $\lambda_2$ , respectively; they will take care of the well condition in the heterogeneous reservoir. It is easy to see that  $v$  and  $w$  satisfy Eq. E.1 and Eq. E.2. The general solution to Eq. E.1 and Eq. E.2 can be obtained by separating variables  $r$  and  $\theta$ :

$$p(r, \theta) = \sum_{k=0}^{\infty} (C_{1k} r^k + C_{2k} r^{-k}) \sin k(\theta - \theta_k) \quad (\text{E.7})$$

Because  $v$  is bounded at  $r = 0$  and  $w$  is bounded at  $r = \infty$ ,

$$v = \sum_{k=0}^{\infty} V_{1k} r^k \cos k\theta + V_{2k} r^k \sin k\theta \quad (\text{E.8})$$

$$w = \sum_{k=0}^{\infty} W_{1k} r^{-k} \cos k\theta + W_{2k} r^{-k} \sin k\theta \quad (\text{E.9})$$

In order to apply the boundary conditions in Eq. E.3 and Eq. E.4,  $\ln R$  needs to be expressed in Fourier series,

$$\ln R = \ln r' - \sum_{k=1}^{\infty} \frac{r^k}{k r'^k} \cos k(\theta - \theta') \quad r < r' \quad (\text{E.10})$$

$$\ln R = \ln r - \sum_{k=1}^{\infty} \frac{r'^k}{k r^k} \cos k(\theta - \theta') \quad r > r' \quad (\text{E.11})$$

Since the derivations for both cases are very similar, discussion below will focus on Case 2 as an example.

Applying boundary conditions, we obtain

$$V_{1k} a^k = -\frac{q}{2\pi\lambda_2 h} \frac{a^k}{k r'^k} \cos k\theta' + W_{1k} a^{-k} \quad (\text{E.12})$$

$$V_{2k} a^k = -\frac{k}{2\pi\lambda_2 h} \frac{a^k}{k r'^k} \sin k\theta' + W_{2k} a^{-k} \quad (\text{E.13})$$

$$\lambda_1 V_{1k} a^{k-1} k = -\frac{q}{2\pi h} \frac{a^{k-1}}{r'^k} \cos k\theta' - \lambda_2 W_{1k} a^{-k-1} k \quad (\text{E.14})$$

$$\lambda_1 V_{2k} a^{k-1} k = -\frac{q}{2\pi h} \frac{a^{k-1}}{r'^k} \sin k\theta' - \lambda_2 W_{2k} a^{-k-1} k \quad (\text{E.15})$$

Solving Eqs. E.12, E.13, E.14 and E.15 yields

$$V_{1k} = -\frac{q}{\pi h r'^k} \frac{\cos k\theta'}{k(\lambda_1 + \lambda_2)}$$

$$V_{2k} = -\frac{q}{\pi h r'^k} \frac{\sin k\theta'}{k(\lambda_1 + \lambda_2)}$$

$$W_{1k} = \left(\frac{\lambda_1}{\lambda_2} - 1\right) \frac{q}{2\pi h r'^k} \frac{a^{2k} \cos k\theta'}{k(\lambda_1 + \lambda_2)}$$

$$W_{2k} = \left(\frac{\lambda_1}{\lambda_2} - 1\right) \frac{q}{2\pi h r'^k} \frac{a^{2k} \sin k\theta'}{k(\lambda_1 + \lambda_2)}$$

Substitute into Eqs. E.8 and E.9, then

$$v = \frac{q}{2\pi h \lambda_2} \ln r' - \frac{q}{\pi h(\lambda_1 + \lambda_2)} \sum_{k=1}^{\infty} \frac{r^k}{k r'^k} \cos k(\theta - \theta') \quad (\text{E.16})$$

$$w = \frac{q}{2\pi h(\lambda_1 + \lambda_2)} \left(\frac{\lambda_1}{\lambda_2} - 1\right) \sum_{k=1}^{\infty} \frac{(aa)^k}{k (r r')^k} \cos k(\theta - \theta') \quad (\text{E.17})$$

Applying the Fourier series expression of  $\ln R$  in Eq. E.10,  $v(r, \theta, r', \theta')$  and  $w(r, \theta, r', \theta')$  can be written as

$$v = \frac{q}{2\pi h \lambda_2} \frac{\lambda_1 - \lambda_2}{\lambda_1 + \lambda_2} \ln r' + \frac{q}{\pi h (\lambda_1 + \lambda_2)} \ln R \quad (\text{E.18})$$

$$w = \frac{q}{2\pi h (\lambda_1 + \lambda_2)} \left( \frac{\lambda_1}{\lambda_2} - 1 \right) \ln \frac{rr'}{\sqrt{a^4 + r^2 r'^2 - 2a^2 r r' \cos(\theta - \theta')}} \quad (\text{E.19})$$

Therefore, for a source well outside circular discontinuity ( $r' > a$ ), the pressure change is

$$p(r, \theta) = \begin{cases} \frac{q\alpha}{2\pi h \lambda_2} \ln r' + \frac{q}{\pi h (\lambda_1 + \lambda_2)} \ln R, & r < a \\ \frac{q}{2\pi h \lambda_2} \ln R + \frac{q\alpha}{2\pi h \lambda_2} \ln(rr') - \frac{q\alpha}{2\pi h \lambda_2} \ln \mathcal{R}, & r > a \end{cases} \quad (\text{E.20})$$

Similarly, for a source well inside circular discontinuity ( $r' < a$ ), we can obtain

$$p(r, \theta) = \begin{cases} \frac{q}{2\pi h \lambda_1} \ln R + \frac{q(\lambda_1 - \lambda_2)\alpha}{2\pi h \lambda_1 \lambda_2} \ln a + \frac{q\alpha}{2\pi h \lambda_1} \ln \mathcal{R}, & r < a \\ \frac{q\alpha}{2\pi h \lambda_2} \ln r + \frac{q}{\pi h (\lambda_1 + \lambda_2)} \ln R, & r > a \end{cases} \quad (\text{E.21})$$

where

$$\begin{aligned} R &= \sqrt{r^2 + r'^2 - 2rr' \cos(\theta - \theta')}, \\ \mathcal{R} &= \sqrt{a^4 + r^2 r'^2 - 2a^2 r r' \cos(\theta - \theta')}, \\ \alpha &= (\lambda_1 - \lambda_2)/(\lambda_1 + \lambda_2), \\ \lambda_1 &= k_1/\mu_1, \\ \lambda_2 &= k_2/\mu_2. \end{aligned}$$

Consider an infinite reservoir with an injection well and  $n$  production wells, where each production well is located at  $(r'_i, \theta'_i)$  and has rate  $q_i$ , ( $i = 1, \dots, n$ ) and the injection well has rate

$$q_0 = - \sum_{i=1}^n q_i \quad (\text{E.22})$$

and position  $(r'_0, \theta'_0)$ . There is a circular discontinuity of radius  $a$  with mobility  $\lambda_1$ . The long time pressure change for this system can be superimposed by the solution in Eqs. E.20 and E.21 for one single well,

$$p(r, \theta) = \sum_{i=0}^n q_i G(r, \theta, r'_i, \theta'_i) \quad (\text{E.23})$$



where

$$G(r, \theta, r'_i, \theta'_i) = \frac{\alpha}{2\pi h \lambda_2} \ln r'_i + \frac{1}{\pi h (\lambda_1 + \lambda_2)} \ln R_i$$

for well  $i$  outside the circular discontinuity and the observation well inside the circular discontinuity, i.e.  $r < a$  and  $r' > a$ ;

$$G(r, \theta, r'_i, \theta'_i) = \frac{1}{2\pi h \lambda_2} \ln R_i + \frac{\alpha}{2\pi h \lambda_2} \ln(rr'_i) - \frac{a}{2\pi h \lambda_2} \ln \mathcal{R}_i$$

for well  $i$  outside the circular discontinuity and the observation well outside the circular discontinuity, i.e.  $r > a$  and  $r' > a$ ;

$$G(r, \theta, r'_i, \theta'_i) = \frac{1}{2\pi h \lambda_1} \ln R_i + \frac{(\lambda_1 - \lambda_2)\alpha}{2\pi h \lambda_1 \lambda_2} \ln a + \frac{\alpha}{2\pi h \lambda_1} \ln \mathcal{R}_i$$

for well  $i$  inside the circular discontinuity and the observation well inside the circular discontinuity, i.e.  $r < a$  and  $r' < a$ ;

$$G(r, \theta, r'_i, \theta'_i) = \frac{\alpha}{2\pi h \lambda_2} \ln r + \frac{1}{\pi h (\lambda_1 + \lambda_2)} \ln R_i$$

for well  $i$  inside the circular discontinuity and the observation well outside the circular discontinuity, i.e.  $r > a$  and  $r' < a$

$$\begin{aligned} R_i &= \sqrt{r^2 + r_i'^2 - 2rr_i' \cos(\theta - \theta_i')} \\ \mathcal{R}_i &= \sqrt{a^4 + r^2 r_i'^2 - 2a^2 r r_i' \cos(\theta - \theta_i')}. \end{aligned}$$

The pressure change for reservoirs of multiple injection wells and multiple production wells can be formulated similarly. Notice that the pressure change observes the principle of reciprocity.

In the above discussion, Darcy units were used. To use field units, just substitute  $\frac{q}{2\pi h \lambda}$  with  $\frac{141.2qB}{h\lambda}$ . Actually, the pressure change in Eq. E.23 is independent of the unit of length; the steady-state model of an infinite reservoir with a circular discontinuity is fully scalable. To verify this, it is sufficient to show that Eqs. E.20 and E.21 will be modified by the same amount when the unit of length is changed. Suppose the old unit is the new unit times a factor  $C$ , then

$$a_{old} = C a_{new}$$

$$r_{old} = C r_{new}$$

$$r'_{old} = Cr'_{new}$$

$$R_{old} = CR_{new}$$

$$\mathcal{R}_{old} = C^2\mathcal{R}_{new}.$$

So the difference between the new expression and the old expression will be

$$\frac{\alpha}{2\pi h\lambda_2} \ln C + \frac{2}{2\pi h(\lambda_1 + \lambda_2)} \ln C = \frac{\ln C}{2\pi h\lambda_2} \quad (\text{E.24})$$

for the expression of  $r' > a$  and  $r < a$ ,

$$\frac{1}{2\pi h\lambda_2} \ln C + \frac{\alpha}{2\pi h\lambda_2} \ln C^2 - \frac{\alpha}{2\pi h\lambda_2} \ln C^2 = \frac{\ln C}{2\pi h\lambda_2} \quad (\text{E.25})$$

for the expression of  $r' > a$  and  $r > a$ ,

$$\frac{1}{2\pi h\lambda_1} \ln C + \frac{(\lambda_1 - \lambda_2)\alpha}{2\pi h\lambda_1\lambda_2} \ln C - \frac{\alpha}{2\pi h\lambda_1} \ln C^2 = \frac{\ln C}{2\pi h\lambda_2} \quad (\text{E.26})$$

for the expression of  $r' < a$  and  $r < a$ , and

$$\frac{\alpha}{2\pi h\lambda_2} \ln C + \frac{2}{2\pi h(\lambda_1 + \lambda_2)} \ln C = \frac{\ln C}{2\pi h\lambda_2} \quad (\text{E.27})$$

for the expression of  $r' < a$  and  $r > a$ . Since

$$\sum_{i=0}^n q_i = 0, \quad (\text{E.28})$$

all the differences incurred by changing the unit of length in Eq. E.23 will cancel out.

# Nomenclature

$a$	radius of circular discontinuity
$a, b$	equal distance between wells in $x, y$ directions
$a_{ij}$	general function
$B$	formation volume factor
$C$	wellbore storage coefficient
$C_n$	constant coefficients
$c$	dimensionless concentration of displacing fluid
$c_i$	concentration of component $i$ in the phase
$c_t$	total system effective compressibility
$D$	differential operator or functional operator
$D$	diffusive coefficient, effective mixing coefficient
$\mathcal{D}$	functional operator
$D_i$	dispersion of component $i$ in the phase
$E$	residual of the least squares
$\mathbf{e}_i$	axis vector of $x_i$
$\mathbf{f}$	general function
$G$	Green's function
$g$	general function
$h$	thickness
$I, K$	modified Bessel functions
$J, Y$	Bessel functions
$k$	permeability
$k_{XX}$	maximum principal permeability

$k_{xx}, k_{xy}, k_{yy}$	components of the permeability tensor
$k_{YY}$	minimum principal permeability
$L$	reference length of flow
$L$	differential operator
$l$	width of reservoir
$L^*$	adjoint differential operator
$\mathcal{L}$	general linear operator
$\mathcal{L}^*$	general linear adjoint operator
$n, \mathbf{n}$	outward normal vector
$p$	pressure
$p_D$	dimensionless pressure response at observation well
$P_e$	Peclet number
$q$	flow rate
$q_{sf}$	sandface flow rate
$r$	radial distance of observation well
$r'$	radial distance of active well
$r_{eD}$	dimensionless reference distance
$r_{nD}$	dimensionless distance between observation and neighbor wells
$r_w$	wellbore radius of active well
$S$	skin factor
$S_e$	boundary, integral variable on boundary
$s$	Laplace variable
$t$	time
$t_{p,D}$	dimensionless producing time before shut-in at testing well
$U$	damping factor
$u$	general function
$v$	general function
$v$	Darcy velocity
$\vec{v}$	Darcy velocity of the phase
$W$	region in the well
$x, y, z$	coordinate in Cartesian system

$x', y', z'$	Cartesian coordinates of source
$x_i$	mole fraction of component $i$ in the system
$z$	Laplace variable
well 0	observation well
well 1	testing well
well $n$	neighboring well or image well( $n > 1$ )
$a$	root of Bessel function equation
$\Gamma$	reservoir boundary
$\Delta p$	pressure drop
$\delta$	Dirac function
$\eta$	hydraulic diffusivity
$\theta$	angle of observation well position
$\theta'$	angle of active well position
$\lambda$	mobility
$\mu$	viscosity
$\nu$	Green's function
$\xi$	dimensionless distance
$\rho$	mole density of the phase
$\rho_i^0$	mole density of component $i$ at standard condition
$\tau$	dimensionless time
$\tau$	integral variable
$\phi$	porosity
$\Omega$	reservoir domain, integral variable
$\nabla$	gradient operator

**Superscripts**

$T$  transpose

**Subscripts**

$D$  dimensionless

1 circular discontinuous region

2                   reservoir, the second region outside discontinuity

# Bibliography

- [1] Abbaszadeh-Dehghani, M.: *Analysis of Unit Mobility Ratio Well-to-Well Tracer Flow to Determine Reservoir Heterogeneity*, PhD dissertation, Stanford University (July 1982).
- [2] Aronofsky, J. S. and Heller, J. P.: “A Diffusion Model to Explain Mixing of Flowing Miscible Fluids in Porous Media,” *Trans. AIME* (1957) 345–349.
- [3] Arya, A., Hewett, T. A., Larson, R. G. and Lake, L. W.: “Dispersion and Reservoir Heterogeneity,” *SPE Reservoir Engineering* (February 1988) 139–148.
- [4] Barua, J., Horne, R. N., Greenstadt, J. L. and Lopez, L.: “Improved Estimation Algorithms for Automated Type Curve Analysis of Well Tests,” *SPE Formation Evaluation* (March 1988) 186–196.
- [5] Bear, J.: “On the Tensor Form of Dispersion in Porous Media,” *J. Geophys. Res.* (1961) 1185–97.
- [6] Bear, J.: *Hydraulics of Groundwater*, McGraw-Hill Book Co. (1979).
- [7] Brzostowski, M. A. and McMechan, G. A.: “4-D Tomographic Monitoring of Enhanced Oil Recovery,” 61st Annual Internat. Mtg., Soc. Expl. Geophys., Expanded Abstracts, Soc. Expl. Geophys. (1991) 367–370.
- [8] Carslaw, H. S. and Jaeger, J. C.: *Conduction of Heat in Solids*, 2nd edition, Oxford University Press (1959).
- [9] Collins, R. E.: *Flow of Fluids Through Porous Media*, Reinhold Publishing Corp., New York (1961).

- [10] Courant, R. and Hilbert, D.: *Methods of Mathematical Physics Volume I*, Interscience Publishers, Inc. (1953).
- [11] Crump, K. S.: "Numerical Inversion of Laplace Transforms Using a Fourier Series Approximation," *Journal of Association for Computing Machinery* (1976) 89-96.
- [12] De Josselin de Jong, G. and Bossen, M. J.: "Discussion of Paper by J. Bear On the Tensor Form of Dispersion in Porous Media," *J. Geophys. Res.* (1961) 3623-24.
- [13] De Wiest, R.: *Flow Through Porous Media*, Academic Press (1969).
- [14] Eipper, M. E.: *Computer Generation of Type Curves*, PhD dissertation, Stanford U. Geothermal Program Report SGP-TR-86, Stanford, CA (1985).
- [15] Falk, R. S.: "Error Estimates for the Numerical Identification of a Variable Coefficient," *Math Comp* (April 1983) **40**, 537-546.
- [16] Fletcher, R.: "A Modified Marquardt Subroutine for Nonlinear Least Squares," *Rep. R6799, AERE, Harwell, England* (1971).
- [17] Frind, E. O. and Pinder, G. F.: "Galerkin Solution of the Inverse Problem for Aquifer Transmissivity," *Water Resources Research* (1973) **9**, 1379-1410.
- [18] Grader, A. S. and Horne, R. N.: "Interference Testing: Detecting A Circular Impermeable or Compressible Subregion," *SPE Formation Evaluation* (June 1988) **3**, No. 2, 420-428.
- [19] Gringarten, A. C. and Ramey, H. J. Jr.: "The Use of Source and Green's Functions in Solving Unsteady-Flow Problems in Reservoirs," *Soc. Pet. Eng. J.* (Oct. 1973) 324-335.
- [20] Harleman, D. R. F., Melhorn, P. F. and Rumer, R. R. Jr.: "Dispersion Permeability Correlation in Porous Media," *Am. Soc. Civil. Engrs. HY 2* (1963) 67-85.



- [21] Hyndman, D. W.: “Estimating Special Patterns of Aquifer Parameters Using Seismic and Tracer Data,” Master’s thesis, Stanford University (March 1993).
- [22] Jaeger, J. C.: “Heat Conduction in Composite Circular Cylinders,” *Phil. Mag.* (1941) **7**, 324–335.
- [23] Jaeger, J. C.: “Some Problems Involving Line Sources in Conduction of Heat,” *Phil. Mag.* (1944) **35**, 169–179.
- [24] Jensen, C. L. and Horne, R. N.: “Matrix Diffusion and its Effect on the Modeling of Tracer Returns from the Fractured Geothermal Reservoir at Wairakei, New Zealand,” Proc. Ninth Workshop on Geothermal Reservoir Engineering, Stanford U., Stanford, CA (Dec. 1983) 323–329.
- [25] Kocabas, I. and Horne, R. N.: “Analysis of Injection Backflow Tracer Tests in Fractured Geothermal Reservoirs,” Proc. 12th Workshop on Geothermal Reservoir Engineering, Stanford U., Stanford, CA (Jan. 1987) 323–329.
- [26] Kravaris, C. and Seinfeld, J. H.: “Identification of Parameter in Distributed Parameter Systems by Regularization,” *SIAM J. Control and Optimization* (March 1985) **23**, 217–241.
- [27] Leaver, J. D., Grader, A. and Ramey, H. J. Jr.: “Multiple-Well Interference Testing in the Ohaaki Geothermal Field,” *SPE Formation Evaluation* (June 1988) 429–437.
- [28] Marquardt, D. W.: “An Algorithm for Least-Squares Estimation of Nonlinear Parameters,” *J. Soc. Indust. Appl. Math.* (June 1963) **11**, No. 2, 431–441.
- [29] McKinley, R. M., Vela, S. and Carlton, L. A.: “A Field Application of Pulse-Testing for Detailed Reservoir Description,” *J. Pet. Tech.* (March 1968) 313–321.
- [30] Mishra, S.: *On the Use Pressure and Tracer Data for Reservoir Description*, PhD dissertation, Stanford University (September 1987).

- [31] Morrey, C. B. Jr.: *Multiple Integrals in the Calculus of Variations*, Springer-Verlag, New York Inc. (1966).
- [32] Nelson, R. W.: "Conditions for Determining Areal Permeability Distribution by Calculation," *SPEJ* (September 1962) 223–224.
- [33] Nelson, R. W.: "In-place Determination of Permeability Distribution for Heterogeneous Porous Media Through Analysis of Energy Dissipation," *Society of Petroleum Engineers Journal* (March 1968) 33–42.
- [34] Newman, A. B.: "Heating and Cooling Rectangular and Cylindrical Solids," *Ind. and. Eng. Chem.* (1936) **28**, 545.
- [35] Nur, A.: "4-D Seismology and (True) Direct Detection of Hydrocarbons: The Petrophysical Basis," 58th Annual Internat. Mtg., Soc. Expl. Geophys., Expanded Abstracts, Soc. Expl. Geophys. (1988) Session:ADV1.6.
- [36] Ogbe, D. O.: *Pulse Testing in the Presence of Wellbore Storage and Skin Effects*, PhD dissertation, Stanford University (1984).
- [37] Ozkan, E. and Raghavan, R.: "New Solutions for Well-Test Analysis Problems: Part 1 - Analytical Considerations," *SPEFE* (Sept. 1991) 359–68.
- [38] Ozkan, E. and Raghavan, R.: "New Solutions for Well-Test Analysis Problems: Part 2 - Computational Considerations and Applications," *SPEFE* (Sept. 1991) 369–78.
- [39] Pan, Y.: "Application of Least Squares and Kriging in Multivariate Optimizations of Field Development Scheduling and Well Placement Design," Master's thesis, Stanford University (July 1995).
- [40] Papadopoulos, I. S.: "Nonsteady Flow to a Well in an Infinite Anisotropic Aquifer," *Symposium International Assn. Sci. Hydrology, Dubrovnik, Yugoslavia* (1965).

- [41] Peters, E. and Afzal, N.: "Characterization of Heterogeneities in Permeable Media with Computed Tomography Imaging," *Journal of Petroleum Science and Engineering* (1992) **7**, 283–296.
- [42] Ramey, H. J. Jr.: "Interference Analysis for Anisotropic Formations – A Case History," *J. Pet. Tech.* (October 1975) 1290–1298.
- [43] Ramey, H. J. Jr.: "A Drawdown and Build-up Type Curve for Interference Testing," *Lawrence Berkeley Laboratory, Energy and Environment Division* (1981) 130–134.
- [44] Richter, G. R.: "An Inverse Problem for the Steady State Diffusion Equation," *SIAM J. APPL. MATH.* (October 1981) No. 2, 210–221.
- [45] Richter, G. R.: "Numerical Identification of a Spatially Varying Diffusion Coefficient," *Mathematics of Computation* (1981) **36**, 375–386.
- [46] Roach, G. F.: *Green's Functions*, 2nd edition, Cambridge University Press (1982).
- [47] Rosa, A. J.: *Reservoir Description by Well Test Analysis Using Cyclic Flow Rate Variations*, PhD dissertation, Stanford University (1991).
- [48] Sagar, B., Yakowitz, S. and Duckstein, L.: "A Direct Method for the Identification of the Parameters of Dynamic Nonhomogeneous Aquifers," *Water Resour. Res.* (1975) 563–570.
- [49] Sageev, A.: *Pressure Transient Analysis of Reservoirs with Linear or Internal Circular Boundaries*, PhD dissertation, Stanford University (1983).
- [50] Starkgold, I.: *Green's Functions and Boundary Value Problems*, John Wiley & Sons (1979).
- [51] Stehfest, H.: "Algorithm 368, Numerical Inversion of Laplace Transforms," *D-5 Communications of the ACM* (Jan. 1970) **13**, No. 1, 47–49.

- [52] Theis, C. V.: "Relation Between the Lowering of the Piezometric Surface and the Rate and Duration of Discharge of a Well Using Ground-Water Storage," *EOS Trans.* (AGU. 1935) **16**, No. 2, 519–24.
- [53] Vela, S.: "Effect of Linear Boundary on Interference and Pulse Tests - The Elliptical Inference Area," *JPT* (Aug. 1977) 947–950.
- [54] Walkup, G. W. J. and Horne, R. N.: "Forecasting Thermal Breakthrough of Reinjecting Water Using a Dispersion-Retention Model for Tracer Test Interpretation," *Trans. Geothermal Resources Council Meeting*, Kona, Hawaii (Aug. 1982) 369–374.
- [55] Walton, W. C.: *Groundwater Resource Evaluation*, McGraw-Hill Book Co., Inc. (1970).
- [56] Yakowitz, S. and Noren, P.: "On the Identification of Inhomogeneous Parameters in Dynamic Linear Partial Differential Equations," *J. Math. Analysis and Application* (1976) **53**, 521–538.
- [57] Yeh, W. W.-G.: "Review of Parameter Identification Procedures in Groundwater Hydrology: the Inverse Problem," *Water Resources Research* (February 1986) **22**, No. 2, 95–108.
- [58] Yeh, W. W., Yoon, Y. S. and Lee, K. S.: "Aquifer Parameter Identification with Kriging and Optimum Parameterization," *Water Resources Research* (1983) 225–233.
- [59] Yu, C.: *Mathematical Evaluation of Effective Hydrogeologic Parameters and Media Nonhomogeneity from Tracer Breakthrough Curve Data*, PhD dissertation, Pennsylvania State University (August 1984).